STATISTICAL ANALYSIS OF SEISMIC DATA
AND
SEISMIC RISK ANALYSIS OF INDIAN PENINSULA

A Thesis Submitted
In Partial Fulfilment of the Requirements
for the Degree of
DOCTOR OF PHILOSOPHY

by
SUSANTA BASU

to the

DEPARTMENT OF CIVIL ENGINEERING
INDIAN INSTITUTE OF TECHNOLOGY KANPUR
JUNE 1977

I.I.T. KANPUR
CENTRAL LIBRARY
Acc. No. A 54055
9 MAY 1978

Thesis
624.1762
B 2998

CE-1977-D-BAS-STA

POST GRADUATE OFFICE
Submitted on 27/6/77

CERTIFICATE

This is to certify that the thesis entitled, "Statistical Analysis of Seismic Data and Seismic Risk Analysis of Indian Peninsula" by Susanta Basu, has been carried out under my supervision and has not been submitted elsewhere for a degree.

June - 1977

(N.C. Nigam)
Professor
Department of Aeronautical Engineering
Indian Institute of Technology, Kanpur
INDIA

POST GRADUATE OFFICE
This thesis has been approved
for the award of the Degree of
Doctor of Philosophy (Ph.D.)
in accordance with the
regulations of the Indian
Institute of Technology Kanpur
Dated: 25.4.1978

ACKNOWLEDGEMENTS

The author expresses his deep sense of gratitude to Prof. N.C. Nigam for his able guidance and constant encouragement during the course of this work.

The author is indebted to Mr. H.M. Chaudhury, The Director Seismology Division, Indian Meteriological Department, New Delhi, for permitting the author to use Earthquake Catalogue of I.M.D. The author thankfully acknowledges the help provided by Prof. A.S. Arya and Dr. P.N. Agarwal of SRTEE, Roorkee during data collection.

The author is thankful to Mr. B. Ghosh, Librarian, Geological Survey of India, Calcutta, for extending the library facilities to the author.

The author expresses his sincere gratitude to Mrs. Katharine Rao, who translated the Spanish references cited in this work.

Part of the financial assistance to the author came from H.B.T.I., Kanpur and the author is grateful to the authorities of the H.B.T.I.

The author is grateful to his colleagues in H.B.T.I. in general and to Dr. C.V.S.K. Rao and Mr. H.S. Niranjan in particular for their generous help and cooperation.

The author acknowledges the help provided by Mr. T.M.S. Raghavan, Mr. G.C. Baral, Dr. S.K. Ray and Mr. S. Banerjee for helpful discussion and correction of manuscript.

The author is very much thankful to Mr. R.C. Adhikari for his help in various ways during the course of the work.

The author is thankful to the staff of the Computer Centre, I.I.T./Kanpur, for their cooperation.

Finally, thanks are due to Mr. G.L. Misra and Mr. S.K. Tewari for their skillful and excellent typing.

LIST OF TABLES

CHAPTER 2 : STATISTICAL ANALYSIS OF SEISMIC DATA OF INDIAN PENINSULA

Table 2.1 : Properties of Earthquake with Magnitude above Five 25

Table 2.2 : Estimated Serial Autocorrelation Coefficients 25

Table 2.3 : Estimated Correlation Matrix 25

Table 2.4 : Mean Squares for Various Block Sizes in Grieg-Smith's Pattern Analysis of Epicentral Location 27

Table 2.5 : Analysis of Variance Table for Linear Regression $\ell n\ N = a + bM$ 35

Table 2.6 : Hyperexponential Distribution of Inter-arrival Time 43

Table 2.7 : State of Markov Chain, its Stationary Probabilities and Parametersof Holding Time Distribution 44

Table 2.8 : Transition Probability Matrix of Markov Chain 47

CHAPTER 3 : MODULAR EARTHQUAKE SOURCE AND SENSITIVITY ANALYSIS

Table 3.1 : Ratio of Return Periods for Normal (ℓ) and Mixed Lognoraml ($m\ell$) Distribution to Focal Depth, H 69

CHAPTER 4 : SEISMIC RISK ANALYSIS OF INDIAN PENINSULA A MODEL HOMOGENEOUS IN TECTONIC FEATURES

Table 4.1 : Analysis of Variance Table for Multiple Linear Regression Model - $C(\mu) = \exp\left[a_0 + a_1\ \ell n\ M + a_2 M \right]$ 87

Table 4.2 : Analysis of Variance Table for Linear Regression Model – $\ell n[n\{1+C^2(\mu')\}/(n+1)] = \gamma\,\ell n(V/V')$ 90

Table 4.3 : Estimated Intensity and Coefficient of Variation Square for Earthquake and Peak Generalized Seismic Intensity at Grid Points. Lognormal Focal Depth Distribution, $m \varepsilon (5,9]$, $b = 150$ kms. and $H_0=600$ kms. 93–101

CHAPTER 5 : SEISMIC RISK ANALYSIS OF INDIAN PENINSULA-A MODEL NONHOMOGENEOUS IN TECTONIC FEATURES

Table 5.1 : Geometric and Associated Seismic Activity of Tectonic Units and Faults of Indian Peninsula 121–122

CHAPTER 6 : EFFECT OF SCATTER IN THE ATTENUATION LAW ON SEISMIC RISK

Table 6.1 : Parameter of Envelopes 137

Table 6.2 : Values of C_1 and C_2 for Different Probability Levels for Envelopes A and B 138

CHAPTER 7 : SEISMIC ZONNING MAPS OF INDIA

Table 7.1 : Comparison of IS:1893–1975 with Present Work 158

Table 7.2 : Peak Ground Acceleration in g for Different Cities 159

APPENDIX A7.1 : LIST OF EARTHQUAKES BEFORE 1917

Table A7.1 : List of Earthquake Before 1917 230

LIST OF FIGURES

Page No.

CHAPTER 2 : STATISTICAL ANALYSIS OF SEISMIC DATA OF INDIAN PENINSULA

Fig. 2.1 : Number of Earthquakes in each Year with Magnitude > 5 21

Fig. 2.2 : Histogram of Spatial Occurrence of Earthquakes of Magnitude, M > 5, from January 1917 to December 1975, total Number 1375 23

Fig. 2.3 : Histogram of Focal Depth with Magnitude, M > 5 30

Fig. 2.4 : Frequency-Magnitude Relation 36

Fig. 2.5 : Seismicity of Indian Peninsula: Energy Contours in 10^{15} ergs km^{-2} yr^{-1} 37

Fig. 2.6 : Arrival of Earthquakes 39

CHAPTER 3 : MODULAR EARTHQUAKE SOURCE AND SENSITIVITY ANALYSIS

Fig. 3.1 : Earthquake Source at site: Volume of Revolution of Sector about X_3 53

Fig. 3.2 : Effect of arc Length, b, on Return Period, T_y, of Peak Ground Acceleration, y 65

Fig. 3.3 : Effect of arc Length, b, on Return Period, T_y, of Peak Ground Velocity, y 66

Fig. 3.4 : Effect of arc length, b, on Return Period T_y, of Peak Ground Displacement, y 67

Fig. 3.5 : Effect of Maximum Focal Depth H_o on the Probability of the Peak Ground Acceleration Y Exceeding y; $m \varepsilon (5,9]$ 70

Fig. 3.6 : Effect of Maximum Focal Depth H_o on the Probability of the Peak Ground Velocity Y Exceeding y; $m \epsilon (5,9]$ 71

Fig. 3.7 : Effect of Maximum Focal Depth H_o on the Probability of the Peak Ground Displacement Y Exceeding y; $m \epsilon (5,9]$ 72

Fig. 3.8 : Effect of Maximum Focal Depth H_o on the Probability of the Peak Ground Acceleration Y Exceeding y; $m \epsilon (m_o, \infty)$ 73

Fig. 3.9 : Effect of Maximum Focal Depth H_o on the Probability of the Peak Ground Velocity Y Exceeding y; $m \epsilon (m_o, \infty)$ 74

Fig. 3.10 : Effect of Maximum Focal Depth H_o on the Probability of the Peak Ground Displacement Y Exceeding y; $m \epsilon (m_o, \infty)$ 75

Fig. 3.11 : Effect of Magnitude Cutoff on the Probability of Peak Ground Acceleration Y Exceeding y 76

Fig. 3.12 : Effect of Magnitude Cutoff on the Probability of the Peak Ground Velocity Y Exceeding y 77

Fig. 3.13 : Effect of Magnitude Cutoff on the Probability of the Peak Ground Displacement Y Exceeding y 78

CHAPTER 4 : SEISMIC RISK ANALYSIS OF INDIAN PENINSULA A MODEL HOMOGENEOUS IN TECTONIC FEATURE

Fig. 4.1 : Grid Numbers 82

Fig. 4.2 : Coefficient of Variation of μ and Magnitude Relation 88

Fig. 4.3 : Variability of Local Seismicity within Indian Peninsula for Magnitude, $M > 5$. 91

Fig. 4.4 : Peak Acceleration (cm/sec^2) Contours Focal Depth Lognormally Distributed & $M \epsilon (5,9]$ 102

Fig. 4.5 : Peak Velocity (cm/sec) Contours-Lognormal Distribution of Focal Depth & $M \epsilon (5,9]$ 103

Fig. 4.6 : Peak Displacement (cm) Contours - Lognormal Distribution of Focal Depth & $M \in (5,9]$ 104

Fig. 4.7 : Variation of μ_T with Peak Ground Acceleration, Y 107

Fig. 4.8 : Variation of μ_T with Peak Ground Velocity, Y 108

Fig. 4.9 : Variation of μ_T with Peak Ground Displacement, Y 109

CHAPTER 5 : SEISMIC RISK ANALYSIS OF INDIAN PENINSULA A MODEL NONHOMOGENEOUS IN TECTONIC FEATURES

Fig. 5.1 : Seismo-Tectonic Map of India 116

Fig. 5.2 : Idealized Tectonic Features of Indian Peninsula 117

Fig. 5.3 : Peak Acceleration (cm/sec^2) Contours-Lognormal Distribution of Focal Depth, $M \in (5,9]$ & Nonhomogeneous in Tectonic Features 124

Fig. 5.4 : Peak Velocity (cm/sec) Contours-Lognormal Distribution of Focal Depth, $M \in (5,9]$ & Nonhomogeneous in Tectonic Features 125

Fig. 5.5 : Peak Displacement (cm) Contours-Lognoraml Distribution of Focal Depth, $M \in (5,9]$ & Nonhomogeneous in Tectonic Features 126

CHAPTER 6 : EFFECT OF SCATTER IN THE ATTENUATION LAWS ON SEISMIC RISK ANALYSIS

Fig. 6.1 : Attenuation Law for Peak Ground Acceleration, Y 129

Fig. 6.2 : Attenuation Law for Peak Ground Velocity,Y 130

Fig. 6.3 : Envelope of Scatter 134

Fig. 6.4 : Effect of Model-1 on the Exceedance Probability of Peak Acceleration, Y 139

Fig. 6.5 : Effect of Model-1 on the Exceedance Probability of Peak Velocity, Y 140

Fig. 6.6 : Effect of Model-1 on the Exceedance Probability of Peak Displacement, Y 141

Fig. 6.7 : Effect of Model-2 and Gaussian Model on the Exceedance Probability of Peak Acceleration, Y 144

Fig. 6.8 : Effect of Model-2 and Gaussian Model on the Exceedance Probability of Peak Velocity,Y 145

Fig. 6.9 : Effect of Model-2 and Gaussian Model on the Exceedance Probability of Peak Displacement,Y 146

CHAPTER 7 : SEISMIC ZONING MAPS OF INDIA

Fig. 7.1 : Peak Acceleration Contours 150

Fig. 7.2 : Zoning Map Based on Acceleration 152

Fig. 7.3 : Peak Velocity (cm/sec.) Contours 154

Fig. 7.4 : Zoning Map Based on Velocity 155

Fig. 7.5 : Peak Displacement (cm) Contours 156

Fig. 7.6 : Zoning Map Based on Displacement 157

APPENDIX A3.8.1 PROBABILITY DISTRIBUTION FUNCTION AND PROBABILITY DENSITY FUNCTION OF FOCAL DISTANCE, R, FOR VOLUME SOURCE AT SITE

Fig. A3.8.1.1 Earthquake Source at Site: Volume of Revolution of Sector About X_3 180

Fig. A3.8.1.2 $r \varepsilon [0, a \sin \nu]$ 187

Fig. A3.8.1.3 $r \varepsilon [a \sin \nu, 2a \sin (\nu/2)]$ 187

Fig. A3.8.1.4 $r \varepsilon [2a \sin (\nu/2), H_o]$ 187

Fig. A3.8.1.5 $r \varepsilon [H_o, R_o]$ 187

APPENDIX A3.8.2 PROBABILITY OF GENERALIZED PEAK SEISMIC INTENSITY

Fig. A3.8.2.1 Domain of Different $[Y > y]$; $z \varepsilon (z_1, \infty)$ 196

Fig. A3.8.2.2 Domain of Different $[Y > y]$; $z \varepsilon (z_1, z_2]$ 197

APPENDIX A5.1 SECTION OF A SPHERE (EARTH) BY A PLANE (FAULT)

Fig. A5.1 Rotation of Axis for Fault Plane X' O Y' 202

APPENDIX A5.2 PROBABILITY DISTRIBUTION FUNCTION AND PROBABILITY DENSITY FUNCTION OF FOCAL DISTANCE, R, FOR AREA SOURCE

Fig. A5.2.1 Area Source due to Fault with Projection of Site 0 at Fault Plane 206

APPENDIX A6.4.1 THE PROBABILITY DISTRIBUTION FUNCTION OF Z

Fig. A6.4.1.1 $Z \leq z_1$ 216
Fig. A6.4.1.2 $z_1 \leq Z \leq z_2$ 216
Fig. A6.4.1.3 Domain of Z 216

APPENDIX A6.4.2 THE PROBABILITY DENSITY AND DISTRIBUTION FUNCTION OF W

Fig. A6.4.2.1 Event $[\ W \leq w_1\ ]$ 222
Fig. A6.4.2.2 Event $[\ w_1 \leq W \leq \min\ (w_2, w_4)\ ]$ 222

APPENDIX A6.4.3 PROBABILITY OF PEAK GENERALIZED SEISMIC INTENSITY, Y

Fig. A6.4.3.1 Event $[\ Y \leq y_1\ ]$ 227
Fig. A6.4.3.2 Event $[\ y_1 \leq Y \leq y_2\ ]$ 227
Fig. A6.4.3.3 Domain of Z and W 227

SYNOPSIS

STATISTICAL ANALYSIS OF SEISMIC DATA
AND
SEISMIC RISK ANALYSIS OF INDIAN PENINSULA

The Thesis Submitted
In Partial Fulfilment of the Requirements
For the Degree of
DOCTOR OF PHILOSOPHY
by
SUSANTA BASU
to the
Department of Civil Engineering
Indian Institute of Technology Kanpur
June 1977

Earthquakes constitute a major potential cause of natural disaster over a large part of the earth. During an earthquake the surface of the earth and all earth-based structural systems are subjected to dynamic loads. Aseismic design and analysis of such systems, therefore, requires a prediction of the occurrence of earthquakes and accompanying ground motions at a location during the service life of the structure. The history of recorded earthquakes and ground motions during earthquakes indicate that the occurrence of earthquakes, their size, temporal and spatial characteristics, and the ground motion at a site are random in nature. The prediction of the design

seismic loads during the service life of a structure, therefore, involves statistical analysis and extrapolation ofavailable seismic data. The paucity of seismic data available in most parts of the world, however, puts severe limitations on the use of mere statistical results. For meaningful results, it becomes necessary to synthesise the statistical results with judgement based on geotectonic features and any other related information available, even if it is subjective.

Due to the random nature of the earthquakes, a probabilistic approach provides a rational framework for aseismic design. Engineering interest in earthquakes encompasses location of a structure at the 'best' site, based on relative seismic risk, and establishing design loads for the structural system to provide the optimum balance between cost and acceptable risk to life and property. To a designer this information is available through codes containing zoning maps and algorithm for computatio of design loads.

The current code of practice for earthquake resistant design of structures in India is contained in IS: 1893-1975. The code divides the Indian peninsula in five zones and gives lateral force coefficients for each zone. The seismic zoning map is based on the subjective judgement of the seismicity of the different parts of the country on the basis of epicenters of the past earthquakes, isoseismals and geotectoni features. The code specifies the design acceleration in each zone without accounting for the service life of the structure in the evaluation of the seismic risk. The code also does not provide information regarding other design parameters, such as, peak displacement and velocity which govern the design of some structures.

The objective of the present work is to improve the available techniques for seismic zoning based on stochastic models of earthquake phenomena, and to develop rational seismic zoning maps of Indian peninsula. The Indian peninsula is defined by latitude (6°, 40°] and longitude (66°, 98°] and the seismic data available for a period of 55 years (January 1917 to December 1972) is used to determine the parameters of the stochastic models. An attempt is made to quantity the notion of seismic risk based on T-year generalised intensity.

Statistical analysis of the past seismic activities of the Indian peninsula is carried out in the first part of the investigation. Histograms of origin-times, latitude, longitude and focal depth are obtained. A stochastic model based on origin-times only is made to investigate the structure of mainshock and aftershocks for different magnitudes. However the exact location of earthquake focus is largely ignored in the model. The model parameters are estimated based on the fact that an apriori discrimination between mainshocks and aftershocks from the earthquake catalogue is indistinguishable. An attempt is made to obtain a semi-Markov model of earthquakes occurrence for magnitude greater than five. The focal depths are considered to be spatially homogeneous and temporally stationary. The focal depth data is fitted with truncated lognormal and a bimodal distribution by the method of maximum likelihood. Tests of goodness of fit are performed in each case.

The seismic risk analysis of the Indian peninsula is investigated for two different cases. The earthquake process is assumed to be Poisson in both the cases. In the first case the seismic risk is determined assuming that the earthquake source is homogeneous in tectonic features.

Sensitivity analysis of seismic risk with respect to various dimensional parameters of earthquake source, magnitude cutoff and three assumed distributions of focal depth is performed. Based on the sensitivity analysis model parameters are chosen to evaluate seismic risk of the Indian peninsula. The results are plotted in a contour form for 100 year return period. Method of extrapolation to obtain seismic risk for any other return period and specified acceptable risk from this map is indicated. In the second case, the Indian peninsula is assumed to be nonhomogeneous in tectonic features based on available geotectonic data. The earthquake source now consists of area sources associated with faults, and volume sources corresponding to major geological zones. The seismic risk is obtained and compared with the risk evaluated in the first case.

The available data shows a large scatter around assumed attenuation laws. A true evaluation of seismic risk must incorporate the effect of this uncertainity. Two new models are proposed to incorporate the effect of the scatter and compared with the deterministic and Gaussian model due to Esteva. Steps to incorporate the effect of scatter in the seismic risk analysis at a site are indicated.

Based on the stochastic models discussed in this thesis, the available information regarding the geotectonic features of Indian peninsula and the current seismic zoning maps of the I.S. Code, seismic zoning maps of peak ground acceleration, velocity and displacement are prepared for a 100 year return period. The maps reflect the synthesis of all available information to the best judgement of the author.

TABLE OF CONTENTS

CHAPTER Page No.

LIST OF TABLES v

LIST OF FIGURES vii

SYNOPSIS xii

1 INTRODUCTION 1

1.1 General 1
1.2 Engineering Aspects of Earthquakes 3
1.2.1 Causes and mechanism 3
1.2.2 Earthquake parameters and attenuation law 5

1.3 Seismic Data 7
1.4 Geology 8
1.5 Seismic Zonning 8

1.5.1 Deterministic approach 9
1.5.2 Probabilistic approach 11

1.6 Present Work 17

2 STATISTICAL ANALYSIS OF SEISMIC DATA OF INDIAN PENINSULA 20

2.1 Introduction 20
2.2 Data and General Observation 20
2.3 Spatial Pattern 26
2.4 Focal Depth 29
2.5 Magnitude and Energy 34
2.6 Interarrival Times 38
2.7 Summary of Results 49

3 MODULAR EARTHQUAKE SOURCE AND SENSITIVITY ANALYSIS 50

3.1 Introduction 50
3.2 Modular Earthquake Source-Geometry 52
3.3 Magnitude-Frequency Law 54
3.4 Focal Depth 56
3.5 Temporal Model of Earthquake Source 57
3.6 Attenuation Law 58
3.7 General Formulation of Seismic Risk at a Site 58

CHAPTER Page No.

3.7.1 Probability distribution function of generalized peak seismic intensity 58
3.7.2 T-year generalized peak seismic intensity 60

3.8 Probability Distribution of Peak Generalized Seismic Intensity for Assumed Distribution of Focal Depth, H, and Magnitude, M, of Earthquake 62

3.8.1 Magnitude, M, cutoff at lower level i.e. $m \varepsilon (m_o, \infty)$ 62
3.8.2 Magnitude, M, cutoff at both ends i.e. $m \varepsilon (m_o, m_1)$ 62

3.9 Results & Discussion 63

4 SEISMIC RISK ANALYSIS OF INDIAN PENINSULA - A MODEL HOMOGENEOUS IN TECTONIC FEATURES 81

4.1 Introduction 81
4.2 Local Seismicity 83

4.2.1 Bayes' Theorem 84
4.2.2 Estimation of Local Seismicity 85

4.3 Estimation of Regional Seismicity at Grid Points 89
4.4 Results and Discussion 92
4.5 Extrapolation of Generalized Intensity at a Location 105

4.5.1 Extrapolation for return period 106
4.5.2 Extrapolation for specified exceedance probability 110
4.5.3 Extrapolation for specified exceedance probability and specified return period 111
4.5.4 Extrapolation for magnitude cutoff 111

5 SEISMIC RISK ANALYSIS OF INDIAN PENINSULA- A MODEL NONHOMOGENEOUS IN TECTONIC FEATURES 113

5.1 Introduction 113
5.2 Tectonic Features of Indian Peninsula 113
5.3 Earthquake Source 118
5.4 T-year Generalised Peak Seismic Intensity 119
5.5 Estimation of Parameter of Earthquake Arrival Process of Various Seismo-Tectonic Provinces and Faults 120
5.6 Estimation of Parameter of Arrival Process at Grid Points 123
5.7 Results and Discussion 123

CHAPTER Page No.

6 EFFECT OF SCATTER IN THE ATTENUATION LAW ON SEISMIC RISK 128

6.1 Introduction 128
6.2 A Gaussian Model 128

6.2.1 Probability of generalised intensity 131

6.2.1.1 The probability of generalised intensity for magnitude cutoff at lower level i.e. $m \varepsilon (m_o, \infty)$ 131
6.2.1.2 The probability of generalised seismic intensity for magnitude cutoff at both ends i.e. $m \varepsilon (m_o, m_1]$ 133

6.3 Proposed Model for Scatter in Attenuation Law-Model-1 134

6.3.1 The choice of envelopes 136

6.4 Proposed Modelfor Scatter in Attenuation Law 136
6.5 Results and Discussion 143
6.6 Incorporation of the Effect of Scatter on Seismic Risk 143

7 SEISMIC ZONING MAPS OF INDIA 148

7.1 Introduction 148
7.2 Seismic Zoning Map 149
7.3 Discussion of the Seismic Zoning Maps 153

8 SUMMARY OF RESULTS AND CONCLUSIONS AND SUGGESTIONS FOR FURTHER WORK 161

8.1 Results and Conclusions 161
8.2 Suggestionsfor Further Work 163

REFERENCES 166

APPENDIX A2.4.1 MAXIMUM-LIKELIHOOD ESTIMATION FOR FOCAL DEPTH 172

APPENDIX A2.6.1 MAXIMUM-LIKELIHOOD ESTIMATION OF HYPER-EXPONENTIAL DISTRIBUTION 177

APPENDIX A3.8.1 PROBABILITY DISTRIBUTION FUNCTION AND PROBABILITY DENSITY FUNCTION OF FOCAL DISTANCE, R, FOR VOLUME SOURCE AT SITE 179

Page No.

APPENDIX A3.8.2 PROBABILITY OF GENERALIZED PEAK SEISMIC INTENSITY, Y 194

APPENDIX A5.1 SECTION OF A SPHERE (EARTH) BY A PLANE (FAULT) 201

APPENDIX A5.2 PROBABILITY DISTRIBUTION FUNCTION AND PROBABILITY DENSITY FUNCTION OF FOCAL DISTANCE, R, FOR AREA SOURCE 205

APPENDIX A6.4.1 THE PROBABILITY DISTRIBUTION FUNCTION OF Z 215

APPENDIX A6.4.2 THE PROBABILITY DENSITY AND DISTRIBUTION FUNCTION OF W 221

APPENDIX A6.4.3 PROBABILITY OF PEAK GENERALIZED SEISMIC INTENSITY, Y 226

APPENDIX A7.1 LIST OF EARTHQUAKES BEFORE 1917 230

CHAPTER 1

INTRODUCTION

1.1 General

Soil, air and water are basic to the creation and sustenance of life and civilization on the earth. It is ironical that each one of them is also the cause of major natural disaster through earthquakes, hurricanes, floods and tsunamis . Of these, earthquakes occur over a large part of the earth, without prior warning,and have, therefore, caused severe loss to life and property. With increasing population, spillover of cities and industries into seismically active regions are inevitable. The risk to life and economic loss during future earthquakes is, therefore, increasing at an accelerated rate. The engineering aspects of earthquake cover:

i) Minimising damage to existing structures, through strengthening and modification, if possible. Demolition of unsafe structures to avoid loss of life.

ii) Contingency plans to deal with the likely disruption of life-line facilities, such as, water-supply, electricity, sewarage after an earthquake.

iii) Location, design and construction of new structures to withstand future earthquakes.

An earthquake is caused by the release of energy below the surface of the earth. The energy is propagated in the form of the wave and causes the shaking of the soil deposits, reservoirs and all manmade structures in contact with the ground. The shaking causes dynamic loads which must be resisted to avoid damage during an earthquake. Aseismic design and analysis of any system, therefore, require a prediction of the occurrence of earthquakes and the nature of accompanying ground motions at a site during the service life of the system.

Earthquakes must have occured since the earth came to acquire its present form. However, the documentation and scientific study of earthquakes called seismology, is relatively recent. The history of recorded earthquakes indicates that the occurrence of earthquakes, their size, temporal and spatial characteristics and the ground motion at a site are random in nature. The prediction of the design seismic loads during the service life of a structure, therefore, involves construction of stochastic models, based on available seismic data, and its extrapolation. The paucity of seismic data available in most parts of the world, however, puts severe limitations on the reliability of mere statistical predictions. For meaningful results, it becomes necessary to synthesise the statistical results with judgment based on geotectonic features and any other related information.

Due to the random nature of the earthquake phenomena, a probabilistic approach provides a rational framework for aseismic design. Engineering interest in earthquakes encompasses location of a structure at the 'best' site and adopting design loads to provide optimum balance between cost and acceptable risk to life and property. The codes containing zoning maps and algorithm for the computation of design loads are expected to provide this information. There are several ways by which the zoning maps may be prepared. Housner and Jenings(1) have classified the maps as (a) seismicity maps, (b) fault maps, seismotectonic maps and seismic probability maps, and (c) engineering maps. Seismicity maps provide subjective information regarding shaking in terms of Modified Mercalli (MM) Intensity Scale or other similar scales. Maps showing active faults are called fault maps. Seismotectonic maps are augmented fault maps with geological information (e.g. local geology, tectonic process etc.). Seismic probability or seismic risk maps assign probability of occurrence of earthquakes of different magnitudes at each fault and provide information regarding areal distribution of intensity. Each of these maps is largely subjective in predicting the ground shaking. Engineering maps provide quantitative information regarding ground motion which can be used to fix the seismic load on a structure. Preparation of accurate engineering maps is, therefore, of utmost importance.

1.2 Engineering Aspects of Earthquakes

1.2.1 Causes and Mechanism.

The earthquakes of engineering interest are primarily associated with tectonic activity in the earth's crust. The process leading to an earthquake is essentially one of the transformations of the vast store of energy in the earth's interior. According to Belousov, as reported by Medvedev(2), the vertical oscillatory movement of the earth's crust is the basic factor in the tectonic process of earthquake occurrence. The earthquake mechanism consists of disruption of continuity in earth's crust composed of more rigid blocks adjoining less rigid blocks. Relative movements of these blocks develope high shearing strain at the junction of the blocks causing earthquakes. These junction zones are known as faults. The mechanical rupture at a single point within a fault leads to a redistribution of shearing strain over the entire fault which causes possibility of occurrence of earthquakes in the fault or an adjoining fault. A second theory due to Evison(3,4) describes the earthquake process as the effect of phase change in rocks accompanied by a volume change in relatively small volumes of the crust. The validity of the above theories cannot be established conclusively due to lack of seismic data. The generally accepted theory of earthquake occurrence is the slip along geological faults. However, these faults cannot extend beyond a certain depth owing to high confining pressure and temperature in the mantle. The evidence of the occurrence of earthquake at a depth between 600 to 800 kilometers, as catalogued by Gutenberg and Richter(5), stands against the fault slip mechanism. On the other hand, the study of Southern California earthquakes by Allen et. al(6) strongly supports the view that most of these motions originate as slips along geological faults. It is now recognised that more than one mechanism may be possible for the generation of tectonic earthquakes(7).

Two entirely different approaches, namely, physical and stochastic, are available to understand the mechanism of the origin of earthquakes. A physical model, proposed by Burridge and Knopoff(8), consisted of sliding masses resting on a level surface with coulomb friction and connected by linear springs and dashpots. This model yielded insights into the earthquake mechanisms regarding foreshocks, afterschocks and fault creep. A second approach due to Vere-Jones(9,10) treated earthquake mechanism as a stochastic process analogous to a leaking reservoir. An essentially Compound Poisson Process model was proposed by Shlein and Toksöz(11) where mainshocks were assumed to trigger the earthquake mechanism. Later Hawkes(12,13,14) introduced a class of stationary marked point process in which the value taken by marks (e.g. the energy released by earthquakes) influenced the future intensity of the process. Although mechanical and stochastic models are based on apparently different analogies, they provide a realistic mathematical treatment of the behaviour of earthquake mechanisms.

The importance of the study of earthquake mechanism was evident from the study of Rascón and Cornell(15) showing that strong motion characteristics near the focus of earthquakes were dependent on the conditions leading to earthquakes. Housner(16) with some assumptions regarding bedrock mechanical properties concluded that the peak ground acceleration was 50% of gravity. Similar conclusion could be made regarding peak ground velocity(17,18).

1.2.2 Earthquake Parameters and Attenuation Law

An earthquake is characterized by its location (latitude, longitude, depth of focus), its time of origin and the amount of energy released by it. The latter is a quantitative measure of the size of the earthquakes.

Richter's(19,20) magnitude, M, is intended to rate an earthquake independent of the place of occurrence. The magnitude was originally defined as the common logarithm of maximum amplitude of surface waves in microns, measured at a distance of 100 Kms. on a Wood Anderson Seisomograph. The empirical relation between energy, E, released and magnitude, M, is(19,20)

$$\log E = 1.5M + 11.4 \qquad (1.1)$$

where E is in ergs. The magnitude, M, characterizes the relative strength of earthquake at focus.

The intensity, I, of earthquake is a subjective measure of shaking at a point on the earth's surface. This is usually reported on a non instrumental ordinal scale. Most commonly used scale is modified Mercalli Scale. Empirical relation between magnitude, M, and intensity, I_o, at epicentre for different focal depth, h (in kms.), is(5,21,22)

$$I_o = 1.5M - 3.5 \log h + 3 \qquad (1.2)$$

Relationship between the magnitude, M, the intensity, I, and the focal distance, R (in kms.), has been proposed for different regions(23). The relation given by Esteva and Rosenblueth(24) is

$$I = 8.16 + 1.45M - 2.46 \log R \qquad (1.3)$$

To quantify the historical data which is available in the form of the description of damage during past earthquakes, an attempt has been made to correlate the intensity with peak ground acceleration or velocity. The correlation proposed by Esteva and Rosenblueth(24), and Rosenblueth(25) between MM intensity, I, and peak ground velocity, v, is

$$I = \log(14v)/\log 2 \qquad (1.4)$$

Several authors(23) have proposed correlation between peak ground motion (displacement, velocity, acceleration), Y, with magnitude, M, and focal distance, R. These relations are also called, attenuation laws, and can be expressed in the following general form

$$Y = C_1 \exp\left[C_2 M - C_3 \ln R\right] \qquad (1.5)$$

where Y is in c.g.s. units, R is in kms. C_1, C_2 and C_3 are empirical constants.

1.3 Seismic Data

The historical data regarding past earthquakes are available in the following forms.

(i) Narration of the human reaction and effect on structures.

(ii) Isoseismal maps or intensity information on MM or similar scale.

(iii) Instrumental data in the form of time of occurrence, magnitude, latitude, longitude and depth of focus.

(iv) Instrumental data giving ground motion records and attenuation of earthquake parameters, such as, ground acceleration, velocity or displacement with distance.

The instrumental data have become available recently. However, this data is not complete for many events. For a quantitative treatment of risk due to earthquakes, data under serial (i) and (ii) can be converted into quantitative measures through relations given in the previous sections. One of the major problems in the quantitative treatment of earthquake risk is the paucity of data at the regional level.

1.4 Geology

A realistic evaluation of seismic risk requires information regarding geological features in particular the structure of geological formation. Links between seismicity and geological formations can be estimated by compairing the geological evidence with seismometric materials. However, these links vary widely(2). An important general feature is the fact that the stronger the differences in the rate of vertical movement within a certain zone, the stronger is the seismic activity. However, zones of different seismic intensities cannot be demarcated by seismometric data owing to its validity for short period in comparison with geological times.

The geological information is given in the map of tectonic features giving various folds, faults, thrust etc. and the lithologic group map showing the various type of rock groups in different parts of the country.

1.5 Seismic Zoning

Seismic zoning maps divide a country or a region in zones with a specified intensity of ground shaking due to earthquakes. The intensity of shaking may be specified in terms of MM intensity, Peak ground displacement, velocity or acceleration or similar site-based parameters. Seismic zoning maps represent a synthesis of hystorical data, geological features, attenuation laws and an acceptable balance between cost and risk of damage due to earthquakes. Depending upon the treatment of uncertainty associated with the occurrence of earthquakes and attenuation laws, the available zoning methods may be classified in two groups

1. Deterministric
2. Probabilistic

1.5.1 Deterministic Approach

During the last four decades considerable efforts have been made to prepare and update seismic zoning maps in all countries lying in the seismically active regions. Although the ultimate purpose of seismic zoning maps is the same, there exist differences in the approach used by different countries. Early maps were prepared on a deterministic approach. In Soviet Union, the first zoning map was prepared in 1937 by the seismological Institute (Academy of Sciences of the U.S.S.R.). The procedure adopted to prepare the maps consisted of two steps. The first step was the identification of various zones on the basis of seismometric (magnitude or energy) and geological data. The second step consisted of forecasting intensity and joining them by isoseismals(2). The procedure adopted in China was understood to be same as in U.S.S.R. The basis of preparing zoning maps in Japan was seismicity map(26). The development of seismic zoning in U.S.A. was closely related to building codes.

Each county /state has its own building provision. Uniform Building Code of 1967(27) provided a seismic probability map of United States of America. In 1959, Richter(28,29) produced a zoning map using Soviet concept of zoning. According to Medvedev(2) the map was an over-estimation. The work on the seismic zoning map of U.S.A. based on seismic risk analysis is currently being done by the Applied Technology Council.

The first seismic zoning map of India indicating three earthquake zones, demarcating on qualitative basis, as heavy, moderate and light was produced by Geological Survey of India in 1934. Jai Krishna(30) in 1959 published a four zone map in terms of likely peak ground acceleration in different zones. In 1962, Indian Standard Institution introduced a seismic zone map in the code, namely, Indian Standard Recommendation for Earthquake Resistant Design of Structure IS: 1893-1962(31). The map was produced by plotting all known epicenters with magnitude five and above, drawing assumed circular isoseismal using the average intensity-magnitude-distance relationship and modifying marginally with regional tectonic features. Seven seismic zones were demarcated in this map according to MM intensity. A revision of previous map was made in 1966 (IS: 1893-1966)(32). The zone I of IS: 1893-1962 was extended to cover only the "marginal depression" in accordance with Tectonic Map of Geological Survey of India. The zones at the foot of Himalaya were made parallel to its tectonic trend. Revision of shape of location and grade of isoseismal around Delhi, Kashmir, Assam, Nagaland, Andaman, Manipur, Tripura and Satpura were made. Seismic zone map IS: 1893-1970(33) was produced in accordance with Oldham's hypothesis of the faulted coast line along West Coast owing to the occurrence of Koyna Earthquake of 1967. Different seismic zones were demarcated on the probable distribution of the general intensity of future shocks as guided by the specific tectonic features and past seismic history. In the second revision of IS: 1893 seismic zones were reduced to five by combining zone 0 and zone I as zone I and by combining zone V and VI as zone V. Four separate islands were added in Kashmir, H.P., U.P. and near Nepal. Andaman was entirely under zone V. A zone IV in the Koyna region surrounded by a zone III all along West coast was introduced. Boundary of zone II and zone III were redemarcated raising the seismicity in parts of Gangetic plane. Latest version of IS: 1893-1975(34) contained the seismic zone map of IS: 1893-1970. The earthquake likely to occur in the five zones were of magnitude less than, 5, 5 to 6, 6 to 6.5, 6.5 to 7 and greater than 7 respectively in Ricter's scale. Kaila et. al.(35,36) produced a seismicity map of India which agreed quite well with other maps prepared by different methods.

1.5.2 Probabilistic Approach

A large measure of uncertainty associated with the occurrence of earthquakes, their sizes, locations and attenuation laws makes it necessary to use the probabilistic approach to develop a rational basis for earthquake resistant design. To quote Newmark and Rosenblueth(7)

"In the past the orthodox viewpoint maintained that the objective of design was to prevent failure; it idealized variables as deterministic.

This simple approach is still fruitful when applied to design under mild uncertainty, and in situations in which the possibility of failure may be contemplated at such a distant future as to be almost irrelevant; but when confronted with the effects of earthquakes, this orthodox viewpoint seems so naive as to be sterile".

While the need for a probabilistic approach is generally recognised but the difficulty lies in the scarcity of data. During the last decade intensive efforts have been made all over the world in the application of probabilistic method. Assessment of seismic risk forms the basis of probabilistic approach(37). A seismologist defines a seismic risk as the probability of the occurrence of an earthquake of a specified size or more in a region during a specified interval of time. To an engineer it is more meaningful to define seismic risk as the probability of occurrence of generalized intensity (e.g. peak ground acceleration, velocity, displacement etc.) greater than a specified value at a site in a specified interval of time (service life). To distinguish the two definitions, henceforth the former is termed as geological risk. The seismic risk at a site not only calls for the assessment of geological risk of an earthquake source located at a distance from a site but also accounts for its effect by the attenuation of ground motion Eq. (1.5).

It is generally assumed in both types of analyses that the earthquake arrival process is Poisson and the magnitudes are exponentially distributed. These two assumptionslead to Gumbel's(38) Type I extreme value distribution for maximum earthquake magnitudes and generalized intensities.

Choosing a critical size of earthquakes, Lomnitz(39) produced a geological risk map of Chile in 1964, for a time period less than the time period of the available seismic data. He subdivided the entire region by grid of m × n points, where m is the past epicenters of earthquake in the region, and assuming statistical independence of origin of critical size earthquake at each grid point obtained geological risk at each node.

Lomnitz and Epstein(40) used extreme value theory to obtain geological risk of California. The results were in return periods of extreme magnitude of earthquakes. However, California region was too big to be considered a single unit.

A major contribution to the seismic risk analysis was made independently by Cornell(41) and Esteva(42,43). In their work, earthquake source geometry was assumed to be either a point, or a line, or an area located at constant depth. An attenuation law incorporating the effect of attenuation during wave travel from source to site was used to evaluate the peak generalized seismic intensity at the site for a specified return period. The unobservable Gaussian error, obtained from the linear regression analysis in fitting the attenuation law to data, was also incorporated in the analysis of Esteva. He estimated the intensity of source by Bayesian statistics to account for regional variation in the parameter of magnitude-frequency law. Cornell on the other hand opted for classical statistics to obtain the intensity of occurrence of earthquake at a source.

Later, Cornell and Vanmarcke(44) performed sensitivity analysis of the parameters involved in the seismic risk model(41). They arrived at the conclusion that major contribution to the risk comes from the more frequent smaller events at close proximity to the site.

Goto and Kameda(45) used discrete analogue of Poisson process, the Bernouli random variables, to model the arrival process of earthquakes of different intensities. This result was a multinomial distribution of earthquakes of different intensities during a specified time interval. The return period of exceedance intensity was obtained from the above distribution. They further assumed that the ground motion record was a Gaussian process and level crossing was a Poisson process in obtaining the probability distribution of maximum ground motion in a single earthquake. Intensity parameters of the model were matched with the empirical formula. Several samples of accelerogram were simulated for different correlation time(46) to obtain probability distribution of maximum ground acceleration. Combining assumed model of earthquake process and probability distribution of maximum ground acceleration, the probability distribution of maximum ground acceleration at a site in a 75 year period was obtained and the expected maximum ground acceleration was computed. Same procedure was used for the ground velocity. The results were presented in contour forms showing expected maximum ground acceleration and velocity to occur in 75 years in Japan.

Benjamin(47) assumed a multinomial model for earthquakes of different intensities. Bayesian forecasting technique was adopted with diffuse prior(48) to optimize design decision at a site. Lomnitz(49) incorporated the historical data and obtained a geological risk map of Chilie using his previous technique(39).

Milne and Davenport(50) obtained a least square solution with number of earthquakes at a site that produced an acceleration equal to or greater than a specified value at a site per annum. A risk map in terms of the return period of an acceleration of 10% gravity for eastern part of Canada was prepared. They also compared their result with that obtained from extreme value theory.

Algermissen(51) obtained a geological risk map of United States of America using distribution of MM intensity and strain release data and association of strain release data with geological features.

Relation between fault length and magnitude, the spatial distribution of intensity of ground shaking and magnitude, the felt area and magnitude, and the frequency of occurrence of earthquakes and magnitude were given by Housner(52). For an average site in California effective upper bound of magnitude was given as a function of seismicity.

A comparison of geological risk for various models of earthquake arrival process at a site in Alaska was presented by Chou et. al.(53). Inter-arrivals of earthquakes were considered to be exponential distribution and Weibull distribution. Both classical and Bayesian estimation procedure were used for comparison of geological risk for various distributional model. They also obtained geological risk of Alaska site using Benjamin's(47) approach.

In 1971, Cornell(54) incorporated the Gaussian error term in the attenuation law in his seismic risk model(41) discussed earlier. He also introduced a random aspect in this paper for the structural response. Assuming damage measure a monotonic increasing function of intensity of ground motion the probability distribution of cummulative damage of Palmgren -Miner type was obtained. Finally the probability distribution of commulative damage of structure was obtained approximately using approximate probability distributions, extreme value distribution of Type I, of peak structural response and assuming coefficient of variation of peak response given that the site intensity is small.

Algermissen and Perkins(55) following somewhat similar technique proposed by Cornell(41) obtained a seismic risk map for Utah and Arizona. They prepared maps for the region on the basis of peak ground acceleration of 50-year return period and 50-year maximum acceleration with 10% exceedance probability.

Merz and Cornell(56) developed a seismic risk model using a quadratic-magnitude-frequency law based on observed data(57) to provide a better fit for large magnitude. Later, Merz and Cornell(58) used a trigger model in seismic risk analysis to account for aftershocks. Spatial distribution of aftershocks were assumed according to a distribution obtained by Utsu(59,60) and temporal characteristics in accordance with Omari's(61) law. Based on this investigation it was concluded that equivalent event model (no discrimination between shocks) provided a conservative estimate of the seismic risk.

In 1975, Liu and Fagel(62) provided geological risk of United States using available methods. The risk was presented in terms of magnitude and return period.

The essential feature of the probabilistic approach to seismic zoning is the synthesis of the stochastic model of the earthquake phenomena incorporating the temporal and spatial uncertainties, a distribution function for magnitude, attenuation laws and geotectonic features. In view of the paucity of instrument data, Bayes' theorem is used for parameter estimation to make the best use of historical and future data. In the investigation known to author the random nature of focal depth(7) has not been incorporated. There is also scope for improvement in the available methods to account for the scatter in attenuation laws and extrapolation of specified intensities at a site for different return periods, cutoff magnitude and acceptable risk. The goodness-of-fit of assumed distributions is rarely reported. The approach adopted to prepare the current seismic zoning map for the Indian peninsula(34) explicitly states, "The Sectional Committee has appreciated that there cannot be any statistical approach to the problem of earthquake intensity and an entirely scientific basis for zoning is also not possible in view of the scanty data available". The map has been prepared for ground acceleration only and does not account for the return period.

1.6 Present Work

The present work is an attempt to improve the available technique for seismic zoning based on stochastic models of earthquake phenomena, and to develop rational seismic zoning map of Indian peninsula. The Indian peninsula is defined by latitude (6°, 40°] and longitude (66°, 98°] .

Chapter 2 presents an analysis of the seismic data of the Indian peninsula for the period of 55 year (January 1917 - December 1972). Histogram for spatial location of earthquake is obtained first. A contour map showing energy released by earthquakes of magnitude above five is presented. Frequency-magnitude relation for Indian peninsula is obtained. A stochastic model ignoring exact location of earthquake focus and based only on origintimes is constructed to investigate the structure of mainshocks and aftershocks for earthquakes above different magnitude threshold. A Semi-Markov model incorporating spatial (epicentral) and temporal location of earthquakes is fitted to the past seismic data of the region. The focal depth data is assumed to be spatially and temporally homogeneous and stationary. The focal depth data is fitted to the truncated lognormal and bimodal distributions. The goodness-of-fit is discussed in each case.

Seismic risk formulation for a modular volume source centered at a site is presented in chapter 3. Sensitivity analysis with respect to various geometric parameters of the earthquake source, magnitude cutoff and three assumed focal depth distributions is performed.

The Indian peninsula is divided into a 2° × 2° grid and seismic risk is evaluated assuming homogeneous in tectonic features at each grid point for a 100 year return period based on modular volume source.

These results are presented in Chapter 4. The geometric and other parameters are chosen on the basis of the sensitivity analysis in Chapter 3. Regional variation of magnitude-frequency law is taken into account by Bayesian procedure. The results are plotted in contour forms. Extrapolation and interpolation procedure for different return periods as well as procedure to obtain T-year maximum generalized intensity with exceedance probability α is discussed.

Chapter 5 gives a brief description of the structural geology of Indian peninsula and their idealisation for the study. Seismic risk analysis of Indian peninsula is carried out assuming it to be nonhomogeneous in tectonic features. The earthquake source consists of area source due to known faults and volume sources based on geological character. Contour maps obtained from this analysis are compared with that of the homogeneous analysis prepared in the previous chapter.

Three different methods of incorporating the scatter in the attenuation laws are discussed in Chapter 6. Examples are given to show the method of accounting the scatter in the contour maps.

Based on the results of the present investigation, available geotectonic information and the current I.S. Code, seismic zoning maps are prepared for a 100-year return period in terms of peak ground acceleration, velocity and displacement. These are presented in Chapter 7. Thesis is concluded with a summary of results and a discussion of the scope of future research in Chapter 8.

CHAPTER 2

STATISTICAL ANALYSIS OF SEISMIC DATA OF INDIAN PENINSULA

2.1 Introduction

The earthquake process is essentially a stochastic field process. However, at present it is not possible to carry out complete and successful investigation assuming it as a stochastic field process, primarily, because of the insufficient nature of available seismic data. Nevertheless the statistical analysis of the available data has its importance towards proper understanding of the mechanism of earthquake in a region. It is with this aim that the statistical analysis of seismic data of Indian peninsula (latitude (6°,40°] and longitude (66°, 98°]) has been carried out and presented in this chapter.

The data analysis is primarily aimed at to investigate the earthquake characteristics with respect to space, time and its magnitude. To this end distribution of focal depth and magnitude frequency relation are established in this chapter. Further, some stochastic models on interarrival times are developed and parameters of these models are estimated. The goodness of fit criteria is determined in each case and is discussed.

2.2 Data and General Observation

The seismic data are obtained from Indian Meteriological Department, New Delhi. The catalogue of earthquakes contains data from the year 893.

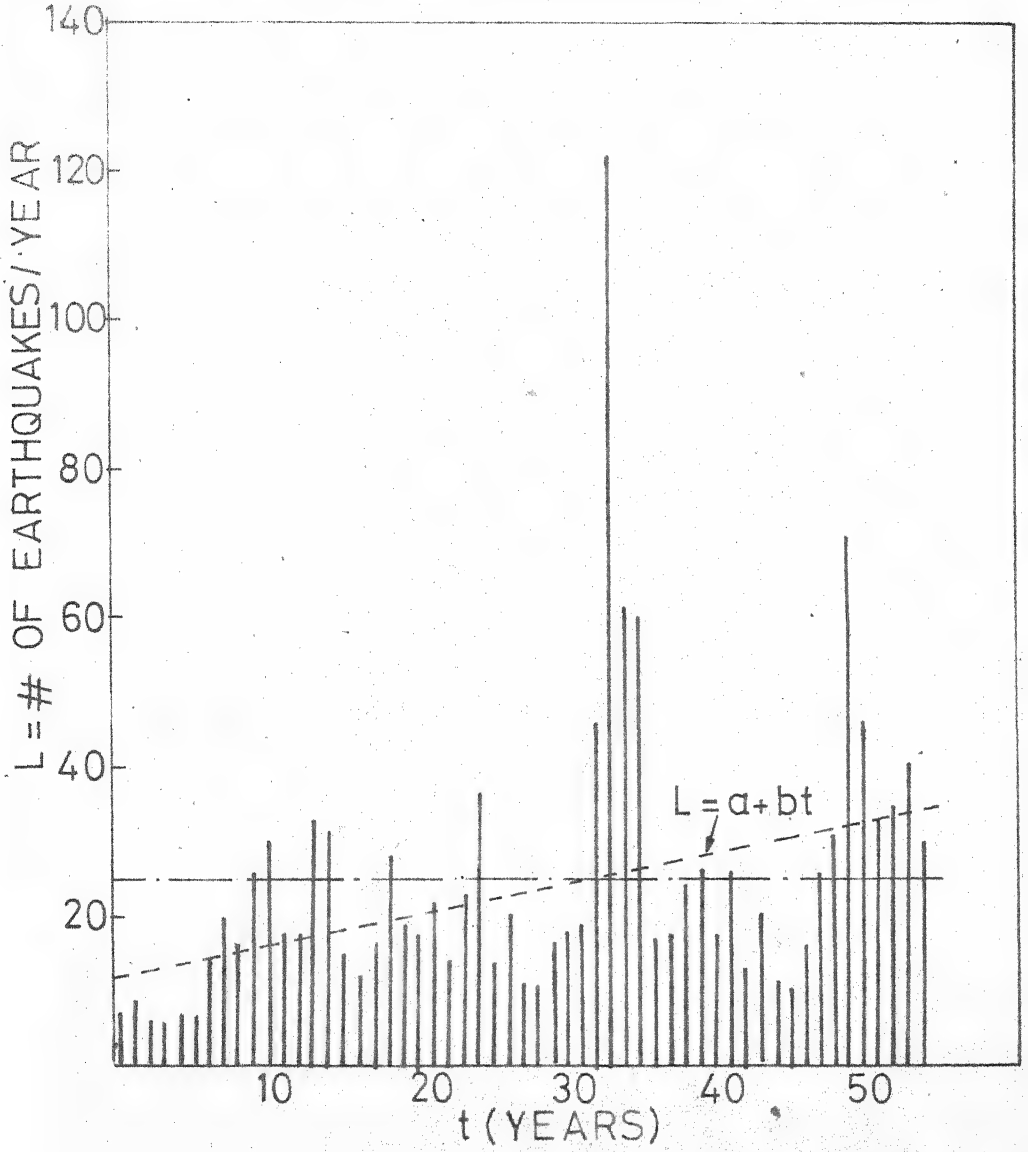

FIG 2·1 NUMBER OF EARTHQUAKES IN EACH YEAR WITH MAGNITUDE > 5

But upto the year 1917 the data are very sparse and cannot meaningfully be used in the statistical analysis. It is for this reason that earthquake data from 1917 onwards have been used in this study. The early part of the catalogue contains earthquake data with magnitude above 5 only. However with the availability of sophisticated instruments during the last decade the catalogue contains earthquake data with magnitude less than five from 1965 onwards. In the present analysis except for magnitude-frequency relation the data of earthquake with magnitude above five are used. The focal depth data of all the earthquakes are not mentioned in the catalogue. Further the catalogue contains a large number of earthquakes with focal depth exactly equal to 33 kms. It is suspected that 33.0 kms. is attributed to all those cases where focal depth has not been recorded properly or some doubt exists on the value of focal depth. Hence, all data with focal depth of 33.0 kms have been rejected. It also appears that magnitude data of some of the early earthquakes of the catalogue might have been derived from intensities. However, this indication is available only for a few cases. In some magnitude data only range is specified. The mid point of the specified range is taken as the actual data.

Fig. (2.1) shows the yearly number of earthquakes with magnitude above five in the region for 55 years. The mean rate is 25 earthquakes/yr A linear regression $L = a+bt$ is performed. The parameter L represents earthquakes/yr and t is in years. The results of the analysis are

$\hat{a}$ = 11.57 earthquakes/yr

$\hat{b}$ = 0.488 earthquakes/yr./yr

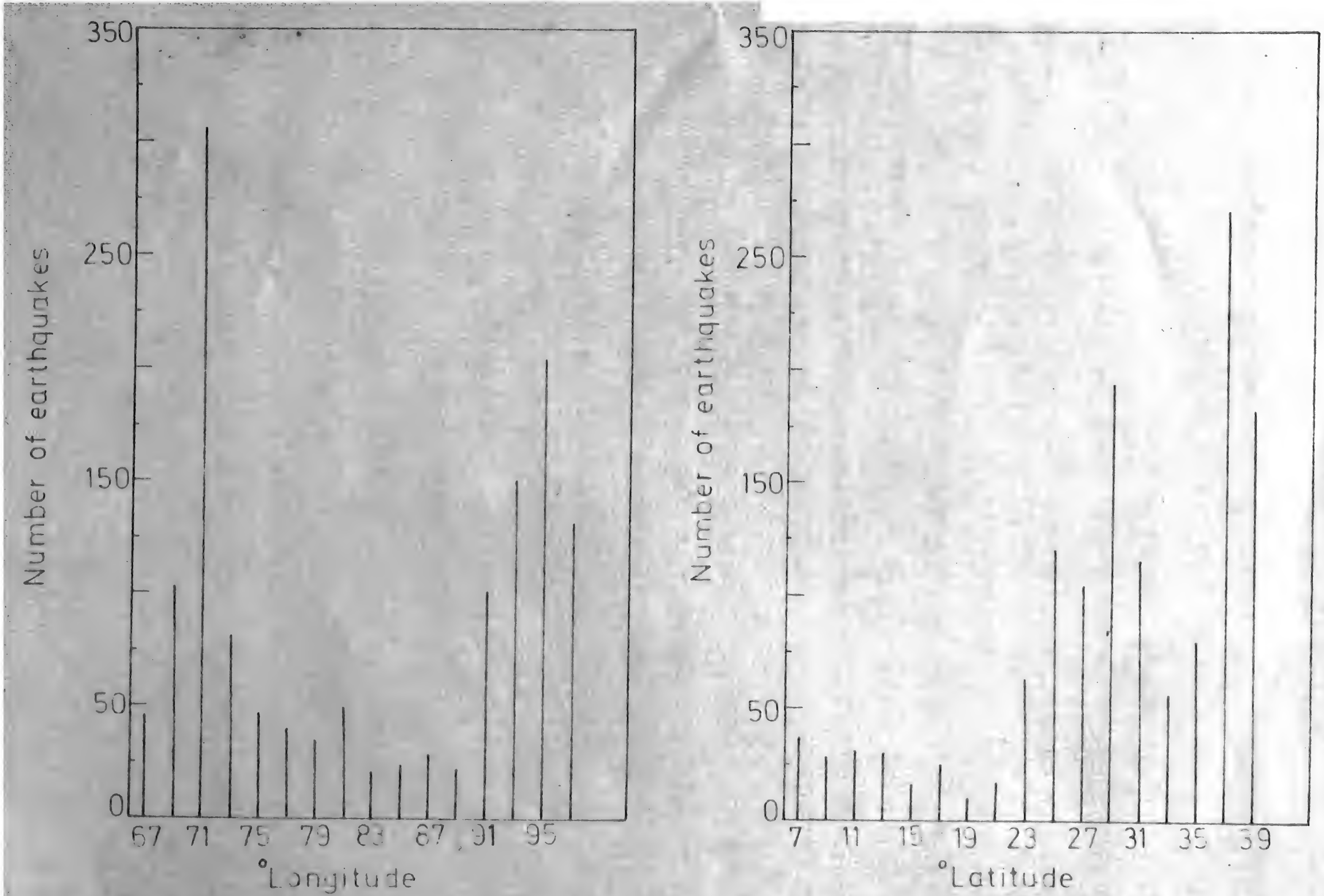

FIG 2·2 HISTOGRAM OF SPATIAL OCCURRENCE OF EARTHQUAKES OF MAGNITUDE, M >5, FROM JANUARY 1917 TO DECEMBER 1972, TOTAL NUMBER 1375

Multiple correlation coefficient square = 0.1605
The null hypothesis H_o: b = 0 is tested by F-test. The regression coefficient b obtained is significant because F_o=18.05 > $F_{o.999}$ (1,53) $\simeq$ 12.2. The result implies that on an average about 26 more earthquakes/yr of magnitude above five were recorded at the end of period than at the begining.

Fig. (2.2) gives the histrogram of latitude and longitude data at 2° interval. It can be seen that maximum earthquakes during the period have occurred between longitude of (70°,72°] and between latitude of (36°, 38°].

The Table 2.1 provides length of the period; the number of sample, the sample mean dispersion and the coefficient of variation, for interarrival time, magnitude, longitude, latitude and focal depth data. Table 2.2 gives the sample serial correlation coefficient of interarrival time, magnitude, longitude and latitude of lag upto 10. None of the series is completely random since values of the serial correlation coefficient of lag one is far above the standard error(63), $\sigma \simeq 0.03$.

The correlation matrix of longitudes, latitudes, magnitudes and interarrival times are given in Table 2.3. The correlation between latitude and longitude is significant and it confirms the presence of Himalayan belt and indicates that on an average epicenters of earthquake have high latitude and small longitude or viceversa. However, other correlations are vary small.

Table 2.1

Properties* of Earthquakes with Magnitude above Five

	Interarrival times (days)	Magnitude (log(erg))	Latitude (degrees)	Longitude (degrees)	Focal depth. (kms.)
1. Length of Data	20064.95**	-	-	-	-
2. Nos. of Samples	1374	1374	1374	1374	624
3. Mean	14.603	5.743	29.597	82.635	98.861
4. Dispersion	455.979	0.234	70.772	120.954	5829.710†
5. Coefficient of variation	1.463	0.082	0.284	1.333	0.773

* Origin is fixed at the first event after 1917

** Indicates total time period of the data (1917-1972) less time to the first event

† The number is high due to widely separated data.

Table 2.2

Estimated Serial Autocorrelation Coefficients

Lag	1	2	3	4	5	6	7	8	9	10
Interarrival time	0.234	0.181	0.185	0.170	0.281	0.261	0.209	0.200	0.179	0.174
Magnitude	0.191	0.201	0.198	0.214	0.224	0.213	0.202	0.202	0.219	0.190
Latitude	0.147	0.183	0.134	0.066	0.073	0.078	0.060	0.098	0.048	0.097
Longitude	0.235	0.224	0.184	0.184	0.162	0.108	0.110	0.114	0.141	0.122

Table 2.3

Estimated Correlation Matrix

Interarrival times	1.0			
Magnitude	0.0396	1.0		
Latitude	0.0015	-0.0429	1.0	
Longitude	-0.0265	0.1038	-0.6192	1.0

2.3 Spatial Pattern

In this section spatial pattern of earthquakes is studied. Only position of epicenter is considered. Focal position is not considered owing to the nonavailability of focal depth data at all origin times. In the first part location of epicenter is tested for two different time periods (from 1917 to 1947 and from 1917 to 1972) to investigate stationarity of spatial pattern. In the later part the data are tested for space-time correlation.

The spatial pattern is analysed by the method suggested by Greig-Smith(64). The method uses contiguous quadrats (small areas) covering the entire region. The number in each quadrats is counted. Adjacent pair of quadrats are then combined to give quadrats of double area. This procedure is followed until the quadrat itself becomes the region. The total sum of squares about the mean of the smallest quadrat or single unit block is apportioned as in the analysis of variance. The results of the analysis provide mean squares for different block size and are reported in Table 2.4. However, choice of period (1917-1947) is arbitrary. According to Greig-Smith the mean square value remains small for block size being small in relation to the mosaic patches of the pattern. However, the mean square increases with increase in block size till area of block becomes equal to the area of patch. The mean square value remains in this high level with further increase in block size. This indicates that the patches themselves are random or aggregated. The fall of mean square value from this high level ensures regular arrangement of patches.

Table 2.4

Mean squares for various block sizes in Greig-Smith's pattern analysis of epicentral location

Period	1917-1947	1917-1972
Block size	Mean Squares	
1	0.711	3.095
2	0.641	3.083
4	0.798	2.728
8	0.429	3.172
16	1.392	9.581
32	1.031	5.743
64	2.221	22.683
128	4.073	30.477
256	5.936	51.090
512	6.686	62.940
1024	2.337	11.124
2048	29.907	242.678

Number of quadrats is 4096

Number of earthquakes for the period 1917-1947 is 515

Number of earthquakes for the period 1917-1972 is 1375

The result for the period (1917-1947) shows three different mean size of patch area while that of period (1917 to 1972) shows two different mean size patch area. This indicates that the pattern in different time periods are different i.e. the pattern is not stationary. For the period (1917 to 1972) the spatial pattern is composed of patches of mean size of area between 256-1024 units within which patches of mean size area between 8-32 units exist and these patches have regular pattern. A regular pattern of patches of three different mean size of area between 256-1024 units, 8-32 units and 2-8 units constitutes the epicentral pattern for the period (1917-1947).

A second investigation has been carried out to ascertain whether earthquakes occuring at small epicentral distances from each other have also occurred close in time. Existance of space-time clustering will imply the sympathetic behaviour of earthquakes' occurrence. The method(65) requires a priori specification of closeness of event both in space and time. A 2 × 2 contingency table is made by taking every possible pair of earthquakes and classifying them in accordance to a priori choice of closeness. The a priori closeness specification used in this study are spatial distance of 150 kms. and time interval of 180 days. The 2 × 2 continency table obtained from data is given below

Time in	Distances	in Kms.	
days	< 150	≥ 150	Total
<180	X = 3329	23010	26339
≥180	38659	879627	918286
Total	41988	9082637	944625

The null hypothesis of no space-time correlation, suggested by Knox(65) and later proved by Barton and David(66) by graph theoretic approach, is to test that the statistics X is Poisson with mean

$$\lambda = (26339 \times 41988)/944625 = 1170.75$$

The null hypothesis is rejected by approximating the Poisson by Normal random variable at P value less than 5×10^{-6}. This test confirms that earthquake data are composed of main shock and aftershock data. However, the test performed has the drawback of a priori choice of critical distance and time. The end result of the test is strongly dependent on this choice.

2.4 Focal Depth

In this section focal depth distribution is chosen and estimated. The focal depth data contain missing data which are supposed to be that of 'normal' depth earthquakes. The variation of focal depth of earthquakes with respect to time cannot be investigated because of these gaps in data. Hence focal depth is assumed to be stationary parameter of earthquakes. It is also assumed to be homogeneous in Indian peninsula. The maximum focal depth of earthquake in the data is 383 kms. Histogram of focal depth is shown in Fig. (2.3). The histogram clearly shows a major peak at 30 kms. and a minor peak at 230 kms. for earthquakes with magnitude above five. The sample properties of focal depth are reported in Table 2.1. Two distributions, truncated lognormal which is a unimodal distribution and a mixed truncated lognormal

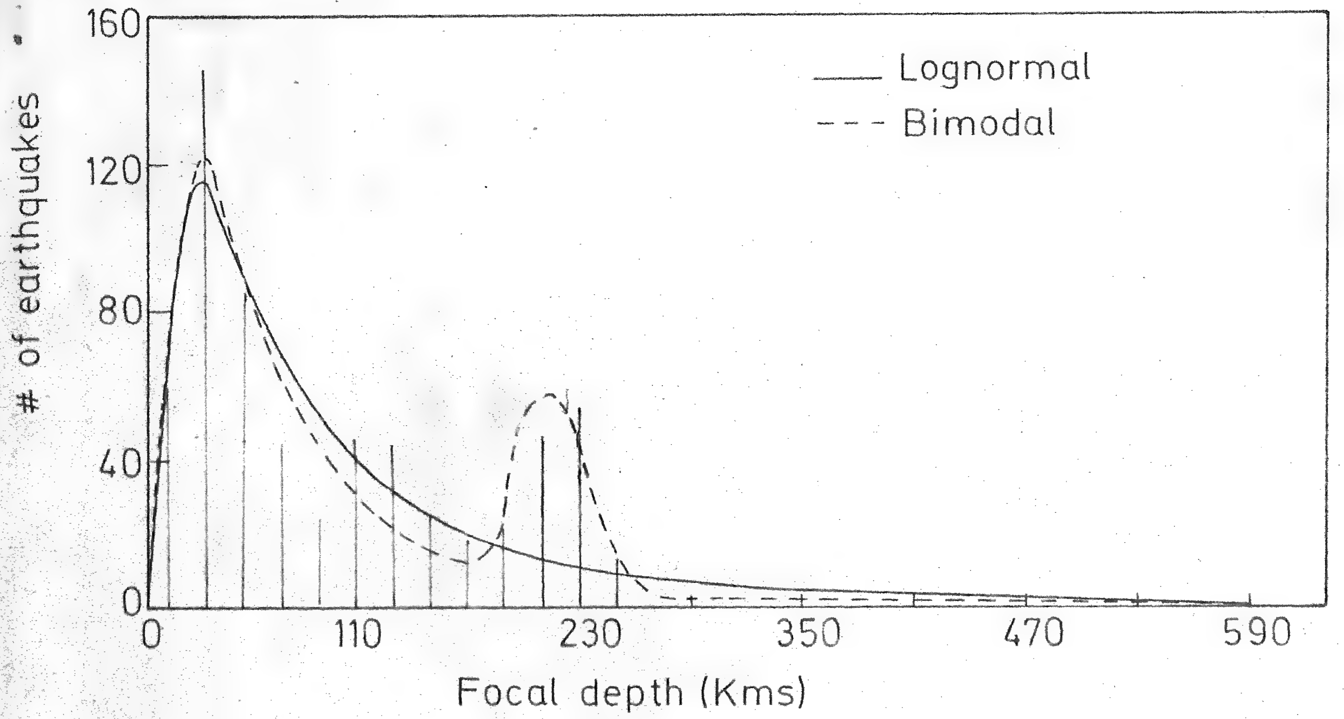

FIG. 2·3 HISTOGRAM OF FOCAL DEPTH WITH MAGNITUDE, M >5 distribution which incorporates both the peaks observed in histogram, are tried to fit the focal depth data. The truncation level is chosen as 600 kms. The subjective judgement in the cutoff is the assertion that earthquakes with focal depth greater than 600 kms are not likely to cause damage to the structure with foundation in ground.

The focal depth data is first fitted to a lognormal distribution with maximum focal depth, $H_o = 600$ kms. The focal depth data is a sample from

$$f_H(x) = \exp\left[-0.5(\ell n\, x-\theta_1)^2/\theta_2\right] / \left[\sqrt{2\pi\theta_2}\;\; x\, \Phi\{(\ell n\, H_o-\theta_1)/\sqrt{\theta_2}\,\}\right] \quad ;\, x \;\varepsilon\; (0, H_o] \qquad (2.1)$$

where θ_1, θ_2 are parameters of the distribution and $\Phi(.)$ is probability density of $N(0,1)$. The details of the method of maximum-likelihood estimation of the parameters θ_1 and θ_2 are given in Appendix A2.4.1 . The estimated values are:

$$\hat{\theta}_1 = 4.252 \quad \text{and} \quad \hat{\theta}_2 = 1.0761$$

and the large sample covariances of the estimated parameter are:

$\hat{\theta}_1$	2.02×10^{-3}	
$\hat{\theta}_2$	7.38×10^{-4}	5.33×10^{-3}

The goodness of fit is tested by Kolmogorov-Smirnov test. The test statistics for two-sided test is $D=0.0866 > D_{624,0.05} = 0.0544$. Hence the null hypothesis that the sample is from lognormal distribution is rejected at significance level, $\alpha = 0.05$.

A bimodal distribution for focal depth is used to fit the data. The distribution is mixed lognormal with probability density function

$$f_H(x) = \sum_{i=1}^{2} p_i \exp\left[-0.5(\ln x - \theta_{1i})^2/\theta_{2i}\right] / \left[\sqrt{2\pi\theta_{2i}} \; x \; \Phi\{(\ln H_o - \theta_{1i})/\sqrt{\theta_{2i}}\}\right] \; ; \; x \, \varepsilon \, (0, H_o] \qquad (2.2)$$

where

$\sum p_i = 1$

$H_o = 600$ kms

$\theta_{12} > \theta_{11}$

and θ_{1i}, θ_{2i}; $i=1,2$ are parameters of the distribution and $\Phi(.)$ is the probability density of $N(0,1)$. The details of the method of maximum-likelihood estimation are given in Appendix A2.4.1. The values of the estimated parameters are:

$\hat{p}_1 = 0.8258$

$\hat{\theta}_{11} = 3.966$

$\hat{\theta}_{12} = 5.373$

$\hat{\theta}_{21} = 0.8475$

$\hat{\theta}_{22} = 0.00466$

The large sample covariances of the estimate are:

p_1	3.227×10^{-4}	
θ_{11}	1.678×10^{-4}	2.016×10^{-3}

θ_{12}	1.561×10^{-4}	4.633×10^{-4}	3.523×10^{-3}		
θ_{21}	1.772×10^{-4}	2.668×10^{-5}	1.461×10^{-5}	6.838×10^{-5}	
θ_{22}	-3.996×10^{-6}	-7.023×10^{-6}	-6.107×10^{-6}	-1.811×10^{-6}	8.317×10^{-7}

The goodness of fit is tested both by Chi-square and Kolmogorov-Smirnov test. **The test statistics** for two sided test is given by $D = 0.0614 < D_{624,0.005} = .06525$. Hence the null hypothesis can be accepted at significance level $\alpha = 0.005$. For Chi-square test the number of class, k, is chosen according to Mann and Wald(67). The class limits are chosen such that the number of theoretical frequency in each class is equal to N/k, where N is the number of samples. The number of class is 49 for 624 samples and significance level, $\alpha = 0.05$. The test statistics is $T = 135.87 > 59.034 = \chi^2_{0.05}(43)$. Hence the null hypothesis that the focal depth distribution is mixed lognormal is rejected at $\alpha = 0.05$.

Basic weaknesses of Chi-square test are the requirement for large sample, heavy dependence upon the choice of number and position of intervals which are generally subjective in nature, and the possibility of very high type II error for some feasible alternative distributions.

The parameters of focal depth distribution for different truncation are estimated for the distribution given by Eq. (2.2) and is reported in the following:

H_o	$\hat{\theta}_1$	$\hat{\theta}_2$
400	4.3808	1.289
500	4.2900	1.429

However, none of these satisfies goodness of fit criteria. Graphically mixed lognormal distribution (Fig. 2.3) gives the best fit of the data.

2.5 Magnitude and Energy

In this section frequency-magnitude relation(5,19,20) indicating correlation between the number of earthquakes with magnitude above a level, M, and the magnitude, M, is established. The data of earthquakes below magnitude five are used in this section. In the latter part a seismicity map giving contours of average yearly energy released by the earthquake is obtained.

A linear regression analysis

$$\ell n\, N = a + bM \tag{2.3}$$

where

M = magnitude of earthquakes

N = # earthquakes/day with magnitude above M is performed in this section to obtain "magnitude-frequency" relation. The analysis of variance table, confidence intervals of the estimate are given in Table 2.5. The test of hypothesis indicates that the coefficient b is highly significant. The regression line with 95% confidence intervals is shown in Fig. (2.4).

A contour map of early energy released is shown in Fig. (2.5). The energy released, E, by an earthquake is obtained from the empirical relation(5,19,20)

Table 2.5

Analysis of Variance Table for Linear Regression Model

$\ell n \quad N = a + bM$

Number of sample = 23

Source of Variation	sum of squares	Degree of freedom	Root Mean square	F-Ratio
Due Regression	146.609	1	12.11	1572.87
Due Residual	1.957	21	0.093	
Total	148.566	22		

	Value	Standard deviation	T-value
a	6.997	0.304	23.00
b	-1.903	0.048	39.66

The covariances of the estimate are

a	0.09256	
b	-0.01428	0.002303

The multiple coefficient correlation square = 0.9868

The null hypothesis $H_0: b = 0$ is rejected at $P << 0.001$

since $F_0 = 1572.87 >> F_{0.999}(1,21) = 14.6$

The 95% confidence interval for a and b are

a = (6.365, 7.630)

b = (-2.003, -1.803).

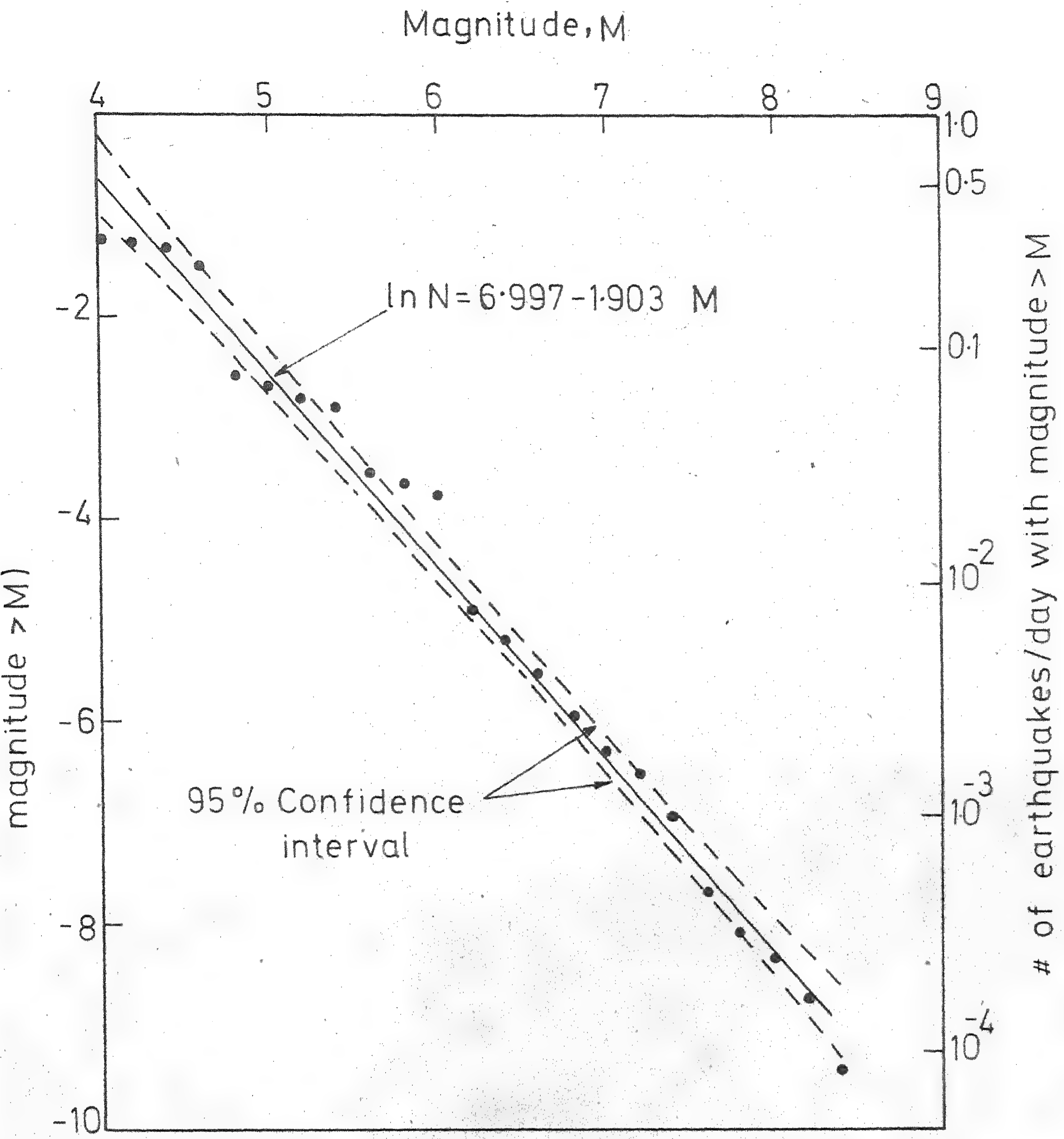

FIG. 2·4 FREQUENCY - MAGNITUDE RELATION

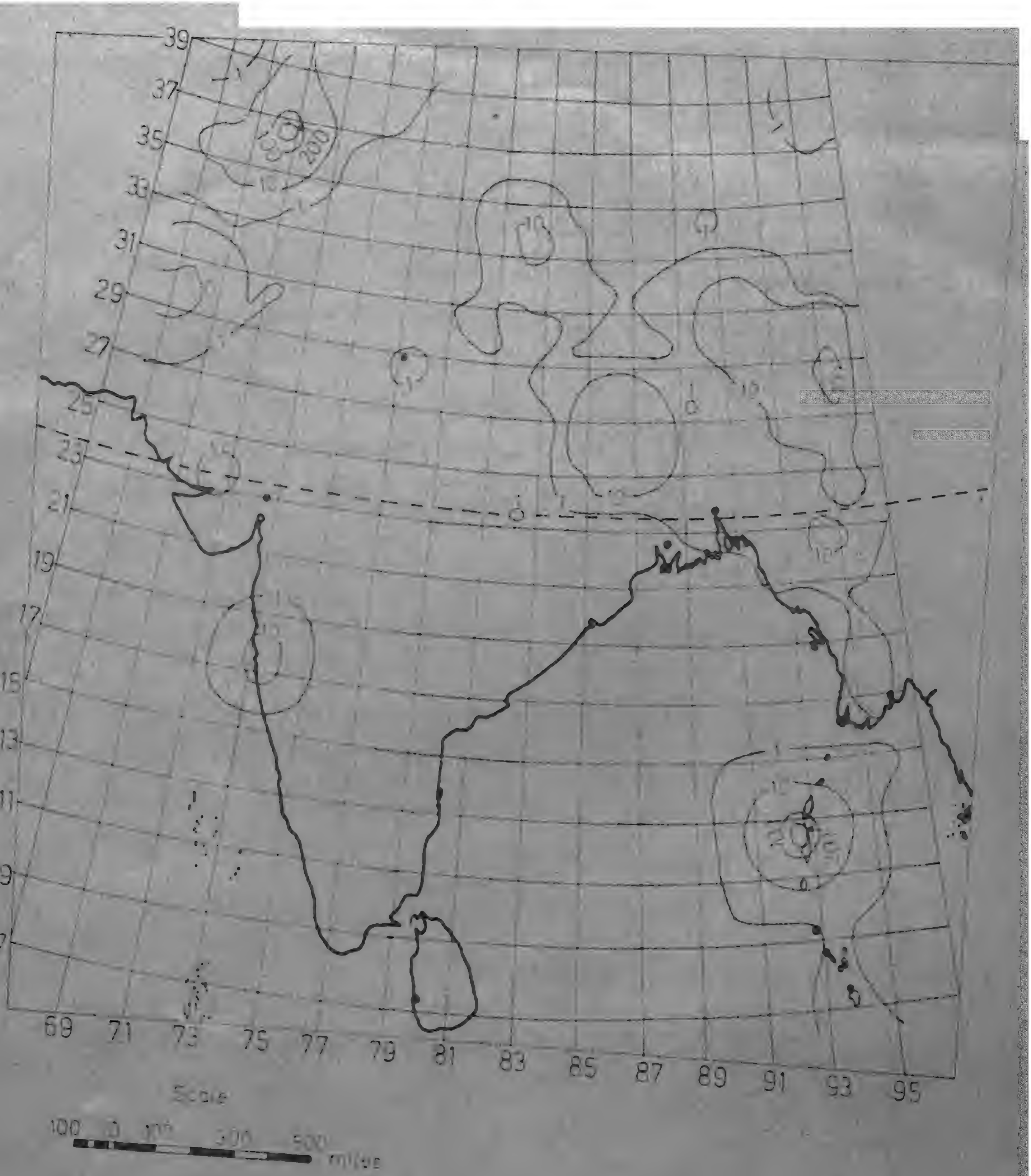
39
37
35
33
31
29
27
25
23
21
19
17
15
13
11
9
7
69
71
73
75
77
79
81
83
85
87
89
91
93
95
200
10
1
Scale
100 0 100 300 500
miles

FIG. 2·5 SIESMICITY OF INDIAN PENINSULA: ENERGY CONTOURS IN 10^{15} ergs km^{-2} y_r^{-1}

$$\log E = 1.5 M + 11.4 \tag{2.4}$$

where M is the magnitude of an earthquake. The energy released by earthquake at 1° by 1° grid point is obtained. Smoothing of the result is done prior contouring over a 5° by 5° window and using a curve which gives a weight 0.5 at the central square and weight in other square in proportion to the inverse square of their distance from the centre. The contour map shows that maximum energy is released in Hindukush and Andaman-Nicobar region. Entire Himalayan, Assam, Delhi, Kutch and Koyna region also release considerable amount of energy.

2.6 Interarrival Times

The purpose of this section is to investigate properties of interarrival times of earthquakes. In the latter part of the section stochastic models based on origin time are developed to describe earthquake occurrences. The parameters of the models are estimated and goodness of fit criteria is discussed in each case.

Sample statistics of interarrival times are given in section 2.2. Fig. (2.6) shows average of successive group of 20 interarrival times of earthquake. It is evident from the Fig. (2.6) that a quadratic trend exist. Test for homogenity of variance(68) for the entire period with 69 groups yields

over all average = 14.603 day

estimated variance =348.857 $(\text{day})^2$

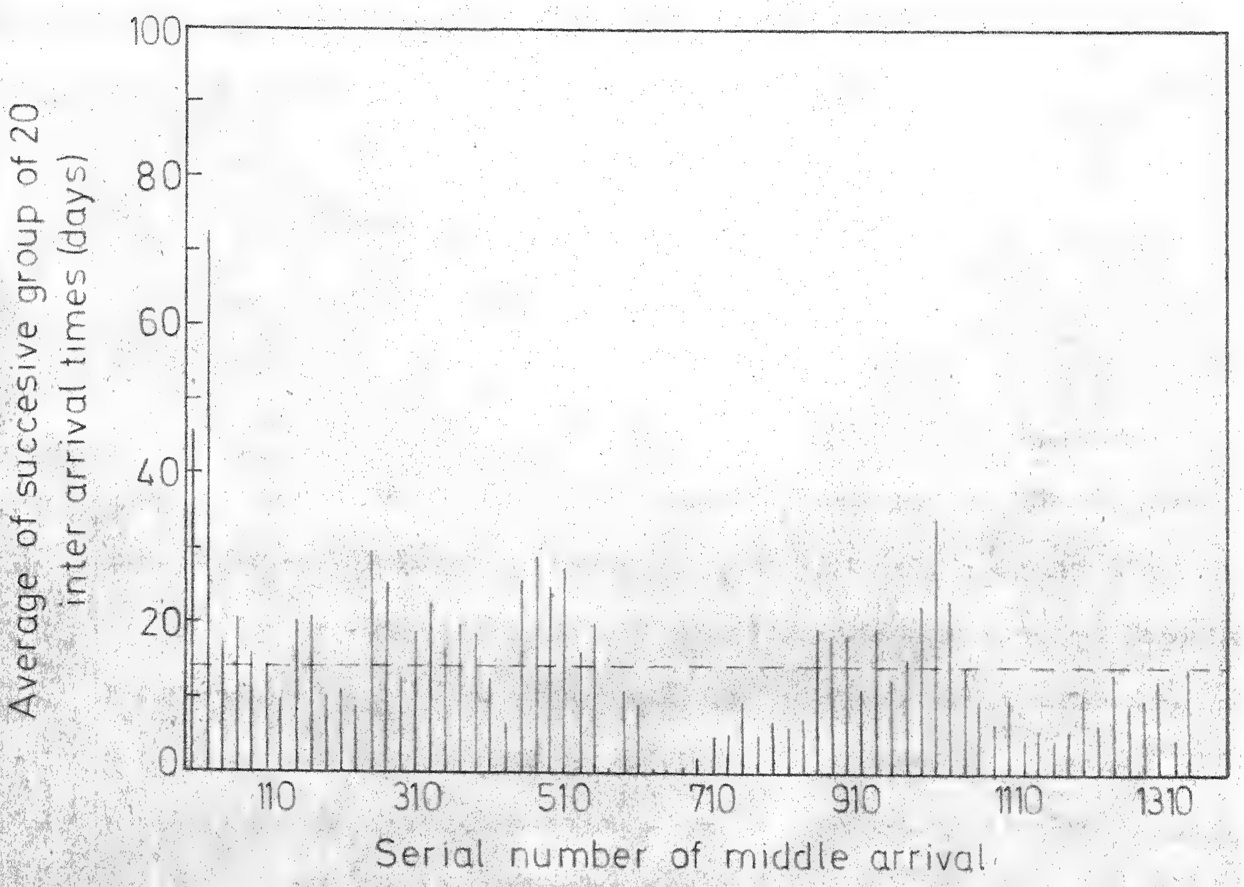

FIG. 2·6 ARRIVAL OF EARTHQUAKES

and corrected chi-square test statistics, T = 1452.3. The test statistics is greater than 95% point of chi-square distribution with 68 degrees of freedom. This indicates that there is less than 0.05 chance that these variance estimates are samples from populations with the same variance. This test implies either intensity of the earthquake arrival process is different for different time intervals or there exist gaps in the data.

Because of the simplicity of Poisson Process and its success in describing many natural phenomena, identification of a point process data is first tested for Poisson process. A Poisson process is a stationary point process with independent increment. The interarrival time of Poisson process is exponentially distributed. A rough indication of departure of the earthquake data from the Poisson process is indicated in Tables (2.1 and 2.2). The coefficient of variation of earthquake data is greater than one and the existance of significantly nonzero positive serial correlation coefficient of lag one are the most striking features of the results presented in those tables. However, estimated mean intensity of earthquake process with magnitude above five is $1/\mu = 14.603$ day/earthquake. The goodness of fit criteria is tested by chi-square test at significance level, $\alpha = 0.05$. For earthquake sample of 1374, the number of classes is obtained as 67. The intervals are chosen so that the theoretical frequency in each interval is equal. The test statistics is, $T = 873.47 > 84.821 = \chi^2_{0.05}(65)$. Hence the null hypothesis of exponentially distributed interarrival time is rejected at significance level, $\alpha = 0.05$. The Kolmogorov-Smirnov Test also rejects the null hypothesis because the statistics for two sided test is $D = 0.1515 > D_{1374,.05} = .0367$.

A two-state Semi-Markov process$^{(69-70)}$ with two types of interval is considered next to fit interarrival data. The probability density of the interarrival time is hyperexponentially distributed for this process and is given by

$$f_T(t) = \sum_{i=1}^{2} p_i \mu_i \exp(-\mu_i t) \tag{2.5}$$

where

$$\sum p_i = 1 \tag{2.6}$$

Eq. (2.5) states that the earthquake process is composed of two types of shock, namely, mainshock and aftershock but a priori discrimination from the catalogue is not possible. Both main shock and after shock posses exponential distribution with parameter μ_1 and μ_2 respectively. The aftershocks are likely to occur within a short interval in comparison to mainshocks. This is ensured by the condition

$$\mu_2 > \mu_1 \tag{2.7}$$

The parameters of the distribution Eq. (2.5) are estimated by the method of maximum-likelihood. The details of the method of estimation are given in Appendix A2.6.1. The estimation and test for goodness of fit are carried out for earthquakes with magnitude above various levels and are reported in Table 2.6. The hypothesis that the interarrival time is hyperexponentially distributed is rejected for earthquake with magnitude above 5.0, 5.5 and 6.0. A peculiarity for earthquakes with magnitude above 5.5 is that it contains less mainshocks than the mainshocks in earthquakes with magnitude above 5. The mean value of mainshock distribution reduces with increase in magnitude. The mean value of aftershock distribution reduces with increase in magnitude excluding the earthquakes with magnitude above six. The results (Table 2.6) indicate that the catalogue of earthquake contain very few aftershocks (less than 20%).

Lastly in view of the analysis of epicentral pattern result, the Indian peninsula is arbitrarily divided in 16 equal areas and the boundaries of these areas are given in Table 2.7. A test for Markov Chain proposed by Kullback et al(71) is made for the transition of earthquakes in the areas defined by Table 2.7. The results of the test are

	Statistics	Degree of freedom
Two way independence	503.1974	225
Markovity	881.4358	3600
Two way/one way independence	1384.633	3825

These statistics are to be compared with chi-square distribution with given degree of freedom. The two way independence test implying $P[E_j|E_i] = P[E_j]$, where E_j is the state of the Markov chain, is rejected at significance level, $\alpha = 0.05$. However, both Markovity

Table 2.6

Hyperexponential Distribution of Interarrival time

Magnitude >	Nos. of Samples N	$\hat{p}_1$	$\hat{\mu}_1 \times 10^2$	$\hat{\mu}_2$	Chi-square Test				Kolomogorov-Smirnov Test		
					Statistics	d.f. M	$\chi^2_{M,0.05}$	H_o	Statistics $\times 10^2$	$D_{N,0.05} \times 10^2$	H_o
5.0	1374	0.8238	5.670	2.668	109.95	63	82.529	Rejected	5.880	3.669	Rejected
5.5	609	0.8182	2.490	1.860	125.5	44	60.481	Rejected	7.707	5.511	Rejected
6.0	473	0.8307	1.963	1.964	80.58	40	55.758	Rejected	10.314	6.250	Rejected
6.5	86	0.9054	0.4215	0.575	14.28	18	28.869	Accepted	6.165	14.665	Accepted
7.0	34	0.9991	0.1885	0.497	–	–	–	–	21.89	23.32	Accepted

# of class = M + 4

Table 2.7

State of Markov Chain, its Stationary Probabilities and Parameters of Holding Time Distribution

State	Latitude	Longitude	$\Pi_i \times 10^3$	$\lambda_i \times 10^2$
1	(6,00,13.83]	(66,74]	1.39	6.209
2	(6.00,13.83]	(74,82]	0.71	3.798
3	(6,00,13.83]	(82,90]	0.76	1.619
4	(6,00,13.83]	(90,98]	87.23	5.706
5	(13.83, 21.94]	(66,74]	13.02	20.891
6	(13.83, 21.94]	(74.82]	2.87	6.093
7	(13.83, 21.94]	(82,90]	3.03	3.021
8	(13.83, 21.94]	(90,98]	27.68	4.372
9	(21.94, 30.55]	(66,74]	63.32	8.962
10	(21.94, 30.55]	(74,82]	32.62	6.871
11	(21.94, 30.55]	(82,90]	33.67	5.473
12	(21.94, 30.55]	(90,98]	258.05	8.377
13	(30.55, 40.00]	(66,74]	309.73	7.117
14	(30.55, 40.00]	(74,82]	84.57	5.057
15	(30.55, 40.00]	(82.90]	30.63	7.467
16	(30.55, 40.00]	(90,98]	50.72	6.082

and two way/one way independence are accepted. The two way/one way independence test says whether rr × r tables are homogeneous. The acceptance of Markovity implies that transition between these regions can be considered as Markov chain of order one i.e. $P[E_k \mid E_j E_i] = P[E_k \mid E_j]$. In view of this result a Semi-Markov process is defined in which the states are the areas given in Table 2.7 and holding time in the states are exponentially distributed. Formally, let p_{ij} represent the probability of the next transition to state j given that it just made a transition to state i and the time between these transitions has an exponential distribution which depends only on the state it just entered and is given by $H_i(t)$. During a time interval t, let $N(t)$ represents the total number of transition, $N_j(t)$ represents the number of transition to state j and $N_{ij}(t)$ represents the next transition to state j given that it has just entered state i, i.e.

$$N(t) = \sum_{j=1}^{m} N_j(t) = \sum_{i=1}^{m} \sum_{j=1}^{m} N_{ij}(t) \qquad (2.8)$$

where m is the number of states of the embeded Markov-chain. Pyke(70) has shown that for a fixed time interval t and when the transition probability matrix, $[P]$, and holding time distribution function, $H_i(.)$; $i = 1,\ldots,m$ are not functionally related, the problem of maximum-likelihood estimation reduces to three separate maximum-likelihood estimation problems. These are (i) maximum-likelihood estimation of $\hat{p}_{ij}$ the transition matrix of Markov-chain;

(ii) maximum-likelihood estimation, based on non random sample size, of $H_i(.)$ for $i=1,\dots,m$ and $i \neq J$; where J is the last state in which the process has entered before t, and (iii) maximum likelihood estimation of $\hat{H}_J(.)$ of the renewal process.

The solution to the problem of maximum-likelihood estimation of the transition matrix $[\,P\,]$ of the Markov chain is given(72) by

$$\hat{p}_{ij} = N_{ij}(t)/N_i(t) \tag{2.9}$$

The transition probability matrix for the data is estimated using Eq. (2.9) and is reported in Table 2.8.

Let X_{ij} denotes the holding time of jth visit to state i. The maximum likelihood estimate of the distribution $\hat{H}_i(.)$; $i=1,\dots,m$ and $i \neq J$ is

$$\hat{\lambda}_i = N_i(t)/\sum_{j=1}^{N_i(t)} X_{ij} \tag{2.10}$$

where $\hat{\lambda}_i$ is the parameter of the distribution function, $H_i(.)$. The maximum-likelihood estimation for $\hat{H}_J(.)$ is

$$\hat{\lambda}_J = N_J(t)/\left[u + \sum_{k=1}^{N_J(t)} X_{Jk}\right] \tag{2.11}$$

where

$$u = t - \sum_{i=1}^{m} \sum_{j=1}^{N_i(t)} X_{ij} \tag{2.12}$$

The parameters of the distribution of holding time are estimated from the data and are reported in Table 2.7.

Table 2.8

Transition Probability Matrix of Markov Chain

1	2	3	4	5	6	7	8	9	10	11	12	13	14	15	16
0.000	0.000	0.000	0.000	0.000	0.000	0.000	0.000	0.000	0.000	0.000	0.000	1.000	0.000	0.000	0.000
0.000	0.000	0.000	1.000	0.000	0.000	0.000	0.000	0.000	0.000	0.000	0.000	0.000	0.000	0.000	0.000
0.000	0.000	0.000	0.000	0.000	0.000	0.000	0.000	0.000	0.000	0.000	0.000	0.000	0.000	0.000	1.000
0.000	0.000	0.000	0.240	0.008	0.000	0.000	0.033	0.050	0.050	0.033	0.174	0.281	0.066	0.041	0.024
0.000	0.000	0.000	0.000	0.333	0.000	0.000	0.000	0.000	0.056	0.056	0.111	0.388	0.000	0.000	0.056
0.000	0.000	0.000	0.000	0.000	0.250	0.000	0.250	0.000	0.000	0.000	0.500	0.000	0.000	0.000	0.000
0.000	0.000	0.000	0.000	0.000	0.000	0.000	0.000	0.000	0.000	0.250	0.250	0.500	0.000	0.000	0.000
0.000	0.000	0.000	0.079	0.026	0.000	0.000	0.105	0.079	0.026	0.033	0.211	0.184	0.131	0.053	0.053
0.000	0.000	0.000	0.046	0.012	0.012	0.000	0.034	0.368	0.012	0.034	0.080	0.345	0.034	0.000	0.023
0.000	0.000	0.000	0.089	0.000	0.000	0.022	0.022	0.044	0.311	0.067	0.178	0.200	0.067	0.000	0.000
0.000	0.000	0.000	0.043	0.022	0.000	0.000	0.000	0.043	0.065	0.109	0.261	0.326	0.087	0.022	0.022
0.003	0.000	0.000	0.063	0.011	0.003	0.006	0.023	0.042	0.011	0.020	0.450	0.218	0.074	0.017	0.059
0.002	0.000	0.000	0.096	0.007	0.002	0.000	0.033	0.038	0.028	0.045	0.186	0.408	0.080	0.026	0.049
0.000	0.000	0.009	0.060	0.009	0.000	0.009	0.017	0.077	0.009	0.000	0.224	0.319	0.198	0.026	0.043
0.000	0.000	0.000	0.071	0.000	0.000	0.000	0.000	0.000	0.024	0.024	0.214	0.238	0.119	0.310	0.000
0.000	0.014	0.000	0.057	0.000	0.000	0.000	0.014	0.029	0.014	0.000	0.286	0.314	0.072	0.014	0.186

The stationary distribution[69] associated with $[P]$ of the Markov-Chain is determined by

$$<\Pi> = <\Pi> [P] \tag{2.13}$$

where $<\Pi>$ is a row vector of Π_i; $i=1,\ldots,m$ and is reported in Table 2.7.

The probability density function of the interarrival time is then simply[69]

$$f_T(t) = \sum_{i=1}^{\ell} \Pi_i h_i(t); \quad t \geq 0 \tag{2.14}$$

where $h_i(\cdot)$ is the probability density function corresponding to $H_i(\cdot)$.

The goodness of fit criteria is tested first by chi-square test at significance level, $\alpha = 0.05$, with 1374 samples. The number of class is 67 and the test statistics is $T=80.092 > 48.602 = \chi^2_{0.05}(34)$. Hence the null hypothesis that interarrival of earthquakes is distributed as given by Eq. (2.14) is rejected. The Kolmogorov-Smirnov test yields statistics for both-sided test, $D=0.01468 > 0.03669 = D_{1374,.05}$. Hence the null hypothesis is rejected.

Among the models tried to fit the interarrival time data the best fit is obtained by Eq. (2.14). However all these models donot satisfy any of the goodness of fit test for earthquakes above magnitude five. The semi-Markov model can be used for seismic risk analysis if sufficient data in a region are available.

2.7 Summary of the Results

The results of the statistical analysis can be summerized as:

(i) the spatial pattern is not stationary ,

(ii) the earthquake data is space time correlated,

(iii) the intensity of arrival process might be different in different periods,

(iv) a long cycle trend might exist in the data and

(v) among all the models tested the Semi-Markov model provides the best fit. However, these conclusions are arrived through first order and graphical analysis only.

CHAPTER 3

MODULAR EARTHQUAKE SOURCE AND SENSITIVITY ANALYSIS

3.1 Introduction

To construct the seismic zoning maps of the Indian peninsula, on a macroscopic scale, the seismic risk at a location is expressed in this thesis in two ways:

1. Generalised intensity for a specified return period.
2. Generalised intensity corresponding to a specified exceedance probability and return period.

The peninsula is divided in $2^\circ \times 2^\circ$ grid points and the generalised intensity is determined at each point. The zoning maps are prepared by drawing the contours of equal intensity. The requirements for evaluation of generalised seismic intensity at a location are:

1. Identification of the sources of earthquakes which may be idealised into point, area or volume sources.
2. Construction of stochastic model of the earthquake activity in the sources incorporating the temporal, spatial and magnitude characteristics based on seismic data.
3. Assumptions regarding the attenuation laws.

The identification of earthquake sources near a location can be done on the basis of geotectonic information and/or epicentral data of past earthquakes. Due to tectonic nature of earthquakes, epicentral data, if available over a long period of time, should exhibit a strong correlation with the geotectonic features. To construct the seismic zoning map of the peninsula on this basis, earthquake sources can be identified at each grid point and the seismic risk can be evaluated. Such an approach explicitly accounts for the non-homogeneous nature of the geotectonic features in a large peninsula like India and is adopted in Chapter 5.

While explicit incorporation of nonhomogeneous nature of geotectonic feature is desireable in calculating the seismic risk for preparing the zoning maps, there are two aspects connected with it which should be considered:

1. In many locations, particularly in alluvial areas, it is difficult to identify distinct earthquake sources and estimate parameters associated with the stochastic model at each source.

2. Use of zoning maps for design of engineering systems may require extrapolation of specified intensities for different return periods (service life), exceedance probability, cutoff magnitudes and effect of scatter on attenuation laws. For maps based on non-homogeneous tectonic features such extrapolations will be different for each grid point and, therefore, too cumbersome to be incorporated in the codes of practice for earthquake resistant design.

In view of the above comments the viability of assuming the Indian peninsula to be homogeneous in tectonic features is examined. A modular volume source centered at each grid point is proposed as a

I.I.T. KANPUR
CENTRAL LIBRARY
Acc. No. A 54055

standard earthquake source. The earthquake occurrance at the source is assumed to be spatially homogeneous and temporally stationary. Uniform, truncated lognormal and mixed truncated lognormal distributions are assumed for the focal depth. The mean arrival rate is, however, calculated at each grid point based on regional seismic data which, as pointed earlier, is expected to show strong correlation with tectonic features. Contour maps based on homogeneous and non-homogeneous tectonic feature assumptions are compared in Chapter 5.

The geometry of the modular volume source, distribution functions of magnitude, focal depth, temporal model of earthquake occurrence and assumed attenuation laws are described in this chapter. The influence of each of these parameters is synthesised to determine the seismic risk at the grid point for the modular source. Effects of geometric parameters of the source and magnitude cutoff are studied to establish the parameters for the modular source and are used in the next chapter for preparing seismic zoning map.

3.2 Modular Earthquake Source-Geometry

The modular earthquake source, to determine the peak intensity at a site, is a volume element formed by a sector of revolution about the site with an arc, length, b, and maximum focal depth, H_o, in which future earthquakes can potentially occur as shown in Fig. (3.1). The volume element is assumed to be homogeneous in tectonic features and presence of faults, if any, within it is disregarded. Location of an earthquake within the earthquake source is temporally stationary and

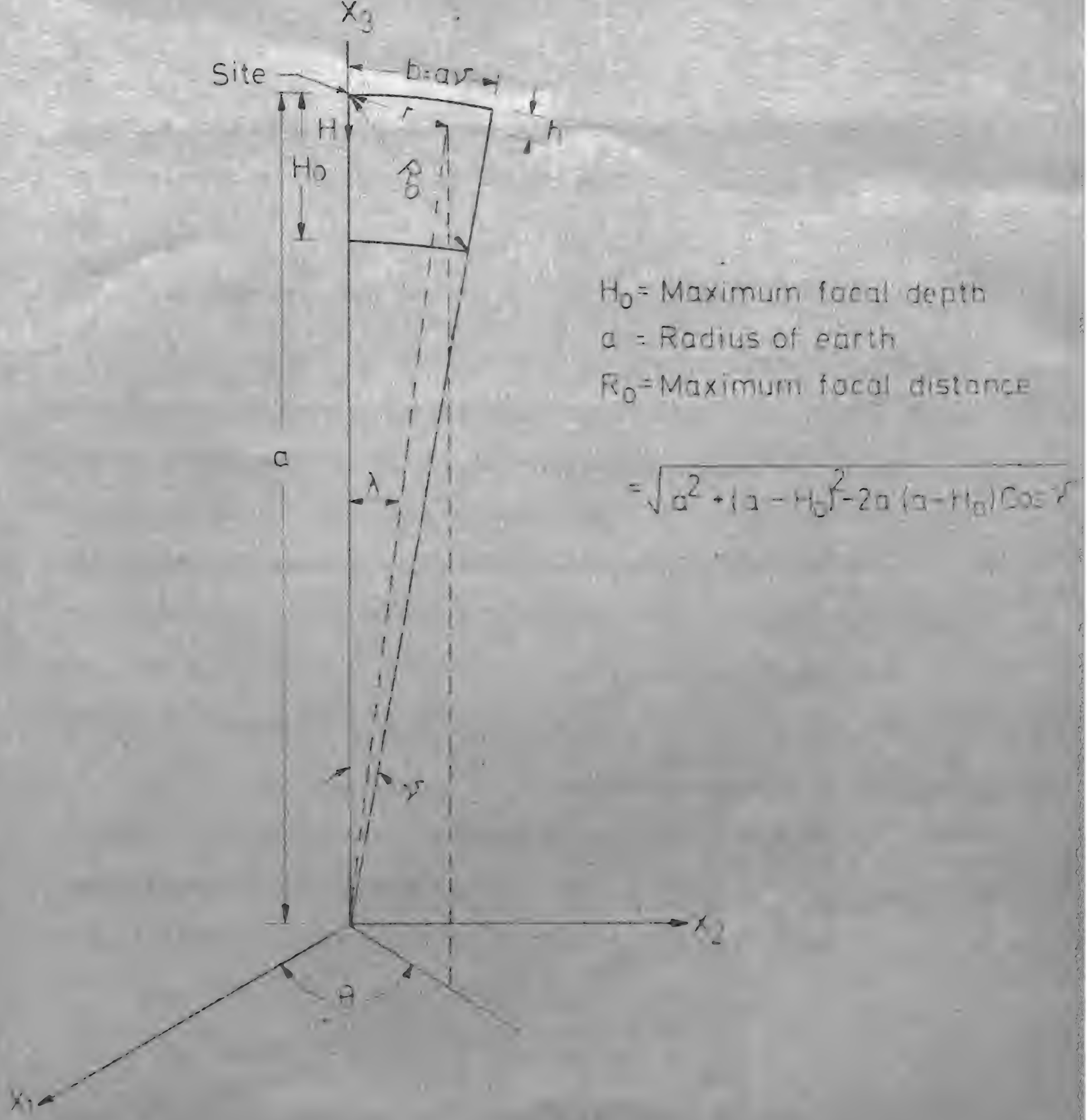
X_3
Site
$b = a\nu$
r
h
H
H_0
$\hat{\delta}$
a
λ
ν
X_2
θ
X_1
H_0 = Maximum focal depth
a = Radius of earth
R_0 = Maximum focal distance
$= \sqrt{a^2 + (a - H_0)^2 - 2a\,(a - H_0)\,\mathrm{Cos}\,\nu}$

FIG 3·1 EARTHQUAKE SOURCE AT SITE: VOLUME OF REVOLUTION OF SECTOR ABOUT AXIS X_3

spatially homogeneous. Occurrence of earthquake is equally likely in the azimuth direction, Λ , and in the latitude direction, Θ , Fig. (3.1).

3.3 Magnitude-Frequency Law

Hypothesis of magnitude stability, i.e. in any given realization of the earthquake process the magnitude distribution is (a) stationary and (b) independent of rate of occurrence of earthquakes(73-78), is accepted in this study. This assumption implies that the magnitude of earthquakes is a regional variable and the magnitude distribution is represented by a 'space-series' independent of time. Consequently the magnitude distribution is assumed to posses a continuous probability density function denoted by $f_M(\cdot)$.

In early forties Japanese and American scientist independently discovered that the number of earthquakes in a region decrease exponentially with their magnitudes. This relationship is known as "magnitude-frequency equation" due to Ishimoto and Iida(79) and Gutenberg and Richter(5) and expressed as

$$\log N_m = a - bm \tag{3.1}$$

where N_m is the number of earthquakes greater than a specified threshold magnitude m and a and b are empirical parameters. Normalization of Eq. (3.1) and subsequent differentiation with respect to m yields the probability density function of magnitude, M, as

$$f_M(m) = \beta \exp [-\beta m] \quad ; m \geq 0 \tag{3.2}$$

where $\beta = b \ \ell n\ 10$

where

$$1/K = 1 - \exp\ [\ \beta(m_o - m_1)\ ] \tag{3.5}$$

3.4 Focal Depth

In the investigation of seismic risk analysis known to the author, focal depth of earthquakes has been treated as a deterministic parameter. It is well known that focal depth has a measure of uncertainty associated with it(7). The focal depth, H, is assumed to be temporally stationary and posses a continuous probability density function $f_H(.)$ with a maximum focal depth, H_o.

If past seismic data of focal depth is not available, it is logical to assume that earthquake is equally likely to occur upto a depth, H_o. The probability density of focal depth, H, corresponding to this assumption is 'uniform' and is given by

$$f_H(h) = \begin{cases} 1/H_o & ;\ h \in (0, H_o\,] \\ 0 & ;\ \text{otherwise} \end{cases} \tag{3.6}$$

An analysis of available focal depth data indicates that the shallow focus earthquakes predominate over intermediate and deep focus earthquakes in Indian peninsula. The histogram in Fig. (2.3) shows a distinctive minor peak at 230 kms. To incorporate the above features, a truncated lognormal and mixed truncated lognormal distribution are proposed. The probability density function of these distributions are

1. Lognormal distribution

$$f_H(h) = \exp\left[-0.5\,(\ell n\, h-\theta_1)^2/\theta_2\right] / \left[\sqrt{2\pi\theta_2}\, h\, \Phi\{(\ell n\, H_o-\theta_1)/\sqrt{\theta_2}\}\right] \quad ; h \in (0, H_o] \qquad (3.7)$$

2. Mixed lognormal distribution

$$f_H(h) = \sum_{i=1}^{2} p_i \exp\left[-0.5(\ell n\, h-\theta_{1i})^2/\theta_{2i}\right] / \left[\sqrt{2\pi\theta_2}\, h\, \Phi\{(\ell n\, H_o-\theta_{1i})/\sqrt{\theta_{2i}}\}\right] \; ; h \in (0, H_o] \qquad (3.8)$$

where

$$\sum_{i=1}^{2} p_i = 1 \qquad (3.9)$$

and $\Phi(.)$ is the probability distribution function of $N(0,1)$.
θ_1 and $\{\theta_{ij}\ ; i,j = 1,2\}$ are the parameters of the distributions.

3.5 Temporal Model of Earthquake Source

An earthquake process is essentially a clustered marked point process with memory owing to the well accepted hypothesis of elastic rebound theory, presence of aftershocks and often presence of swarms of earthquakes. However, quite extensive amount of past seismic data is required to model earthquake process as a clustered marked point process with memory. In this analysis, the earthquake process is assumed to be Poisson process with an intensity, μ , for magnitude greater than a threshold magnitude, m_o. This assumption is physically inconsistent but is considered adequate for engineering purpose(82,83). Statistical test on past seismic data after removal of swarms and aftershocks from the catalogue do not reject the null hypothesis that the earthquake process is Poisson decisively(84-88).

3.6 Attenuation Law

To include the effect of wave propagation within the modular earthquake source, deterministic attenuation law which estimate the peak seismic intensity (e.g. acceleration) at a site as a function of earthquake magnitude, M, and focal distance, R, from the site to the location of the hypocenter of earthquake is assumed. The generalized attenuation law proposed by Kanai(89) and Esteva and Rosenbleeth(24) is used and is given by

$$Y = C_1 \exp \left[C_2M - C_3 \ln (R + C_4)\right] \tag{3.10}$$

where Y is the required peak ground intensity, C_1, C_2, C_3 and C_4 are empirical constants. The unit of R is in kilometers and the values of (C_1, C_2, C_3, C_4) are taken as (2000.0, 0.8, 2.0, 25.0), (16.0, 1.0, 1.7, 25.0) and (7.0, 1.2, 1.6, 25.0) for peak ground acceleration (cm/sec^2), peak ground velocity (cm/sec) and peak ground displacement (cm) respectively.

3.7 General Formulation of Seismic Risk at a Site

3.7.1 Probability distribution function of generalized peak seismic intensity

In the Eq. (3.10) let

$$Z = C_1 \exp (C_2M) \tag{3.11}$$

and $$W = \exp [\, -C_3 \;\ell n(R + C_4)\,] \tag{3.12}$$

The joint probability density function of Z and W, assuming statistical independence of focal distance, R, and magnitude, M, of earthquake is given by

$$f_{ZW}(z,w) = f_Z(z)\, f_W(w) \tag{3.13}$$

where

$$f_W(w) = 1/[\, C_3 \, w^{(C_3+1)/C_3}\,]\; f_R(w^{-1/C_3} - C_4) \quad ; \; w \;\varepsilon [w_1, w_2) \tag{3.14}$$

$$f_Z(z) = 1/(zC_2)\, f_M \,\{(\ell n\, z - \ell n\, C_1)/C_2\} \tag{3.15}$$

with

$$w_1 = (R_o + C_4)^{-C_3} \tag{3.16}$$

$$w_2 = C_4^{-C_3} \tag{3.17}$$

and R_o = maximum focal distance

$$= \sqrt{a^2 + (a - H_o)^2 - 2a\,(a - H_o)\cos \nu} \tag{3.18}$$

The parameters a, H_o and ν are the radius of earth, maximum focal depth and the angle subtended at the centre of earth by an extreme point in the modular earthquake source (Fig. 3.1) respectively. The probability density function, $f_R(.)$, of focal distance, R, is derived on the assumed probability density functions of the location variables of future earthquakes in the source. The exceedance probability of generalized seismic peak intensity, Y, is obtained from Eq. (3.13) and is given by

$$S_Y(y) = P[\,Y > y\,] = \iint_{\{(z,w):\, zw > y\}} f_{ZW}(z,w)\, dz\, dw \qquad (3.19)$$

The above result yields the probability that peak seismic intensity, Y, at the site will exceed a certain value, y, given that an earthquake with a magnitude in the domain of interest occurs somewhere in the modular earthquake source.

3.7.2 T-year generalized peak seismic intensity

To consider the random number of occurrences in a given time period, it is assumed that the arrival of earthquakes is a Poisson process with intensity, μ , in the entire earthquake source. The number of earthquakes, $\{N(t),\ t \geq 0\}$, which occur in the earthquake source during a time interval, t, is given by

$$P_N(n,t) = P[\,N(t) = n\,] = (\mu t)^n/n!\ \exp(-\mu t);\ n=0,1,2,3,\ldots \qquad (3.20)$$

Among all these events, the earthquakes which produce peak generalized seismic intensity at site above a threshold value, y, is given by Eq. (3.19). Since the events, $[\,Y > y\,]$, arrive independent of each other and the earthquake process as such is a Poisson arrival process, it can be shown(90) that the number of earthquakes, $\{L(t), t \geq 0\}$, which produce peak generalized seismic intensity at a site greater than a value, y, during a time interval, t, is given by

$$P_L(\ell,t) = P[L(t) = \ell] = \{\mu t\, S_Y(y)\}^{\ell}/\ell!\ \exp[\,-\mu t\, S_Y(y)\,] \quad ;\ \ell = 0,1,2,\ldots \qquad (3.21)$$

The probability of no occurrence of the event, $[Y > y]$, during a time interval, t, is obtained by substituting $\ell = 0$ into Eq. (3.21). This gives the probability distribution function of maximum peak generalized seismic intensity in a time interval, t, and is formally written as

$$F_{Y_{max}}(y;t) = P[Y_{max} \leq y;t] = P_L(0,t) = \exp[-\mu t\, S_Y(y)] \quad (3.22)$$

The annual maximum peak generalized seismic intensity is obtained by putting $t = 1$ in the Eq. (3.22) and is given by

$$F_{Y_{max}}(y;1) = P[Y_{max} \leq y;1] = P_L(0,1) = \exp[-\mu\, S_Y(y)]$$

$$\simeq 1 - \mu S_Y(y) \qquad (\because \mu S_Y(y) \ll 1)$$

Therefore

$$P[Y_{max} > y;1] = \mu S_Y(y) \quad (3.23)$$

The average return period, T_y, of peak generalized seismic intensity exceeding y is defined as

$$T_y = 1/P[Y_{max} > y;1] = 1/[\mu S_Y(y)] \quad (3.24)$$

The T-year peak generalized seismic intensity at a site is obtained by solving Eq. (3.24) for y given a service life, T_y.

The general formulation of the problem of seismic risk analysis at a site for the modular earthquake source involves two probability density functions, namely, the probability density function, $f_M(\cdot)$, of the magnitude, M, and that of the focal depth, H, $f_H(\cdot)$. These must be established on the basis of local seismic data.

3.8 Probability Distribution of Peak Generalized Seismic Intensity for Assumed Distributions of Focal Depth, H, and Magnitude, M, of Earthquakes

3.8.1 Magnitude, M, cutoff at lower level i.e. $m \varepsilon (m_o, \infty)$

The probability of peak generalized seismic intensity, $Y = ZW$, exceeding a specified value, y, is obtained from Eq. (3.19) for magnitude, M, cutoff at lower level, m_o, and is given by

$$S_Y(y) = P[Y > y] = 1 \quad ; \; y \leq y_1 = C_1 \exp [C_2 m_o - C_3 \, \ell n(R_o + C_4)] \tag{3.25}$$

$$S_Y(y) = \int_{x_1}^{R_o} S(r) \, f_R(r) \, dr + F_R(x_1) \; ; \; y_1 \leq y \leq y_2 \tag{3.26}$$

$$S_Y(y) = \int_{o}^{R_o} S(r) \, f_R(r) \, dr \; ; \; y \geq y_2 = C_1 \exp [C_2 m_o - C_3 \ell n \; C_4] \tag{3.27}$$

where

$$S(r) = \exp [\beta \{ m_o + [\ell n \; C_1 - C_3 \; \ell n(r + C_4) - \ell n \; y] / C_2 \}] \tag{3.28}$$

$$x_1 = \exp \; [(C_2 m_o + \ell n \; C_1 - \ell n \; y) / C_3] - C_4 \tag{3.29}$$

The $f_R(.)$ and $F_R(.)$ are the probability density and probability distribution function of focal distance, R, for different assumed distribution of focal depth Eqs. (3.6-3.8). The detailed derivation of these functions are given in Appendix A3.8.1. The details of Eqs. (3.25-3.27) are given in Appendix A3.8.2.

3.8.2 Magnitude, M, cutoff at both ends i.e. $m \varepsilon (m_o, m_1]$

The probability of the event, $[Y > y]$ is obtained from Eq. (3.19) when magnitude, M, of earthquakes is being cutoff at both ends and is given by

$$S_Y(y) = P[Y > y] = 1 \quad ; \; y \leq y_1 = C_1 \exp[C_2 m_o - C_3 \ln(R_o + C_4)] \tag{3.30}$$

$$S_Y(y) = 1 - [1 - F_R(x_1)]K + K \int_{x_1}^{R_o} S(r)\, f_R(r) dr$$

$$; \; y_1 \leq y \leq \min(y_2, y_3) \tag{3.31}$$

$$S_Y(y) = (1-K)\, F_R(x_2) + K\, F_R(x_1) + \int_{x_1}^{x_2} S(r)\, f_R(r) dr$$

$$; \; y_3 \leq y \leq y_2 = C_1 \exp[C_2 m_o - C_3 \ln C_4] \tag{3.32}$$

$$S_Y(y) = 1 - K + K \int_{o}^{R_o} S(r)\, f_R(r) dr \; ; \; y_2 \leq y \leq y_3 =$$

$$C_1 \exp[C_2 m_1 - C_3 \ln(R_o + C_4)] \tag{3.33}$$

$$S_Y(y) = (1-K)\, F_R(x_2) + K \int_{o}^{x_2} S(r)\, f_R(r) dr ; \; y \geq \max(y_2, y_3) \tag{3.34}$$

where

$$x_2 = \exp[(C_2 m_1 + \ln C_1 - \ln y)/C_3] - C_4 \tag{3.35}$$

One of the Eq. (3.32) and Eq. (3.33) is to be used according to the numerical values of the relevant parameters. Details of the above are given in Appendix A3.8.2.

The integrand in Eqs. (3.25-3.27) and Eqs. (3.31-3.34) cannot be obtained analytically. Numerical integration by the method of Gaussian quadrature is used to obtain the results.

3.9 Results and Discusstion

The parameters of the probability density function of focal depth, H, for various assumptionsand that of magnitude, M, are estimated in Chapter 2. The intensity of the arrival process, μ, is estimated in this chapter by the ratio of number of past earthquakes in the modular source at a site and the time period of the seismic data. The radius of earth, a, is assumed to be 6371 kms.

The effect of variation in modular source geometry parameters, namely, arc length and maximum focal depth, on seismic risk is investigated.

The sensitivity of seismic risk due to variation in arc length, b, is investigated assuming the intensity, μ, of the earthquake arrival process at a source is directly proportional to the volume of the source. The return periods for different arc length, b, are calculated at a site (latitude 31°, longitude 95°) for various level of peak ground displacement, velocity and acceleration. The results are shown in Figs. (3.2-3.4) for uniform and lognormal focal depth distribution with maximum focal depth, $H_o = 600$ kms, and magnitude, $m \varepsilon (5,9]$. Figs. (3.2-3.4) indicate that the smaller the arc length the larger is the return period (lesser seismic risk) for all levels of generalized peak seismic intensity. However, the increase in return period due to the reduction of arc length, b, reduces as the peak generalized seismic intensity increases. From Figs.(3.2-3.4) it is also observed that the return period remains constant beyond arc length, b = 150 kms, for all practical purposes. The seismic risk is less for uniform distribution of focal depth in comparison with lognormal focal depth distribution with the assumed maximum focal depth, $H_o = 600$ kms., and a given level of peak ground intensity.

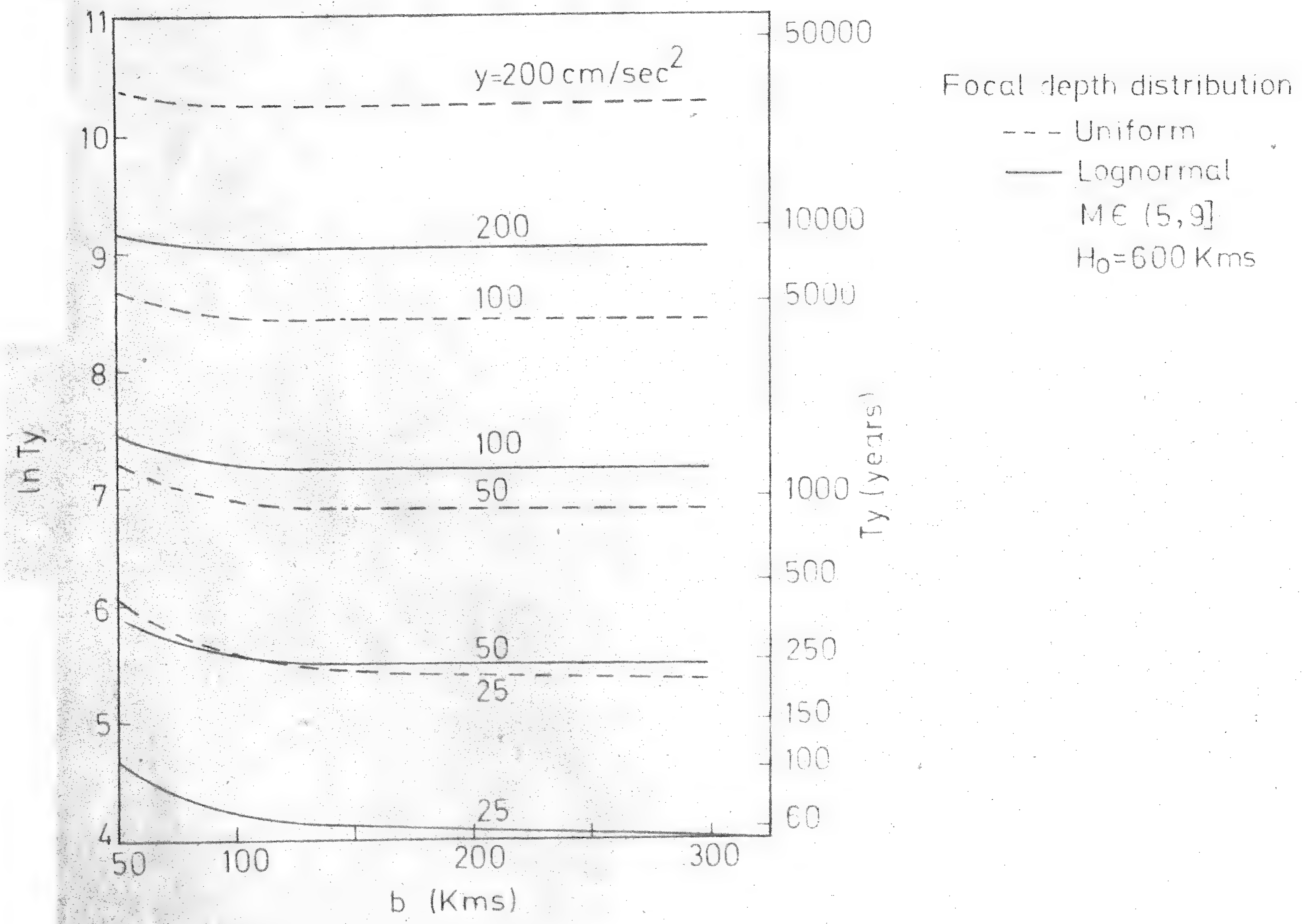

FIG.3.2 EFFECT OF ARC LENGTH, b, ON RETURN PERIOD, Ty, OF PEAK GROUND ACCELERATION, y

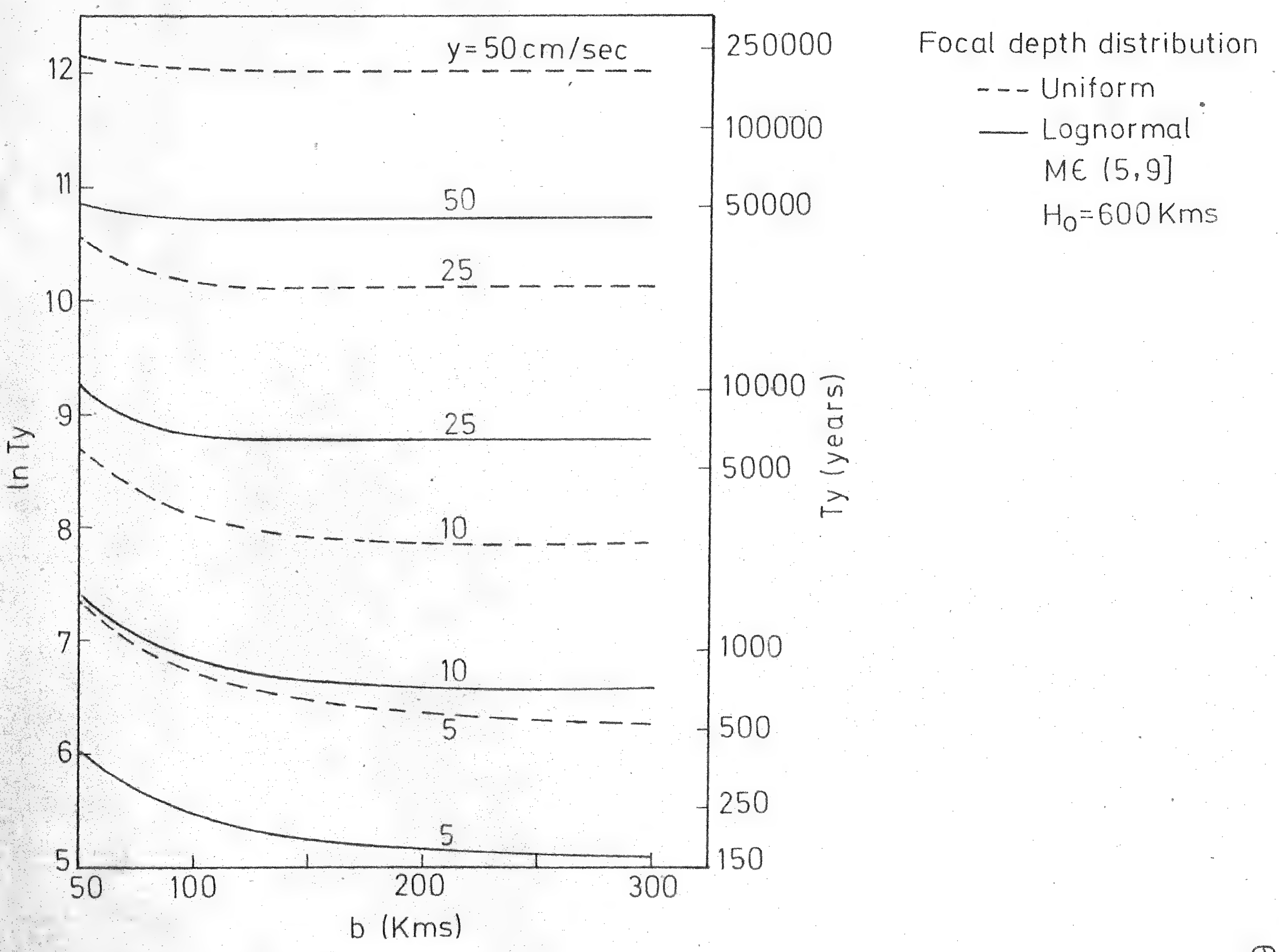

FIG. 3·3 EFFECT OF ARC LENGTH, b, ON RETURN PERIOD, Ty, OF PEAK GROUND VELOCITY, y

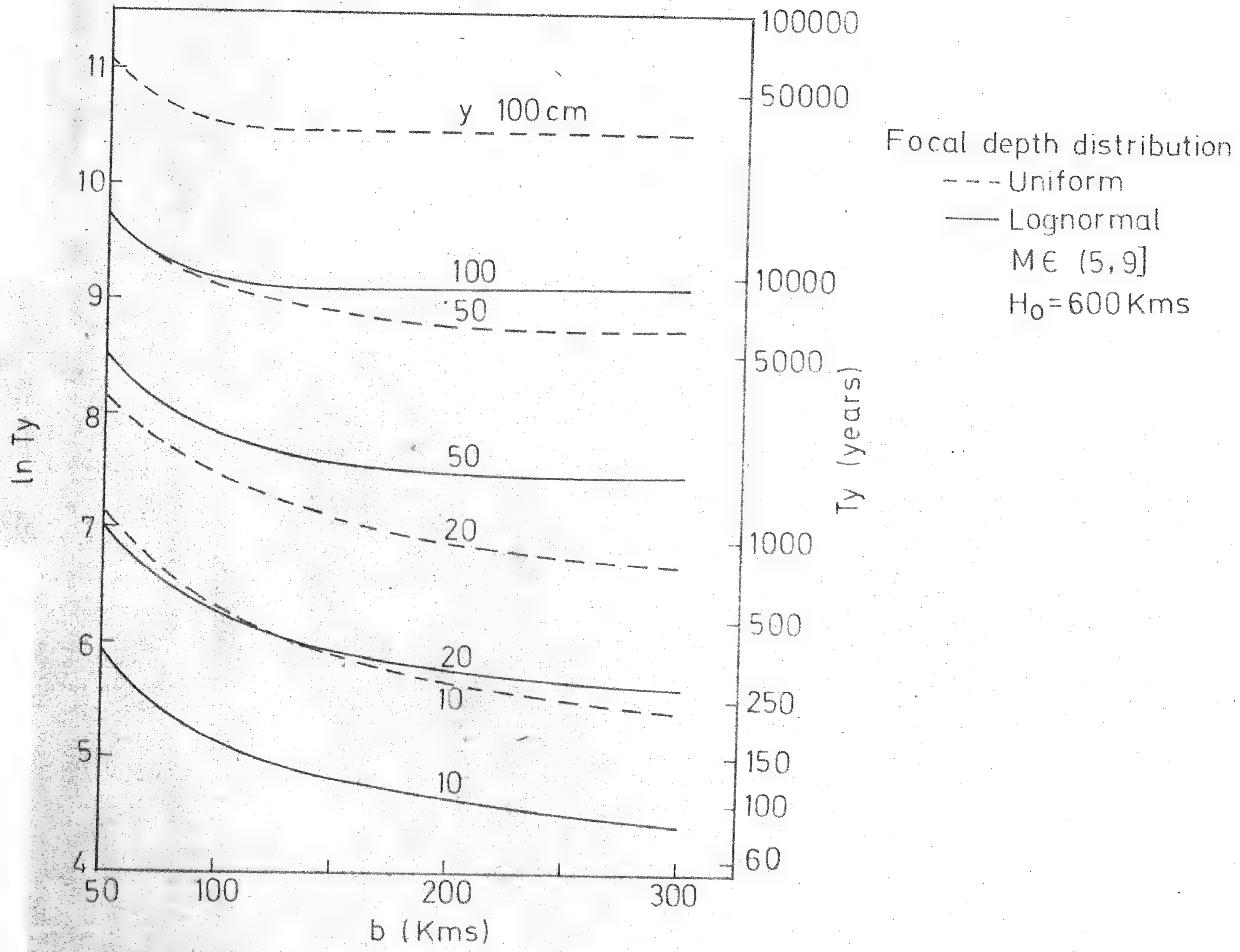

FIG.3·4 EFFECT OF ARC LENGTH, b, ON RETURN PERIOD, Ty, OF PEAK GROUND DISPLACEMNT, y

The effect of variation of maximum focal depth, H_0, on the seismic risk is investigated firstly for uniform distribution of focal depth assuming constant intensity parameter, μ, of the earthquake arrival process for various geometric configuration of sources. The results for magnitude, $m \in (5,9]$ are shown in Figs. (3.5-3.7) and that for magnitude, $m \in (5,\infty)$ are shown in Figs. (3.8-3.10). It is concluded from these figures that for a constant return period peak ground intensity increases with decrease in maximum focal depth, H_0. Seismic risk changes marginally for various peak seismic intensities (Table 3.1) when intensity, μ, of arrival process for various geometry of sources having lognormal or mixed lognormal distribution of focal depth is constant.

A difference in behaviour Table 3.1 and Figs. (3.5-3.7) is observed between the cases of uniform and lognormal distribution of focal depth when maximum focal depth, H_0, is cutoff at different level. Since maximum focal depth of past earthquake data of Indian peninsula is 383 kms. the minimum cutoff of H_0 is considered to be 400 kms. for the lognormal distribution of focal depth. The estimation of parameter involved in uniform distribution of focal depth does not require the past earthquake data and hence does not properly reflect the earthquake activity in the source. Moreover this assumption increases the number of deep focus earthquakes in comparison with lognormal distribution of focal depth and consequently lesser risk is predicted for equal maximum focal depth cutoff. The risk for various cutoff of maximum focal depth, H_0, remain almost constant in the lognormal distribution of focal depth. The insignificant variation of risk is essentially the

Table 3.1

Ratio of return periods for lognormal (ℓ) and mixed lognormal ($m\ell$) distribution of focal depth, H.

$b = 150$ kms.

$m \epsilon (5,9]$

Ratio of return period is defined as the ratio of return period of any assumed focal depth distribution and lognormal focal depth distribution with maximum focal depth, $H_o = 600$ kms.

Distribution of focal depth maximum focal depth, H_o	$m\ell$ 600 kms.	ℓ 500 kms.	ℓ 400 kms.
peak ground acceleration in cm/sec^2	Ratio of return periods		
25	0.983	1.007	1.065
50	0.973	1.002	1.078
100	0.970	0.987	1.084
200	0.962	0.994	1.097
500	0.999	0.984	1.115
peak ground velocity in cm/sec			
5	0.996	1.005	1.053
10	0.999	1.005	1.059
25	0.975	1.004	1.076
50	0.958	0.998	1.095
90	0.956	0.998	1.112
peak ground displacement in cm			
10	1.005	1.005	1.038
20	1.005	1.005	1.041
30	1.006	1.006	1.044
50	1.009	1.006	1.051
100	0.982	1.006	1.069

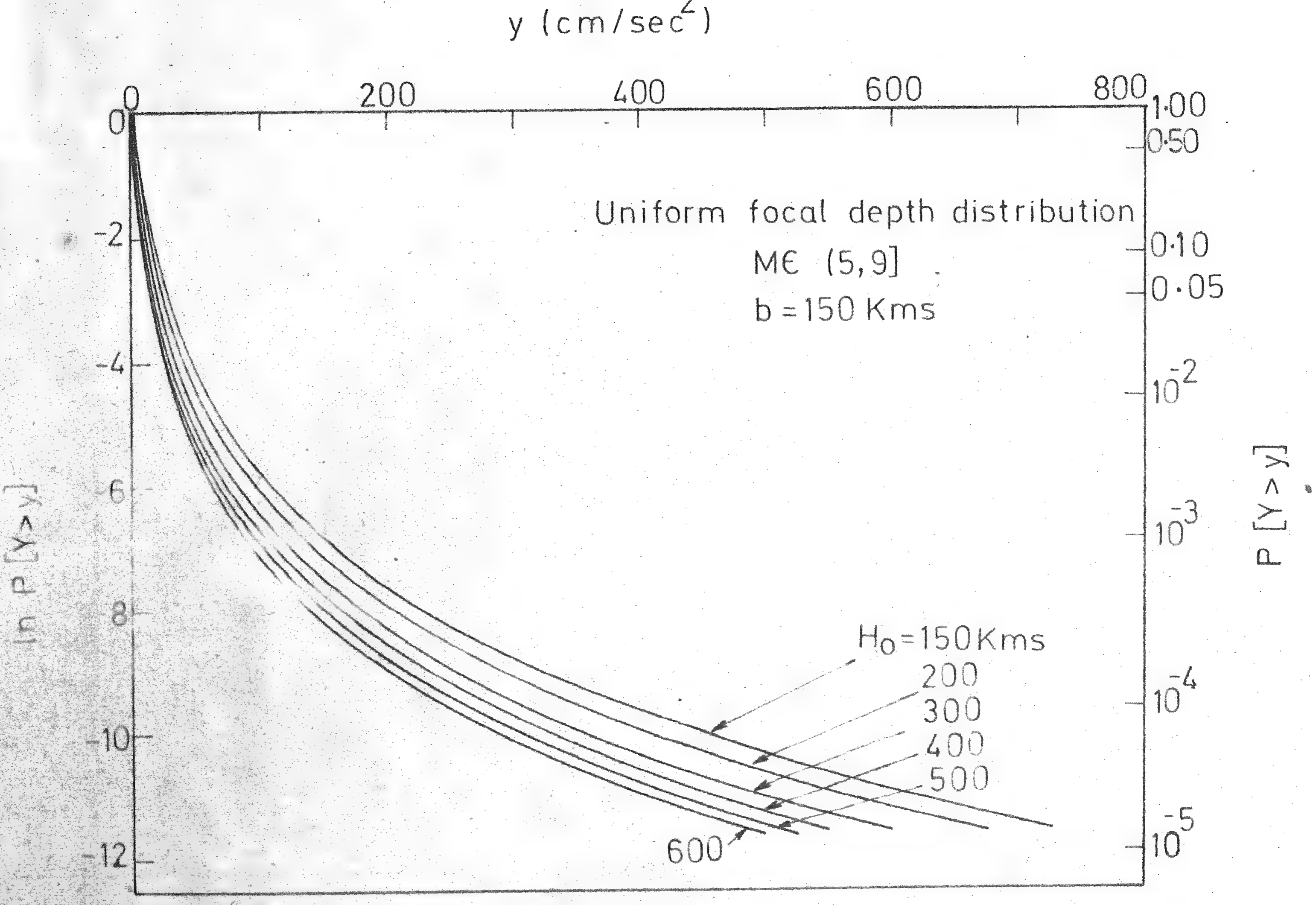

FIG.3·5 EFFECT OF MAXIMUM FOCAL DEPTH, H_o, ON THE PROBABILITY OF THE PEAK GROUND ACCELERATION, Y, EXCEEDING y

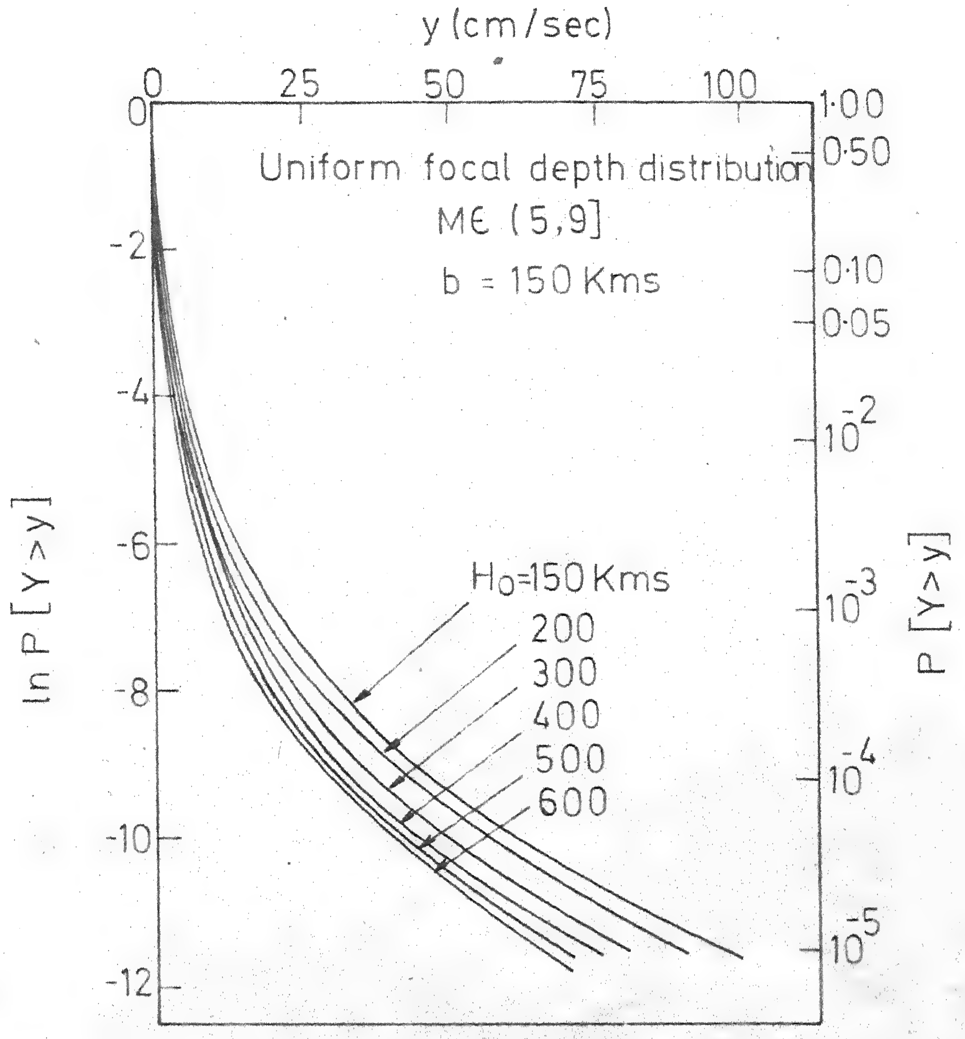

FIG. 3·6 EFFECT OF MAXIMUM FOCAL DEPTH, H_0 ON THE PROBABILITY OF THE PEAK GROUND VELOCITY, Y, EXCEEDING y

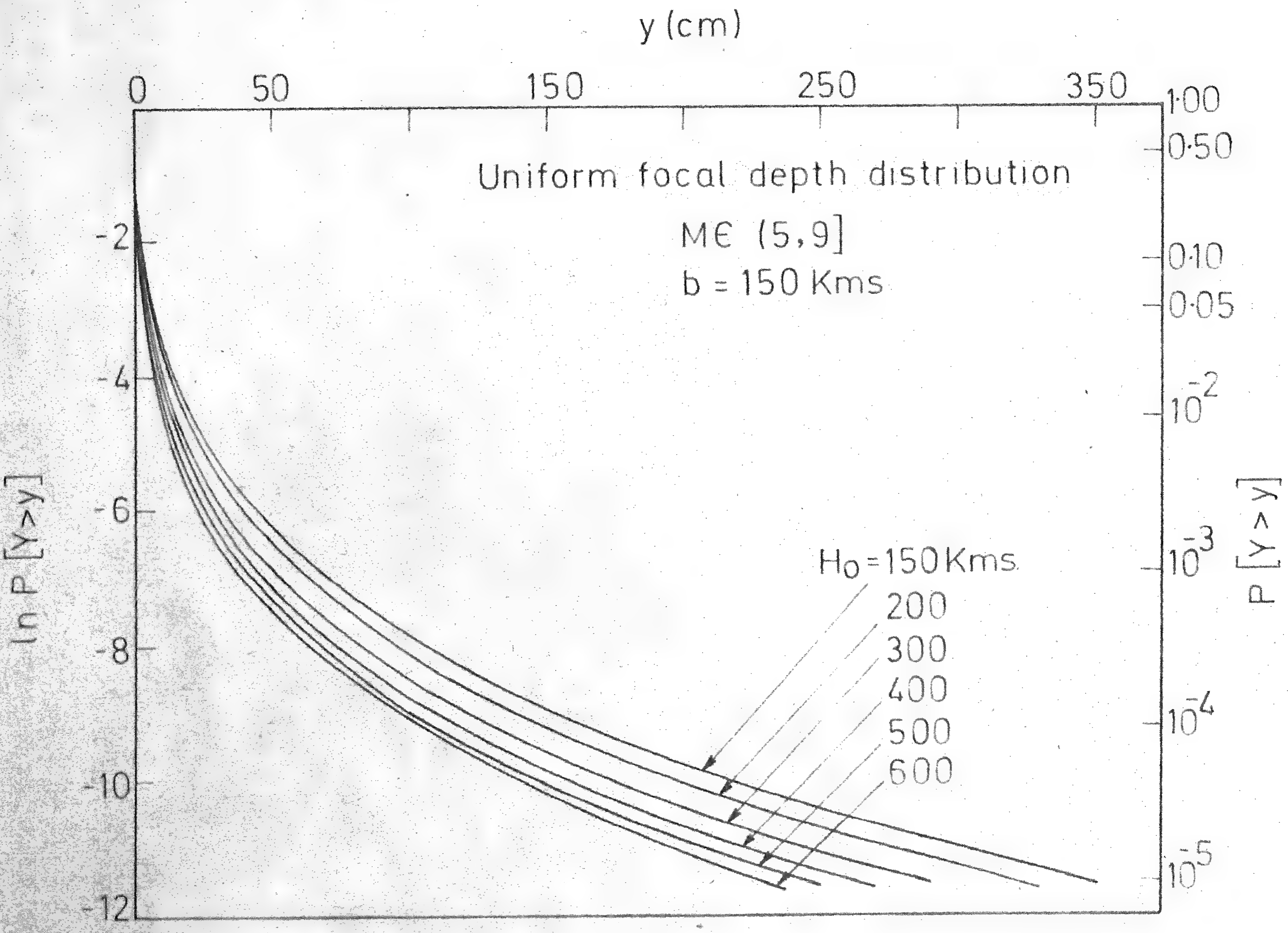

FIG 3·7 EFFECT OF MAXIMUM FOCAL DEPTH, H_0, ON THE PROBABILITY OF THE PEAK GROUND DISPLACEMENT, Y, EXCEEDING y

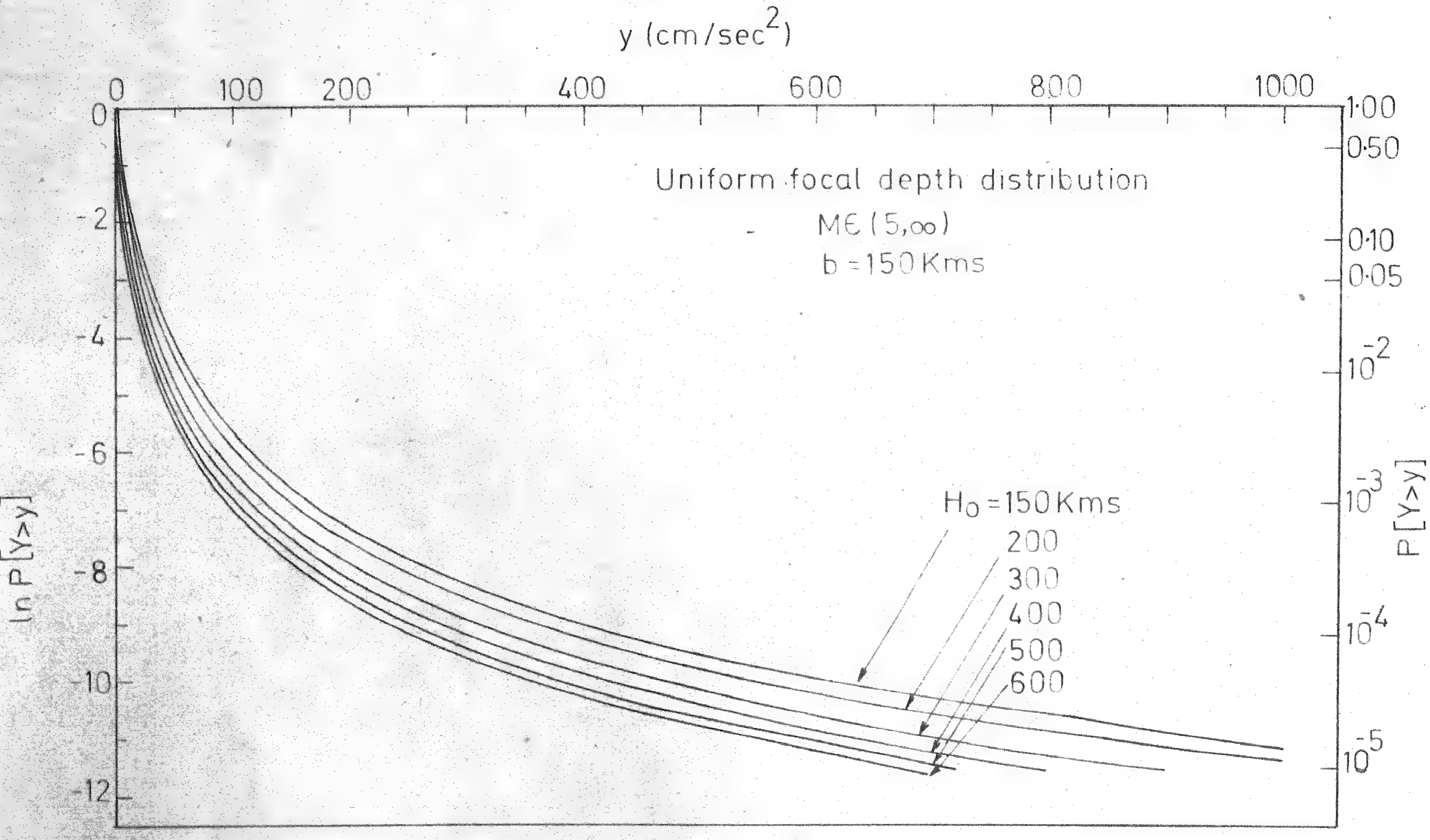

FIG. 3·8 EFFECT OF MAXIMUM FOCAL DEPTH, H_0, ON THE PROBABILITY OF THE PEAK GROUND ACCELERATION, Y, EXCEEDING y

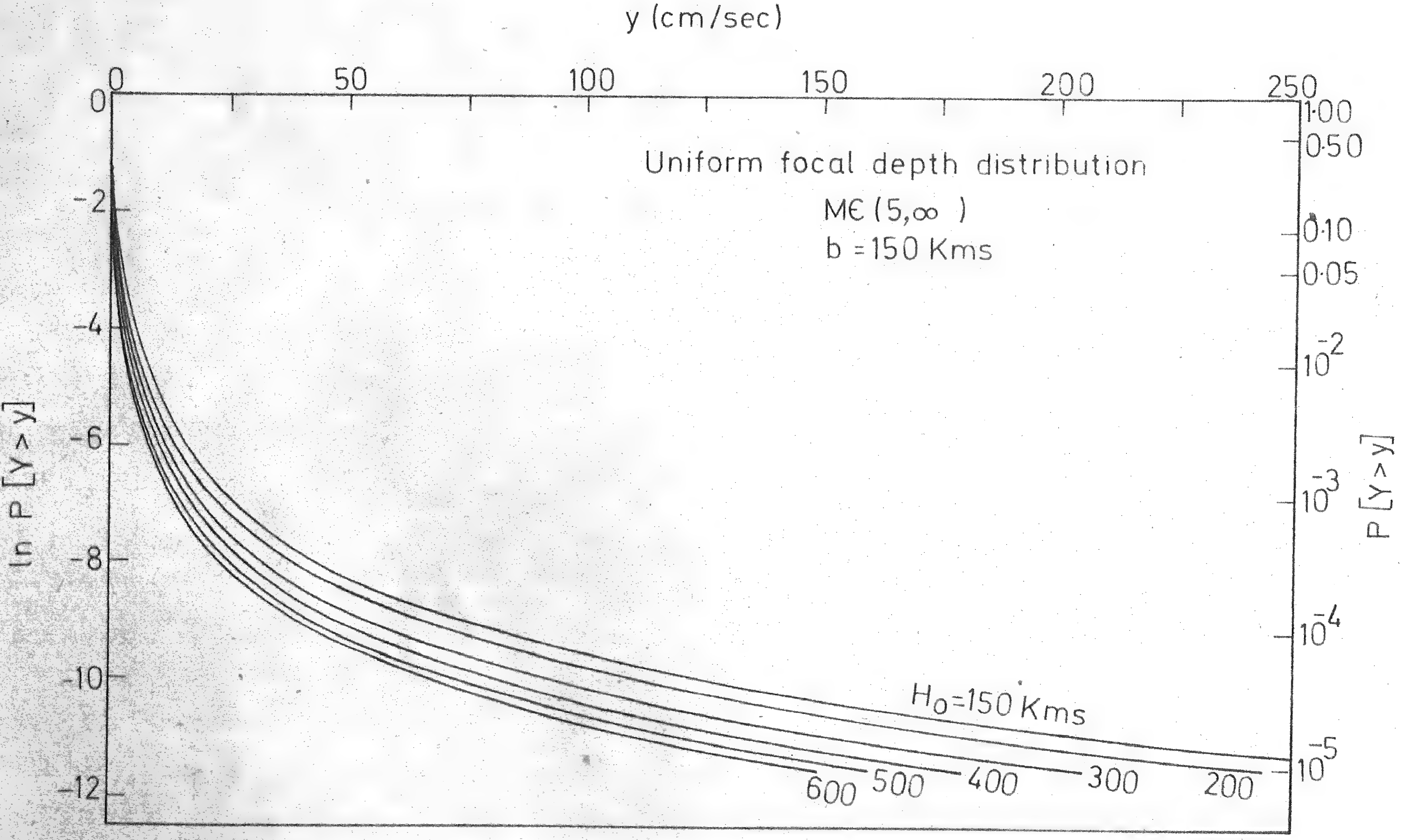

FIG. 3·9 EFFECT OF MAXIMUM FOCAL DEPTH, H_0, ON THE PROBABILITY OF THE PEAK GROUND VELOCITY, Y, EXCEEDING y

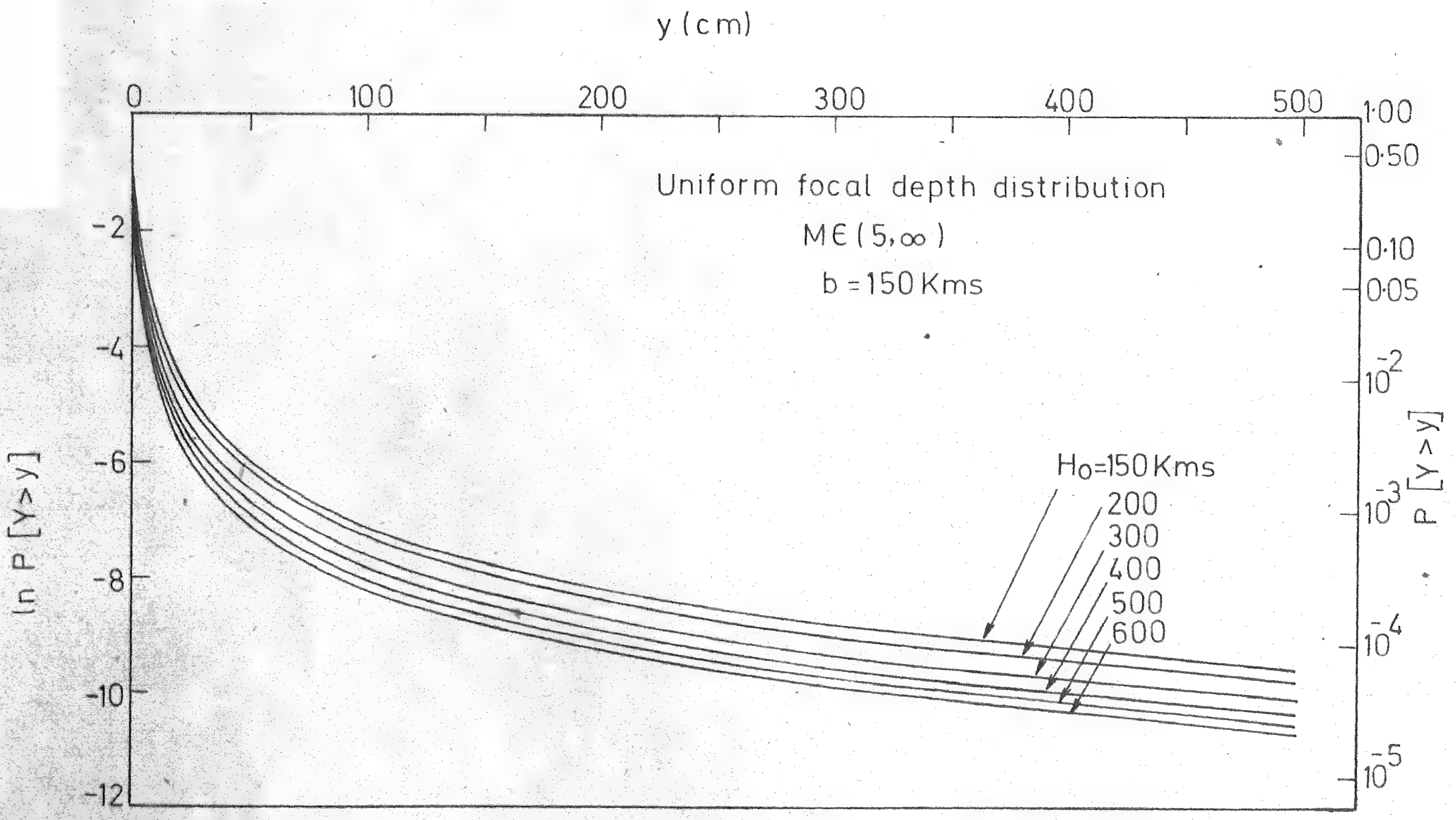

FIG. 3·10 EFFECT OF MAXIMUM FOCAL DEPTH, H_o, ON THE PROBABILITY OF THE PEAK GROUND DISPLACEMENT, Y, EXCEEDING y

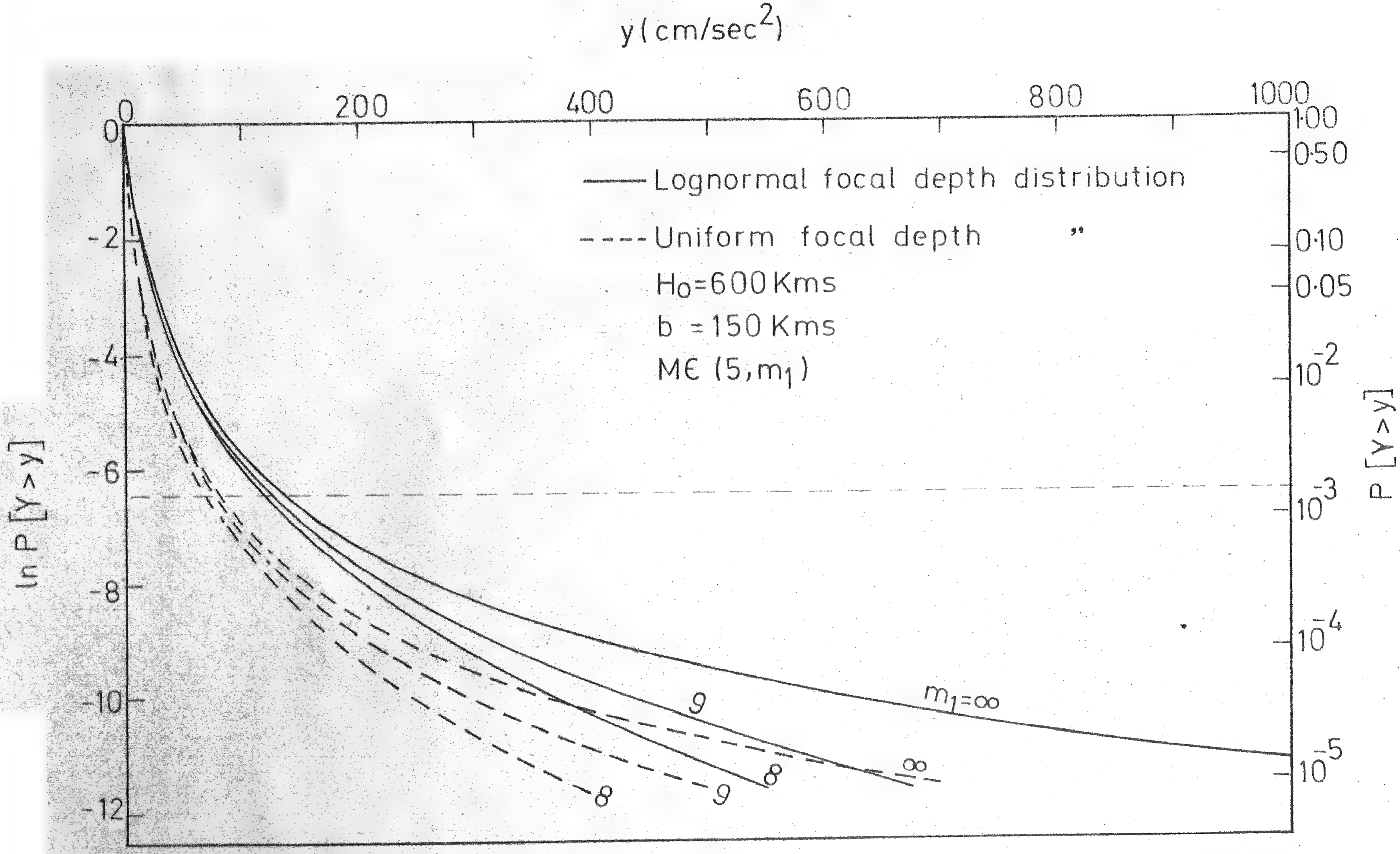

FIG. 3·11 EFFECT OF MAGNITUDE CUTOFF ON THE PROBABILITY OF THE PEAK GROUND ACCELERATION, Y, EXCEEDING y

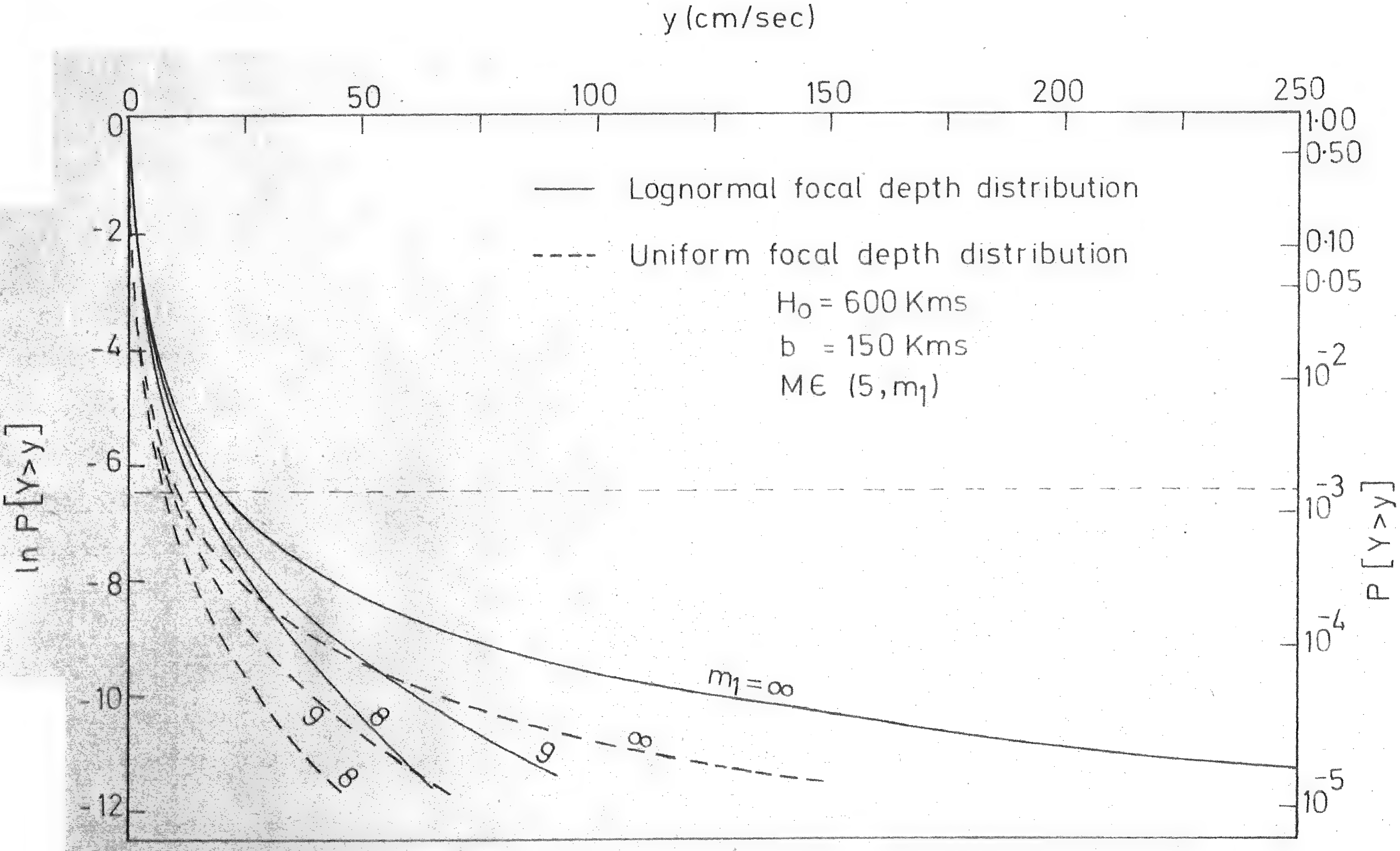

FIG. 3·12 EFFECT OF MAGNITUDE CUTOFF ON THE PROBABILITY OF THE PEAK GROUND VELOCITY, Y, EXCEEDING v

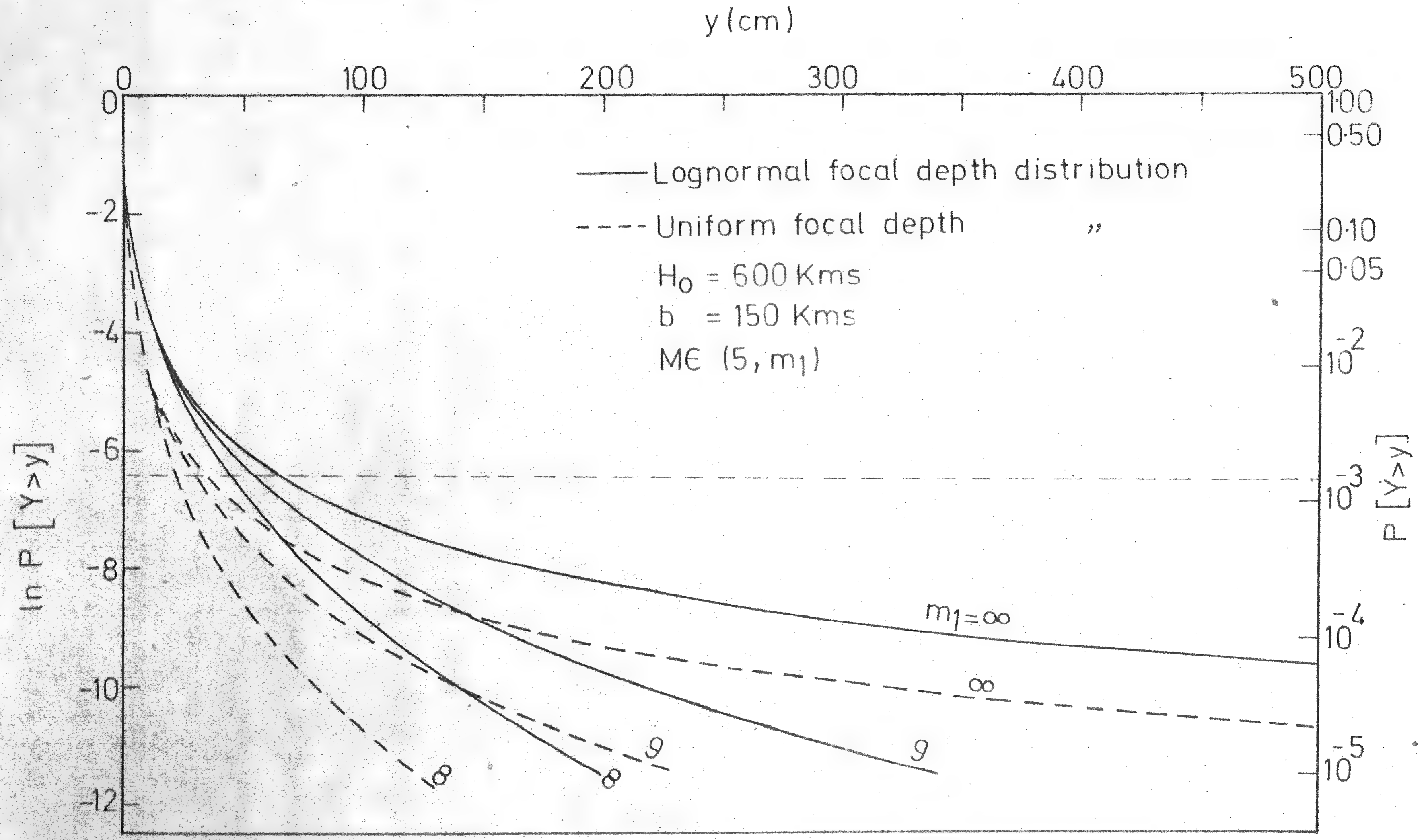

FIG. 3·13 EFFECT OF MAGNITUDE CUTOFF ON THE PROBABILITY OF THE PEAK GROUND DISPLACEMENT, Y, EXCEEDING y reflection of the estimated parameter values involved in that distribution. Contrary to the simple conjecture that the seismic risk for lognormal distribution of focal depth is upper bound, for uniform distribution is lower bound and for mixed lognormal distribution of focal depth is inbetween two extreme bounds, it is observed that the seismic risk is maximum for mixed lognormal distribution. This observation suggests that in the Indian peninsula a better fit of past seismic data in the intermediate focus region increases the frequency of occurrence of earthquake in the shallow focus region also and hence the increment of risk. The modular source with uniform focal depth distribution and having maximum focal depth, H_o= 150 kms., gives compairable seismic risk at a site with a modular source of maximum focal depth, H_o= 600 kms., and having a lognormal distribution of focal depth. The arc length of the both earthquake sources is 150 kms.

The sensitivity of seismic risk due to magnitude cutoff is shown in Figs. (3.11-3.13). For constant return period the increase in upper magnitude, m_1, cutoff increases the peak ground generalized intensity. The dashed line in Figs. (3.11-3.13) represents the range of exceedance probability of Y in Indian peninsula. The effect of magnitude cutoff at upper level on seismic risk is insignificant for larger exceedance probability of Y. From these figures it is seen that the distribution assumption of focal depth is more pronounced for peak ground acceleration and peak ground velocity than for peak ground displacement.

From the results presented in this section it is concluded that modular source with arc length, $b = 150$ kms, and maximum focal depth, $H_o = 600$ kms is to be used for evaluation of seismic risk of Indian peninsula. The distribution of focal depth is lognormal and magnitude, $m \varepsilon (5,9]$.

CHAPTER 4

SEISMIC RISK ANALYSIS OF INDIAN PENINSULA-A MODEL HOMOGENEOUS IN TECTONIC FEATURES

4.1 Introduction

The modular volume source of earthquakes presented in the previous chapter is used for the seismic risk analysis of the Indian peninsula in this chapter. The peninsula is divided in 2° × 2° grid as shown in Fig. (4.1). Peak generalised seismic intensity in terms of peak ground acceleration, velocity and displacement are determined at each grid point. The earthquake source at grid points are assumed to be homogeneous in tectonic features i.e. precise information regarding location of faults within the modular earthquake source at grid point is either not available or ignored. Every region within Indian peninsula is assumed to be prone to earthquakes. Nonavailability of evidence of occurrence of earthquakes in the available data of past earthquakes does not imply that the region is free from earthquakes. The acceptance of the hypothesis that any region is free from seismic activity is synonymous of a dying planet.

The scarcity of data leads to a situation where classical statistics fail to provide meaningful results. A Bayesian approach is, therefore, used to estimate the intensity parameter, μ, of the earthquake arrival process at a source. The local seismicity i.e. the probabilities of occurrence of earthquakes in the Indian peninsula

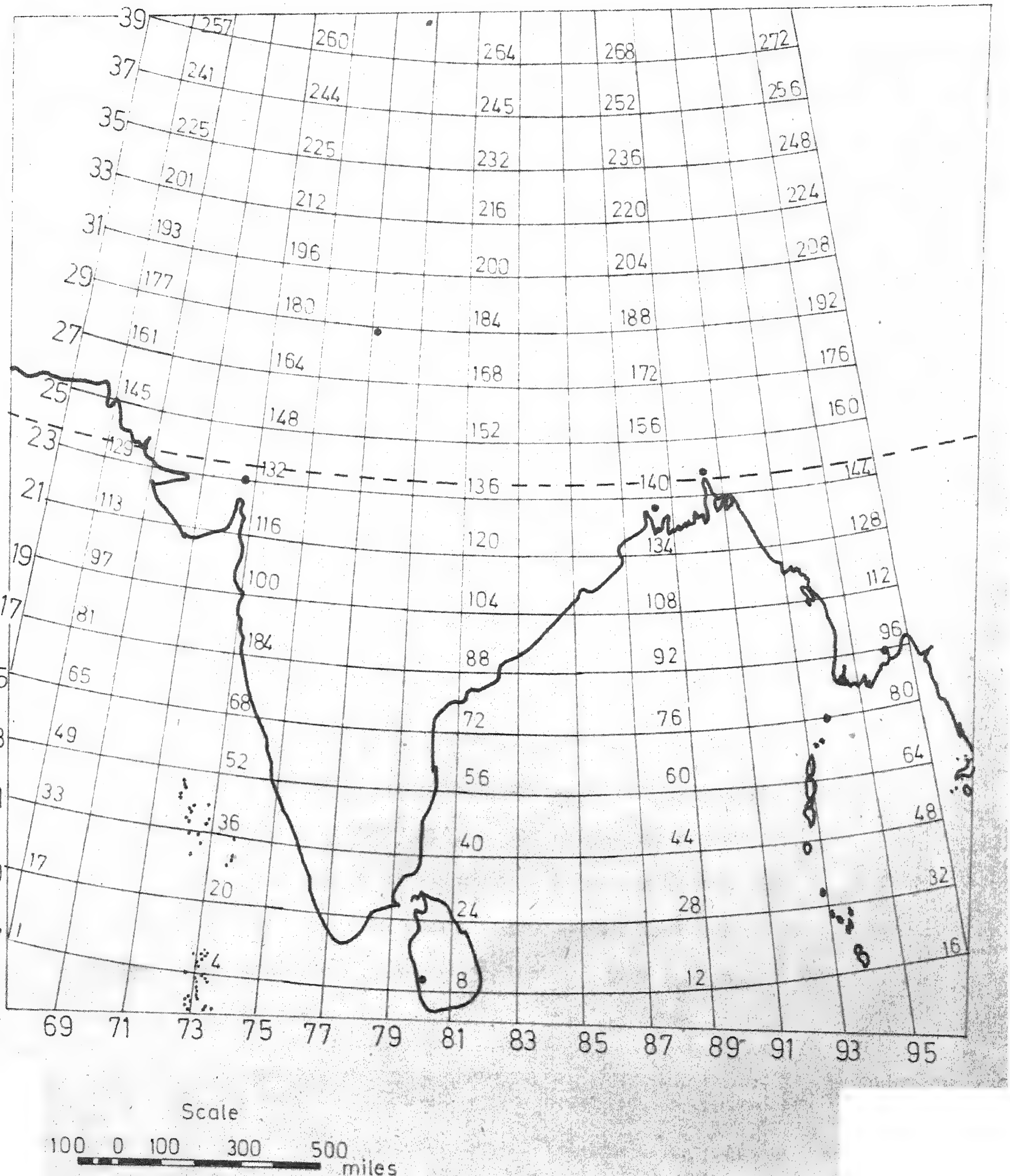
39
37
35
33
31
29
27
25
23
21
19
17
15
13
11
9
7
69
71
73
75
77
79
81
83
85
87
89
91
93
95
257
260
264
268
272
241
244
245
252
256
225
225
232
236
248
201
212
216
220
224
193
196
200
204
208
177
180
184
188
192
161
164
168
172
176
145
148
152
156
160
129
132
136
140
144
113
116
120
134
128
97
100
104
108
112
81
184
88
92
96
65
68
72
76
80
49
52
56
60
64
33
36
40
44
48
17
20
24
28
32
1
4
8
12
16
Scale
100 0 100 300 500
miles

FIG. 4·1 GRID NUMBERS

is obtained in Section 4.2. The regional seismicity in different regions within the Indian peninsula is estimated next. The peak generalised seismic intensities for 100-year return period are estimated at each grid point and contours of equal intensity are drawn. Curves to extrapolate 100-year intensity at a site for a different return period, or for other specified exceedance probability are presented.

4.2 Local Seismicity

The local seismicity of Indian peninsula possessing a volume, V, of earth is assumed to be constant. The intensity parameter, μ, of the earthquake arrival process for magnitude greater than a threshold value, M, is assumed to be a function of magnitude, M, and volume, V, and is given by

$$\ell n\ \mu = \ell n(\alpha V) - \beta M \qquad (4.1)$$

where α and β are empirical constants. The relation Eq. (4.1) is a representation of magnitude-frequency law. The parameter, a, of the magnitude-frequency law (Eq. 3.1) is a function of volume. Since the assumed arrival of earthquakes is Poisson process, the interarrival of earthquakes is a sample from exponential distribution. The probability density of interarrival time is given by

$$f_X(x) = \mu \ \exp(-\mu x) \qquad ; x > 0 \qquad (4.2)$$

The parameter, μ, will be different for various regions of Indian peninsula as stated in the Introduction and is estimated by Bayes' theorem.

4.2.1 Bayes' Theorem

Bayes' Theorem states that 'posterior probabilities' are equal to the 'prior probabilities' and the corresponding likelihood values disregarding the normalising constant. This formula can, of course, be stated in logarithmic form, in which Bayes' Theorem is rule of addition of information. In the language of Bayesian statistics, the model density is

$$m_\mu(x) = \mu \exp(-\mu x) \qquad ; x > 0 \qquad (4.3)$$

The likelihood with respect to μ of the observations (interarrival times) z_i is

$$\ell(\mu) = \exp(m \ln \mu - \mu \sum z_i) \qquad (4.4)$$

The natural conjugate Bayes density may be taken to be

$$b(\mu) = 1/\Gamma(m) \exp[m \ln(\sum z_i) + (m-1) \ln \mu - \mu \sum z_i] \qquad (4.5)$$

where $\Gamma(.)$ is a Gamma function.

The natural conjugate Bayes density with $m = z = 0$ reduces to the density $1/\mu$ i.e. uniform on $\theta = \ln \mu$, which is a valid indifference density but provides neither a stochastic upper bound nor a stochastic lower bound on μ.

Let the first arrival occurs at $x > 0$. The posterior density is given by

$$b_m(\mu) = 1/\Gamma(m+1) \exp[(m+1) \ln(x+\sum z_i) + m \ln \mu$$
$$- \mu(x + \sum z_i)] \qquad (4.6)$$

With $m = z = 0$ the posterior is proper as long as $x > 0$, and is given by, $x \exp(-\mu x)$. As $x \to 0$, $b(\mu)$ approaches a uniform density.

Let n events have occurred with interarrival, τ_j. The posterior density is

$$b(\mu) = 1/\Gamma(n+m) \exp\left[(n+m) \ln \left(\sum z_i + \sum \tau_j\right) + (n+m-1) \ln \mu - \mu\left(\sum z_i + \sum \tau_j\right)\right] \quad ; \quad \mu \geq 0 \qquad (4.7)$$

The Bayes estimate of μ under quadratic loss function is $\hat{\mu}$ and is given by

$$\hat{\mu} = E[\mu] = (n+m)/\left(\sum z_i + \sum \tau_j\right) \qquad (4.8)$$

and coefficient of variation of μ is

$$C(\mu) = 1/\sqrt{n+m} \qquad (4.9)$$

4.2.2 Estimation of Local Seismicity

In the estimation of local seismicity the historic evidence is neglected. Thus, $m = z = 0$, in Eq. (4.8) and

$$\hat{\mu} = E[\mu] = n/t_o \qquad (4.10)$$

$$C(\mu) = 1/\sqrt{n} \qquad (4.11)$$

where t_o = the period of record

$$= \sum \tau_j \qquad (4.12)$$

and $\hat{}$ refers estimated value and $E[\,.\,]$ is expectation.

Neglect of historic evidence will not change $\hat{\mu}$ sufficiently but will increase disperssion. The above method of estimation leads to a point estimation of μ for different magnitude ranges. To obtain a continuous variation of $\hat{\mu}$ the values obtained from Eq. (4.10) are fitted to the Eq. (4.1). It is to be noted that this fit will be identical with the magnitude-frequency law given in Chapter 2.

The coefficient of variation of μ, $C(\mu)$, Eq. (4.11) is fitted with a Horel function

$$C(\mu) = \exp\ [a_0 + a_1 \ \ell n\ M + a_2 M] \tag{4.13}$$

The analysis of variance table is given in Table 4.1. The fitted plot is shown in Fig. (4.2). The 95% confidence interval of coefficients a_0, a_1 and a_2 are (5.826 ± 2.605), (-17.097 ± 3.345) and (3.653 ± 0.558) respectively.

The local seismicity of a smaller volume, say V', is obtained assuming μ'/μ and μ are statistically independent and μ' refers to the intensity of arrival for volume V'. The spatial variation of seismicity within Indian peninsula is accounted for by μ'/μ . It can be shown from Eq. (4.1) that

$$\hat{\mu}' = V'/V\ \hat{\mu} \tag{4.14}$$

$$C^2(\mu') = C^2(\mu'/\mu) + C^2(\mu'/\mu)\ C^2(\mu) + C^2(\mu) \tag{4.15}$$

where $C^2(.)$ is coefficient of variation square. Esteva$^{(43)}$ has shown that by restriction of condition $V' \rightarrow V \Longrightarrow \mu' \rightarrow \mu$ to Eq. (4.15) yields the solution

Table 4.1

Analysis of Variance Table for Multiple Linear Regression
Model - $C(\mu) = \exp\left[\, a_o + a_1 \, \ell n \, M + a_2 M \,\right]$

Number of sample = 23

Source of Variation	Sum of square	Degree of freedom	Root Mean square	F-ratio
Due regression	30.1023	2	3.8796	530.2
Due residual	0.5677	20	0.1685	
Total	30.6700	22		

Multiple correlation coefficient square = 0.981

i	Coeff. a_i	σ_{a_i}	t-value	$\max(X_i)$	$\min(X_i)$
0	5.826	1.249	4.66		
1	-17.097	1.605	10.65	2.128	1.386
2	3.653	0.268	13.65	8.400	4.000

Covariance of coefficients

$$\mathrm{Cov}\left[\underset{\sim}{a}\right] = \begin{bmatrix} 1.561 & -1.987 & 0.325 \\ -1.987 & 2.575 & -0.427 \\ 0.325 & -0.427 & 0.072 \end{bmatrix}$$

The null hypothesis: $a_1 = a_2 = 0$ is rejected at $P < 0.001$ since $F_o = 530.2 > F_{.999\,;\,2,20} = 9.5$ and the null hypothesis regarding $a_i = 0$, $i = 0, 1, 2$ is rejected at P-value much less than 0.001.

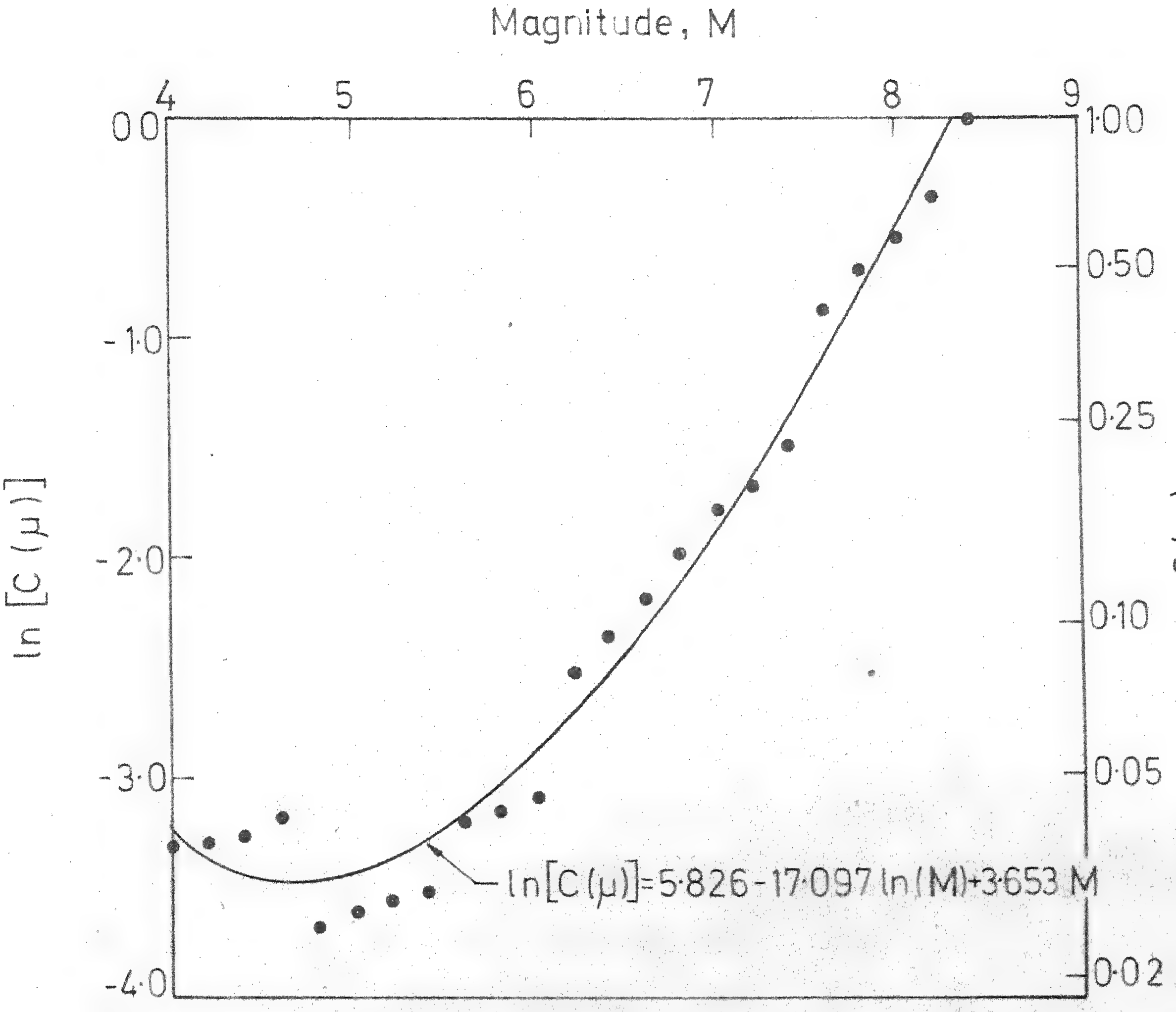

FIG 4·2 COEFFICIENT OF VARIATION OF μ AND MAGNITUDE RELATION

$$C^2(\mu'/\mu) = (V/V')^{\gamma} - 1 \qquad (4.16)$$

Use of Eqs. (4.15, 4.16 and 4.11) yields

$$(V/V')^{\gamma} = n\,[1 + C^2(\mu')]\,/(n+1) \qquad (4.17)$$

For each volume ratio 250 random volume samples of V' are generated within Indian peninsula to estimate $C^2(\mu')$. This estimated value is used to obtain γ and shown in Fig. (4.3). The results of this analysis are given in Table 4.2. The 95% confidence interval of γ is (0.408 ± 0.021).

The relations developed are used to estimate the intensity of arrival process and its coefficient of variation at each grid point.

4.3 Estimation of Regional Seismicity at Grid Points

To estimate intensity of arrival process at a grid point, the number, r, of earthquakes over a given magnitude threshold originated at earthquake source, centred at a grid point, in the time period, T, of available seismic data is counted. The intensity of arrival $\hat{\mu}_1$, and coefficient of variation, $C(\mu_1)$, are obtained from Figs. (2.4 and 4.2). The intensity, $\hat{\mu}'_1$, for earthquake source of volume, V', is obtained by substitution $\hat{\mu}_1$ in Eq. (4.14). The parameter, m, and, $\sum z_i$, of the natural conjugate Bayes density Eq. (4.5) are

$$m = 1/C^2(\mu_1) \qquad (4.18)$$

$$\sum z_i = 1/\,[\,\hat{\mu}'_1\, C^2(\mu_1)\,] = m/\,\hat{\mu}'_1 \qquad (4.19)$$

where $C^2(\mu'_1)$ is obtained from Eq. (4.15) and Eq. (4.16) as

Table 4.2

Analysis of Variance Table for Linear Regression Model

$$- \ln [n \{1+C^2(\mu')\} /(n+1)] = \gamma \ln (V/V')$$

Number of samples = 20

Source of variation	Sum of Squares	Degree of Freedom	Root Mean square	F-Ratio
Due regression	37.233	1	6.102	400.76
Due residual	1.756	19		
Total	38.989	20		

Multiple Correlation Coefficient Square = 0.955

$\hat{\gamma}$ = 0.408

σ_γ = 0.012

t-value = 39.93

Since $F_0 = 400.76 > F_{0.999;1,18} = 15.4$, the null hypothesis H_0: $\gamma = 0$ is rejected at $P < 0.001$. P-value $= 2P [t(18) > 39.93] < 2 \times 0.0005 = 0.001$, hence H_0: $\gamma = 0$ is rejected at $P << 0.001$.

A 95% confidence interval for γ is (0.408 ± 0.021)

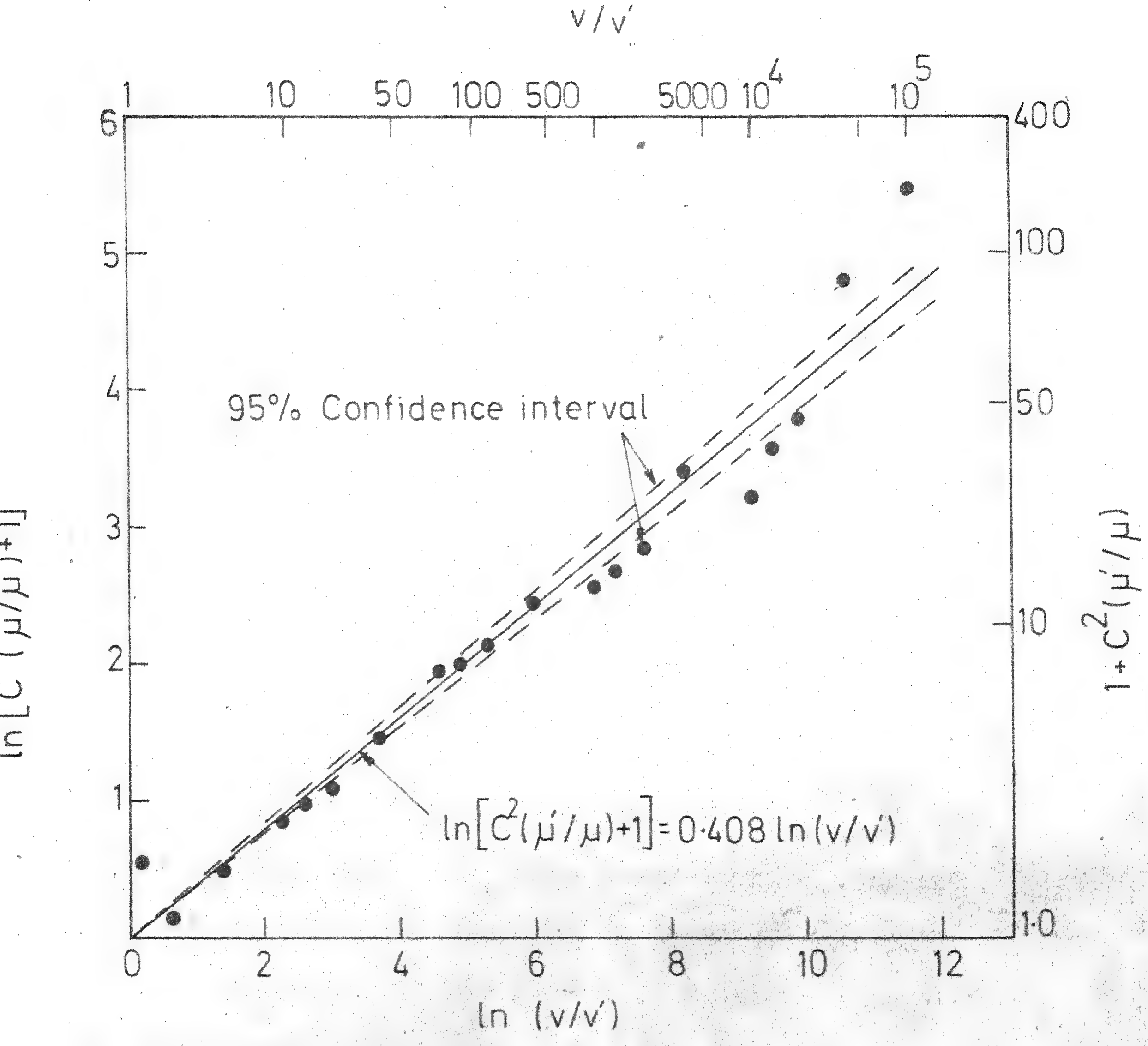

FIG. 4·3 VARIABILITY OF LOCAL SEISMICITY WITHIN INDIAN PENINSULA FOR MAGNITUDE, M>5

$$C^2(\mu_1') = \{(V/V')^{\gamma} -1\} \{1 + C^2(\mu_1)\} + C^2(\mu_1) \quad (4.20)$$

The Bayes estimate of μ' under quadratic loss function when r earthquakes occured in the earthquake source during a time interval, T, is $\hat{\mu}'$ and is given by

$$\hat{\mu}' = (r+m)/(\sum z_i + T) \quad (4.21)$$

and coefficient of variation of μ' is from Eq. (4.9) as

$$\hat{C}(\mu') = 1/\sqrt{(r+m)} \quad (4.22)$$

The regional seismicity at each grid point is estimated from Eqs. (4.21 and 4.22) and is reported in Table 4.3.

4.4 Results and Discussion

The results in terms of peak ground acceleration, velocity and displacement are obtained numerically from Eq. (3.24) for a specified return period, T_y = 100 years. The generalized intensity is obtained in an iterative procedure with tolerance such that

$$100 \text{ years} \le T_y \le 101 \text{ years.}$$

The generalized intensities are obtained (Table 4.3) at each 2° × 2° grid points and are plotted in contour forms in Figs. (4.4–4.6). The general shape of the contour in the three maps is similar. However, spread in contours for displacement and velocity are more than that for acceleration. Significant differences are present in the central and north-eastern region. Although the tectonic features are not taken into account explicitly, a clear indication of Himalayan belt is

Table 4.3

Estimated intensity and coefficient of variation square for earthquake arrival process and peak generalized seismic intensity at grid points.

Lognormal focal depth distribution, $m \in (5,9]$, $b = 150$ Kms. and $H_o = 600$ Kms.

Grid point	$\hat{\mu}\times10^6$ (≠ /day)	$C^2(\mu)\times10^2$	100 years ≤ return period ≤ 101 years		
			Acceleration (Cm/Sec^2)	Velocity$\times10^2$ (Cm/Sec)	Displacement $\times10^2$ (Cm)
1	8.287	849.6	0.2651	4.009	9.101
2	8.287	849.6	0.2651	4.009	9.101
3	8.287	849.6	0.2651	4.009	9.101
4	78.70	89.47	8.290	89.00	193.0
5	8.287	849.6	0.2651	4.009	9.101
6	8.287	849.6	0.2651	4.009	9.101
7	78.70	89.47	8.290	89.00	193.0
8	8.287	849.6	0.2651	4.009	9.101
9	8.287	849.6	0.2651	4.009	9.101
10	8.287	849.6	0.2651	4.009	9.101
11	8.287	849.6	0.2651	4.009	9.101
12	8.287	849.6	0.2651	4.009	9.101
13	78.70	89.47	8.290	89.00	193.0
14	1346	5.2307	43.77	487.3	128.8
15	994.0	7.083	37.86	415.9	106.9
16	78.70	89.47	8.290	89.00	193.0
17	8.309	851.5	0.2651	4.009	9.101
18	8.309	851.5	0.2651	4.009	9.101
19	79.06	89.49	8.320	89.31	193.7
20	8.309	851.5	0.2651	4.009	9.101
21	8.309	851.5	0.2651	4.009	9.101
22	8.309	851.5	0.2651	4.009	9.101

Table 4.3 contd.

23	8.309	851.5	0.2651	4.009	9.101
24	8.309	851.5	0.2651	4.009	9.101
25	8.309	851.5	0.2651	4.009	9.101
26	8.309	851.5	0.2651	4.009	9.101
27	8.309	851.5	0.2651	4.009	9.101
28	8.309	851.5	0.2651	4.009	9.101
29	8.309	851.5	0.2651	4.009	9.101
30	1636	4.326	47.90	538.9	145.1
31	291.3	24.29	19.72	210.8	491.2
32	8.309	851.5	0.2651	4.009	9.101
33	8.337	853.9	0.2651	4.009	9.101
34	8.337	853.9	0.2651	4.009	9.101
35	8.337	853.9	0.2651	4.009	9.101
36	8.337	853.9	0.2651	4.009	9.101
37	8.337	853.9	0.2651	4.009	9.101
38	8.337	853.9	0.2651	4.009	9.101
39	8.337	853.9	0.2651	4.009	9.101
40	8.337	853.9	0.2651	4.009	9.101
41	8.337	853.9	0.2651	4.009	9.101
42	8.337	853.9	0.2651	4.009	9.101
43	8.337	853.9	0.2651	4.009	9.101
44	8.337	853.9	0.2651	4.009	9.101
45	293.1	24.29	19.78	211.6	493.2
46	1076	6.615	39.34	433.6	1122
47	862.6	8.253	35.30	385.8	978.2
48	8.337	853.9	0.2651	4.009	9.101
49	8.370	856.8	0.2651	4.009	9.101
50	8.370	856.8	0.2651	4.009	9.101
51	8.370	856.8	0.2651	4.009	9.101
52	8.370	856.8	0.2651	4.009	9.101
53	8.370	856.8	0.2651	4.009	9.101
54	8.370	856.8	0.2651	4.009	9.101
55	8.370	856.8	0.2651	4.009	9.101

Table 4.3 contd.

56	8.370	856.8	0.2651	4.009	9.101
57	8.370	856.8	0.2651	4.009	9.101
58	8.370	856.8	0.2651	4.009	9.101
59	8.370	856.8	0.2651	4.009	9.001
60	80.08	89.55	8.402	90.19	195.7
61	8.370	856.8	0.2651	4.009	9.101
62	1443	4.971	45.21	505.1	1344
63	510.4	14.05	26.94	290.2	704.1
64	80.08	89.55	8.402	90.19	195.7
65	8.409	860.2	0.2651	4.009	9.101
66	8.409	860.2	0.2651	4.009	9.101
67	8.409	860.2	0.2651	4.009	9.101
68	8.409	860.2	0.2651	4.009	9.101
69	8.409	860.2	0.2651	4.009	9.101
70	8.409	860.2	0.2651	4.009	9.101
71	80.74	89.59	8.455	90.75	197.0
72	8.409	860.2	0.2651	4.009	9.101
73	80.74	89.59	8.455	90.75	197.0
74	8.409	860.2	0.2651	4.009	9.101
75	8.409	860.2	0.2651	4.009	9.101
76	80.74	89.59	8.455	90.75	197.0
77	8.409	860.2	0.2651	4.009	9.101
78	514.7	14.05	27.07	291.6	707.9
79	153.1	47.25	13.27	141.8	317.9
80	225.4	32.09	16.93	180.8	414.5
81	8.454	864.1	0.2651	4.009	9.101
82	8.454	864.1	0.2651	4.009	9.101
83	8.454	864.1	0.2651	4.009	9.101
84	1031	7.084	38.54	424.0	109.3
85	8.454	864.1	0.2651	4.009	9.101
86	8.454	864.1	0.2651	4.009	9.101
87	8.454	864.1	0.2651	4.009	9.101
88	154.6	47.27	13.35	14.27	320.1

Table 4.3 contd.

89	8.454	864.1	0.2651	4.009	9.101
90	8.454	864.1	0.2651	4.009	9.101
91	8.454	864.1	0.2651	4.009	9.101
92	8.454	864.1	0.2651	4.009	9.101
93	8.454	864.1	0.2651	4.009	9.101
94	154.6	47.27	13.35	142.7	320.1
95	81.51	89.63	8.517	91.40	198.5
96	373.7	19.55	22.73	243.5	577.3
97	8.505	868.6	0.2651	4.009	9.101
98	8.505	868.6	0.2651	4.009	9.101
99	82.38	89.68	8.587	92.14	200.2
100	82.38	89.68	8.587	92.14	200.2
101	8.505	868.6	0.2651	4.009	9.101
102	8.505	868.6	0.2651	4.009	9.101
103	8.505	868.6	0.2651	4.009	9.101
104	8.505	868.6	0.2651	4.009	9.101
105	8.505	868.6	0.2651	4.009	9.101
106	8.505	868.6	0.2651	4.009	9.101
107	8.505	868.6	0.2651	4.009	9.101
108	8.505	868.6	0.2651	4.009	9.101
109	8.505	868.6	0.2651	4.009	9.101
110	8.505	868.6	0.2651	4.009	9.101
111	451.8	16.35	25.23	271.1	651.7
112	156.3	47.28	13.45	143.7	322.5
113	83.38	89.73	8.665	92.97	202.2
114	8.563	873.7	0.2651	4.009	9.101
115	8.563	873.7	0.2651	4.009	9.101
116	83.38	89.73	8.665	92.97	202.2
117	83.38	89.73	8.665	92.97	202.2
118	8.563	873.7	0.2651	4.009	9.101
119	8.563	873.7	0.2651	4.009	9.101
120	8.563	873.7	0.2651	4.009	9.101
121	8.563	873.7	0.2651	4.009	9.101

Table 4.3 Contd.

122	8.563	873.7	0.2651	4.009	9.101
123	158.2	47.29	13.55	144.8	325.3
124	83.38	89.73	8.665	92.97	202.2
125	8.563	873.7	0.2651	4.009	9.101
126	158.2	47.29	13.55	144.8	325.3
127	532.3	14.06	27.55	297.0	723.0
128	158.2	47.29	13.55	144.8	325.3
129	84.49	89.79	8.753	93.90	204.3
130	84.49	89.79	8.753	93.90	204.3
131	84.49	89.79	8.753	93.90	204.3
132	8.628	879.3	0.2651	4.009	9.101
133	8.628	879.3	0.2651	4.009	9.101
134	84.49	89.79	8.753	93.90	204.3
135	8.628	879.3	0.2651	4.009	9.101
136	8.628	879.3	0.2651	4.009	9.101
137	84.49	89.79	8.753	93.90	204.3
138	84.49	89.79	8.753	93.90	204.3
139	84.49	89.79	8.753	93.90	204.3
140	8.628	879.3	0.2651	4.009	9.101
141	312.1	24.31	20.52	219.5	513.8
142	919.0	8.255	36.43	399.0	1017
143	2436	3.114	57.27	660.6	1850
144	615.6	12.32	29.74	321.7	792.3
145	239.8	32.12	17.57	187.7	432.1
146	239.8	32.12	17.57	187.7	432.1
147	85.74	89.85	8.851	94.93	206.7
148	85.74	89.85	8.851	94.93	206.7
149	8.700	885.5	0.2651	4.009	9.101
150	239.8	32.12	17.57	187.7	432.1
151	8.700	885.5	0.2651	4.009	9.101
152	8.700	885.5	0.2651	4.009	9.101
153	8.700	885.5	0.2651	4.009	9.101
154	8.700	885.5	0.2651	4.009	9.101

Table 4.3 contd.

155	8.700	885.5	0.2651	4.009	9.101
156	239.8	32.12	17.57	187.7	432.1
157	1550	4.972	46.72	524.1	1404
158	1087	7.086	39.54	436.0	1130
159	2859	2.694	61.39	715.7	2037
160	2782	2.769	60.67	706.0	2004
161	322.2	24.32	20.89	223.6	524.6
162	165.5	47.34	13.95	149.1	335.7
163	8.780	892.4	0.2651	4.009	9.101
164	8.780	892.4	0.2651	4.009	9.101
165	8.780	892.4	0.2651	4.009	9.101
166	8.780	892.4	0.2651	4.009	9.101
167	87.13	89.92	8.958	96.07	209.4
168	87.13	89.92	8.958	96.07	209.4
169	243.8	32.13	17.75	189.6	436.8
170	400.5	19.56	23.62	253.3	603.5
171	557.2	14.06	28.23	304.6	744.2
172	243.8	32.13	17.75	189.6	436.8
173	1889	4.147	51.15	580.1	1585
174	1341	5.843	43.69	486.3	1284
175	949.0	8.256	37.01	405.8	1038
176	1968	3.982	52.09	592.3	1625
177	1206	6.618	41.55	460.2	1203
178	2164	3.689	54.35	621.6	1721
179	727.1	10.98	32.40	352.1	879.4
180	88.68	90.00	9.076	97.32	212.3
181	88.68	90.00	0.2651	4.009	9.101
182	168.5	47.37	14.12	150.8	339.9
183	168.5	47.37	14.12	150.8	339.9
184	2004	3.982	52.52	597.8	1643
185	567.5	14.06	28.50	307.7	752.8
186	88.68	90.00	9.076	97.32	212.2
187	647.3	12.33	30.53	330.6	817.7

Table 4.3 contd.

188	248.3	32.14	17.94	191.7	442.1
189	647.3	12.33	30.53	330.6	817.7
190	248.3	32.14	17.94	191.7	442.1
191	4159	1.919	71.91	861.8	2545
192	2403	3.321	56.92	656.0	1834
193	497.4	16.37	26.58	286.1	692.7
194	1067	7.628	39.19	431.7	1117
195	578.8	14.06	28.80	311.1	762.3
196	90.38	90.08	9.206	98.69	215.4
197	171.8	47.39	14.29	152.7	344.5
198	171.8	47.39	14.29	152.7	344.5
199	904.5	9.001	36.14	395.6	1007
200	660.3	12.33	30.84	334.2	827.9
201	334.6	24.33	21.35	228.6	537.6
202	660.3	12.33	30.84	334.2	827.9
203	497.4	16.37	26.58	286.1	692.7
204	497.4	16.37	26.58	286.1	692.7
205	1800	4.522	50.04	566.0	1539
206	171.8	47.39	14.29	152.7	344.5
207	741.7	10.98	32.73	355.9	890.3
208	578.8	14.06	28.80	311.1	762.3
209	175.4	47.42	14.49	154.7	349.6
210	591.4	14.07	29.13	314.7	772.6
211	175.4	47.42	14.49	154.7	349.6
212	341.8	24.34	21.61	231.3	545.0
213	591.4	14.07	29.13	314.7	772.6
214	175.4	47.42	14.49	154.7	349.6
215	425.0	19.57	24.40	262.0	626.8
216	92.26	90.17	9.347	100.2	218.9
217	258.6	32.16	18.38	196.5	454.3
218	175.4	47.42	14.49	154.7	349.6
219	92.26	90.17	9.347	100.2	218.9
220	9.070	917.2	0.2651	4.009	9.101

Table 4.3 contd.

221	341.8	24.34	21.61	231.3	545.0
222	924.1	9.002	36.52	400.2	1021
223	341.8	24.34	21.61	231.3	545.0
224	175.4	47.42	14.49	154.7	349.6
225	349.8	24.34	21.89	234.4	553.2
226	1116	7.629	40.04	442.0	1148
227	1457	5.845	45.41	507.6	1352
228	690.4	12.33	31.55	342.4	851.3
229	264.6	32.18	18.63	199.2	461.2
230	520.1	16.38	27.21	293.3	712.5
231	264.6	32.18	18.63	199.2	461.2
232	690.4	12.33	31.55	342.3	851.3
233	94.33	90.26	9.501	101.8	222.7
234	9.186	927.0	0.2651	4.009	9.101
235	94.33	90.26	9.501	101.8	222.7
236	179.4	47.44	14.70	157.0	355.1
237	775.5	10.98	33.48	364.5	915.5
238	179.5	47.44	14.70	157.0	355.1
239	9.186	927.0	0.2651	4.009	9.101
240	264.6	32.18	18.63	199.2	461.2
241	620.5	14.07	29.87	323.1	796.3
242	2192	3.983	54.66	626.5	1735
243	17210	0.5073	125.8	1663	5554
244	1406	6.209	44.67	498.5	1323
245	358.6	24.35	22.20	237.8	562.1
246	533.2	16.38	27.58	297.3	723.8
247	96.62	90.36	9.669	103.6	226.9
248	96.62	90.36	9.669	103.6	226.9
249	9.312	937.7	0.2651	4.009	9.101
250	533.2	16.38	27.58	297.3	723.8
251	96.62	90.36	9.669	103.6	226.9
252	183.9	47.47	14.93	159.4	361.2

Table 4.3 contd.

253	96.62	90.36	9.669	103.6	226.9
254	96.62	90.36	9.667	103.6	226.9
255	96.62	90.36	9.669	103.6	226.9
256	96.62	90.36	9.669	103.6	226.9
257	188.8	47.50	15.18	162.1	367.7
258	996.1	9.005	37.90	416.3	1070
259	6288	1.426	85.06	1053	3234
260	2880	3.115	61.58	718.2	2046
261	2611	3.436	59.02	683.9	1929
262	1534	5.846	46.52	521.4	1395
263	727.0	12.34	32.40	352.1	879.3
264	188.8	47.50	15.18	162.1	367.7
265	9.449	949.3	0.2651	4.009	9.101
266	9.449	949.3	0.2651	4.009	9.101
267	99.15	90.47	9.851	105.5	231.4
268	9.449	949.3	0.2651	4.009	9.101
269	278.5	32.20	19.21	205.3	477.0
270	9.449	949.3	0.2651	4.009	9.101
271	278.5	32.20	19.21	205.3	477.0
272	368.2	24.36	22.54	241.5	571.8

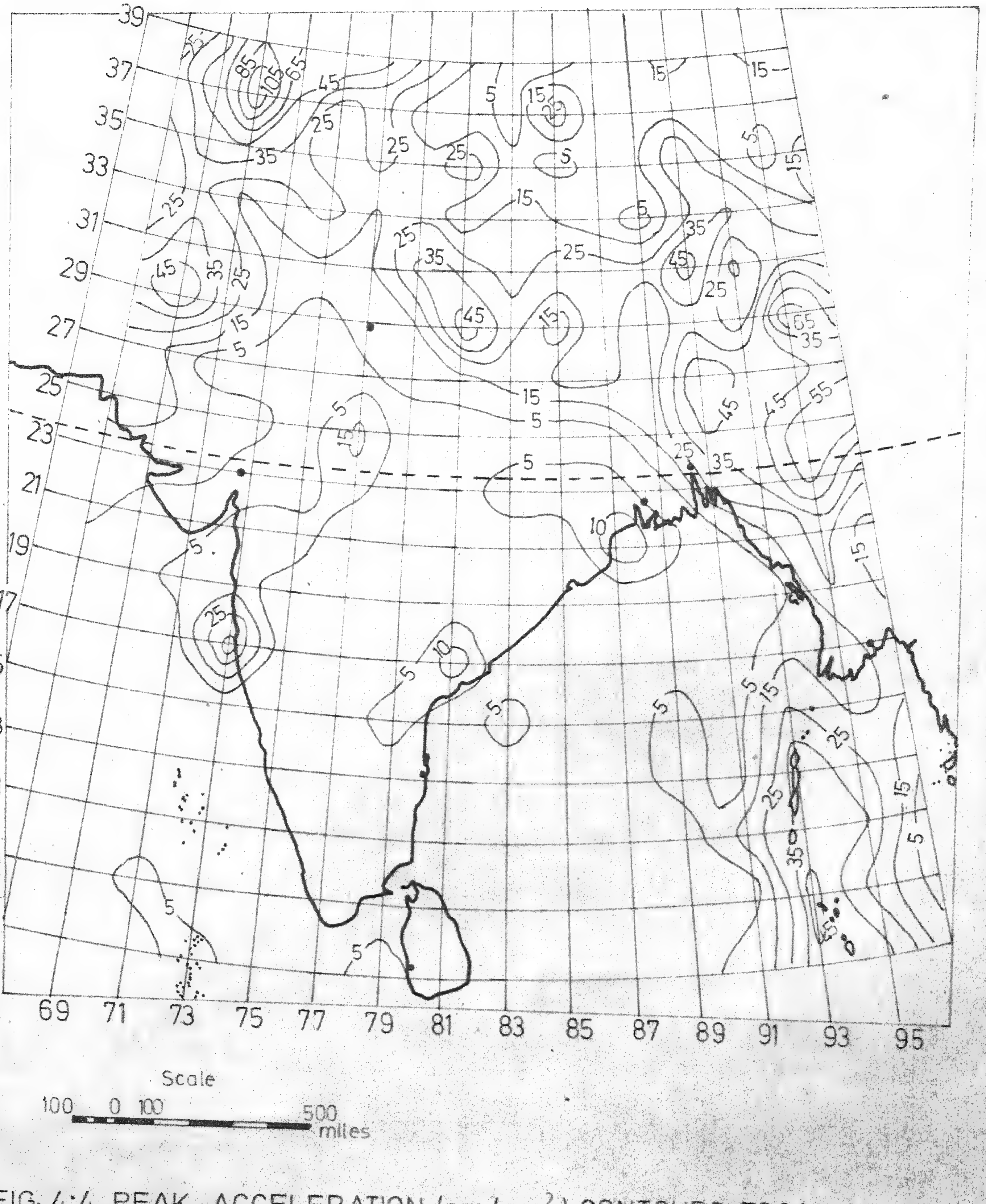
39
37
35
33
31
29
27
25
23
21
19
17
15
13
11
9
7
69
71
73
75
77
79
81
83
85
87
89
91
93
95
105
85
65
45
35
25
15
10
5
55
Scale
100
0
100
500
miles

FIG. 4·4 PEAK ACCELERATION (cm/sec^2) CONTOURS-FOCAL DEPTH LOG-NORMALLY DISTRIBUTED & M∈[5,9]

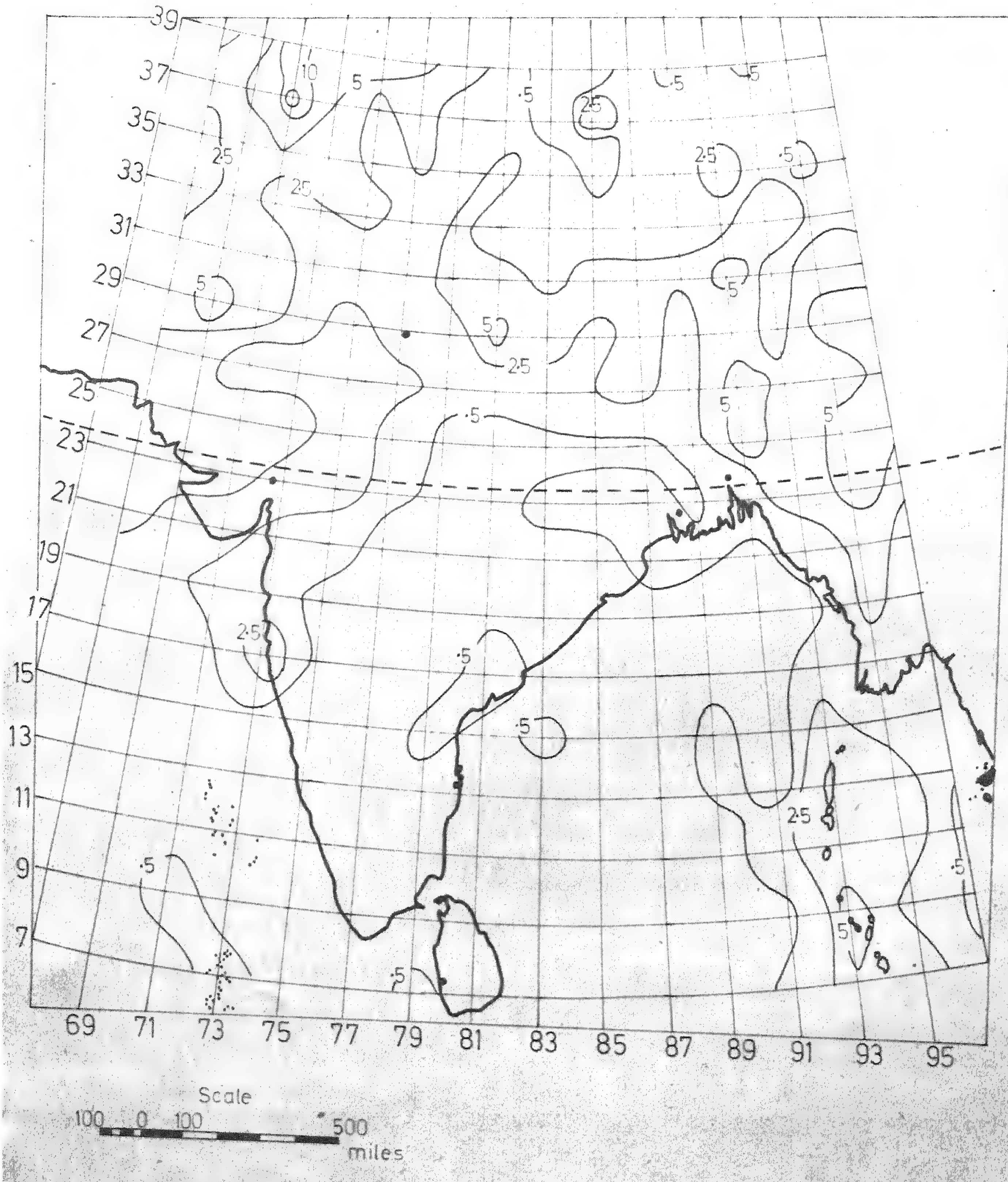
39
37
35
33
31
29
27
25
23
21
19
17
15
13
11
9
7
10
5
·5
2·5
69
71
73
75
77
79
81
83
85
87
89
91
93
95
Scale
100 0 100 500
miles

FIG. 4·5 PEAK VELOCITY (cm/sec) CONTOURS-LOGNORMAL DISTRIBUTION OF FOCAL DEPTH & M∈(5, 9]

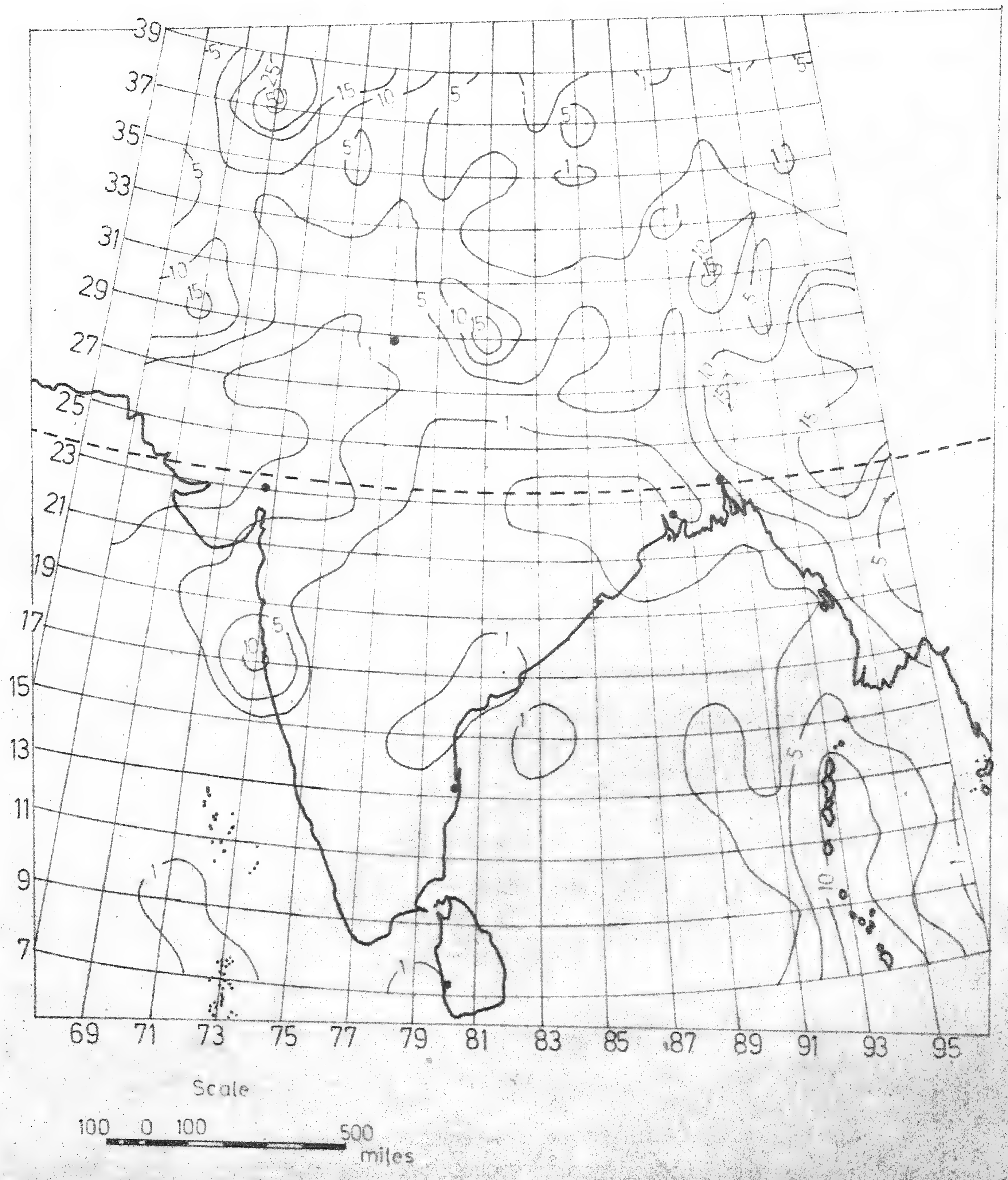
39
37
35
33
31
29
27
25
23
21
19
17
15
13
11
9
7
69
71
73
75
77
79
81
83
85
87
89
91
93
95
Scale
100 0 100 500
miles

FIG. 4·6 PEAK DISPLACEMENT (cm) CONTOURS-LOGNORMAL DISTRIBUTION OF FOCAL DEPTH & Mϵ [5,9] reflected by the contour maps. It is expected that a substantial change in contour pattern is likely to occur in the proximaty of geological faults when faults are taken into account in the seismic risk analysis. The focal depth distribution is identical at each grid point in this analysis. This distribution reflects shallow focus earthquakes. However, from past focal depth data it is observed that grid point 243 has a dominant intermediate focus earthquakes. The analysis with identical focal depth distribution will overestimate generalised intensity at this grid point.

4.5 Extrapolation of Generalized Intensity at a Location

The contour maps prepared in the previous section provide estimates of peak ground acceleration, velocity and displacement at any location in the Indian peninsula for 100-year return period. The return period is estimated from Eq. (3.24) which can also be written as

$$\mu T_y \; P[\, Y > y \,] = 1 \tag{4.23}$$

Substituting $t = T_y$ from Eq. (4.23) into Eq. (3.22) gives

$$F_{Y_{max}} (y; T_y) = \exp(-1) = 0.37 \tag{4.24}$$

Thus a generalized intensity based on T_y-year return period has a probability of 0.63 being exceeded.

While using the contour maps to establish the design loads for a structure at a location, it is quite often necessary to extrapolate the generalized intensity for a 100-year return period given in the map to some other return period (service life). It may also become necessary to determine the generalized intensity for a specified exceedance probability over a given period (service life).

Since the maps presented in the previous section have been drawn on the basis of seismic risk determined from modulur earthquake source at each grid point, these extrapolation can be done in a very simple manner as explained below.

Figs. (4.7 - 4.9) give the plot of generalized intensity against $\ell n(\mu T_y)$ for 0.63, 0.25, 0.10 and 0.05 values of exceedance probabilities at any point in the Indian peninsula.

4.5.1 Extrapolation for Return Period

Let the design intensity required for a return period be $T_y = CT$. Generalized intensity is determined by solving for y from the equation

$$\ell n(\mu T) + \ell n\ C = -\ \ell n\ P[Y > y] \tag{4.25}$$

which is obtained from Eq. (4.23).

Extrapolation can be done in the following steps as shown in Figs. (4.7 - 4.9):

1. Determine the generalized intensity for a T = 100-year return period from the contour map.
2. Locate point B on the curve with p = 0.63 Add ℓn C to the ordinate and locate point C on the curve with p = 0.63.

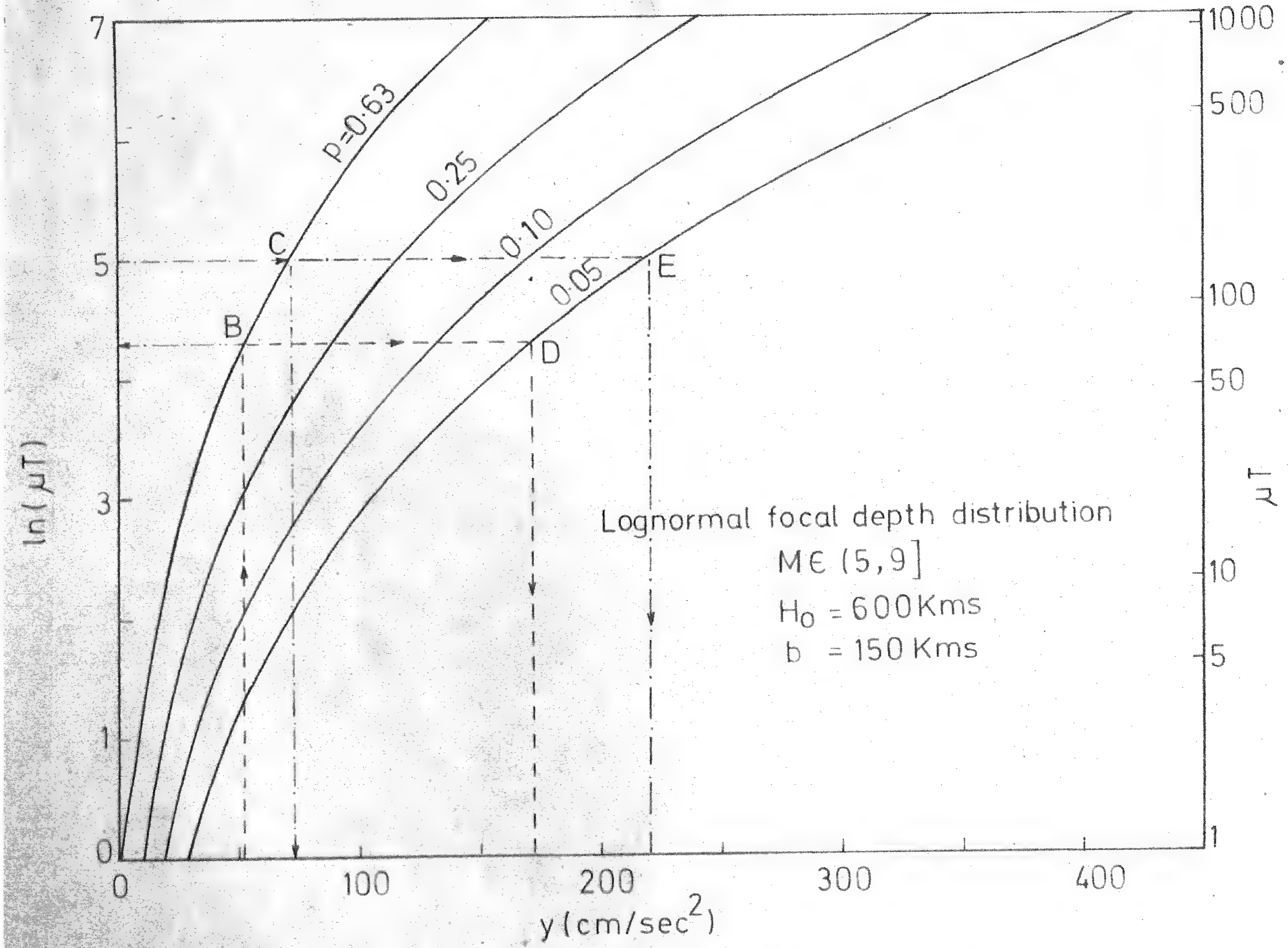

FIG 4·7 VARIATION OF μT WITH PEAK GROUND ACCELERATION, Y

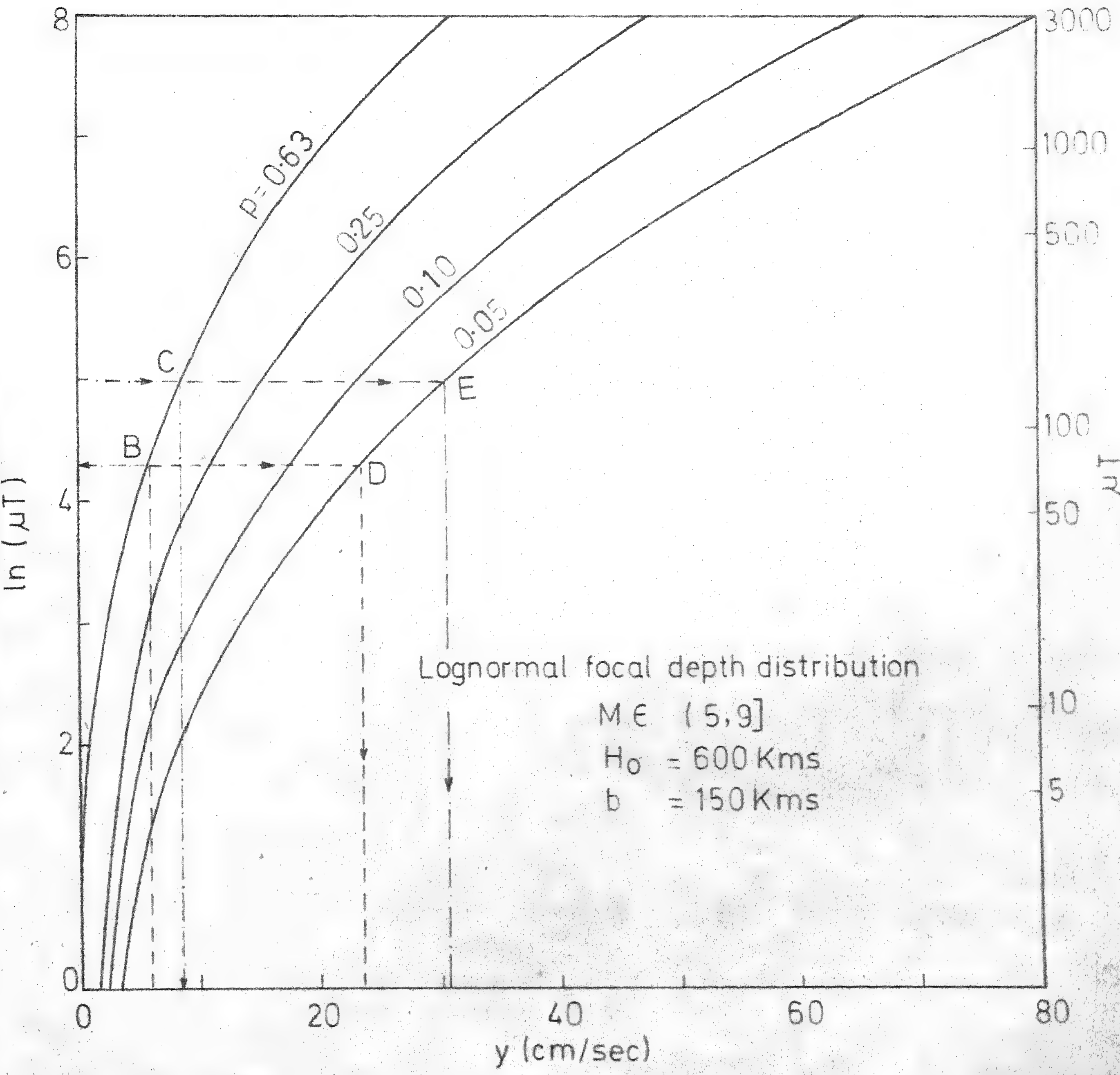

FIG. 4·8 VARIATION OF μT WITH PEAK GROUND VELOCITY, Y.

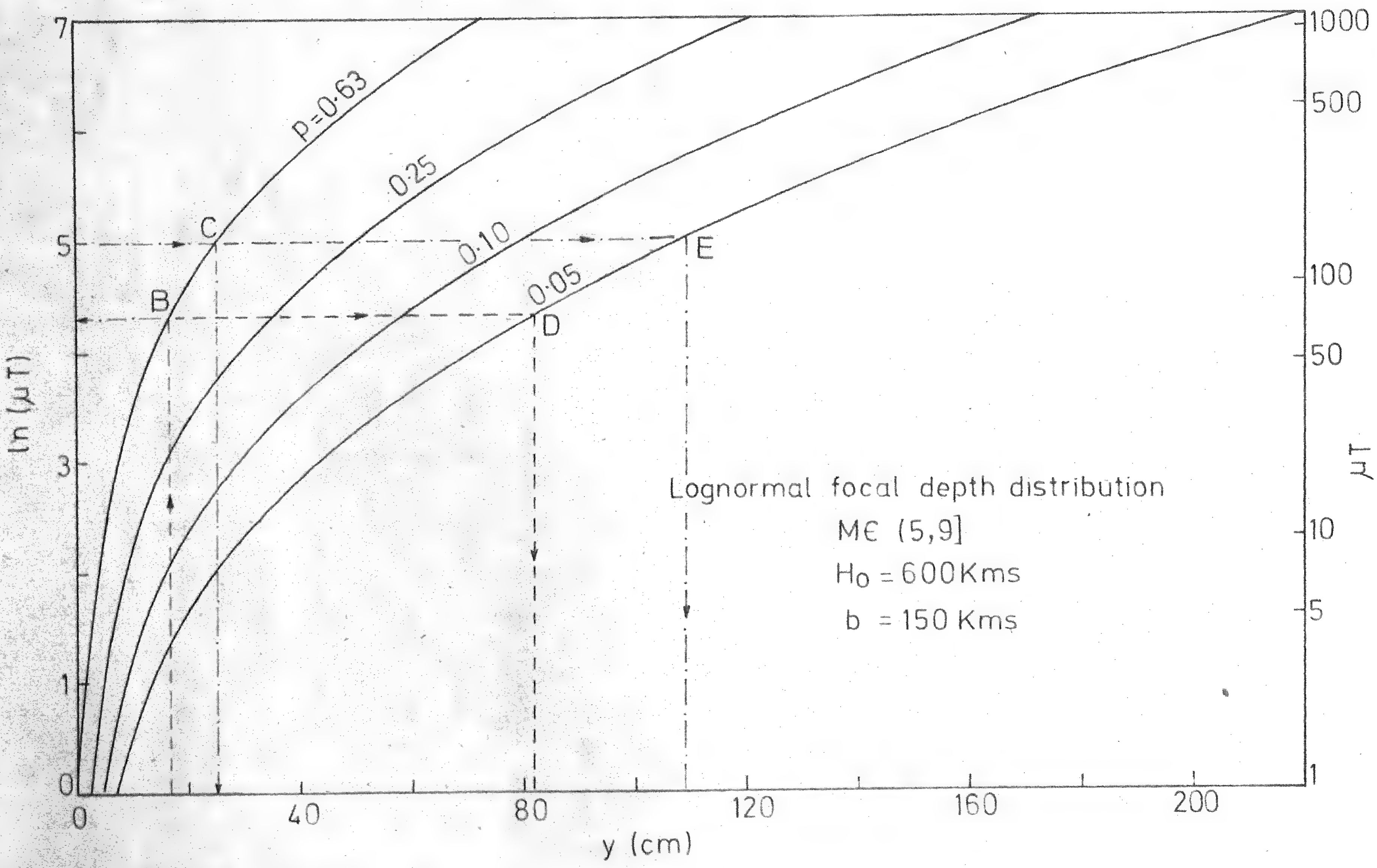

FIG. 4·9 VARIATION OF μT WITH PEAK GROUND DISPLACEMENT, Y

3. Project vertically from C to the abscissa to get the extrapolated generalized intensity for T_y year return period.

Example:

Let T_y=200 years at a location where 100-year peak acceleration is 52.5 cm/sec^2. Following the above procedure the intensity is obtained as 72 cm/sec^2.

4.5.2 Extrapolation for specified exceedance probability

Let the generalized intensity at a location be required for a specified exceedance probability p, over a T year return period. From Eq. (3.22)

$$p=1-F_{Y_{max}}(y;T) = 1-P_M(0,T) = 1-\exp\{-\mu TP[Y > y]\} \qquad (4.26)$$

Graphically the extrapolation can be done in the following steps:

1. Determine the generalized intensity for a T-year return period from the contour map.
2. Locate the point B on the curve marked p = 0.63. Project horizontally to the curve corresponding to required p and locate the point D on it.
3. Project vertically from D to the abscissa to get the extrapolated generalized intensity for the specified exceedance probability, p, and return period, T.

Example

Let peak acceleration is 52.5 cm/sec^2 at a location for 100-year return period. Following the above procedure the intensity is 172.5 cm/sec^2 if design intensity for 100-year return period with exceedance probability, $p = 0.05$, is required. The exceedance probability, $p = 0.05$, is the specified level for nuclear facilities(55).

4.5.3 Extrapolation for specified exceedance probability and specified return period.

If the period T is different from the return period in the contour map, adopt upto step 2 of the procedure for extrapolation for return period. Then

3. Project horizontally from the point C to the specified p-curve and locate point E on it.
4. Project vertically from E to the abscissa to obtain the required generalized intensity.

Example

Let $p = 5\%$ over a 200-year period at a site where 100-year return period peak ground acceleration = 52.5 cm/sec^2. The extrapolation as explained above yields 220 cm/sec^2.

4.5.4 Extrapolation for magnitude cutoff

Let the generalized intensity at a location is required when magnitude, $m \in (5, m_2)$, for a T-year return period. Graphically this extrapolation is achieved from Figs. (3.11-3.13) by following procedure:

1. Determine the generalized intensity for a T-year return period from contour map.
2. Locate the point A on the curve marked, $m_1 = 9$. Project horizontally to the m_2-curve to mark point B on it.
3. Project vertically from B to the abscissa to obtain extrapolated value.

Example

Let $m_2 = \infty$ at a location with peak acceleration of 125 cm/sec^2 for 100-year return period. By above procedure the extrapolated value for 100-year is 135 cm/sec^2.

Any additional extrapolation may be carried out by choosing the proper procedure (4.5.1-4.5.3) as per requirements.

As explained above, the generalised intensity obtained from the 100 year return period contour maps can be easily extrapolated for different return periods and exceedance probability using a set of curves. Such a simple procedure which can be easily incorporated in the codes, has been possible due to the assumption that the peninsula is homogeneous in tectonic features and use of a modular earthquake source. This is the most significant feature of the contour maps presented in this section.

CHAPTER 5

SEISMIC RISK ANALYSIS OF INDIAN PENINSULA-A MODEL NONHOMOGENEOUS IN TECTONIC FEATURES

5.1 Introduction

The contour maps of peak generalised seismic intensities prepared in the previous chapter are based on homogeneous source model which ignores the geotectonic information. In estimating the seismic risk the natural conjugate Bayes density at each grid point is assumed to have identical values of the parameter. In this chapter, the earthquake sources are identified based on available geotectonic information. The natural conjugate Bayes density at different grid points is determined based on its location in the Indian peninsula. For this purpose the tectonic features are idealized. Contour maps of generalised intensities are prepared and compared with the maps based on homogeneous tectonic features.

5.2 Tectonic Features of Indian Peninsula

The tectonogenesis of the Indian peninsula can be pieced together on the basis of the continental drift theory. Starting with Pangae in the late Paleozoic or early Mesozoic period, the formation of Indian peninsula can be traced to its present state. The Indian peninsula is a part of Eurasia composed of mountains of Altaid and Alpide systems. The geological structure varies considerably within both the systems. The Indian peninsula can be classified broadly in three different regions as south of Vindhyas, the regions of Alpide systems and the regions of Altaid system.

The south of Vindhyas is a precambrian shield and consist of Deccan and Sri Lanka. The Deccan is a peneplain composed of ancient metamorphic rocks and partly covered by Late Cretaceous basalts in the western region. The south of Vindhyas has never been submerged totally under the sea. The region is a shield of great rigidity unaffected by any folding. The structural disturbances in this region are'block movement' i.e. displacement in the vertical direction of large land masses between radial faults within the region. The mountains in the Deccan are of 'relict type'.

The regions of Alpide system consist of Indo-Gangetic plain and Himalya and have evidence, in the form of marine deposits starting from Cambrian period, to indicate that the land masses have remained beneath the sea for the greater part of its existence. The Himalaya , a part of Alpide system , is formed during Tertiary age and is composed of comparatively weak and yielding type of rocks. Himalayan tectonics have been interpreted as the compression between the Asian main land and shield of India. These regions are associated with large-scale concentric folding and thrusting. The characteristics of earth-movements are of flexible nature. The wrinkles and folds formed by the tangential thrust on more or less linear zones of earth's surface are the mountain-chains of this region. The indo-gangetic plain is originally a deep depression between north of Vindhyas and Himalaya and is covered up by alluvial deposits of river-clays and silts. The Geological Survey of India considers this great depression as a 'Fore-deep', fronting the Himalayan earth waves, and a sagging part of the Deccan arresting the southward advance of mountain-waves. A second theory considers the depression as a 'Rift-Valley'(91).

A sequence of parallel ranges and high plateaus in the north of Himalaya and a part of Altai region at the edge of Siberia shield form the region of Altaid systems. The Altaids are mostly Paleozoic ranges with intense and wide spread metamorphism. The plateau of Tibet is a stable high platform surrounded by seismically active ranges.

The major tectonic features of India and epicenters of the earthquakes in Indian peninsula are shown in Fig. (5.1). The tectonic features have been idealized in this investigation following closely the suggestion of Srivastava(92) and are shown in Fig. (5.2). The idealized map consists of twentyone faults and eight tectonic units. Among all the tectonic units the 'orogenic unit' and the 'foredeep and marginal depression unit' have undergone maximum tectonic disturbances in comparison to remaining units. The geometric property and the associated seismic activity of each fault and tectonic unit are given in Table 5.1. The significant tectonic features of the idealized map are:

(i) Orogenic unit containing Shillong massif and major thrust of Himalaya

(ii) Foredeep and Marginal depression unit of Himalaya containing Patna, Moradabad, Lucknow faults.

(iii) West Coast and Narmada-Tapti unit containing the tectonic rift that crosses India from the Gulf of Cambay to Bihar.

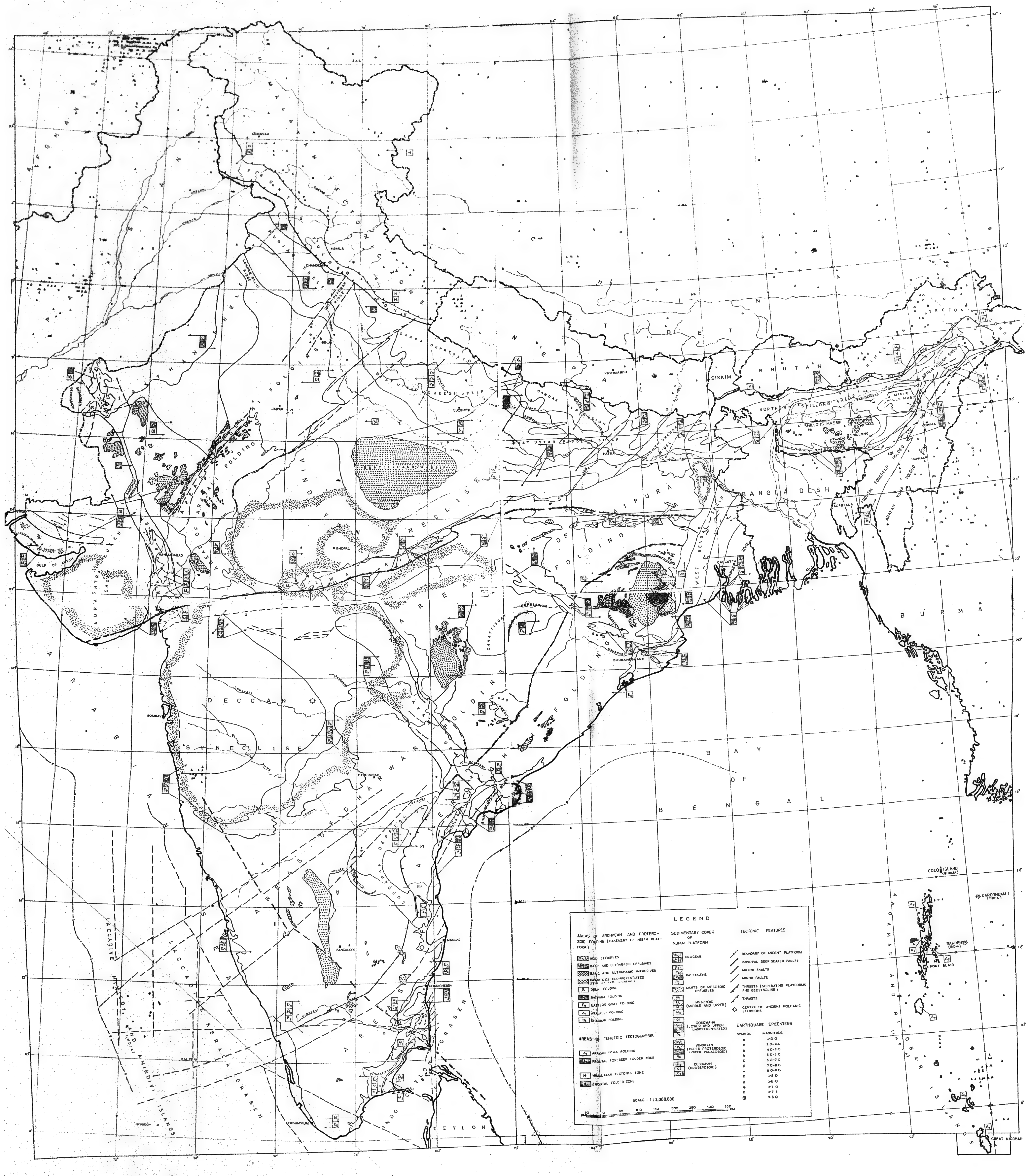
LEGEND
AREAS OF ARCHAEAN AND PROTEROZOIC FOLDING (BASEMENT OF INDIAN PLATFORM)
ACID EFFUSIVES
BASIC AND ULTRABASIC EFFUSIVES
BASIC AND ULTRABASIC INTRUSIVES
GRANITOIDS UNDIFFERENTIATED (SYN OR LATE OROGENIC)
D₁ DELHI FOLDING
SATPURA FOLDING
Eg EASTERN GHAT FOLDING
Ar ARAVALLI FOLDING
Dh DHARWAR FOLDING
AREAS OF CENOZOIC TECTOGENESIS
Ay ARAKAN YOMA FOLDING
Ay FRONTAL FOREDEEP FOLDED ZONE
H HIMALAYAN TECTONIC ZONE
H FRONTAL FOLDED ZONE
SEDIMENTARY COVER OF INDIAN PLATFORM
Ng NEOGENE
Pg PALEOGENE
LIMITS OF MESOZOIC EFFUSIVES
Mz MESOZOIC (MIDDLE AND UPPER)
Gn GONDWANA (LOWER AND UPPER UNDIFFERENTIATED)
Vn VINDHYAN (UPPER PROTEROZOIC LOWER PALAEOZOIC)
Cd CUDDAPAH (PROTEROZOIC)
TECTONIC FEATURES
BOUNDARY OF ANCIENT PLATFORM
PRINCIPAL DEEP SEATED FAULTS
MAJOR FAULTS
MINOR FAULTS
THRUSTS (SEPERATING PLATFORMS AND GEOSYNCLINE)
THRUSTS
CENTRE OF ANCIENT VOLCANIC EFFUSIONS
EARTHQUAKE EPICENTERS
SYMBOL MAGNITUDE
>0.0
2.0-4.0
4.0-5.0
5.0-6.0
6.0-7.0
7.0-8.0
8.0-9.0
>5.0
>6.0
>7.0
>7.5
>8.0
SCALE - 1: 2,000,000
KM 50 0 50 100 150 200 250 300 350 KM
AFGHANISTAN
PAKISTAN
TIBET
NEPAL
SIKKIM
BHUTAN
BANGLA DESH
BURMA
CEYLON
ARABIAN SEA
BAY OF BENGAL
SRINAGAR
SIMLA
CHANDIGARH
DELHI
JAIPUR
LUCKNOW
KATHMANDU
PATNA
SHILLONG
IMPHAL
AGARTALA
CALCUTTA
BHOPAL
AHMADABAD
BOMBAY
HYDERABAD
BHUBANESHWAR
MADRAS
BANGALORE
PONDICHERRY
TRIVANDRUM
PORT BLAIR
GULF OF KUTCH
SAURASHTRA
DECCAN SYNECLISE
HIMALAYAN TECTONIC ZONE
SHILLONG MASSIF
NORTHERN SHILLONG SHELF
MIKIR HILLS MASSIF
UPPER ASSAM SHELF
WEST BENGAL SHELF
CHHATTISGARH
AREAS OF SATPURA FOLDING
AREAS OF ARAVALLI FOLDING
AREAS OF DELHI FOLDING
AREAS OF DHARWAR FOLDING
AREAS OF EASTERN GHAT FOLDING
GANDAK DEPRESSION
SARDA DEPRESSION
WEST UTTAR PRADESH SHELF
EAST UTTAR PRADESH SHELF
VINDHYAN SYNECLISE
LACCADIVE
LACCADIVE MINICOY AND AMINDIVI ISLANDS
KERALA GRABEN
INDO CEYLON GRABEN
ANDAMAN AND NICOBAR ISLANDS
COCO ISLAND (BURMA)
NARCONDAM I. (INDIA)
BARREN I. (INDIA)
GREAT NICOBAR

FIG. 5.1 SEISMO-TECTONIC MAP OF INDIA

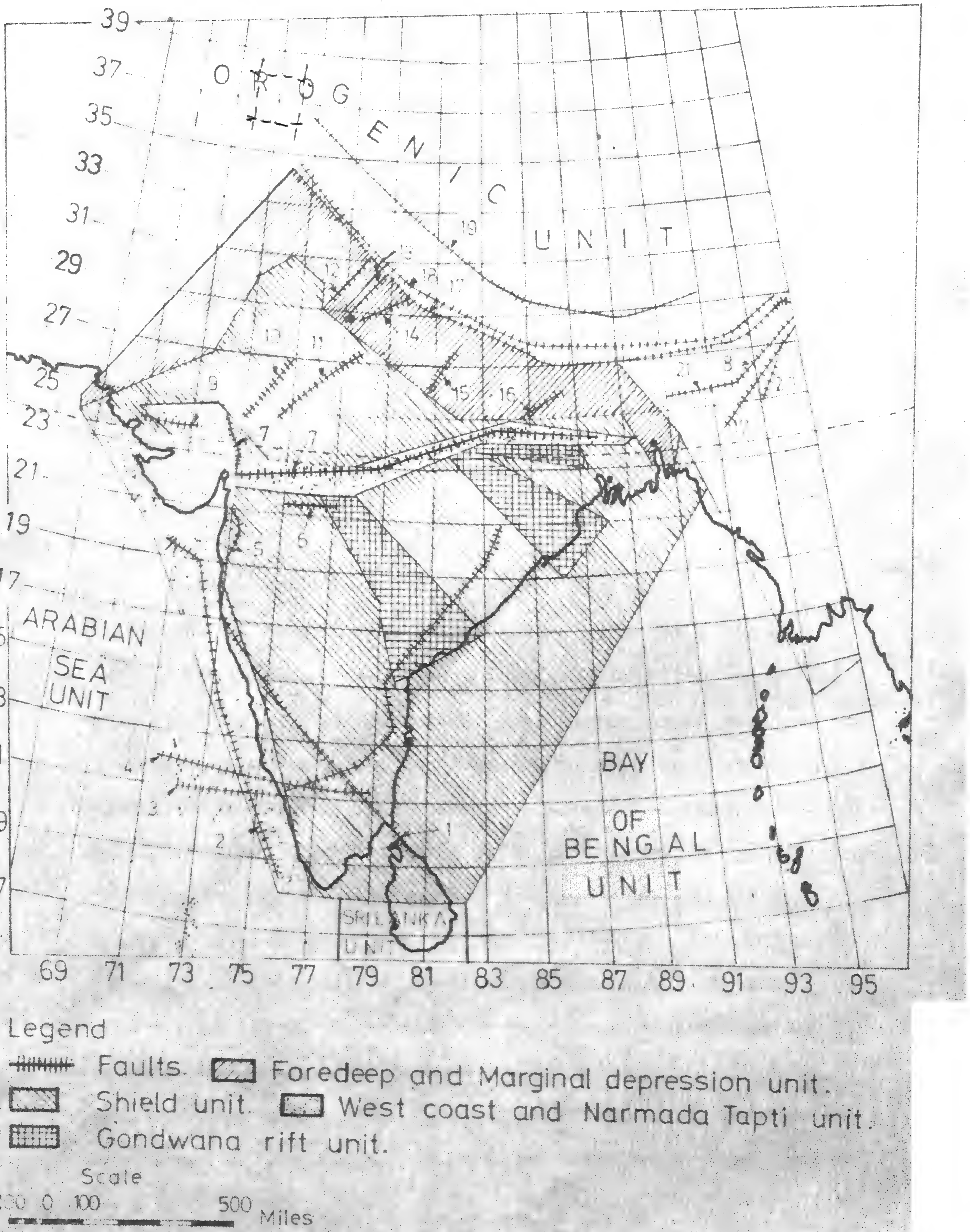
O R O G E N I C U N I T
ARABIAN SEA UNIT
BAY OF BENGAL UNIT
SRI LANKA UNIT
39
37
35
33
31
29
27
25
23
21
19
17
15
13
11
9
7
69
71
73
75
77
79
81
83
85
87
89
91
93
95
Legend
Faults.
Foredeep and Marginal depression unit.
Shield unit.
West coast and Narmada Tapti unit.
Gondwana rift unit.
Scale
100 0 100 500 Miles

IDEALIZED TECTONIC FEATURES OF INDIAN PENINSULA..
FIG. 5·2

(iv) Gondowana Rift unit - a part of the southern shield with Mesozoic or early cenozoic sedimentary cover.

(v) Shield unit containing non active ancient faults.

(vi) Bay of Bengal unit containing seismically active Andaman and Nicobar island of the Burma arc.

(vii) The Arabian sea unit containing Chagos-Laccadive ridge of ballastic magma.

(viii) Sri Lanka unit containing part of Sri Lanka which is a part of Indian shield

5.3 Earthquake Sources

The earthquake sources in the seismic risk analysis, based, on non-homogeneous tectonic features, consist of faults, which are area sources, and volume sources. The risk analysis for volume sources has been treated in the previous chapter. The probability of exceedance of generalised intensity (Eq. 3.19) for faults, which is idealized as segment of great circle, is obtained by passing a plane through the fault and transforming the plane to the equatorial position. The transformation enabling to rotate a fault plane to the position of the equator is given in Appendix A5.1. The formulae (Eqs. 3.25-3.27 and 3.30-3.34) for probability of exceedance of peak generalised seismic intensity for assumed distribution of focal depth, H, and magnitude, M, of earthquakes with suitable changes in the probability density, $f_R(.)$, and probability distribution, $F_R(.)$, of focal distance, R, remain valid even in case of area source. The detailed derivation of these functions are given in Appendix A5.2.

5.4 T-year Generalised Peak Seismic Intensity

The faults within a volume source at a site are assumed to be mutually statistically independent and also statistically independent with respect to the volume source. Let the number of faults at a particular site be n. The probability distribution function of maximum peak generalized seismic intensity can be formally written as

$$F_{Y_{max}}(y;t) = \prod_{i=1}^{n+1} P\,[\,Y_{max_i} \leq y;\ t\,] \tag{5.1}$$

in which Y_{max_i} is the maximum peak generalised intensity for the source, i. The source $n+1$ represent the volume source at the site and the sources $i=1,\ldots,n$ represent n number of area sources associated with the faults. If $\{L_i(t);\ t \geq 0,\ i=1,\ldots,n+1\}$ are the number of earthquakes owing to sources which produce peak generalised seismic intensity at a site greater than a value, y, during a time interval, t, the Eq. (5.1) can be further simplified as

$$F_{Y_{max}}(y;t) = \prod_{i=1}^{n+1} P_{L_i}(o,t) = \exp\,[\,-\sum_{i=1}^{n+1} \mu_i t\ S_{Y_i}(y)\,] \tag{5.2}$$

in which μ_i is the intensity of earthquake arrival in the ith source and $S_{Y_i}(y) = P\,[\,Y_i > y\,]$ is the probability of exceedance of peak generalised seismic intensity, Y_i, at a site owing to ith source. The probability distribution of annual maximum peak generalized seismic intensity is obtained by substitution of $t=1$ in the Eq. (5.2):

$$\begin{aligned} F_{Y_{max}}(y;1) &= P\,[\,Y_{max} \leq y\ ;\ 1\,] \\ &= \exp\,[-\sum \mu_i\ S_{Y_i}(y)\,] \qquad (5.3) \\ &\simeq 1 - \sum \mu_i\ S_{Y_i}(y) \qquad [\because \sum \mu_i\ S_{Y_i}(y) << 1\,] \end{aligned}$$

which yields

$$P[\, Y_{max} > y;\ 1\,] = \sum \mu_i \;\; S_{Y_i}(y)$$

The average return period, T_y, of peak generalised seismic intensity exceeding a value, y, is given by

$$T_y = 1/P\,[\,Y_{max} > y; 1\,] = 1/\ \{ \sum \mu_i \;\; S_{Y_i}(y) \} \qquad (5.4)$$

The T-year generalised seismic intensity at a site for a given time period T_y is obtained by solving Eq. (5.4) for y.

5.5 Estimation of parameters of earthquake arrival process for various seismo-tectonic provinces and faults.

The intensity and the coefficient of variation of intensity of arrival process in the required magnitude range are estimated from Eqs. (4.1 and 4.12) for the Indian peninsula. The volume of each seismo-tectonic province is calculated. Using Eqs. (4.13-14) and variability of seismicity in Indian peninsula (Fig. 4.3), the intensity and coefficient of variation of intensity of earthquake process for each seismotectonic province is obtained. These results are reported in Table 5.1.

Assuming each fault is of unit thickness, the intensity and coefficient of variation of intensity of arrival process are estimated following the procedure of estimation for seismotectonic province. The results are shown in Table 5.1.

Table 5.1

Geometric and associated Seismic activity of Tectonic units and Faults of Indian Peninsula.

Tectonic Units

Name	V*	$\hat{\mu} \times 10^4$ (#/day)	$C^2(\mu) \times 10$
Orogenic unit	110.01	295.0	5.085
Foredeep and Marginal depression unit	20.29	54.4	20.060
West coast and Narmada-Tapti unit	16.12	43.2	23.021
Gondowana rift unit	8.73	23.4	32.347
Shield unit	64.76	173.7	8.723
Bay of Bengal unit	43.63	117.0	11.997
Arabian Sea unit	34.96	93.7	14.078
Sri Lanka unit	2.12	5.7	65.582

Actual volume of unit = $V^* \; \{3a(a-H_o) + H_o^2\} H_o \; 10^{-3}/3 \; Km^3$

Faults

Fault Number	Length (Kms.)	$\hat{\mu} \times 10^6$ (#/day)	$C^2(\mu)$
1	1209.7	8.38	41.19
2	1512.3	10.48	37.51
3	2293.0	5.88	31.50
4	848.5	5.88	47.75
5	258.0	1.79	78.22

Table 5.1 contd.

6	260.4	1.80	77.93
7	1846.9	12.79	34.50
8	388.7	2.69	66.03
9	279.3	15.88	31.50
10	342.6	2.37	69.57
11	464.6	3.22	61.33
12	205.7	1.43	85.90
13	265.6	1.84	77.30
14	233.9	1.62	81.46
15	279.2	1.93	75.71
16	316.2	2.19	71.91
17	3275.5	22.69	27.10
18	2575	17.84	29.99
19	2079.9	14.41	32.82
20	218.8	1.52	83.74
21	302.1	2.09	73.29

5.6 Estimation of Parameters of Arrival Process at Grid Points.

The procedure of Section 4.3 is used to estimate the parameters of volume source at the site. However, the number, r, of earthquakes originated in the volume source at site exclude earthquakes originated in the faults. All earthquakes which have epicenter within 50 kms. from a fault are assumed to be caused by the fault. The effective length of a fault at the site is assumed to be the length of the fault intersected by a circle with centre at the site and having a radius of 150 kms. at the surface of earth. Similar procedure for volume source (Section 4.3) is adopted to estimate the parameters of the arrival process for a fault associated with the site.

5.7 Results and Discussion

The results of the seismic risk analysis for 100-year return period at each grid point is obtained numerically adopting iterative procedure and are plotted in contour forms in Figs. (5.3-5.5). The tolerance of one year in the higher side is used for return period. The regional effects of active faults are reflected in the contours. Comparison of Figs. (4.4-4.6 and 5.3-5.5) shows that the shape of contours for different regions have changed from homogeneous model analysis. The reason is the acceptance of different Bayes natural conjugate density for various seismotectonic provinces and that of faults. However, values of generalised intensities are quite compairable in most of the parts of Indian peninsula for homogeneous and nonhomogeneous analysis. In the Koyna region (grid point 84) contours have enlarged

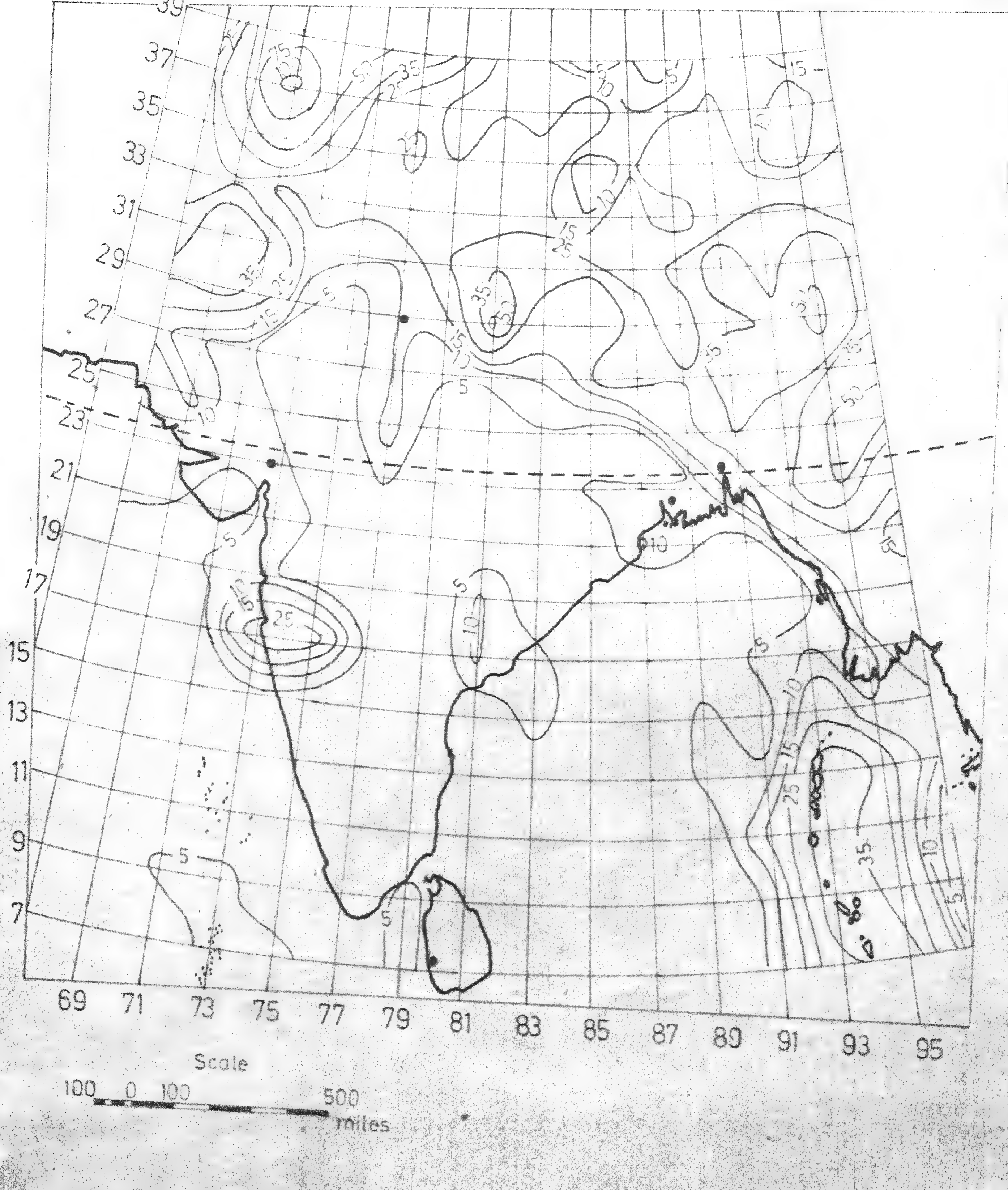
39
37
35
33
31
29
27
25
23
21
19
17
15
13
11
9
7
69
71
73
75
77
79
81
83
85
87
89
91
93
95
75
50
35
25
15
10
5
Scale
100 0 100 500
miles

FIG. 5·3 PEAK ACCELERATION (cm/sec^2) CONTOURS-LOGNORMAL DISTRIBUTION OF FOCAL DEPTH, M$\in$(5,9] & NONHOMOGENEOUS IN TECTONIC FEATURES

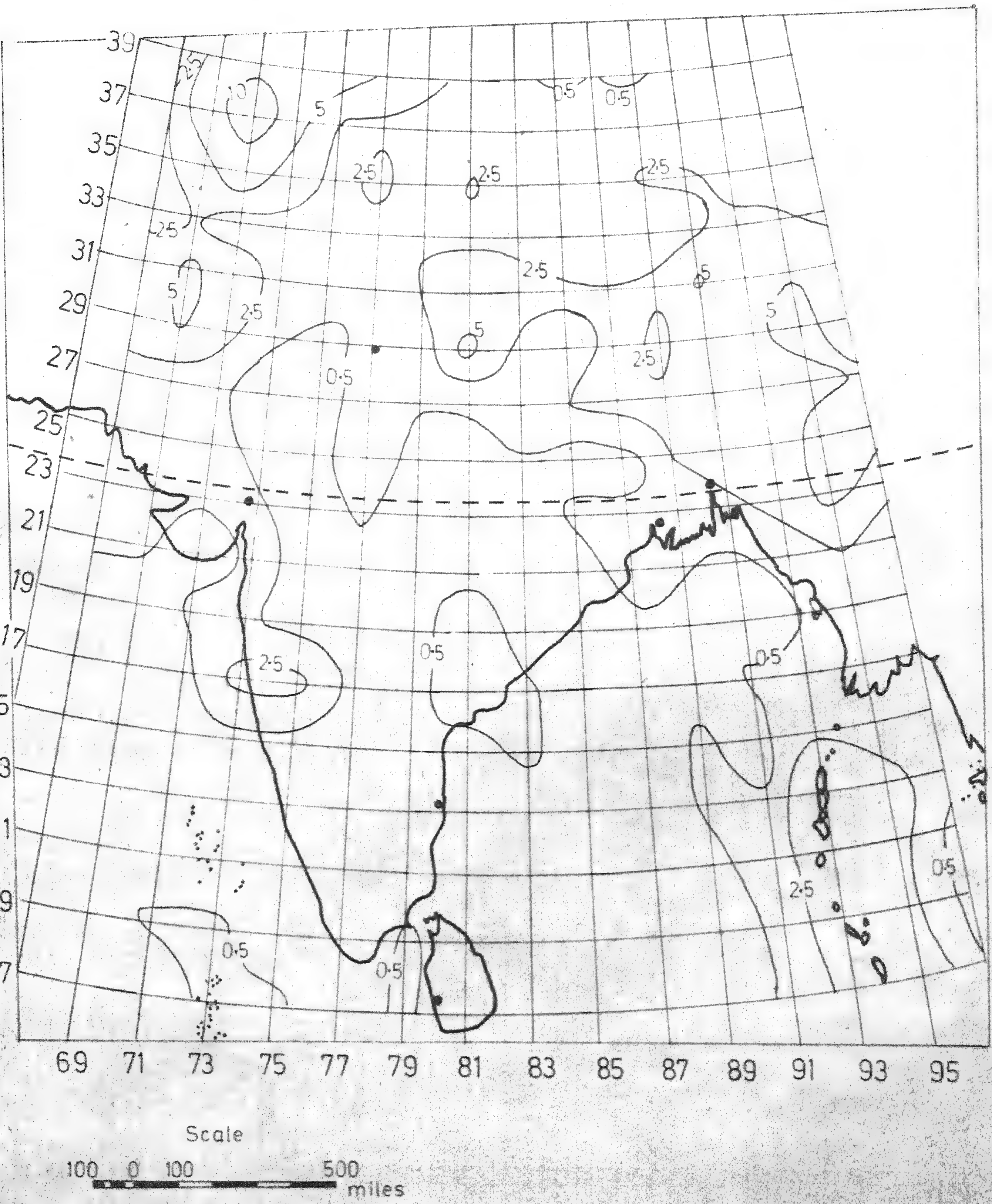
39
37
35
33
31
29
27
25
23
21
19
17
15
13
11
9
7
69
71
73
75
77
79
81
83
85
87
89
91
93
95
2·5
10
5
0·5
0·5
2·5
2·5
2·5
2·5
2·5
5
2·5
5
2·5
5
5
2·5
0·5
2·5
0·5
0·5
0·5
2·5
0·5
0·5
Scale
100 0 100 500
miles

FIG. 5·4 PEAK VELOCITY (cm/sec) CONTOURS-LOGNORMAL DISTRIBUTION OF FOCAL DEPTH, M∈ (5, 9] & NONHOMOGENEOUS IN TECTONIC FEATURES

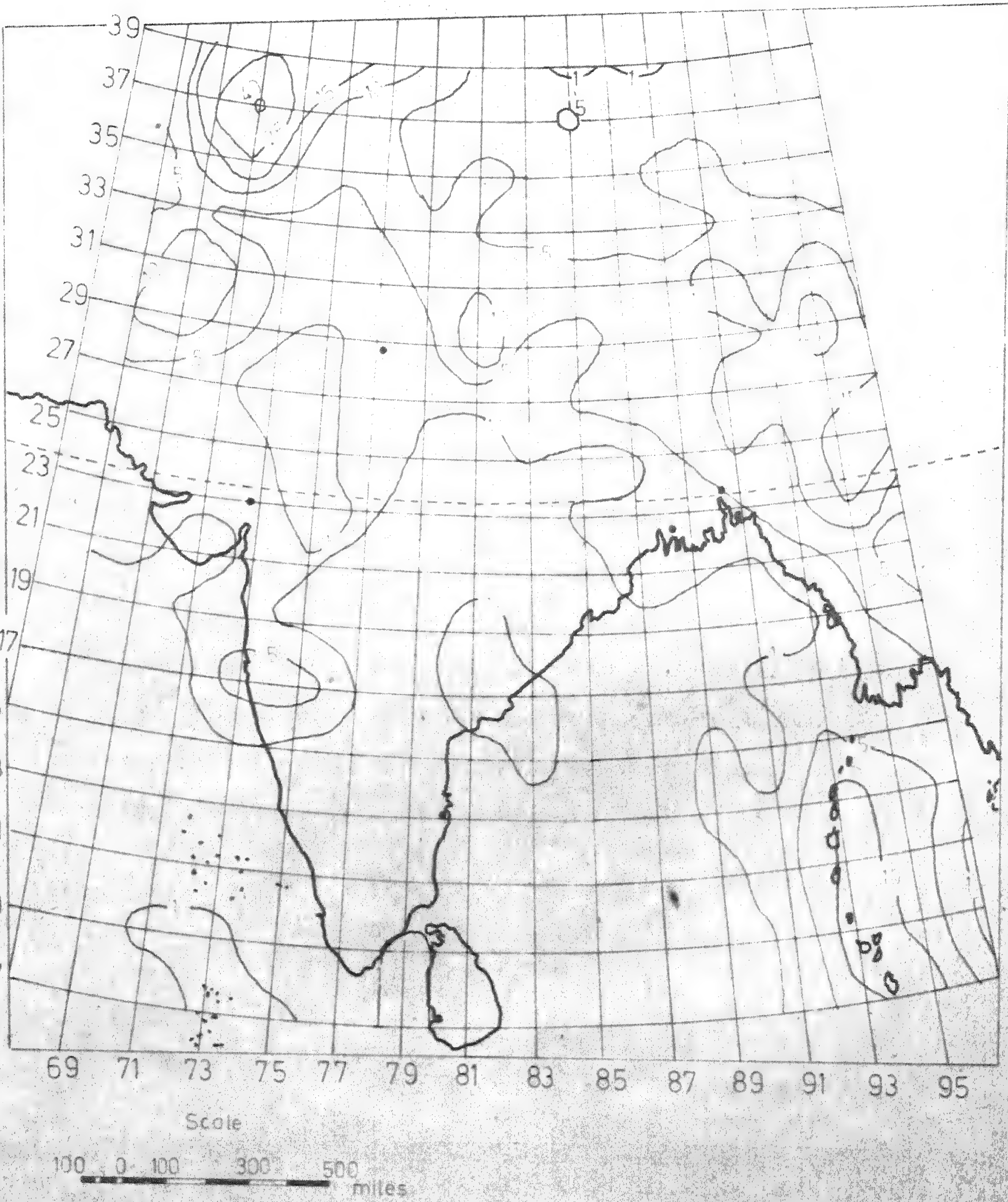
39
37
35
33
31
29
27
25
23
21
19
17
15
13
11
9
7
69
71
73
75
77
79
81
83
85
87
89
91
93
95
1
5
Scale
100 0 100 300 500
miles

FIG. 5·5 PEAK DISPLACEMENT (cm) CONTOURS-LOGNORMAL DISTRIBUTION OF FOCAL DEPTH, M∈ (5,9] AND NONHOMOGENEOUS IN TECTONIC FEATURES because of the fault (number 1). Further the accounting of faults (number 11-14) causes considerable changes in the shape of contours in the central part of India. The contours in the Gondowana rift unit (grid point 88) become parallel to the tectonic province. In general the assumption of nonhomogenity of tectonic feature builds up generalised seismic intensity in the proximity of faults and makes the contours parallel to the seismotectonic province.

In view of the above, it is concluded that the seismic zoning map should be drawn on the basis of seismic risk analysis with sources identified on the basis of tectonic features. However, extrapolation of the contour maps for the nonhomogeneous model is not possible because of the presence of effects of various sources at a site in the denominator of the Eq. (5.4) on which computation of T-year intensity is based. A fresh computation of seismic risk analysis is necessary for information other than that presented in the contour maps in Figs. (5.3-5.5).

CHAPTER 6

EFFECT OF SCATTER IN THE ATTENUATION LAWS ON SEISMIC RISK

6.1 Introduction

In the preceeding chapters the attenuation laws have been assumed to be deterministic. The generalized attenuation law proposed by Kanai(89) and Esteva and Rosenblueth(24) (Eq. 3.10) is used in this thesis. The constants involved in the attenuation laws are taken according to the values suggested by Esteva and Rosenblueth. An excellent review on similar laws is given in Ambraseys(23) paper the parameters of the law are determined from regression analysis. The data used by Esteva and Rosenblueth shows large scatter around the best fit equation as shown in Figs. (6.1 and 6.2). This is because the geological conditions of the data are significantly different. The results of Esteva(42) and Cornell(54) show that the effect of scatter on the seismic risk is significant. In this chapter two models are proposed to incorporate the effect of scatter on seismic risk besides the Gaussian model due to Esteva(42). Steps to incorporate the effect of scatter in the zoning maps are indicated.

6.2 A Gaussian Model

Esteva and Rosenblueth(24) obtained the parameters of attenuation laws by fitting equation to the data. The theory of least sqaere fit assumes the existance of an unobservable error. The attenuation law with the unobservable error is given by

$$Y = C_1 \exp \left[C_2 M - C_3 \ln (R + C_4) + \varepsilon\right] \qquad (6.1)$$

where ε is a Gaussian random variable with mean, ξ, and variance, σ^2. C_1, C_2 and C_3 are empirical constants. The inclusion of the parameter ε

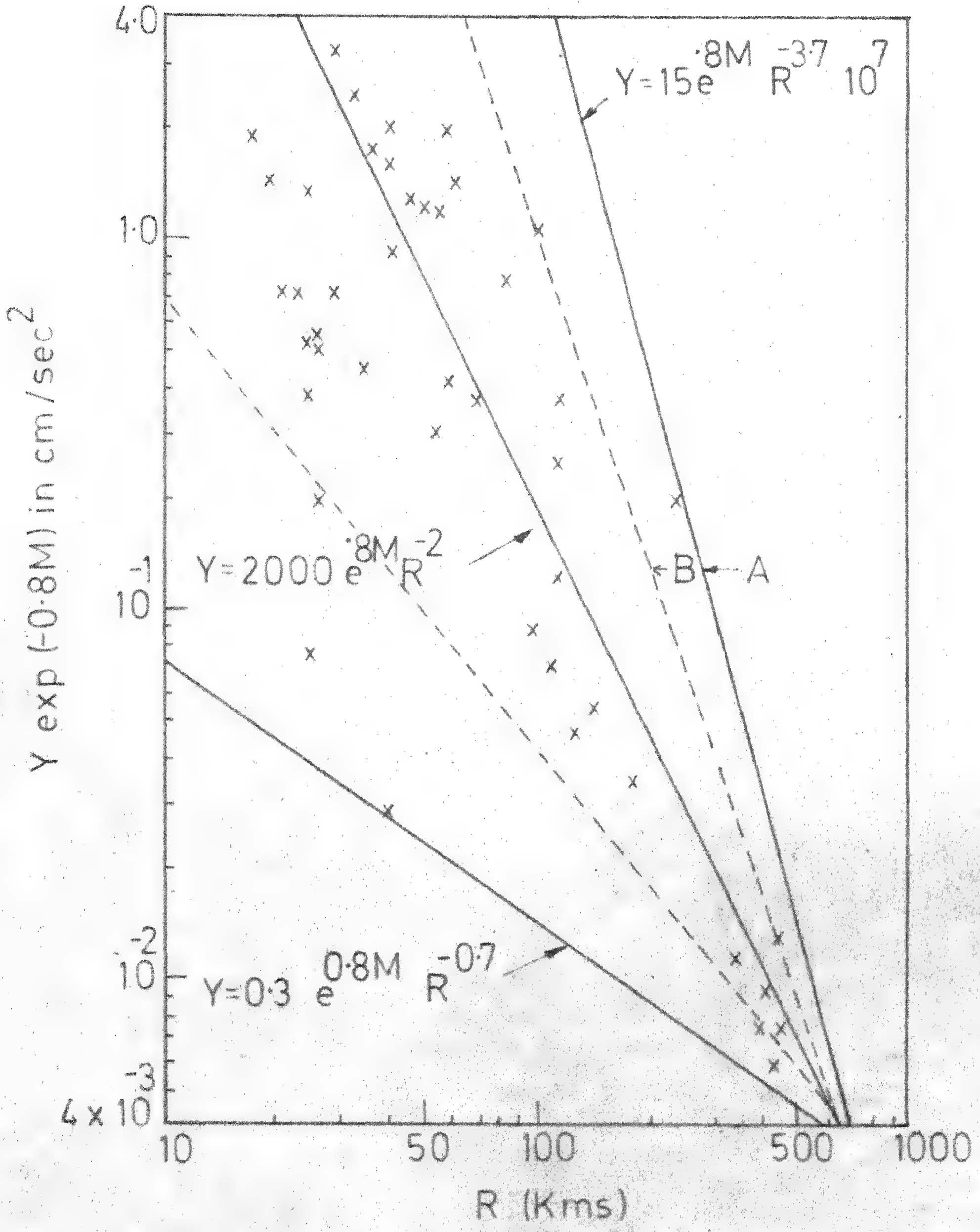

FIG.6·1 ATTENUATION LAW FOR PEAK GROUND ACCELERATION, Y

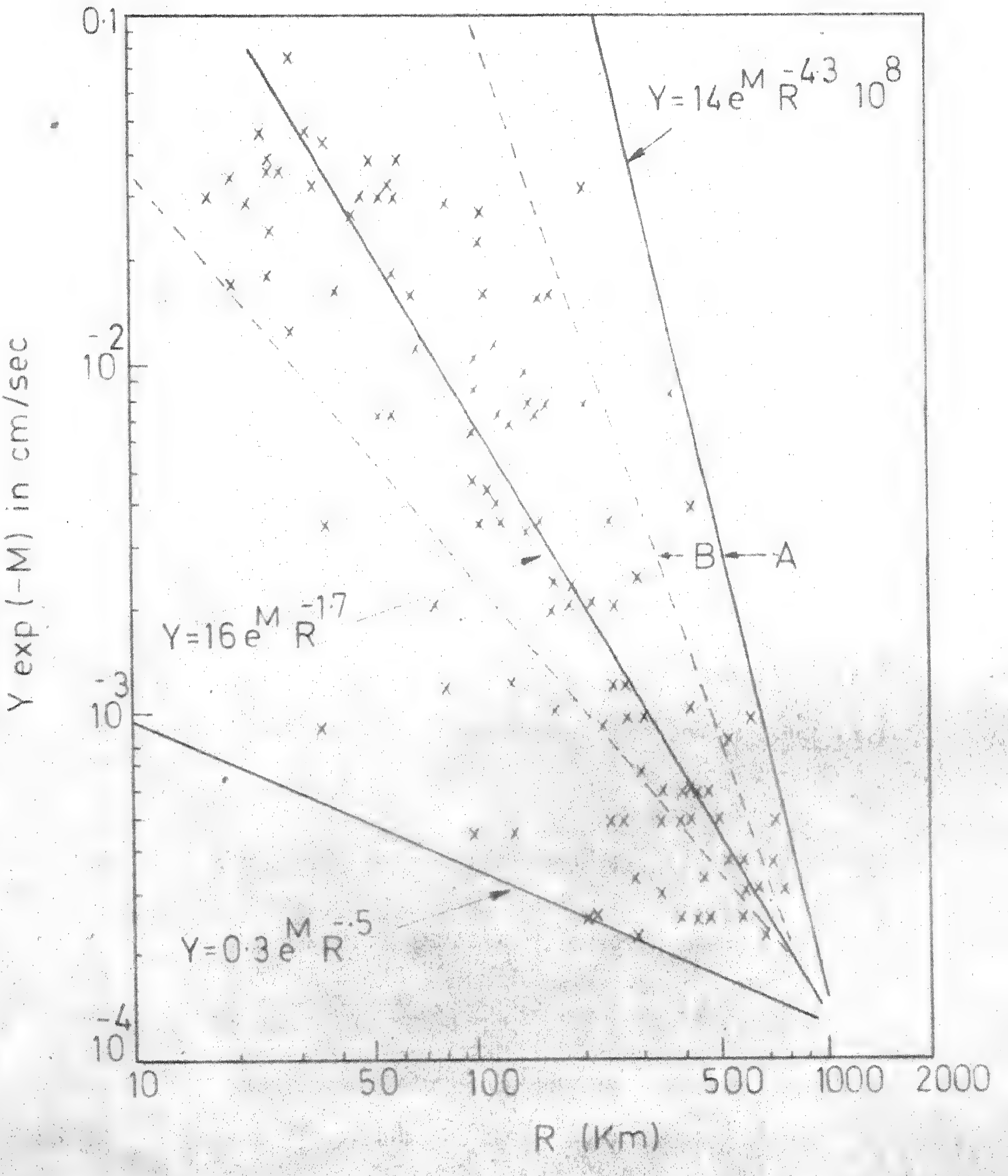

FIG 6.2 ATTENUATION LOW FOR PEAK GROUND VELOCITY Y

changes the exceedance probability of Y in Eq. (3.19) and therefore the seismic risk.

6.2.1 Probability of Generalised intensity

The probability of generalised seismic intensity is obtained using the fact that the random variables M, R and ε are mutually independent. The probability of generalised seismic intensity is given by

$$P\left[Y > y\right] = \int\int P\left[Y > y \mid z,w\right] f_{ZW}(z,w)\, dz\, dw \tag{6.2}$$

where

$$Z = C_1 \exp\left(C_2 M\right) \tag{6.3}$$

and
$$W = (R + C_4)^{-C_3} \tag{6.4}$$

and $f_{ZW}(\cdot,\cdot)$ is the joint probability density function of Z and W. Using the property of statistical independence, the conditional probability in Eq. (6.2) can be evaluated as

$$\begin{aligned} P\left[Y > y \mid z,w\right] &= P\left[\exp(\varepsilon) > y/(zw) \mid z,w\right] \\ &= P\left[\exp(\varepsilon) > y/(zw)\right] \\ &= 1 - \Phi\{(\ell n\, y - \ell n\, z - \ell n\, w - \xi)/\sigma\} \end{aligned} \tag{6.5}$$

where $\Phi(\cdot)$ is the probability distribution function of N(0,1). The probability (Eq. 6.2) can be evaluated by substituting Eq. (6.5) into it and using the distribution law of Z and W.

6.2.1.1 The probability of generalised intensity for magnitude cutoff at lower level i.e. $m \varepsilon (m_0, \infty)$

The probability density function of Z is given by

$$f_Z(z) = \beta \exp[\,\beta\{m_o+(\ell n\ C_1 - \ell n\ z)/C_2\}]/(C_2 z); \quad z\ \varepsilon\ (C_1 \exp\ (C_2\ m_o),\infty) \qquad \ldots \quad (6.6)$$

Substitution of Eq. (6.5) into Eq. (6.2) and use of statistical independence yields

$$P\,[Y > y] = 1 - \int_{w_1}^{w_2} \int_{z_1}^{\infty} \Phi\{(\ell n\ y - \ell n\ z - \ell n\ w - \xi)/\sigma\}\ f_Z(z)\ f_W(w)\ dz\ dw \qquad \ldots \quad (6.7)$$

where

$$z_1 = C_1 \exp\ (C_2\ m_o) \qquad (6.8)$$

$$w_1 = C_4^{-C_3} \qquad (6.9)$$

$$w_2 = (C_4 + R_o)^{-C_3} \qquad (6.10)$$

and R_o is the maximum focal distance.

Integration with respect to z and subsequent substitution of $w = (r + C_4)^{-C_3}$ results in

$$\begin{aligned} S_Y(y) = P\,[Y > y] = 1 - \int_0^{R_o} [\,&\Phi\{(\alpha - \ell n\ z_1)/\sigma\} + \\ &+ \exp\,[\,\beta\{m_o + 1/C_2\ [\ell n\ C_1 - \alpha + \sigma^2 \beta/(2C_2)]\}\,] \\ &\times \Phi\{(\ell n\ z_1 + \sigma^2 \beta/C_2 - \alpha)/\sigma\}]\,f_R(r)\ dr \\ &+ \int_0^{R_o} \exp[\,\beta\{m_o+1/C_2[\,\ell n\ C_1 + \sigma^2\beta/(2C_2) - \alpha]\}\,]\,f_R(r)\ dr; \quad y \geq 0 \end{aligned} \qquad \ldots \quad (6.11)$$

where

$$\alpha = \ell n\ y + C_3\ \ell n(r + C_4) - \xi \qquad (6.12)$$

and $f_R(\cdot)$ is the probability density of R. Details of $f_R(\cdot)$ is given in Appendix A3.8.1. Substitution of Eq. (6.11) in Eq. (3.24) yields average return period, T_Y, of peak generalised seismic intensity.

6.2.1.2 The probability of generalised seismic intensity for magnitude cutoff at both ends i.e. $m \varepsilon (m_o, m_1]$

Use of statistical independence and substitution of Eq. (6.5) into Eq. (6.2) results in

$$S_Y(y) = P[Y > y] = 1 - \int_{w_1}^{w_2} \int_{z_1}^{z_2} \Phi\{(\ell n\, y - \ell n\, z - \ell n\, w - \xi)/\sigma\} f_Z(z)\, f_W(w)\, dz\, dw \qquad (6.13)$$

where

$$f_Z(z) = \exp[\beta\{m_o + (\ell n\, C_1 - \ell n\, z)/C_2\}]\, K\beta/(zC_2);\; z \;\varepsilon\, (z_1, z_2] \qquad (6.14)$$

$$1/K = 1 - \exp[(m_o - m_1)\beta] \qquad (6.15)$$

$$z_2 = C_1 \exp(C_2\, m_1) \qquad (6.16)$$

and w_1, w_2 and z_1 are defined in Eq. (6.8 - 6.10).

The following result is obtained by proceeding in similar lines as in Eq. (6.11).

$$S_Y(y) = P[Y > y] = 1 + K \int_0^{R_o} [\Phi\{(\alpha - \ell n\, z_2)/\sigma\} \exp\{\beta(m_o - m_1)\} - \Phi\{(\alpha - \ell n\, z_1)/\sigma\} + \exp[\beta\{m_o + 1/C_2[\ell n\, C_1 + \sigma^2\beta/(2C_2) - \alpha]\}]$$
$$\times \{\Phi[(\ell n z_2 + \sigma^2\beta/C_2 - \alpha)/\sigma] - \Phi[(\ell n\, z_1 + \sigma^2\beta/C_2 - \alpha)/\sigma]\}] f_R(r)\, dr \;;\; y \geq 0 \qquad (6.17)$$

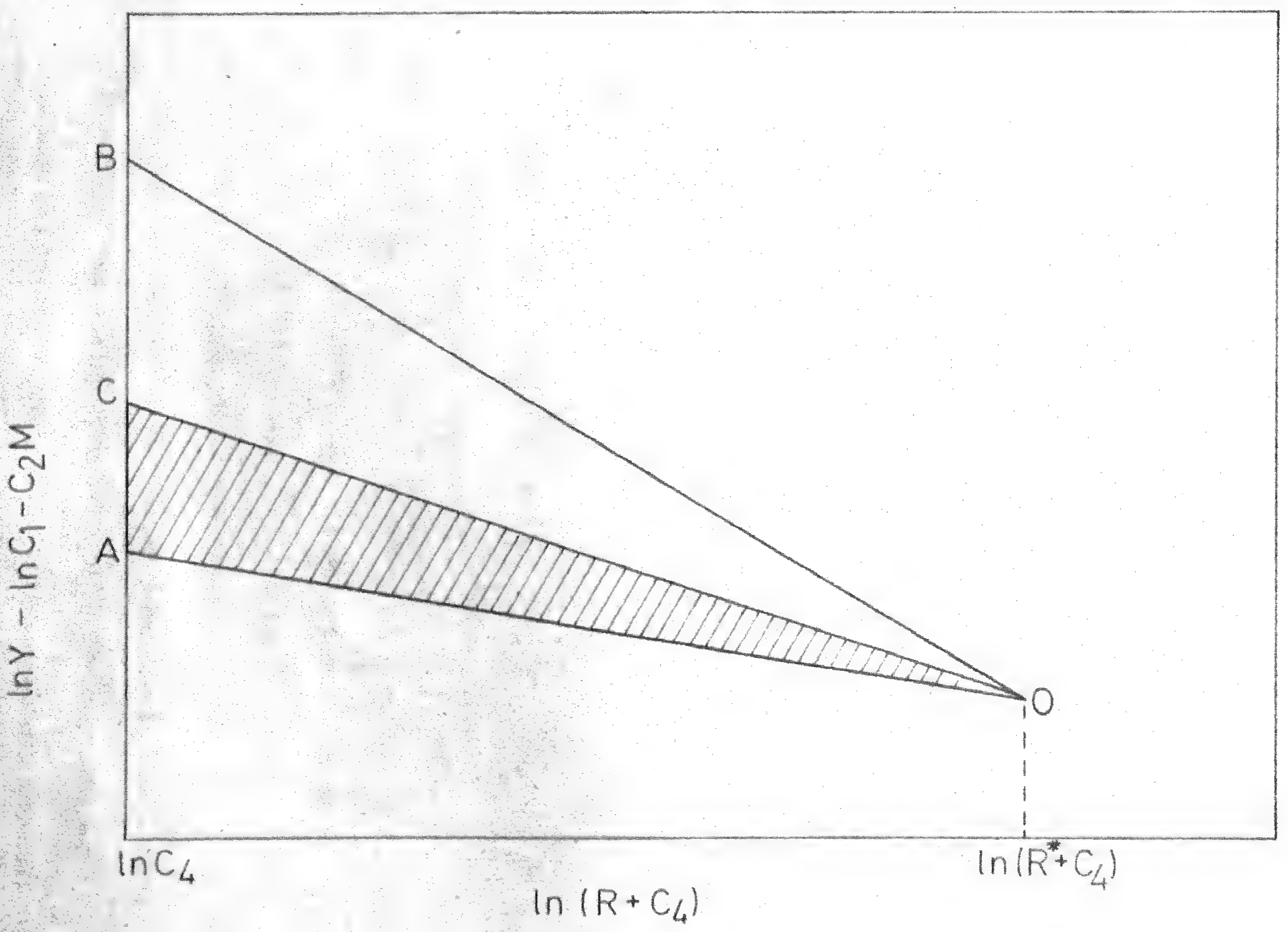
B
C
A
O
$\ln Y - \ln C_1 - C_2M$
$\ln C_4$
$\ln(R^* + C_4)$
$\ln(R + C_4)$

FIG. 6·3 ENVELOPES OF SCATTER

where α is defined by Eq. (6.12). The probability density function, $f_R(\cdot)$ of focal distance, R, is given in Appendix A.3.8.1. Substitution of Eq. (6.17) in Eq. (3.24) yields average return period, T_y, of peak generalised seismic intensity.

The Eq. (6.17) is integrated numerically for different attenuation laws and the results are presented in Figs. (6.7 - 6.9). The in the attenuation law (Eq. 6.1) is taken to be N(0,0.4225) for peak ground acceleration and N(0,0.5625) for peak ground velocity and displacement in accordance with Esteva[(42)].

6.3 Proposed Model for Scatter in Attenuation law - Model - 1

The effect of scatter can also be accounted for by fitting envelope functions of the form

$$Y = C_1 \exp \ [C_2 M - C_3 \ell n (R + C_4)] \qquad (6.18)$$

to the data used by Esteva and Rosenblueth[(24)].
Let R* be the focal distance where both the upper envelope OB and the lower envelope OA, and the attenuation law with the values of the constants as proposed by Esteva and Rosenblueth[(24)] (Section 3.6) meet at O as shown in Fig. (6.3). Any line, OC, drawn through, O, the point of intersection of the envelopes, OA and OB, is considered to be equally likely. The ratio of the shaded area (Fig. 6.3) to the total area bounded by OA and OB gives the probability that the actual generalised intensity will be less than or equal to the generalised intensity predicted by using OC which represent the attenuation law.

6.3.1 The choice of envelopes

Two sets of envelopes are drawn and are marked A and B in Figs. (6.1 and 6.2). The envelope marked A encompases all the data points whereas envelope marked B encompases most of the data points within focal distance of 300 Kms. These envelopes are drawn visually. The values of C_1, C_2 and C_3 for these envelopes are given in Table 6.1. Table 6.2 contains values of parameters C_1 and C_3 for a few probability levels. The envelopes A and B for peak ground displacement are derived from the corresponding envelopes of peak ground acceleration and velocity and satisfying approximate relation

$$ad/v^2 \simeq 1 \tag{6.19}$$

where a, v and d are in cm/sec^2, cm/sec and centimeters respectively.

The results in term of $P[Y > y]$ for a few probability levels are shown in Figs. (6.4 - 6.6) for peak ground acceleration, velocity and displacement and are obtained following procedure discussed in Chapter 3.

6.4 Proposed Model for Scatter in attenuation law - Model - 2

The generalised attenuation law (Eq. 3.10) is given by

$$Y = Z/W \tag{6.20}$$

where

$$Z = C_1 \exp(C_2 M) \tag{6.21}$$

$$W = (R + C_4)^{C_3} \tag{6.22}$$

Table 6.1

Parameters of Envelopes

Envelope A	C_1			C_2	C_3			C_4
	b_1	b_2	b_3		a_1	a_2	a_3	
Acceleration	0.35612	2000.0	1.6×10^8	0.8	0.7	2.0	3.7	25.0
Velocity	0.003348	16.0	1.5×10^9	1.0	0.5	1.7	4.3	25.0
Displacement	0.001514	7.0	1.40625×10^{10}	1.2	0.3	1.6	4.9	25.0
Envelope B								
Acceleration	11.544	2000.0	6.6×10^5	0.8	1.2	2.0	2.9	25.0
Velocity	0.5903	16.0	4.4×10^4	1.0	1.2	1.7	2.9	25.0
Displacement	0.5313	7.0	3.05×10^4	1.2	1.2	1.6	2.9	25.0

Values of b_2 and a_2 correspond to Esteva and Rosenblueth(24).

Table 6.2

Values of C_1 and C_3 for different probability levels for envelopes A and B

Generalised Intensity	Envelope A			Envelope B		
	probability	C_1	C_3	probability	C_1	C_3
Acceleration	0.433	2000.0	2.0	0.471	2000.0	2.000
	0.500	7548.5	2.20	0.500	2760.3	2.050
	0.750	1099.0×10^3	2.95	0.750	42682	2.475
	0.900	2182.1×10^4	3.40	0.900	2207.1×10^2	2.730
	0.950	5908.7×10^4	3.55	0.950	3816.7×10^2	2.815
Velocity	0.316	16.0	1.70	0.294	16.0	1.700
	0.500	2241.0	2.40	0.500	161.2	2.050
	0.750	1833.4×10^3	3.35	0.750	2662.9	2.475
	0.900	1025.6×10^5	3.92	0.900	14329.0	2.730
	0.950	3922.2×10^5	4.11	0.950	25109.0	2.815
Displacement	0.283	7.0	1.60	0.235	7.0	1.600
	0.500	4614.2	2.60	0.500	127.3	2.050
	0.750	8055.2×10^3	3.75	0.750	1970.4	2.475
	0.900	7100.2×10^5	4.44	0.900	10195.0	2.730
	0.950	3159.8×10^6	4.67	0.950	17634.0	2.815

Note : The first row of each generalised intensity corresponds to Esteva's(42) value of parameters C_1 and C_3.

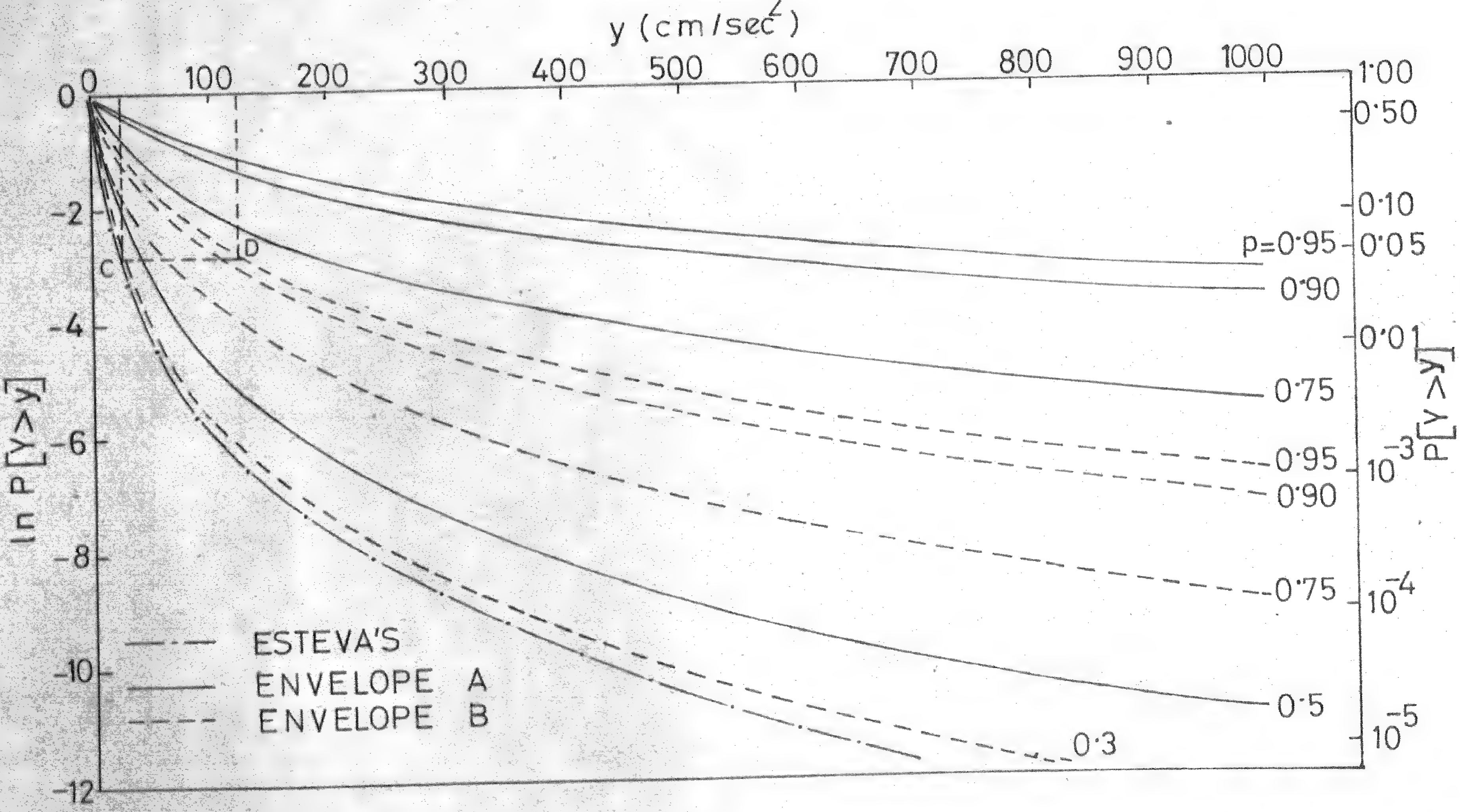

FIG 6·4 EFFECT OF MODEL-1 ON THE EXCEEDANCE PROBABILITY OF PEAK ACCELERATION, Y

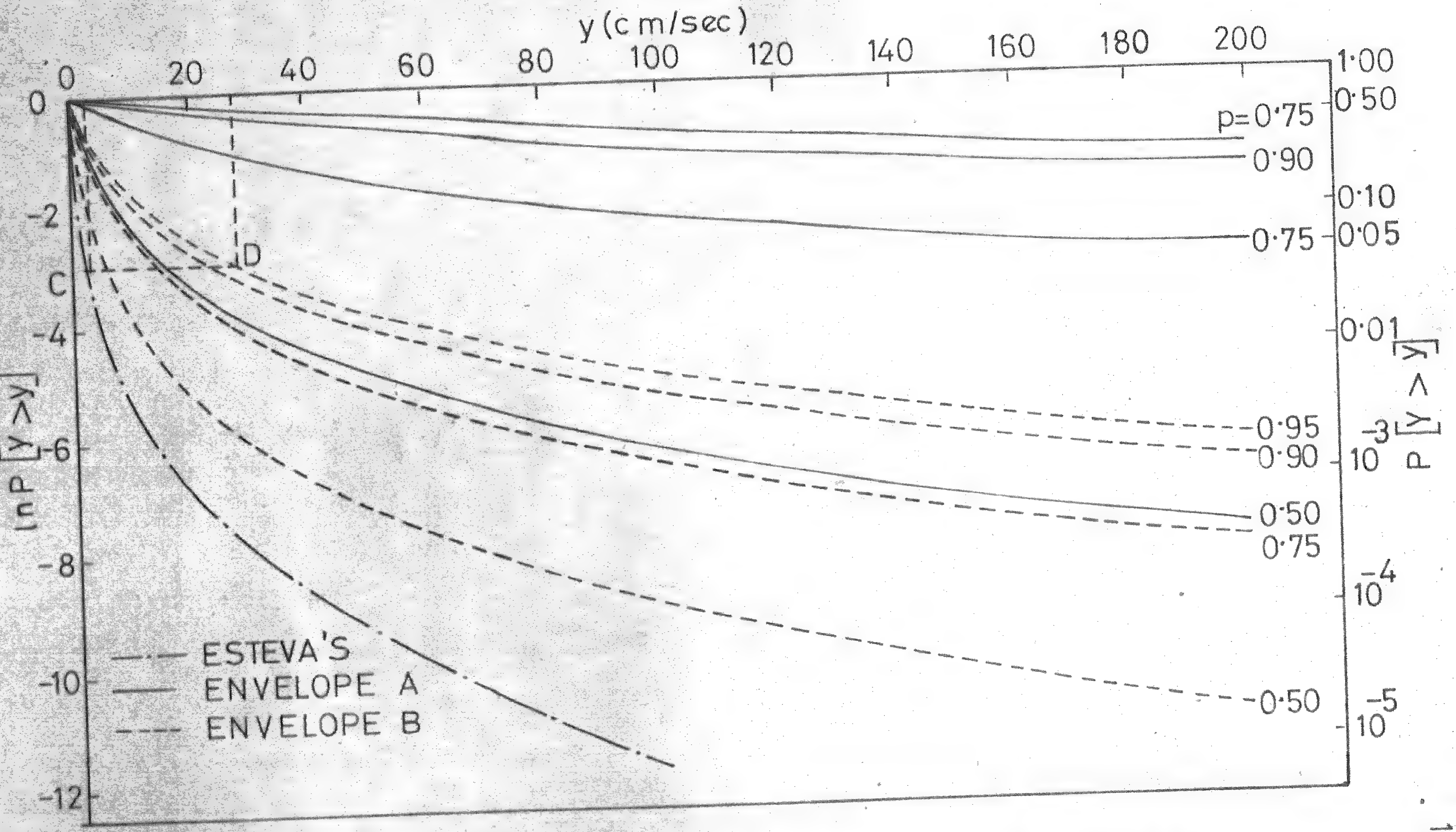

FIG 6·5 EFFECT OF MODEL-1 ON THE EXCEEDANCE PROBABILITY OF PEAK VELOCITY , Y

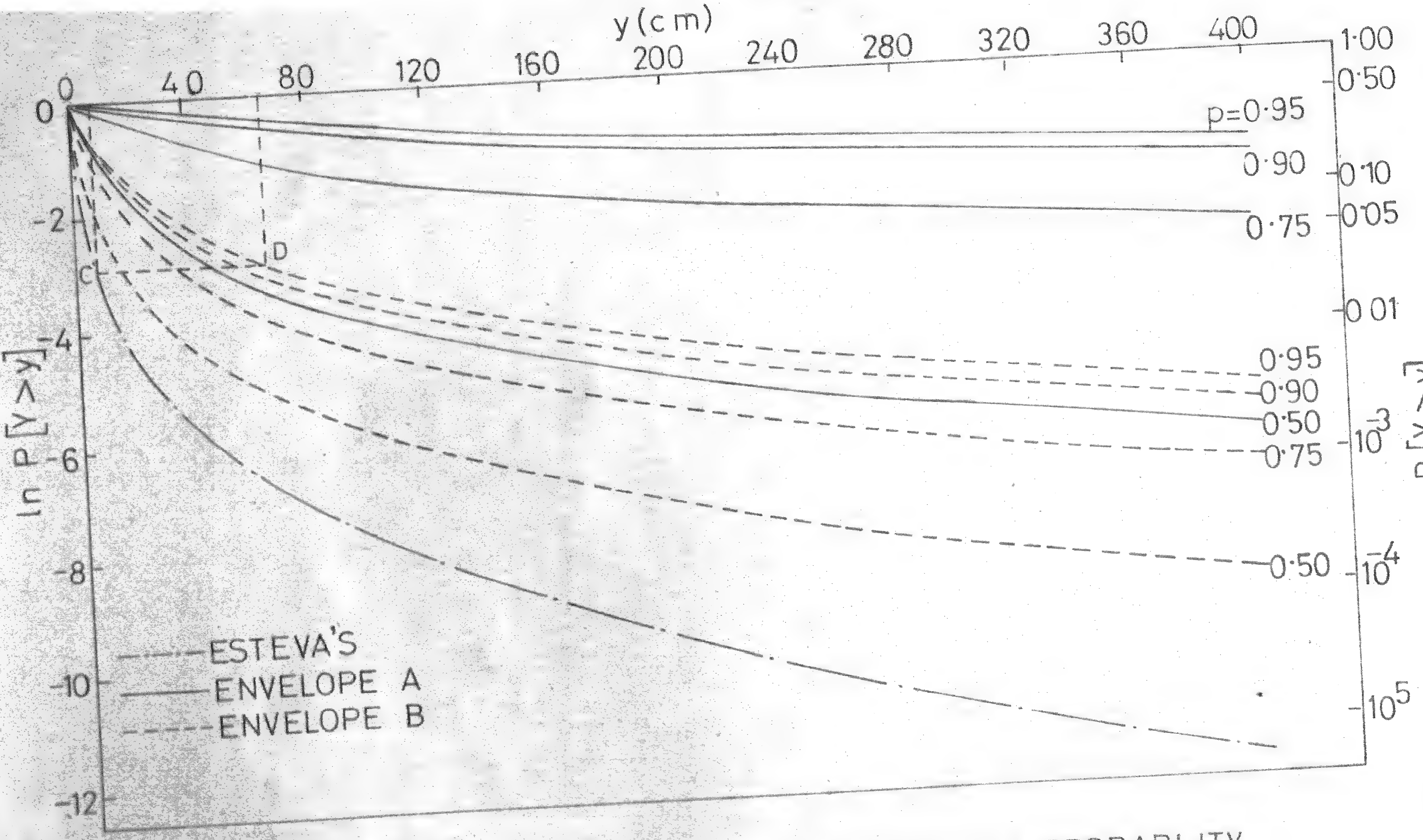

FIG 6·6 EEFECT OF MODEL-1 ON THE EXCEEDANCE PROBABLITY OF PEAK DISPLACEMENT , Y

To account for the scatter in the seismic data C_1 and C_3 are assumed to be random variables in this section. The range of these variables is determined by the upper and lower envelopes discussed in Section 6.3.1. The constants C_2 and C_4 are empirical and are taken as in Section 3.6. The random variables C_1, C_3, M and R are assumed to be mutually independent. The random variable C_1 is assumed to be log – Simpson i.e.

$$X = \ell n\ C_1 \tag{6.23}$$

is a Simpson distributed random variable. The probability density function of X is given by

$$f_X(x) = \begin{cases} 2(x - x_1)/\{(x_3 - x_1)\ (x_2 - x_1)\}; & \ell n\ b_1 = x_1 \leq x \leq x_2 = \ell n\ b_2 \\ 2(x - x_3)/\{(x_3 - x_1)\ (x_2 - x_3)\}; & x_2 \leq x \leq x_3 = \ell n\ b_3 \\ 0 & ; \text{otherwise} \end{cases} \tag{6.24}$$

The random variable C_3 is assumed to be Simpson. The corresponding probability density function is given by

$$f_{C_3}(y) = \begin{cases} 2(y - a_1)/\{(a_3 - a_1)\ (a_2 - a_1)\} & ;\ a_1 \leq y \leq a_2 \\ 2(y - a_3)/\{(a_3 - a_1)\ (a_2 - a_3)\} & ;\ a_2 \leq y \leq a_3 \\ 0 & ;\ \text{otherwise} \end{cases} \tag{6.25}$$

The values of the parameters b_1, b_2 and b_3 in Eq. (6.24) and that of a_1, a_2 and a_3 in Eq. (6.25) are given in Table 6.1.

The probability distribution function of Z(Eq. 6.21) is obtained in Appendix A6.4.1. The details of probability density and distribution function of W(Eq. 6.22) are given in Appendix A6.4.2. Using the distribution laws of Z and W the probability of generalised intensity is obtained in Appendix A6.4.3. The results for peak ground acceleration, velocity and displacement are obtained numerically in terms of $P[Y > y]$ for both envelopes and are marked as A and B corresponding to previous Section. These results are shown in Figs. (6.7 - 6.9).

6.5 Results and Discussion

The results in Figs. (6.4 - 6.9) are for magnitude cutoff at both level i.e. $m \varepsilon (5,9]$ and focal depth lognormally distributed with maximum focal depth, H_o = 600 Kms. The earthquake source is a volume source with arc length b = 150 Kms. Comparison of Gaussian model and Model - 2 (Figs.6.7 - 6.9) shows that Model - 2 predicts higher generalised intensity. The Gaussian Model and Model - 1 (envelope A and 50% chance of actural peak acceleration to be less than or equal to the predicted peak acceleration) for same return period give comparable peak acceleration. However, for peak velocity and displacement, the Model - 1 with chance less than 50% is comparable with the Gaussian model for same return period. The Model - 2 and Gaussian model predict average generalised intensity when scatter in the data are accounted for. However, for Model - 1 specific probability can be specified for predicted intensity. This model might be more useful for important structures (e.g. nuclear facilities).

6.6 Incorporation of the effect of Scatter on Seismic risk

The steps to incorporate the effect of scatter graphically on the seismic risk analysis is given in the followings :

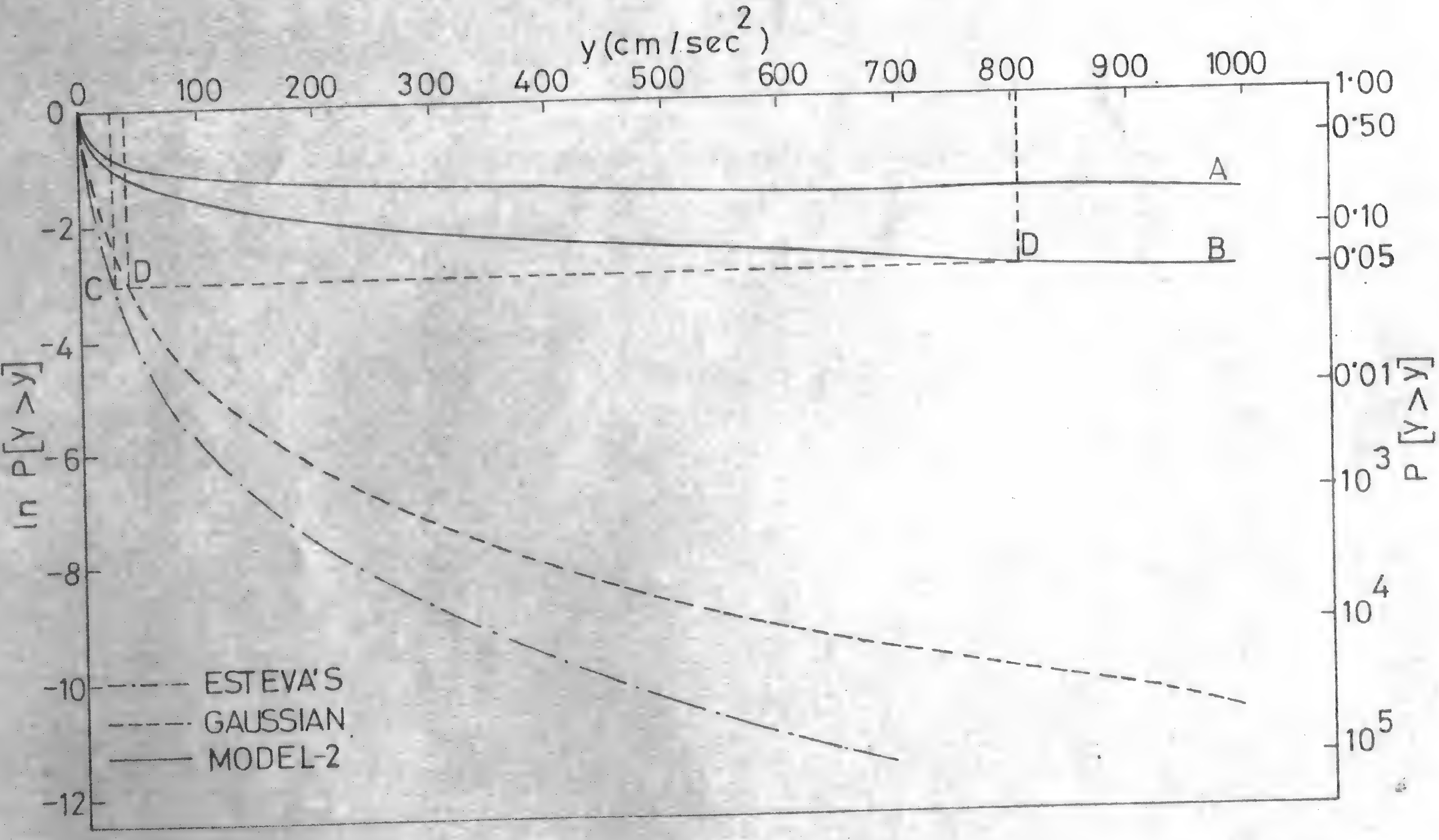

FIG 6·7 EFFECT OF MODEL-2 AND GAUSSIAN MODEL ON THE EXCEEDANCE PROBABILITY OF PEAK ACCELERATION, Y

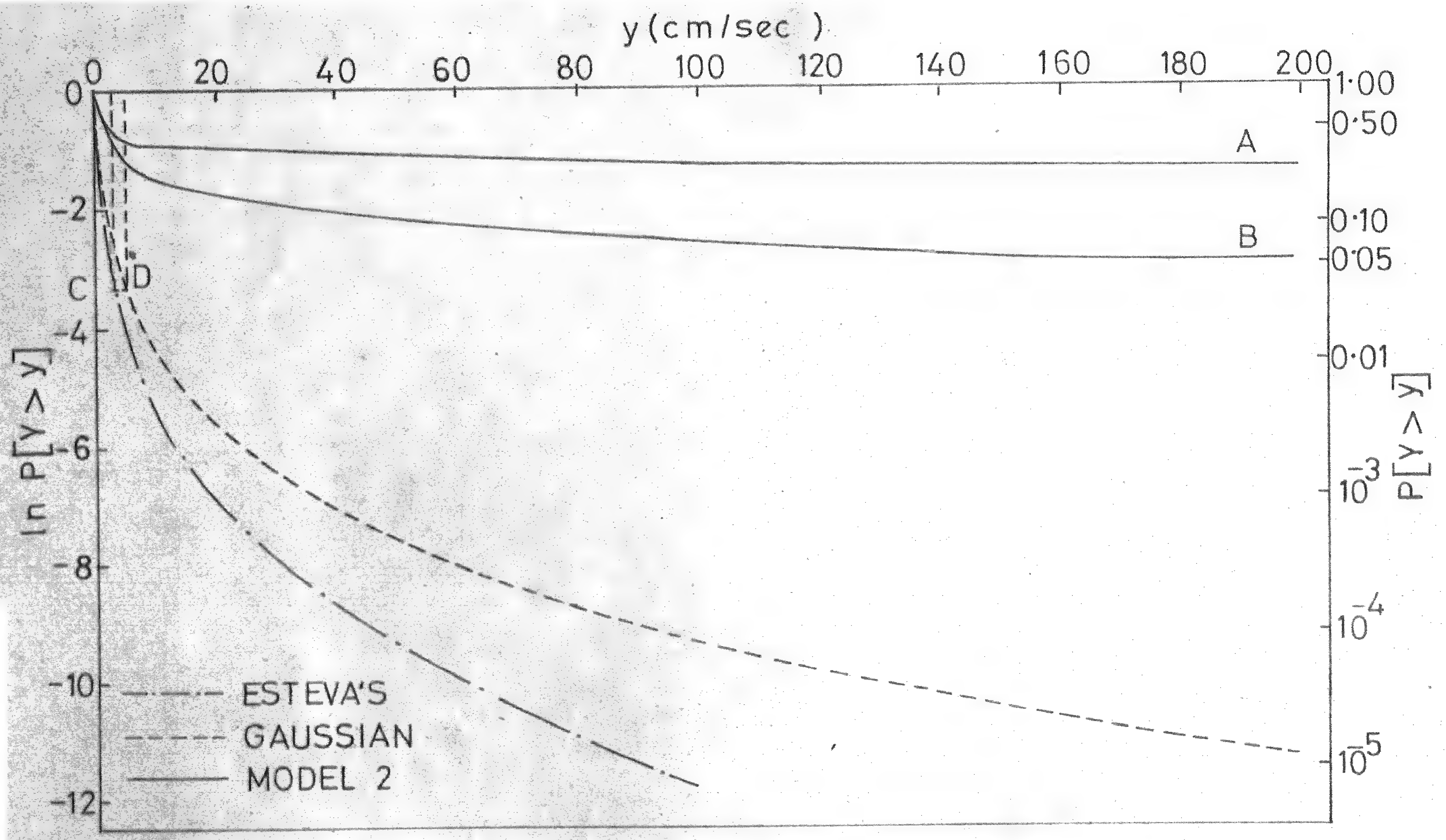

FIG 6·8 EFFECT OF MODEL-2 AND GAUSSIAN MODEL ON THE EXCEEDANCE PROBABILITY OF PEAK VELOCITY, Y

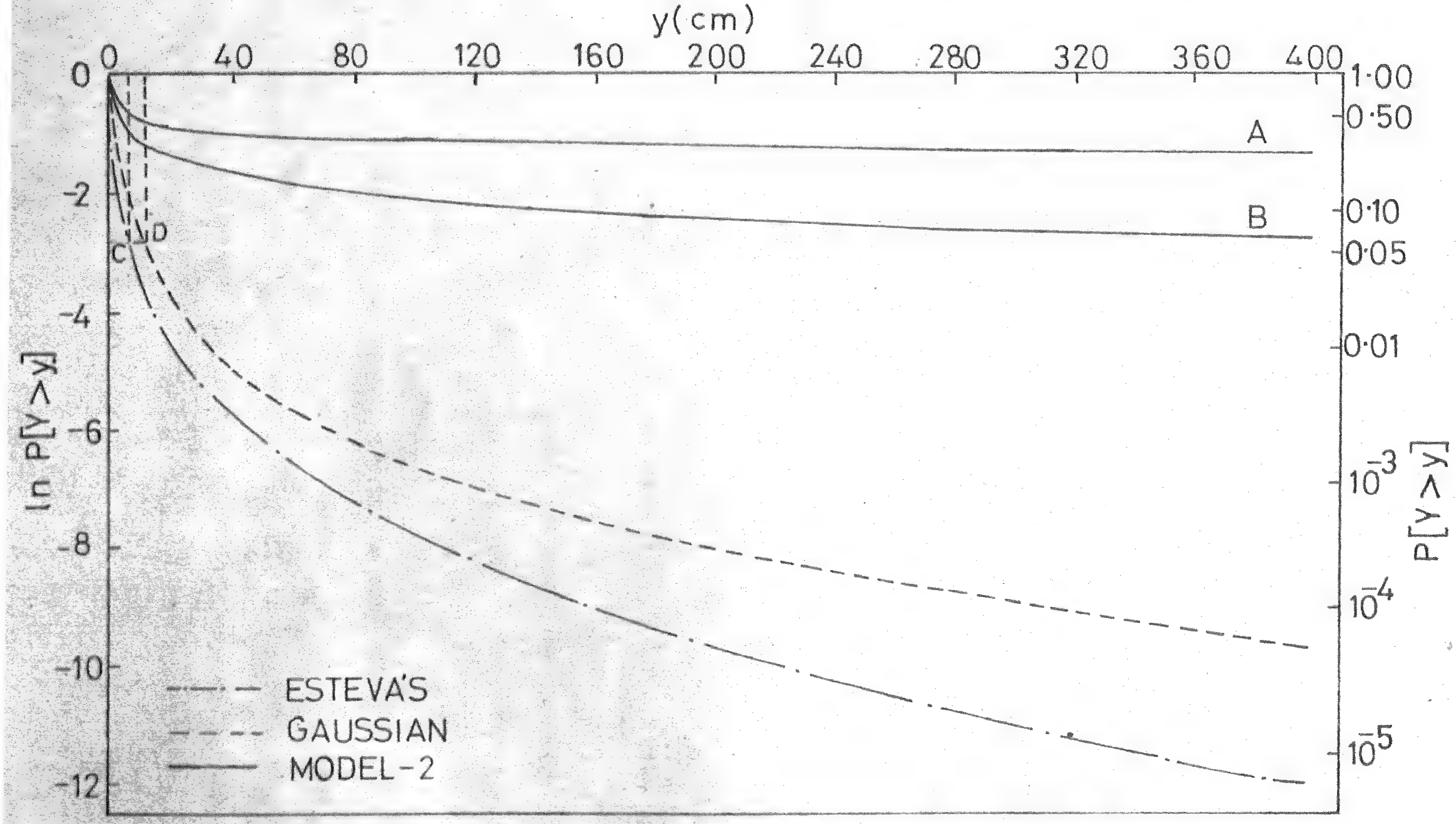

FIG 6·9 EFFECT OF MODEL-2 AND GAUSSIAN MODEL ON THE EXCEEDANCE PROBABILITY OF PEAK DISPLACEMENT, Y

1. Determine the generalised intensity for a T-year return period from the contour map given in Chapter 4.
2. Locate the point C on the curve marked Esteva's in Figs. (6.4 - 6.9). Choose a model of scatter and project horizontally to the curve corresponding to the curve of the chosen model to locate point D.
3. Project vertically from D to the abscissa to get the generalised intensity incorporating scatter in the attenuation law.

Example

Let at a location peak acceleration is 27.5 cm/sec^2 for 100-year return period. The peak acceleration for 100-year return period is obtained following above steps as 37.5 cm/sec^2 for Gaussian model, as 125 cm/sec^2 for Model - 1 with envelope B and 95% chance of probability of actual acceleration to be less than or equal to the predicted value and as 805 cm/sec^2 for Model - 2 with the parameters corresponding to the envelope B.

The extrapolation for return period and for specified exceedance probability may also be incorporated subsequently following procedure reported in Chapter 4.

As explained above, the generalised intensity incorporating the effect of scatter can be easily obtained from contour maps given in Chapter 4. This simple procedure is only possible for sources - homogeneous in tectonic feature. However, for nonhomogeneous source fresh calculation is necessary to include the effect of scatter on seismic risk analysis.

CHAPTER 7

SEISMIC ZONING MAPS OF INDIA

7.1 Introduction

Preparation of the seismic zoning maps of region involves a synthesis of the seismic history, geological features and an acceptable balance between cost and risk. The previous chapters contain the following information of relevance to seismic zoning

1. Seismic data of the Indian peninsula for the period 1917 to 1972 and its analysis of special relevance to seismic zoning is the seismicity map, Fig. (2.5), giving the energy contours.
2. Contour maps for 100-year return period of the peak ground acceleration, velocity and displacement assuming the Indian peninsula to be homogeneous and nonhomogeneous, Figs. (4.4 - 4.6 and 5.3 - 5.5), in tectonic features.
3. Maps of Indian peninsula giving idealized tectonic features, Fig. (5.2), and epicentre of earthquakes, Fig. (5.1).
4. A set of graphs through which the generalised intensities can be extrapolated for i) upper limit on magnitude, Figs. (3.11 - 3.13), ii) different return periods Figs. (4.7 - 4.9), iii) specified exceedance probability for a given service life, Figs. (4.7 - 4.9), and iv) scatter in attenuation laws, Figs. (6.4 - 6.9).

The seismic risk analysis performed in the thesis does not take into account earthquakes prior to 1917. List of these earthquakes, some of which are quite large in size, is placed in Appendix A7.1.

IS : 1893 - 1975, Indian Standard Recommendation for Earthquake Resistant Design of structures(34), contains a zoning map of India. The code also contains maps showing epicentres and sizes of past earthquakes, principal tectonic features and lithological groups.

7.2 Seismic Zoning Maps

In this chapter an attempt is made to prepare a seismic zoning map of India by integrating the results of the investigations presented in this thesis and the information available in the code IS : 1893 - 1975. Three maps have been prepared giving the values of the peak ground acceleration, velocity and displacement for a 100 year return period. Stepswise procedure used in prepairing the map is explained below :

1. Contour map of five levels of peak ground acceleration was prepared on the basis of nonhomogeneous tectonic features. The acceleration values were modifed to include the effect of scatter using the Gaussian Error model and corrected maximum magnitude. The map is shown in Fig. (7.1). It divides the country into five zones with design acceleration for uniform seismic risk.
2. The lateral force coefficients given in the seismic zoning map of IS : 1893 - 1975 are divided by 2.6 to give the peak ground acceleration for 5% damping(93).
3. The map prepared under Step - 1 is compared with zoning map of code. The boundary of the zones are carefully compared and wherever major deviations are noticed, geological and epicentral evidences are examined.

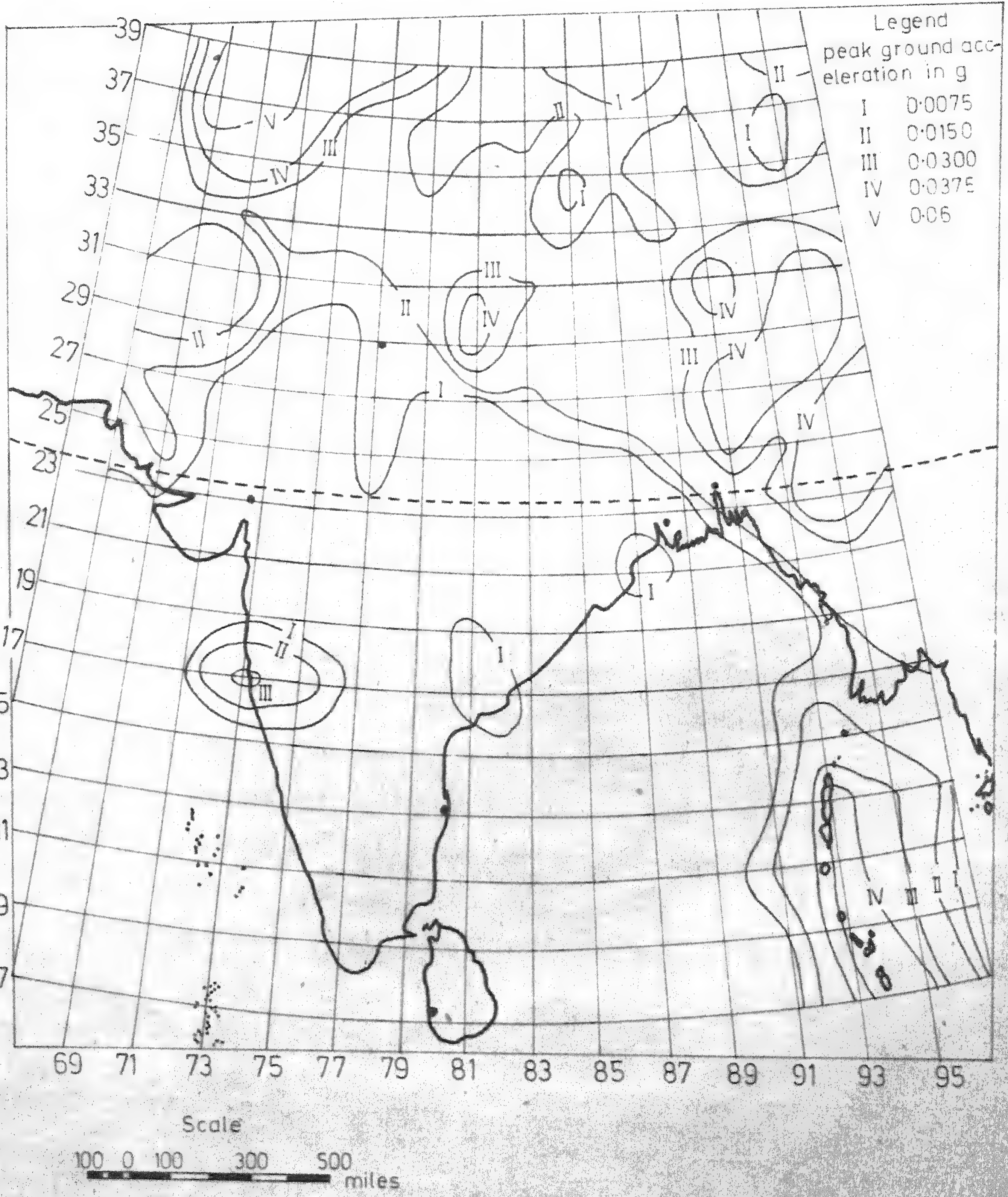
Legend
peak ground acceleration in g
I 0·0075
II 0·0150
III 0·0300
IV 0·0375
V 0·06
39
37
35
33
31
29
27
25
23
21
19
17
15
13
11
9
7
69
71
73
75
77
79
81
83
85
87
89
91
93
95
I
II
III
IV
V
Scale
100 0 100 300 500
miles

FIG. 7·1 PEAK ACCELERATION CONTOURS

4. Integrating all the above informations,the seismic zoning map of India is drawn, (Fig. 7.2), which represents the best judgement of the author.

Salient features and the deviations between the code map and the map prepared by author are :

In the Deccan plateau (below 12° latitude) evidence of earthquake origin exists in the form of past earthquakes. This evidence is accepted and this region is upgraded. In the region of grid point 70 earthquakes of magnitude greater than 6 have occurred in the past and consequently this region is upgraded locally. In the Koyna region (grid point 84) the seismically active region is enlarged as compared to code map. Upgradation of Gondowana rift unit (grid point 88 and 123) is the result of general increment in gradation in the Deccan plateau. The zone boundaries in this region are modifed in conformity with the tectonic features. The presence of inactive seismic fault number 7 in the West coast and Narmada-Tapti unit is largely ignored in the construction of zoning map. In the central zone a narrow higher zone is accepted in the region of fault numbers 11 and 12. In the Himalayan Tectonic zone evidence of historic earthquake in Srinagar, Mandi and Babhange (grid points 229, 214 and 171 respectively) is taken into account by upgrading these regions locally. In the Assam region, adjoining Bangladesh and Burma, a lower zone exists inconformity to the contour maps previously obtained. The region around Bhuj in Gujrat (grid point 130) is also upgraded inconformity with historic data.

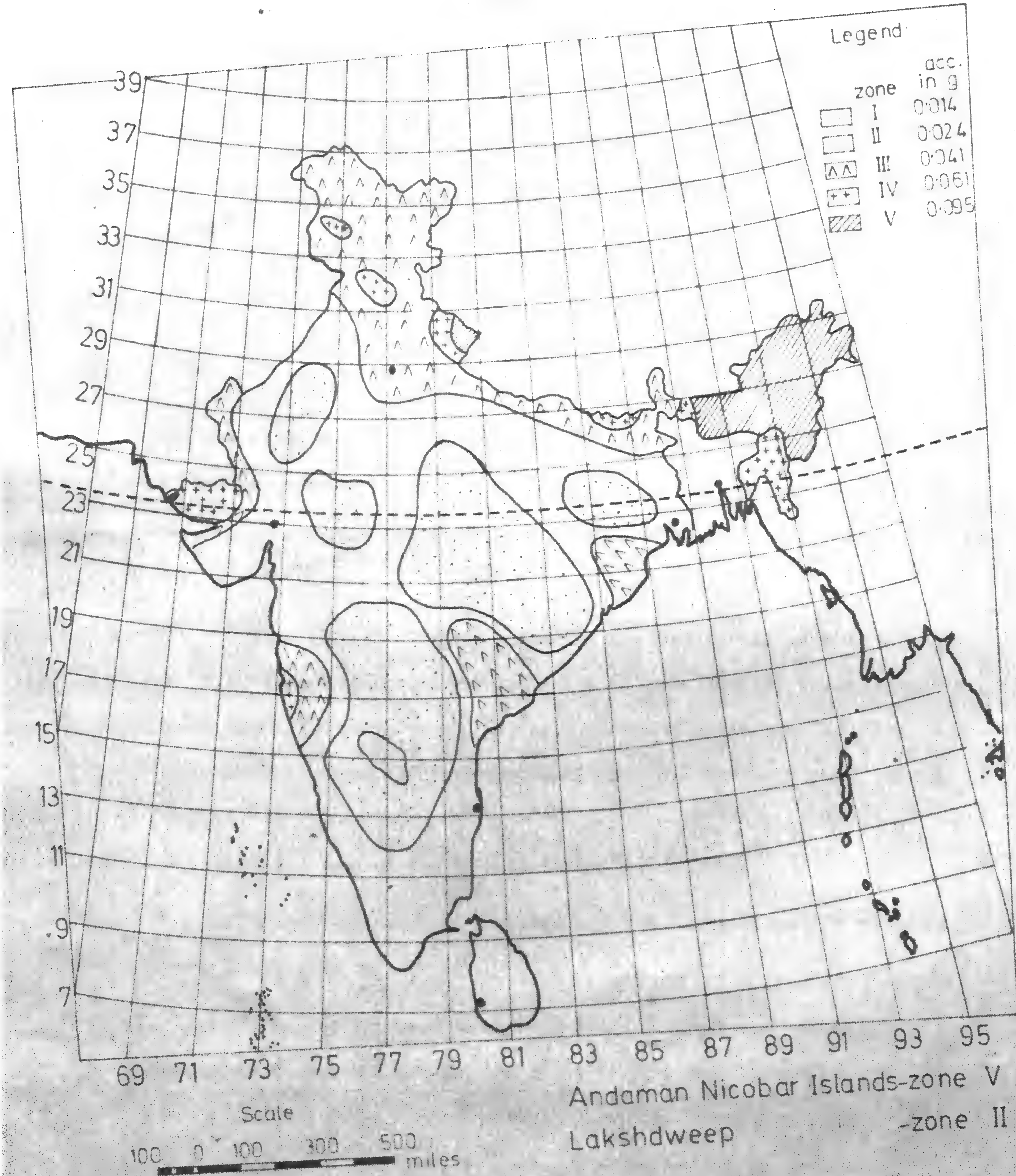
Legend
zone
acc. in g
I 0·014
II 0·024
III 0·041
IV 0·061
V 0·095
39
37
35
33
31
29
27
25
23
21
19
17
15
13
11
9
7
69
71
73
75
77
79
81
83
85
87
89
91
93
95
Scale
100 0 100 300 500 miles

Andaman Nicobar Islands-zone V
Lakshdweep -zone II

FIG. 7·2 ZONING MAP BASED ON ACCELERATION

The seismic zoning maps for peak ground velocity and displacement have been prepared following a similar procedure. The zoning maps and five intensity level contour maps are shown in Figs. (7.3 - 7.6). In these cases, however, code does not provide a map.

7.3 Discussion of the Seismic Zoning Maps

The major deviations in the boundaries of the zones between the code map and that prepared by the author are along the West coast, in Central India and in the Assam region. The code map is based largely on the largest past earthquakes whereas maps based on seismic risk analysis are weighted towards large number of smaller earthquakes close to the site(44).

Table 7.1 shows a comparison of the peak ground acceleration in different zones based on two maps. It is seen from the table that code provision in different zones are not uniform from the view point of acceptable risk and is different by as much as a factor of 4.5. The intensities indicated in the author's map are for 100-year return period and take into account the effects of scatter.

Table 7.2 shows the comparison for 11 major cities in different parts of the country.

Based on the seismic risk analysis of the present work it is recommended that the lateral force coefficient (α_0) in the IS : 1893 - 1975 for zones III, IV and V should be increased to correspond to 25 - 30 year return period. These values are indicated below.

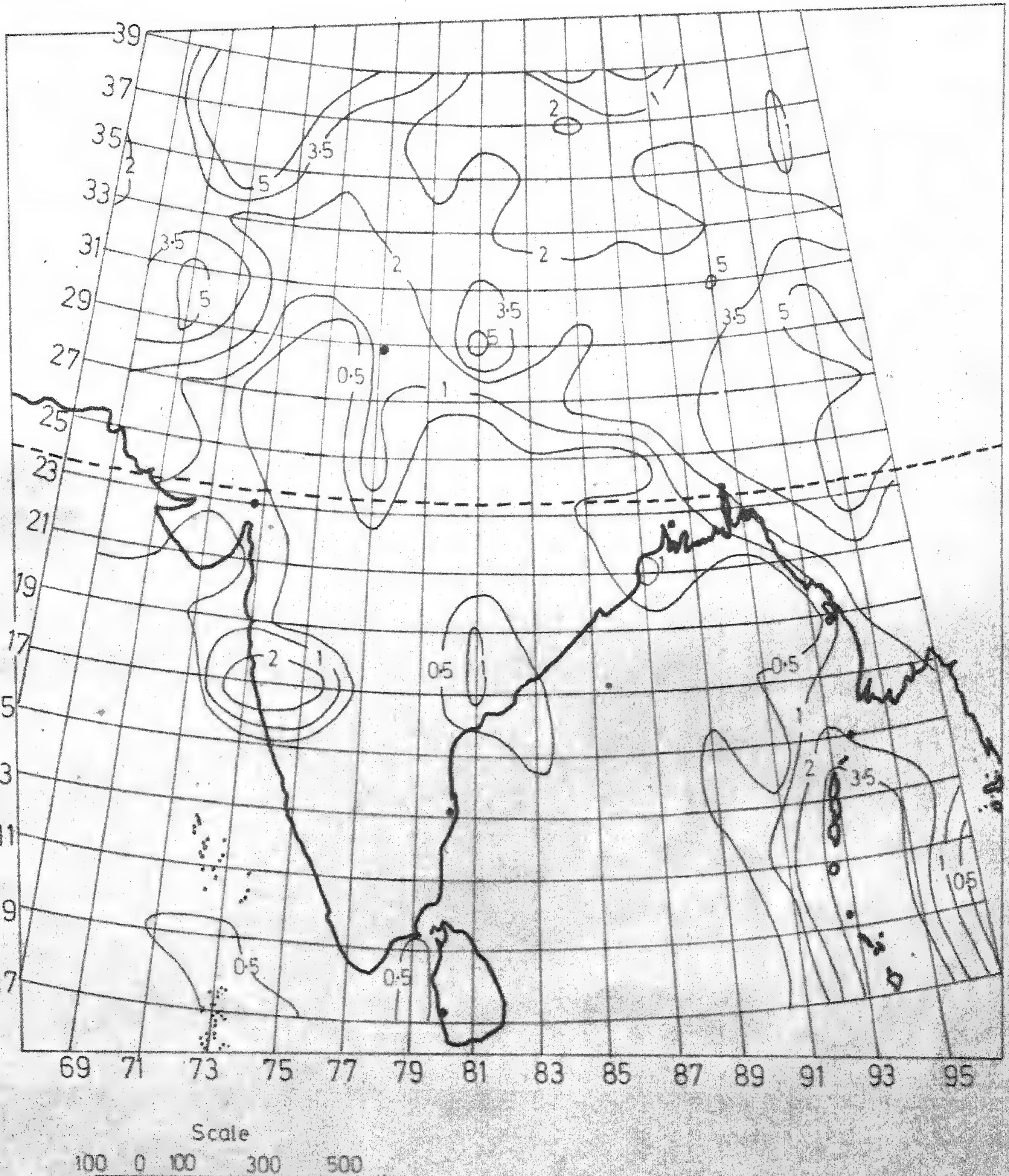
39
37
35
33
31
29
27
25
23
21
19
17
15
13
11
9
7
69
71
73
75
77
79
81
83
85
87
89
91
93
95
2
5
3·5
2
1
3·5
5
0·5
1
5
3·5
5
3·5
5
1
2
0·5
1
0·5
0·5
1
2
3·5
1
0·5
0·5
0·5
Scale
100 0 100 300 500
miles

FIG. 7·3 PEAK VELOCITY (cm/sec) CONTOURS

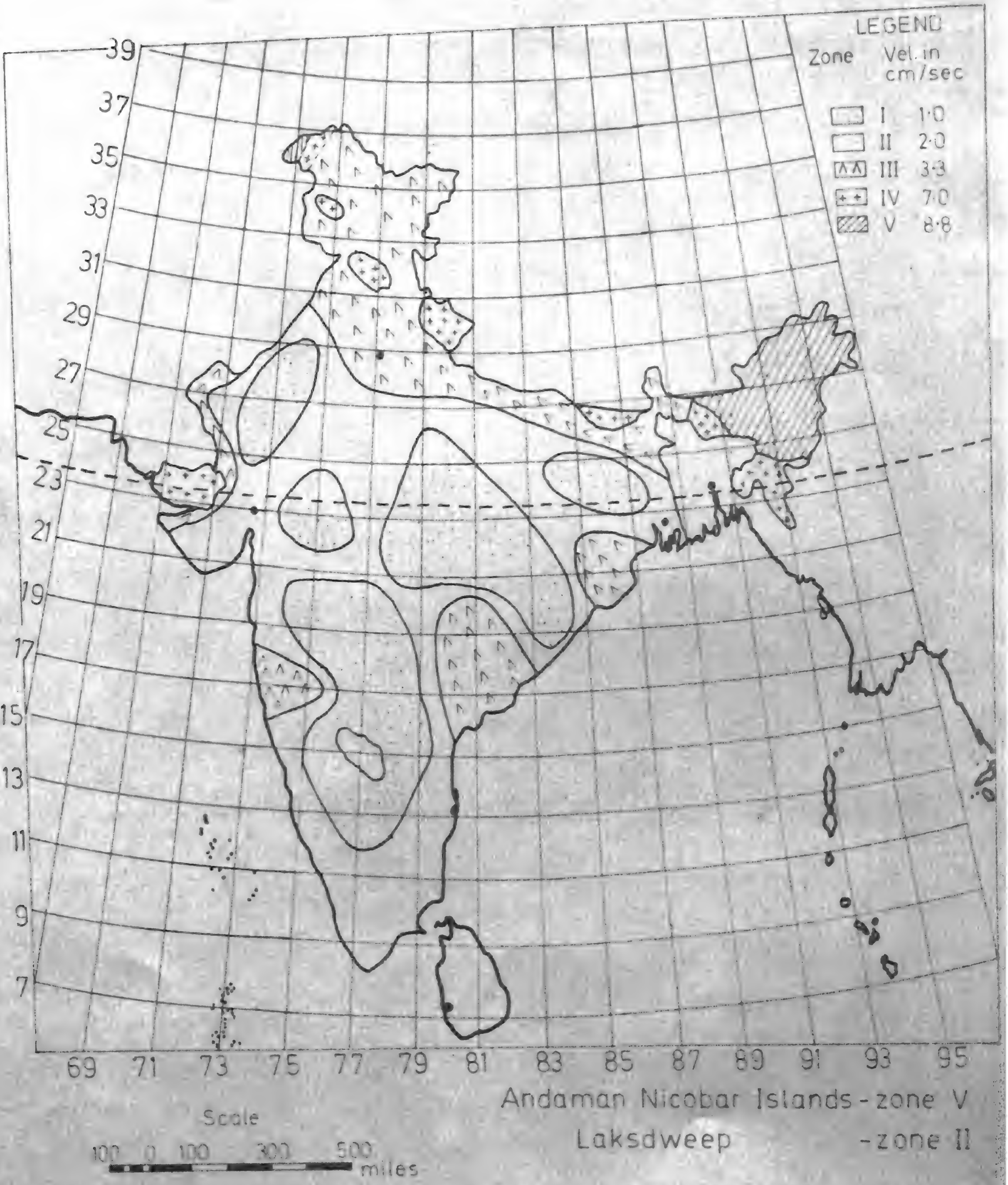
LEGEND
Zone Vel. in cm/sec
I 1·0
II 2·0
III 3·3
IV 7·0
V 8·8
39
37
35
33
31
29
27
25
23
21
19
17
15
13
11
9
7
69
71
73
75
77
79
81
83
85
87
89
91
93
95
Andaman Nicobar Islands - zone V
Laksdweep - zone II
Scale
100 0 100 300 500 miles

FIG. 7·4 ZONING MAP BASED ON VELOCITY

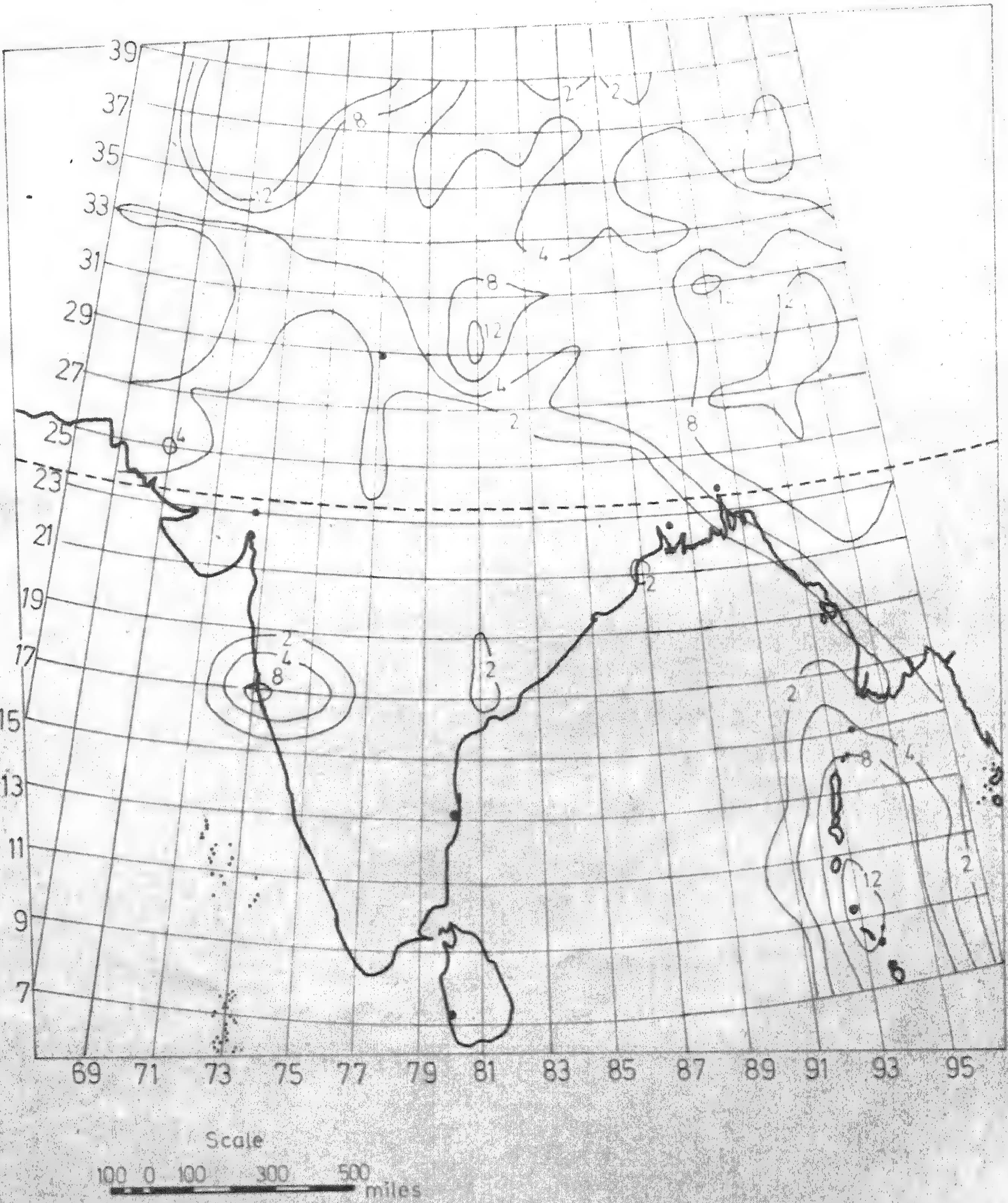
39
37
35
33
31
29
27
25
23
21
19
17
15
13
11
9
7
69
71
73
75
77
79
81
83
85
87
89
91
93
95
2
4
8
12
Scale
100 0 100 300 500
miles

FIG.7.5 PEAK DISPLACEMENT (cm) CONTOURS

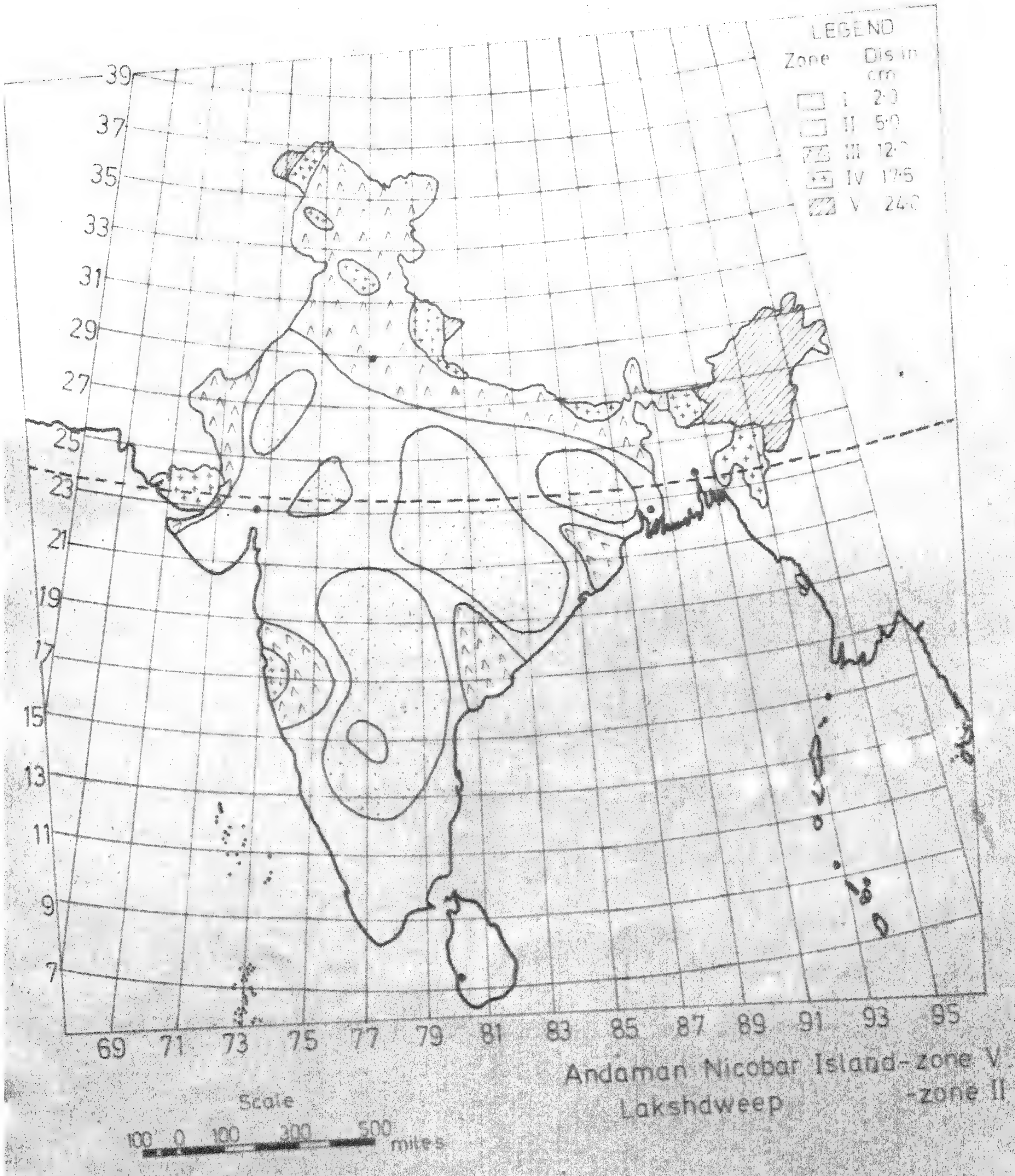
LEGEND
Zone Dis in cm
I 2·0
II 5·0
III 12·0
IV 17·5
V 24·0
39
37
35
33
31
29
27
25
23
21
19
17
15
13
11
9
7
69
71
73
75
77
79
81
83
85
87
89
91
93
95
Andaman Nicobar Island-zone V
Lakshdweep -zone II
Scale
100 0 100 300 500 miles

FIG.7·6 ZONING MAP BASED ON DISPLACEMENT

Table 7.1

Comparison of IS : 1893-1975 with Present Work

Zone	IS : 1893 - 1975				Present work	
	Lateral force coefficient α_o	Acceleration in g $(\alpha_o/2.6)$	Typical return period in years	% exceedance probability for 100-years	Acceleration in g for 100-year return period	5% exceedance acceleration in g for 100-years
V	0.08	0.0308	10	99.99	0.095	0.270
IV	0.05	0.0192	10	99.99	0.061	0.178
III	0.04	0.0154	15	99.90	0.041	0.141
II	0.02	0.0077	25	95.00	0.024	0.087
I	0.01	0.0038	45	80.00	0.010	0.046

Table 7.2

Peak ground Acceleration in g for Different Cities

City	IS : 1893 - 1975			Present work		
	Zone No.	Acceleration	Return period in years	Zone No.	Acceleration for 100-year return period	5% exceedance probability Acceleration for 100-years
Bombay	III	0.0154	60	II	0.024	0.087
Calcutta	III	0.0154	60	II	0.024	0.087
Chandigarh	IV	0.0192	22	III	0.041	0.141
Coimbatore	III	0.0154	60	II	0.024	0.087
Delhi	IV	0.0192	22	III	0.041	0.141
Gauhati	V	0.0308	10	V	0.095	0.270
Hyderabad	I	0.00308	45	I	0.010	0.046
Kanpur	III	0.0154	60	II	0.024	0.087
Madras	II	0.0077	25	II	0.024	0.087
Norora	IV	0.0192	22	III	0.041	0.141
Srinagar	V	0.0308	23	IV	0.061	0.178

Zone	Present Code provision for α_o	Recommended Code provision for α_o
V	0.08	0.13
IV	0.05	0.08
III	0.04	0.07

The generalised intensity in the author's map can be extrapolated for different return periods and specified exceedance probability for a given service life. For example, at Norora, the peak ground acceleration for an exceedance probability of 5% over a 200 year period works out to be 0.257g.

The generalised intensity values in the seismic zoning map are average values for the zones. These values may be exceeded in the close proximity of the epicentre of a large earthquake. The generalised intensity values are for firm soil and shall be modified suitably for local soil condition.

Major difference between acceleration and velocity or displacement maps is the two higher zones in region near grid point 244 as is shown in Figs. (7.2, 7.4 and 7.6). In case of velocity map only zone IV is in the region near grid point 199 and only zone II is present near grid point 84. Both acceleration and displacement map contain two zones near these points. Marginal differences exist between boundaries of various zones in all the three maps.

CHAPTER 8

SUMMARY OF RESULTS AND CONCLUSIONS AND SUGGESTIONS FOR FURTHER WORK

8.1 Results and Conclusions

The statistical analysis of seismic data and the seismic risk analysis of Indian peninsula have been presented in the preceding chapters. The results and conclusions of the investigation can be summarised as :

1. Statistical analysis of seismic data for the period 1917 to 1972 indicates that i) arrival process of earthquakes is not Poisson; (ii) the data are space-time correlated, (iii) the spatial pattern is non-stationary (iv) Markov chain of the Semi-Markov model giving transition of earthquakes from one area to another fits the data. However, final inter-arrival distribution of earthquakes obtained from Semi-Markov model does not fit the data. Semi-Markov model for the earthquake process can be used for seismic risk analysis provided sufficient data are available.

2. Effect of focal depth treated as a random variable on the seismic risk is significant. A mixed lognormal distribution of maximum focal depth, H_o = 600 Kms., gives the best fit to the data. Lognormal distribution with 600 Kms. maximum focal depth gives comparable risk whereas same is true for uniform distribution with 150 Kms. cutoff focal depth.

3. Contour maps of equal generalised intensity based on seismic risk analysis using homogeneous and nonhomogeneous source model show marginal deviations. The tectonic features, such as faults, cause local variations

in the shape of the contours but the value of the generalised intensity is not changed significantly.

In view of the above, it is concluded that the seismic zoning map should be drawn on the basis of seismic risk analysis with sources identified on the basis of tectonic features. However, extrapolation for return period and exceedance probability may be made on the basis of a modular earthquake source. Curves of such extrapolation can be provided in the code.

4. The scatter in attenuation law has a significant effect on seismic risk. Model - 1 proposed in this thesis to account for the scatter agree closely to the Gaussian model due to Esteva(42) for some probability leve whereas proposed Model - 2 predicts significantly higher generalised intensity in comparison to the Gaussian model. The effect of scatter should be included while computing the seismic risk.

5. A generally accepted approach to earthquake resistant design requires the structure to remain elastic for 'small' earthquakes, to undergo repairable limited plastic deformations for 'medium' earthquakes and large plastic deformation, without collapse, for 'large' earthquakes The criteria for choosing small, medium and large earthquakes are not laid. It is proposed that the size of the earthquakes be linked with the return period; small, medium and large earthquake, e.g., may correspond to return periods of 30, 100 and 200 respectively. For a site in zone III the design ground acceleration is given below.

Type of earthquake	Return period years	Design peak ground acceleration in g	Exceedance Probability for 100-year return period
Small	30	0.022	0.50
Medium	100	0.041	0.67
Large	200	0.066	0.85

The small, medium and large earthquakes may also be specified in terms of exceedance probability for 100-years as indicated in the last column of the above table.

6. The lateral force coefficients specified in IS : 1893 - 1975 do not correspond to identical acceptable risk in each zone. The ratio of risk varies as much as 4.5. It is recommended that lateral force coefficients in zone III, IV and V be increased to 0.07, 0.08 and 0.13 to correspond to 25 - 30 year return period.

7. Since ground acceleration, velocity and displacement govern the design of different types of structures, it is meaningful to draw separate zoning maps for each of these. These maps show significant differences in northern and western region.

8. The proposed zoning maps provide design generalised intensities for equal acceptable risk and suggests changes in the boundaries of code map. The design intensities can be modified for different return period and exceedance probabilities.

8.2 Suggestions for Further Work

1. The stochastic model of earthquake occurrence used in this thesis and used by other investigators neglects space-time correlation, magnitude

focal depth correlation and have assumed temporal nature to be Poisson. Efforts should be made to incorporate the space-time and magnitude focal depth correlation in future work. A simulation approach incorporating the above correlations and assuming earthquake process is a stochastic field process may be attempted.

2. The main difficulty in the seismic risk analysis at this stage is the paucity of data which makes the estimation of parameters very difficult. While efforts to collect more data continue, attempts should be made to improve the mechanistic models of earthquake occurrence.

3. At present the attenuation laws are incorporated at the level of local seismicity. Attempt should be made to establish these laws for major geological zones so that they can be used at the regional level. In United States different attenuation laws are used for Eastern and Western regions.

4. It is well known that seismic data reported by different agencies have a measure of uncertainty regarding size and location of earthquakes. The reliability associated with such uncertainties may be established and incorporated in the seismic risk analysis.

5. The seismic zoning maps presented in this thesis may be refined by a more careful and informed identification of earthquake sources and the seismic activity associated with them, use of focal depth and upper limit of magnitude as regional variables and use of 'judgement' factor by a group of seismologists and engineers. After such a map is prepared, the present zoning map in IS : 1893 - 1975 may be reviewed to incorporate some of the features suggested in this thesis.

REFERENCES

1. Housner, G.W. and P.C. Jennings, "Problems of Seismic Zoning", *Proc. 5th World Conf. Eq. ENG.,* Rome, Vol. 2, p. 1626, 1974.

2. Medvedev, S.V., *Engineering Seismology*, Israel Program of Scientific Translation, Jerusalem, 1965.

3. Evison, F.F., "Earthquake and Faults", *Bull. Seism. Soc.Am.,* Vol. 53, p. 873, 1963.

4. Evison, F.F., "On the Occurrence of Volume Change of the Earthquake Source", *Bull. Seism. Soc. Am.*, Vol. 57, p. 9, 1967.

5. Gutenberg, B. and C.F.Richter, *Seismicity of Earth,* Princeton University Press, Princeton, N.J., 1956.

6. Allen, C.R., P.St. Amand, C.F. Richter and J.M. Nordquist, "Relationship Between Seismicity and Geologic Structure in the Southern California", *Bull. Seism. Soc. Am.,* Vol. 55, p. 753, 1965.

7. Newmark, N.M. and E. Rosenblueth, *Fundamentals of Earthquake Engineering*, Prentice-Hall, Inc., Englewood Cliffs, N.J., 1971.

8. Burridge, R. and L. Knopoff, "Model and Theoretical Seismicity", *Bull. Seism. Soc. Am.,* Vol. 57, p. 341, 1967.

9. Vere-Jones, D., "A Markov Model for Aftershock Occurrence", *Pure and Appl. Geophys.,* Vol. 64, p. 31, 1966.

10. Vere-Jones, D., "Stochastic Models for Earthquake Occurrence", *J.R. Stat.Soc., B*, Vol. 32, p. 1, 1970.

11. Shlien, S. and M.N. Toksöz, "A Clustering Model of Earthquake Occurrences", *Bull. Seism. Soc. Am.,* Vol. 60, p. 1765, 1970.

12. Hawkes, A.G., "Point Spectra of Some Mutually Exciting Point Processes", *J.R. Stat. Soc., B,* Vol. 33, p. 438, 1971.

13. Hawkes, A.G., "Spectra of Some Self Exciting and Mutually Exciting Point Processes", *Biometrika,* Vol. 58,p. 83, 1971.

14. Hawkes, A.G., "Spectra of Some Mutually Exciting Point Processes with Associated Variables", *Stochastic Point Process: Statistical Analysis, Theory and Applications"*, P.A.W.Lewis (Editor), Wiley Interscience, 1972.

15. Rascón, O.A. and C.A. Cornell, "A Physical Based Model to Strong Earthquake Records on Firm Ground", *Proc. 4th World Conf. Eq. Eng.*, Santiago, Chile, A-1, p. 84, 1969.

16. Housner, G.W., "Intensity of Earthquake Ground Shaking Near the Causative Fault", *Proc. 3rd World Conf. Eq. Eng.*, Auckland & Wellington,New Zealand, Vol. 1, III-94, 1965.

17. Newmark, N.M., "Problems in Wave Propagation in Soil and Rock", *Symp. Wave Propagation and Dynamic Properties of Earth Materials,* Univ. of New Mexico, Albuquerque, p. 7, 1968.

18. Ambraseys, N.N., "Maximum Intensity of Ground Movements Caused by Faulting", *Proc. 4th World Conf. Eq. Eng.,* Santiago, Chile, A-2, p. 154, 1969.

19. Richter, C.F., *Elementary Seismology*, Freeman, San Francisco, Califf., 1959.

20. Gutenberg, B. and C.F. Richter, "Earthquake Magnitude, Intensity, Energy and Acceleration", *Bull. Seism. Soc. Am.*, Vol. 32, p. 163, 1942.

21. Gutenberg, B. and C.F.Richter, "Earthquake Magnitude, Intensity, Energy and Acceleration", *Bull. Seism. Soc. Am.*, Vol. 46, p. 105, 1956.

22. Gzovsky, M.G., "Tectonophysics and Earthquake Forecasting", *Bull. Seism. Soc.Am.*, Vol. 52, p. 485, 1962.

23. Ambraseys, N.N., "Dynamics and Response of Foundation Materials in Epicentral Regions of Strong Earthquakes", *5th World Conf. Eq. Eng.*, Rome, Invited paper, 1973.

24. Esteva, L. and E. Rosenblueth, "Espectros de Tremblores a Distancias Moderades y Grandes", *Bol. Soc. Mex.Ing. Sismica,* Vol. 2, p. 1, 1964.

25. Rosenblueth, E., "Probabilistic Design to Resist Earthquakes", *Proc. ASCE,* Vol. 90 (EM5), p. 189, 1964.

26. Hisida, T. and K. Nakagawa, *Recent Japanese Developments in Engineering Seismology and their Application to Buildings*, Japan.

27. *Uniform Building Code, 1967 ed.*, Pasadena Califf : International Conference of Building Officials, 1967.

28. Richter, C.F., "Seismic Regionalization", *Bull. Seism. Soc. Am.*, Vol. 49, p. 123, 1959.

29. Wiegel, R.L., *Earthquake Engineering*, Prentice-Hall, Inc., Englewood Cliff., N.J., 1970.

30. Krishna, J., "Seismic Zoning of India", *First Symp. Eq. Eng.*, Univ. of Roorkee, Roorkee, 1954.

31. *Indian Standard Recommendation for Earthquake Resistant Design of Structures*, Indian Standard Institution, New Delhi, IS : 1893-1962.

32. *Indian Standard Recommendation for Earthquake Resistant Design of Structures*, Indian Standard Institution, New Delhi, IS : 1893-1966.

33. *Indian Standard Recommendation for Earthquake Resistant Design of Structures*, Indian Standard Institution, New Delhi, IS : 1893-1970.

34. *Indian Standard Recommendation for Earthquake Resistant Design of Structures*, Indian Standard Institution, New Delhi, IS : 1893-1975.

35. Kaila, K.L. and H.A. Narain, "A new Approach for Preparation of Quantitative Seismicity Map as Applied to Alpide Belt - Sunda Arc and Adjoining Areas", *Bull. Seis. Soc. Am.*, Vol. 61, p. 1275, 1971.

36. Kaila, K.L. , H. A. Narain and V.K. Gaur, "Quantitative Seismicity Map of India", *Bull. Seism. Soc. Am.*, Vol. 62, p. 1119, 1972.

37. Lomnitz, C., *Global Tectonics and Earthquake Risk*, Elsevier Scientific Publishing Co., 1974.

38. Gumbel, E.J., *Statistics of Extremes*, Columbia Univ. Press, N.Y., 1958.

39. Lomnitz, C., "Earthquake Risk of Chile", *Bull. Seis. Soc. Am.*, Vol. 54, p. 1271, 1964.

40. Lomnitz, C. and B.Epstein, "A model for Occurrence of Large Earthquakes", *Nature*, Vol. 211, p. 954, 1966.

41. Cornell,C.A., "Engineering Seismic Risk Analysis", *Bull. Seism. Soc. Am.*, Vol. 58, p. 1583, 1968.

42. Esteva, L., *Bases para la Formulacion de Decisiones de Diseño Sismico*, Instituto de Ingenieria, UNAM, Mexico, 1968.

43. Esteva, L., "Seismicity Prediction : A Bayesian Approach", *Proc. 4th World Conf. Eq.Eng.*, Santiago, Chile, A-1, p. 172, 1969.

44. Cornell, C.A. and E.H.Vanmarcke, "The Major Influence of Seismic Risk", *Proc. 4th World Conf. Eq. Eng.*, Santiago, Chile, A-1, p. 69, 1969.

45. Goto, H. and K. Kameda, "Statistical Inference of the Future Earthquake Ground Motion", *Proc. 4th World Conf. Eq. Eng.*, A-1, p. 39, 1969.

46. Stratonovitch, R.L., *Topics in the Theory of Random Noise*, Vol. I, Gordon and Breach, New York.

47. Benjamin, J.R., "A Probalistic Model for Seismic Force Design", *Proc. 4th World Conf. Eq. Eng.*, Santiago, Chile, B-5,p. 31, 1969.

48. Raiffa, H. and R. Schlaiffer, *Applied Statistical Decision Theory*, Harvard Univ. Press, 1961.

49. Lomnitz, C., "An Earthquake Risk Map of Chile", *Proc. 4th World Conf. Eq. Eng.*, Santiago, Chile, A-1, p. 161, 1969.

50. Milne, W.G.and A.G. Davenport, "Earthquake Probability", *Proc. 4th World Conf. Eq. Eng.*, Santiago, Chile, A-1, p.55,1969.

51. Algermissen, S.T.,"Seismic Risk Studies of United States", *Proc. 4th World Conf. Eq. Eng.*, Santiago, Chile, A-1, p. 55, 1969.

52. Housener, G.W., "Engineering Estimates of Ground Shaking and Maximum Earthquake Magnitude", *Proc. 4th World Conf. Eq. Eng.*, Santiago, Chile, A-1, p. 1, 1969.

53. Chou, I.H., W.J.Zimmer and J.T.P. Yao, "Likelihood of Strong Motion Earthquakes", *Technical Report CE-27(71) NSF-065*, Univ. of New Mexico, Albuquerque, 1971.

54. Cornell, C.A., "Probabilistic Analysis of Damage to Structure Under Seismic Loads", *Dynamic Waves in Civil Engineering*, Howells, D.A., I.P. Haigh and C. Taylor (Editors), John Wiley & Sons., 1971.

55. Algermissen,S.T. and D.M. Perkins, "A Technique for Seismic Zoning : General Consideration and Parameters", *Proc. Intern. Conf. on on Microzonation*, Seattle, p. 865, 1972.

56. Merz, H.A. and C.A. Cornell, "Seismic Risk Analysis Based on A Quadratic Magnitude Frequency Law", *Bull. Seism. Soc. Am.*, Vol. 63,p. 1999,1973.

57. Shelien, S. and M.N.Tosköz, "Frequency-Magnitude Statistics of Earthquake Occurrences", *Earthquake Notes*, Eastern Section of the Seis. Soc. Am., 1970.

58. Merz, H.A. and C.A. Cornell, "Aftershock in Engineering Seismic Risk", Proc. 5th World Conf. Eq. Eng., Rome, Vol. 2, p. 2568, 1974.

59. Utsu, T., "A Statistical Study on Occurrence of Aftershocks", Geophysical Magazine, Tokyo, Vol. 30, p. 521, 1961.

60. Utsu, T., "Aftershocks and Earthquake Statistics", Part I - III, J. of the Faculty of Science, Hokkido Univ., Japan, 1969-1971.

61. Omori, F., "On the Aftershocks of Earthquakes", J.Coll. Sc., Imp. Univ. Tokyo, Japan, p. 111, 1894.

62. Lin, S.C. and L.W.Fagel, "Seismic Risk Analysis Comparison of Three Different Methods of Seismic Regionalization", Bull. Seism. Soc. Am., Vol. 65,p. 1023, 1975.

63. Bartlett, M.S., "On the theoretical specification of Sampling properties of Autocorrelated Time Series", J. Roy. Stat. Soc. (Suppl.), Vol. 8, p. 27, 1946.

64. Greig-Smith, P., Quantitative Plant Ecology, Butterworth, London, 2nd Ed., 1964.

65. Knox, G., "Epidemiology of Childhood Leukemia in Northumberland and Durham," Brt. J. Prev. Med., Vol. 18, p. 17, 1964.

66. Barton, D.E. and F.N. David, "The Random Intersection of Two Graphs", Research Papers in Statistics, F.N. David (Editor), John Wiley, 1966.

67. Mann, H.B. and A. Wald, "On the choice of the Number of Intervals in the Application of Chi-Square Test," Annals of Math. Stat., Vol. 13, p. 306, 1942.

68. Bartlett, M.S., "Some Examples of Statistical Methods of Research in Agriculture and Applied Biology", J. Roy.Stat. Soc. (Suppl.), Vol. 4, p. 137, 1937.

69. Cox, D.R. and P.A.W. Lewis, The Statistical Analysis of Series of Events, Methuen & Co. Ltd., London, 1966.

70. Pyke, R., "Markov Renewal Processes with Finitely Many States", Ann. Math. Statis., Vol. 32, p. 1243, 1961.

71. Kullback, S., M. Kepperman, H.H. Ku, "Tests for Contingency and Markov Chains", Technometrics, Vol. 4, p. 573, 1972.

72. Billingsley, P., "Statistical Methods in Markov Chains", Annals. Math. Statis., Vol. 32, p. 12, 1961.

73. Lomnitz, C., "A study of the Maipo Valley Earthquakes of September 4, 1958", Proc. 2nd Conf. Eq.Eng., Tokyo, Vol. I, p. 501, 1960.

74. Lomnitz, C., "Magnitude Stability in Earthquake Sequences", Bull. Seism. Soc. Am., Vol. 56, p. 247, 1966.

75. Hamada, K. and T. Hagiwara, "High Sensitivity Triparite Observation on Matushiro Earthquakes", Part 4, Bull. Eq. Res. Inst., Tokyo Univ., Vol. 45, p. 159, 1967.

76. Darkopoulos, J.C., "A Statistical Model on the Occurrence of Aftershocks in the Area of Greece", Bull. Int. Inst. Seism. Eq. Eng., Tokyo, Vol. 8,p. 17, 1971.

77. Hamilton, R.M., "The Fiordland Earthquake Sequence of 1960 and Seismic Velocity Beneath, New Zealand", N.Z. J.Geol. Geophys., Vol. 9, p. 224, 1966.

78. López - Arroyo, A. and A. Udias, "Aftershock sequences and focal Parameters of February 28, 1969 Earthquakes of the Azores - Gibraltar fracture Zone", Bull. Seism. Soc. Am., Vol. 62, p.699, 1972.

79. Ishimoto, M. and K. Iida, "Observation Sur les Séims Energistrés per le Microsismographe Construit Derniérement (1)", Bull. Eq. Res. Inst., Tokyo Univ., Vol. 17, p. 443, 1939.

80. Kolmogorov,A.N., "Uber das Logarithmisch Normal Verteilungsgesetz der Dimensionen der Telichen bei Zerstuckelüng", Izv. Akad. Nauk S.S.S.R.,31,p. 1, 1941.

81. Lomnitz, C., "Estimation Problem in Earthquake Science", Tectonophysics, Vol. 2, p. 193, 1964.

82. Rosenblueth, E., "On Seismicity", Seminar in the Application of Statistics to Structural Mechanics, Dept. of Civil Engrg., Univ. of Pennsylvania, 1966.

83. Lomnitz, C., "Statistical Prediction of Earthquakes", Rev. of Geophysics, Vol. 4, p. 337, 1966.

84. Warner, E., "Statistics of Earthquake I, and II", Ger. Geitr. Geophys., Vol. 50, p. 85 and p. 223, 1937.

85. Knopoff, L., "The Statistics of Earthquake in Southern California", Bull. Seism. Soc. Am., Vol. 54,p. 845, 1964.

86. Naizi, M., "Seismicity of Northern and Western Nevada", Bull. Seism. Soc. Am., Vol. 54, p. 845, 1964.

87. Gardner, J.K. and L. Knopoff, "Is the Sequence of Earthquakes in Southern California, with Aftershock Removed, Poissonian", Bull. Seism. Soc. Am., Vol. 63, p. 1363, 1974.

88. Lomnitz, C., "Poisson Process in Earthquake Studies", Bull. Seism. Soc. Am., Vol. 63, p. 735, 1973.

89. Kanai, K., "An Empirical Formula for the Spectrum of Strong Earthquake Motions", Bull. Eq. Res. Inst., Tokyo, Vol. 39, p. 85, 1961.

90. Parzen, E., Stochastic Processes, Holdenday, San Franscisco, 1968.

91. Wadia, D.N., Geology of India, Tata-McGraw Hill Pub. Co., New Delhi, 1975.

92. Srivastava, L.S., "Seismic Zoning of India", Earthquake Engineering, Arya, A.S. et al. (Editor), Sarita Prakashan, Meerut, India, 1974.

93. Newmark, N.M. and W.J. Hall, "Seismic Design of Nuclear Reactor Facilities", Proc. 4th World Conf. of Eq. Eng., Santiago, Chile, B-4, p. 37, 1969.

94. Yakolev, M.N., "The Solution of Systems of Nonlinear Equation by a Method of Differentiation with respect to A Parameters", U.S.S.R. Comput. Math. and Mechanics, Pt. I, Vol. 4, p. 198, 1964.

95. Ralston, A. and H.S. Wilf, Mathematical Methods for Digital Computers, Vol. I, Wiley, N.Y., 1960.

96. Fox, R.L., Optimization Methods for Engineering Design, Addison-Wesley Pub. Co., 1971.

Appendix A2.4.1

MAXIMUM LIKELIHOOD ESTIMATION FOR FOCAL DEPTH

a) Truncated Lognormal Distribution

Let a random sample of size n is drawn from truncated lognormal density:

$$f_H(x) = \exp\left[-0.5(\ell n\, x-\theta_1)^2/\theta_2\right] / \left[\sqrt{2\pi\theta_2}\ \ x\ \ \Phi\{(\ell n\, H_o-\theta_1)/\sqrt{\theta_2}\}\right]$$

$$;\ x \in (0, H_o] \qquad (A2.4.1.1)$$

where θ_1 and θ_2 are parameters of the distribution with specified H_o and $\Phi(.)$ is the probability distribution function of $N(0,1)$.

The logarithm of likelihood function excluding a constant term is

$$L^* = -n\left[1/2\ \{\ell n\ \theta_2 + (\bar{s} - 2\theta_1\ \bar{x} + \theta_1^2)/\theta_2\} + \ell n\ \Phi\right] \qquad (A2.4.1.2)$$

where

$$\bar{x} = (\ \textstyle\sum \ell n\ x_i)/_n \qquad (A2.4.1.3)$$

$$\bar{s} = \textstyle\sum (\ell n\ x_i)^2/n \qquad (A2.4.1.4)$$

and Φ is understood to be a function of θ_1 and θ_2. To find the location of maximum of L^*, following is computed

$$\frac{\partial L^*}{\partial \theta_1} = -n\ \left[(\theta_1 - \bar{x})/\theta_2 + C/\Phi\right] \qquad (A2.4.1.5)$$

$$\frac{\partial L^*}{\partial \theta_2} = -n\ \left[\{1-(\bar{s} - 2\theta_1\bar{x} + \theta_1^2)/\theta_2\}/(2\theta_2) + (\ell n\ H_o-\theta_1)C/(2\theta_2\Phi)\right]$$

$$(A2.4.1.6)$$

where

$$C = -\exp\left[-0.5(\ell n\, H_o-\theta_1)^2/\theta_2\right] / \sqrt{2\pi\theta_2} \qquad (A2.4.1.7)$$

Solution for θ_1 and θ_2 should be obtained from these derivatives (Eq.A2.4.1.5 & A.2.4.1.6) by equating it to zero. These equations are solved by the method of parametric differentiation$^{(94)}$. Assume λ is a parameter such that $\lambda \varepsilon [0,1]$ and at $\lambda = 0$ the values of $\Theta = \Theta^o$. The auxiliary equations from the above derivatives are

$$\partial L^*/\partial\theta_i = (1-\lambda)\left[\partial L^*/\partial\theta_i\right]_{\Theta = \Theta^o} \; ; \; i=1,2 \qquad (A2.4.1.8)$$

The above equations have characteristics that at $\lambda = 0$, $\Theta = \Theta^o$ and at $\lambda = 1$ is the solution of derivatives (Eq. A2.4.1.5 and A2.4.1.6) equal to zero.

Differentiating Eq. (A2.4.1.8) with respect to λ and using the chain rule yields

$$[\,H\,] \begin{Bmatrix} d\theta_1/d\lambda \\ d\theta_2/d\lambda \end{Bmatrix} = - \begin{Bmatrix} \partial L^*/\partial\theta_1 \\ \partial L^*/\partial\theta_2 \end{Bmatrix}_{\Theta = \Theta^o} \qquad (A2.4.1.9)$$

where $[\,H\,]$ is a matrix whose elements are

$$h_{11} = \partial^2 L^*/\partial\theta_1^2 = -n\left[1/\theta_2 + \{[(\ell n\, H_o-\theta_1)/\theta_2 - C/\Phi]C\}/\Phi\right] \qquad (A2.4.1.10)$$

$$h_{12}=h_{21} = \partial^2 L^*/\partial\theta_1\partial\theta_2 = -n[(\bar{x}-\theta_1)/\theta_2^2 + \{[(\ell n\, H_o-\theta_1)^2/\theta_2$$
$$-1-(\ell n\, H_o-\theta_1)C/\Phi]\; C/(2\theta_2)]\}/\Phi] \qquad (A2.4.1.11)$$

$$h_{22} = \partial^2 L^* / \partial\theta_2^2 = -n\,[\,\{(\bar{s} - 2\theta_1\bar{x} + \theta_1^2)/\theta_2 - 1/2\}/\theta_2^2$$

$$+ \{[(\ell n\, H_o - \theta_1)^2/\theta_2 - 3 - (\ell n\, H_o - \theta_1)C/\Phi]\ (\ell n\, H_o - \theta_1)C/(4\theta_2^2)\}/\Phi] \qquad (A2.4.1.12)$$

Equation (A2.4.1.9) represents a set of two simultaneous ordinary differential equationswhich can be solved numerically for $d\theta_i/d\lambda$; $i=1,2$. The resulting ordinary differential equations with initial condition $\Theta = \Theta^o$ at $\lambda = 0$ is numerically integrated upto $\lambda = 1$ to give the solution $\hat{\Theta}$. The Gill variation of Runge-Kutta formulae$^{(95)}$ is used in the numerical integration scheme. Step length for integration will be governed by the accuracy required and the speed of calculation. It is to be noticed that the elements of [H] matrix will have to be computed at every step of numerical integration process. The maximum likelihood estimator $\hat{\Theta}$ for the parameter Θ from sample size n, for large n, is approximately distributed as multivariate normal distribution with mean Θ and with covariance

$$V_\Theta = [-E[H]]^{-1} \simeq [-[H]_{\Theta = \hat{\Theta}}]^{-1} \qquad (A2.4.1.13)$$

b) Truncated Mixed Lognormal Distribution

Let a random sample of size n is drawn from truncated mixed lognormal density function

$$f_H(x) = \sum_{i=1}^{2} p_i \exp[-0.5(\ell n\, x - \theta_{1i})^2/\theta_{2i}]$$

$$/[\sqrt{2\pi\theta_{2i}}\ \times\ \Phi\{(\ell n\, H_o - \theta_{1i})/\sqrt{\theta_{2i}}\}];\ x \in (0, H_o] \qquad (A2.4.1.14)$$

with

$$\sum p_i = 1 \qquad (A2.4.1.15)$$

$$\theta_{12} > \theta_{11} \qquad (A2.4.1.16)$$

and where θ_{1i} and θ_{2i}; $i=1,2$ are parameters of the distribution with specified H_o. $\Phi(.)$ is the probability distribution of $N(0,1)$.

The logarithm of likelihood function is

$$L^* = \sum_{j=1}^{n} \ell n \; f_H(x_j) \qquad (A2.4.1.17)$$

The method of maximum likelihood consists of solving for those estimate $\hat{\Theta}$ of Θ, which maximizes L^* satisfying conditions given in Eqs. (A2.4.1.15 - A2.4.1.16). By transforming the variables as below;

$$p_1 = \sin^2 y_1 \qquad (A2.4.1.18)$$

$$p_2 = 1 - p_1 \qquad (A2.4.1.19)$$

$$\theta_{11} = y_2^2 \qquad (A2.4.1.20)$$

$$\theta_{12} = \theta_{11} + (\ell n \, H_o - \theta_{11}) \sin^2 y_3 \qquad (A2.4.1.21)$$

$$\theta_{21} = y_4^2 \qquad (A2.4.1.22)$$

$$\theta_{22} = y_5^2 \qquad (A2.4.1.23)$$

and changing objective function L^* to

$$L = -L^* \qquad (A2.4.1.2$$

the stated maximization problem is changed to unconstrained minimization problem. The minimization can be done by any standard scheme to estimate the parameters $\hat{\Theta}$. However, Powel's(96) method of unconstrained minimization has been adopted in this work. The covariances of the estimate for large sample may be obtained approximately.

Appendix A2.6.1

MAXIMUM-LIKELIHOOD ESTIMATION OF HYPEREXPONENTIAL DISTRIBUTION

Let an earthquake process has been observed for time t_o, starting from an event at $t = 0$. Let n earthquakes have occurred at $t_1, \ldots\ldots, t_n$. Therefore interarrival times are

$$x_1 = t_1 \tag{A2.6.1.1}$$

$$x_i = t_i - t_{i-1} \quad ; i=2,\ldots,n \tag{A2.6.1.2}$$

and they are samples from hyperexponential distribution with probability density function

$$f_T(t) = \sum_{i=1}^{2} p_i \mu_i \exp(-\mu_i t) \quad ; t \geq 0 \tag{A2.6.1.3}$$

with

$$\sum p_i = 1 \tag{A2.6.1.4}$$

$$\mu_2 > \mu_1 \tag{A2.6.1.5}$$

The log likelihood is given by

$$L^* = (n+1) \ln p_1 + n \ln \mu_1 - \mu_1 t_o + \ln \{1 + p_2/p_1 \exp[(\mu_1 - \mu_2)u]\}$$

$$+ \sum \ln \{1 + p_2 \mu_2 \exp[(\mu_1 - \mu_2)x_i]/(p_1 \mu_1)\} \tag{A2.6.1.6}$$

where

$$u = t_o - t_n \tag{A2.6.1.7}$$

The Eq. (A2.6.1.6) is maximized subject to the conditions given by Eqs. (A2.6.1.4 and A2.6.1.5). Following transformation reduces the constrained maximization problem to an unconstrained minimization problem:

$$\text{minimize} \quad L = -L^*$$

$$\text{with} \quad p_1 = \sin^2(x_1)$$

$$p_2 = 1 - p_1$$

$$\mu_1 = x_2^2$$

$$\mu_2 = \mu_1 + x_3^2$$

Here x_i; $i=1,2,3$ are slack variables and L is a function of slack variables. The solution of the minimization problem can be obtained by any standard method. However, Powel's method(96) is used in this work.

APPENDIX A3.8.1

PROBABILITY DISTRIBUTION FUNCTION AND PROBABILITY DENSITY FUNCTION OF FOCAL DISTANCE, R, FOR VOLUME SOURCE AT SITE

a) Focal depth, H, is uniformly distributed in $(0, H_o]$

It is assumed in this section that an earthquake is equally likely to occur anywhere in the volume source Fig. (A3.8.1.1) which influence the peak generalized intensity of the site. The probability that the focal distance, R, will be less than or equal to r is equal to the ratio of the volume of the earth upto r to the volume of the earth upto maximum focal distance R_o, i.e.

$$F_R(r) = P[R \leq r] = V(r)/V \qquad (A3.8.1.1)$$

where

$$V = \pi \int_0^{a \cos \nu} (y \tan \nu)^2 dy + \pi \int_{a \cos \nu}^{a} (a^2 - y^2) dy$$

$$- \pi \int_0^{(a-H_o)\cos \nu} (y \tan \nu)^2 dy - \pi \int_{(a-H_o)\cos \nu}^{a} (a^2 - y^2) dy$$

$$= 2\pi C \qquad (A3.8.1.2)$$

and

$$C = (1 - \cos \nu)\{a^3 - (a-H_o)^3\}/3 \qquad (A3.8.1.3)$$

For $\epsilon\ [0, a \sin \nu]$, the volume, $V(r)$, upto the focal distance r is given by from Fig. (A3.8.1.1) as

$$V(r) = \pi \int_0^{y_o} (2ay - y^2) dy + \int_{y_o}^{r} \pi (r^2 - y^2) dy \qquad (A3.8.1.4)$$

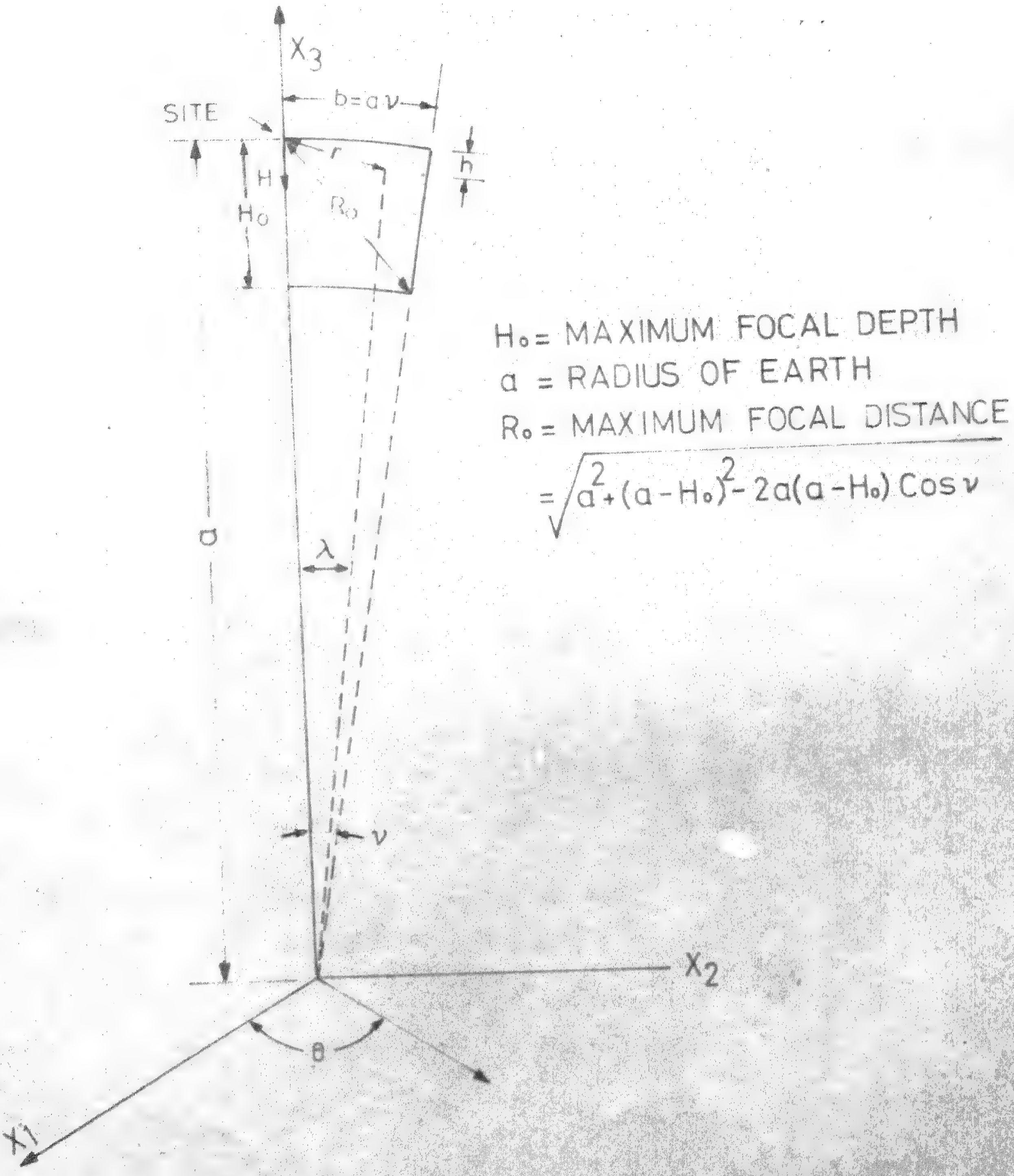
X3
SITE
b=aν
H
H0
r
R0
h
H_0 = MAXIMUM FOCAL DEPTH
a = RADIUS OF EARTH
R_0 = MAXIMUM FOCAL DISTANCE
$= \sqrt{a^2 + (a-H_0)^2 - 2a(a-H_0)\cos\nu}$
a
λ
ν
X2
θ
X1

Fig. A 3·8·1·1 EARTHQUAKE SOURCE AT SITE VOLUME OF REVOLUTION OF SECTOR ABOUT AXIS X_3

where

$$y_o = a\{1 - \cos(r/a)\} \qquad (A3.8.1.5)$$

The integrand of Eq. (A3.8.1.4) results in

$$V(r) = 2\pi\{r^3/3 - y_o(r^2 - ay_o)/2\}$$

Substituting this and Eq. (A3.8.1.2) into Eq. (A3.8.1.1) yields probability distribution function of R and is given by

$$F_R(r) = \{r^3/3 - y_o(r^2 - ay_o)/2\}/C \;;\; 0 \leq r \leq a \sin \nu \qquad (A3.8.1.6)$$

Differentiating with respect to r, the probability density function of R is obtained as

$$f_R(r) = \{r(r - y_o) + 1/2\,\{2ay_o - r^2\}\sin(r/a)\}/C$$

$$;\; 0 \leq r \leq a \sin \nu \qquad (A3.8.1.7)$$

The volume, $V(r)$, for $r \in [\,a \sin \nu,\ 2a \sin(\nu/2)]$ is obtained from Fig. (A3.8.1.1) as

$$V(r) = \pi\Big[\int_0^{y_o} (2ay - y^2)\,dy + \int_{y_o}^{y_1} (r^2 - y^2)\,dy + \int_{y_1}^{y_2} (a - y)^2 \tan^2\nu\,dy + \int_{y_2}^{r} (r^2 - y^2)\,dy\Big]$$

where $y_1 = u_1 - u_2$ (A3.8.1.8)

$y_2 = u_1 + u_2$ (A3.8.1.9)

$u_1 = a \sin^2 \nu$ (A3.8.1.10)

and $u_2 = \cos\nu\sqrt{r^2 - a^2 \sin^2\nu}$ (A3.8.1.11)

After integration and simplification it can be shown that

$$V(r) = \pi [\, 2r^3 + 3y_o \{ay_o - r^2\} - 4u_2(r^2 - a^2 \sin^2 \nu)] /3 \qquad (A3.8.1.12)$$

Probability distribution function of R is obtained from Eq. (A3.8.1.2) and Eq. (A3.8.1.12) as

$$F_R(r) = [\{r^3 - 2u_2(r^2 - a^2 \sin^2 \nu)\}/3 + y_o(ay_o - r^2)/2]/C$$

$$; \ a \sin \nu \leq r \leq 2a \sin (\nu/2) \qquad (A3.8.1.13)$$

Therefore, probability density function of R is

$$f_R(r) = [\, r\, \{r[1 - 1/2 \sin (r/a)] - 2u_2\}]$$

$$+ \{a \sin (r/a) - r\}\, y_o]/C \ ; \ a \sin \nu \leq r \leq 2a \sin (\nu/2)$$

$$(A3.8.1.14)$$

The volume, $V(r)$, for $r \in (2a \sin (\nu/2), H_o]$ is given by Fig. (A3.8.1.1) as

$$V(r) = \pi [\int_0^{y_3} (2ay - y^2)dy + \tan^2 \nu \int_{y_3}^{y_2} (a-y)^2\, dy$$

$$+ \int_{y_2}^{r} \pi(r^2 - y^2)\, dy]$$

$$= \pi [\, 2r^3 - ay_3^2\, (2 + \cos \nu) \cos \nu$$

$$- (2y_2 + u_1)\, (r^2 - a^2 \sin^2 \nu)] /3 \qquad (A3.8.1.16)$$

where

$$y_3 = a(1 - \cos \nu) \qquad (A3.8.1.17)$$

Hence, the probability distribution function of R is obtained as

$$F_R(r) = [\, r^3 - \{ay_3^2\ (2 + \cos\nu)\cos\nu\}/2 - (y_2 + u_1/2)\ (r^2 - a^2\sin^2\nu)]\ /(3C) \qquad (3.8.1.18)$$

Consequently, the probability density of R reduces to

$$f_R(r) = r\,[\, r - y_2\,]/C \qquad (A3.8.1.19)$$

From Fig. (A3.8.1.1), the volume, $V(r)$, for $r \in [H_o, R_o]$ where

$$R_o = \sqrt{a^2 + (a-H_o)^2 - 2a(a-H_o)\cos\nu} \qquad (A3.8.1.20)$$

and $$y_4 = H_o - (r^2 - H_o^2)/(2a) \qquad (A3.8.a.21)$$

is given by

$$V(r) = \pi[\int_0^{y_3} (2ay - y^2)dy + \tan^2\nu \int_{y_3}^{y_2} (a-y)^2 dy + \int_{y_2}^{H_o} (r^2 - y^2)dy + \int_{H_o}^{y_4} [\, r^2 - y^2 - \{(a-H_o)^2 - (a-y)^2\}]dy\,]$$

Above expression after integration and simplification reduces to

$$V(r) = \pi[\{4a\,H_o(3r^2 - H_o^2) + 3(r^2 - H_o^2)^2\}/(4a) - ay_3^2\ (2+\cos\nu)\cos\nu - (2y_2 + u_1)(r^2 - a^2\sin^2\nu)]\ /3 \qquad (A3.8.1.22)$$

Substituting this and Eq. (A3.8.1.2) in Eq. (A3.8.1.1) yields the probability distribution of R as

$$F_R(r) = [\ \{H_o(3r^2 - H_o^2) + 3(r^2 - H_o^2)^2/(4a) - ay_3^2\ (2 + \cos\nu)\cos\nu\}/2 - (y_2 + u_1/2)(r^2 - a^2\sin^2\nu)]\ /(3C)\ ;\ H_o \le r \le R_o \qquad (A3.8.1.23)$$

Differentiating above with respect to r, the probability density function of R is obtained as

$$f_R(r) = r\,[\,H_o - (r^2 - H_o^2)/(2a) - y_2\,]\;/C \qquad (A3.8.1.24)$$

b) Probability distribution function of Focal Depth, H, is mixed lognormal in $(0, H_o\,]$

The probability distribution function of focal distance, R, for volume earthquake source Fig.(A3.8.1.1) is derived based on statistical independence of azimuth, Λ, latitude, Θ, and focal depth, H. The joint probability density function of Λ, Θ and H is given by

$$f_{H\Lambda\Theta}\,(h, \lambda, \theta) = f_H(h)\; f_\Theta(\theta)\; f_\Lambda(\lambda) \qquad (A3.8.1.25)$$

where

$$f_\Lambda(\lambda) = 1/\nu \qquad ;\ \lambda\ \varepsilon\ (0, \nu\,] \qquad (A3.8.1.26)$$

$$f_\Theta(\theta) = 1/(2\pi) \qquad ;\ \theta\ \varepsilon\ (0, 2\pi\,] \qquad (A3.8.1.27)$$

$$f_H(h) = \sum_{i=1}^{2} p_i\; g_i(h)/I_{oi}(H_o) \qquad (A3.8.1.28)$$

$$\sum p_i = 1 \qquad (A3.8.1.29)$$

$$g_i(h) = \exp\,[\,-(\ell n\, h - \theta_{1i})^2/(2\theta_{2i})\,]\,/(\sqrt{2\pi\theta_{2i}}\; h)\ ;\ i=1,2 \qquad (A3.8.1.30)$$

$$I_{mi}(H_o) = \exp\,\{(\theta_{1i} - 1/2\; m\theta_{2i})\; m\}\;\Phi[\,(\ell n\, H_o - \theta_{1i} - m\theta_{2i})/\sqrt{\theta_{2i}}\,]\ ;\ m \geq 0 \qquad (A3.8.1.31)$$

and $\Phi(.)$ is the probability distribution function of $N(0,1)$.

The probability of the event $[R \leq r\,]$ is the ratio of the volume of earth upto focal distance, r, to the volume of earth upto maximum

maximum focal distance, R_o , where earthquakes can potentially occur. In mathematical notation it can be written as

$$P[\,R \leq r\,] = F_R(r) = V(r)/V(R_o) \qquad (A3.8.1.32)$$

To evaluate volume upto maximum focal distance, R_o, a new random variable $Y = a-H$ is defined, where, a, is radius of earth. It can be easily shown that probability density function of Y is given by

$$f_Y(y) = f_H\,(a-y) \quad ;\; y \in [a-H_o, a) \qquad (A3.8.a.33)$$

The joint probability density function of Λ , Θ and Y may be obtained from Eq. (A3.8.1.33) and Eq. (A3.8.1.25) and is given by

$$f_{Y\Lambda\Theta}\,(y, \lambda\,, \theta) = f_Y(y)\, f_\Lambda(\lambda)\, f_\Theta(\theta) \qquad (A3.8.1.34)$$

The volume upto maximum focal distance, R_o, is obtained using Eq. (A3.8.1.34) as

$$\begin{aligned} V(R_o) &= \int_{a-H_o}^{a} y^2 \int_0^{\nu} \sin\lambda \int_0^{2\pi} f_{Y\Lambda\Theta}\,(y\,,\lambda, \theta) d\theta\, d\lambda\, dy \\ &= 1/(2\pi\nu) \int_{a-H_o}^{a} y^2\, f_H(a-y) \int_0^{\nu} \sin\lambda \int_0^{2\pi} d\theta\, d\lambda\, dy \\ &= \sum_{i=1}^{2} p_i(1-\cos\,\nu)[\,a^2 I_{oi}(H_o) + I_{2i}(H_o) \\ &\qquad - 2a\, I_{1i}(H_o)]\,/\,[\,\nu\, I_{oi}(H_o)\,] \end{aligned} \qquad (A3.8.1.35)$$

Defining

$$\lambda' = \arccos\,\{(a^2 + y^2 - r^2)/(2\,ay)\} \qquad (A3.8.1.36)$$

the volume $V(r)$, from Fig. (A3.8.1.2) for $r \varepsilon [0, a \sin \nu]$ can be written as

$$V(r) = \int_{a-r}^{a} y^2 \int_{0}^{\lambda'} \sin \lambda \int_{0}^{2\pi} f_{Y\Lambda\Theta} (y, \lambda, \theta) d\theta \, d\lambda \, dy \qquad (A3.8.1.37)$$

Substitution of Eq. (A3.8.1.36), Eq. (A3.8.1.26) and Eq. (A3.8.1.27) in Eq. (A3.8.1.37) and completion of twofold integral yields

$$V(r) = 1/(2a\nu) \int_{a-r}^{a} y \, [r^2-(a-y)^2] \, f_Y(y) \, dy \qquad (A3.8.1.38)$$

Substituting Eq. (A3.8.1.33), Eq. (A3.8.1.28) and Eq. (A3.8.1.30) in Eq. (A3.8.1.38) and integrating results in

$$V(r) = \sum p_i [\{r^2 I_{oi}(r) - I_{2i}(r)\} + \{I_{3i}(r) - r^2 I_{1i}(r)\} /a] / \{2\nu \, I_{oi} (H_o)\} \qquad (A3.8.1.39)$$

Substituting this and Eq. (A3.8.1.35) into Eq. (A3.8.1.32) yields the probability distribution function of focal distance, R, as

$$F_R(r) = \sum p_i [r^2 I_{oi}(r) - I_{2i}(r) + \{I_{3i}(r) - - r^2 I_{1i}(r)\} /a] /V_i^* \; ; \; 0 \leq r \leq a \sin \nu \qquad (A3.8.1.40)$$

where

$$V_i^* = 2(1-\cos \nu) \sum p_i [a^2 \, I_{oi}(H_o) + I_{2i}(H_o) - 2a \, I_{1i}(H_o)] \qquad (A3.8.1.41)$$

The probability density function of focal distance, R, is obtained by differentiating Eq. (A3.8.1.40) with respect to r and is given by

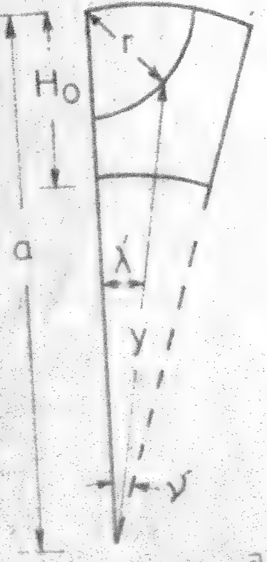

FIG. A3·8·1 2 $r \in [0, a \sin \gamma]$

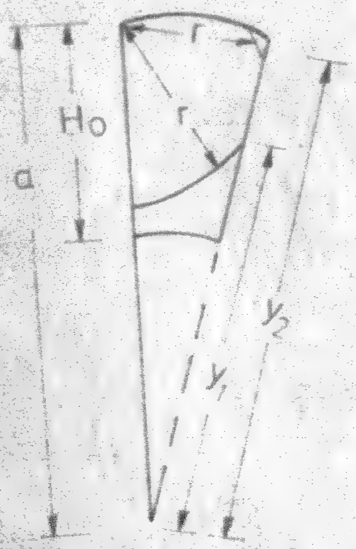

FIG. A3·8·1·3 $r \in [a \sin \gamma, 2a \sin(\gamma/2)]$

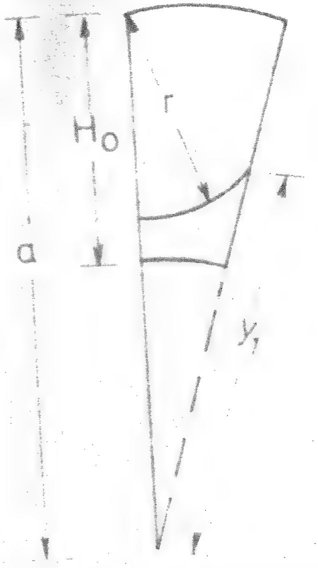

FIG. A3·8·1·4 $r \in [2a \sin(\gamma/2), H_0]$

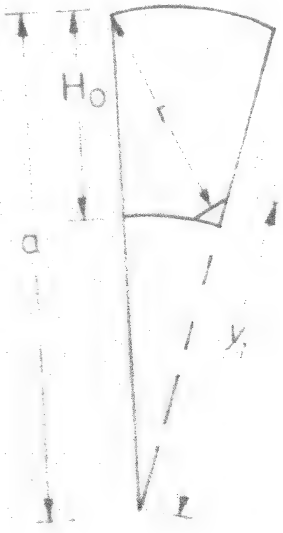

FIG. A3·8·1·5 $r \in [H_0, R_0]$

Event $[R \leq r]$

$$f_R(r) = 2r \sum p_i \left[I_{oi}(r) - I_{1i}(r)/a \right] / V^*; \; 0 \leq r \leq a\sin\nu \qquad (A3.8.1.42)$$

For $r \in [a \sin\nu, 2a \sin(\nu/2)]$, the volume, $V(r)$, from Fig. (3.8.1.3) is

$$V(r) = \int_{y_2}^{a} y^2 \int_0^{\lambda'} \sin\lambda \int_0^{2\pi} f_{Y\Lambda\Theta}(y, \lambda, \theta)\, d\theta\, d\lambda\, dy$$
$$+ \int_{y_2}^{y_1} y^2 \int_0^{\nu} \sin\lambda \int_0^{2\pi} f_{Y\Lambda\Theta}(y, \lambda, \theta)\, d\theta\, d\lambda\, dy$$
$$+ \int_{a-r}^{y_1} y^2 \int_0^{\lambda'} \sin\lambda \int_0^{2\pi} f_{Y\Lambda\Theta}(y, \lambda, \theta)\, d\theta\, d\lambda\, dy \qquad (A3.8.1.43)$$

where

$$\lambda' = \arccos\left[(a^2 + y^2 - r^2)/(2ay) \right] \qquad (A3.8.1.44)$$

$$y_1 = a\cos\nu - \sqrt{r^2 - a^2 \sin^2\nu} \qquad (A3.8.1.45)$$

and $$y_2 = a\cos\nu + \sqrt{r^2 - a^2 \sin^2\nu} \qquad (A3.8.1.46)$$

Substitution of Eq. (A3.8.1.33), Eq. (A3.8.1.28), Eq. (A3.8.1.30) and Eq. (A3.8.1.35) into Eq. (A3.8.1.43) and completion of integration results in

$$V(r) = \sum p_i \left[r^2 I_{oi}(r) - I_{2i}(r) + \{ I_{3i}(r) - r^2 I_{1i}(r) \}/a \right.$$
$$\left. + G_i(a-y_2) - G_i(a-y_1) \right] / \{ 2\nu\, I_{\bullet i}(H_o) \} \qquad (A3.8.1.47)$$

where

$$G_i(x) = \{ r^2 - 2a^2(1-\cos\nu) \} I_{oi}(x) + \{ 4a(1-\cos\nu) - r^2/a \} I_{1i}(x)$$
$$+ \{ 2\cos\nu - 3 \} I_{2i}(x) + I_{3i}(x)/a \qquad (A3.8.1.48)$$

Probability distribution function of R is obtained by substituting Eq. (A3.8.1.47) and Eq. (A3.8.1.35) into Eq. (A3.8.1.32) and is given by

$$F_R(r) = \sum p_i \left[r^2 I_{oi}(r) - I_{2i}(r) + \{ I_{3i}(r) - r^2 I_{1i}(r) \} / a \right.$$

$$\left. + G_i(a-y_2) - G_i(a-y_1) \right] / V_i^* \; ; \; a \sin \nu \le r \le 2a \sin(\nu/2) \tag{A3.8.1.49}$$

Differentiating Eq. (A3.8.1.49) with respect to r yields the probability density function of R as

$$f_R(r) = \sum p_i \left[2r \{ I_{oi}(r) - I_{oi}(a-y_1) + I_{oi}(a-y_2) \right.$$

$$- [I_{1i}(r) - I_{1i}(a-y_1) + I_{1i}(a-y_2)] / a \}$$

$$\left. + \quad q_i(a-y_1) + q_i(a-y_2) \right] / V_i^* \; ; \; a \sin \nu \le r \le 2a \sin(\nu/2) \tag{A3.8.1.50}$$

where

$$q_i(x) = s[2a^2(1-\cos \nu) - r^2 + x \{ r^2/a - 4a(1-\cos \nu) \}$$

$$+ x^2(3-2 \cos \nu) - x^3/a] g_i(x) \tag{A3.8.1.51}$$

and

$$s = r / \sqrt{r^2 - a^2 \sin^2 \nu} \tag{A3.8.1.52}$$

From Fig. (A3.8.1.4), the volume, V(r), for $r \in [2a \sin(\nu/2), H_o]$ can be written as

$$V(r) = \int_{y_1}^{a} y^2 \int_{0}^{\nu} \sin \lambda \int_{0}^{2\pi} f_{Y\Lambda\Theta}(y, \lambda, \theta) \, d\theta \, d\lambda \, dy$$

$$+ \int_{a-r}^{y_1} y^2 \int_{0}^{\lambda'} \sin \lambda \int_{0}^{2\pi} f_{Y\Lambda\Theta}(y, \lambda, \theta) d\theta \, d\lambda \, dy$$

Simplification after substitution of Eq. (A3.8.1.33), Eq. (A3.8.1.26), Eq. (A3.8.1.28) and Eq. (A3.8.1.34) into this and integration results in

$$V(r) = \sum p_i \left[r^2 I_{oi}(r) - I_{2i}(r) + \{I_{3i}(r) - r^2 I_{1i}(r)\}/a - G_i(a-y_1) \right] / \{2\nu \, I_{oi}(H_o)\} \qquad (A3.8.1.53)$$

Substituting Eq. (A3.8.1.53) and Eq. (3.8.1.35) into Eq. (A3.8.1.32) the probability distribution function of R is obtained as

$$F_R(r) = \sum p_i \left[r^2 I_{oi}(r) - I_{2i}(r) + \{ I_{3i}(r) - r^2 I_{1i}(r) \}/a - G_i(a-y_1) \right] / V_i^* \; ; \; 2a \sin(\nu/2) \leq r \leq H_o \qquad (A3.8.1.54)$$

The probability density function of R is obtained by differentiation of Eq. (A3.8.1.54) with respect to r and is given by

$$f_R(r) = \sum p_i \left[2r \{ I_{oi}(r) - I_{oi}(a-y_1) - [I_{1i}(r) - I_{1i}(a-y_1)] /a \} + q_i(a-y_1) \right] / V_i^* \; ; \; 2a \sin(\nu/2) \leq r \leq H_o \qquad (A3.8.1.55)$$

The volume V(r), for $r \in [H_o, R_o]$ from Fig. (A3.8.1.5) is given by

$$V(r) = \int_{a-H_o}^{y_1} y^2 \int_0^{\lambda'} \sin\lambda \int_0^{2\pi} f_{Y\Lambda\Theta}(y, \lambda, \theta) d\theta \, d\lambda \, dy + \int_{y_1}^{a} y^2 \int_0^{\nu} \sin\lambda \int_0^{2\pi} f_{Y\Lambda\Theta}(y, \lambda, \theta) d\theta \, d\lambda \, dy$$

Integrating this after substitution of Eq. (A3.8.1.34), Eq. (A3.8.1.33), Eq. (A3.8.1.28) and Eq. (A3.8.1.26) yields

$$V(r) = \sum p_i \left[r^2 I_{oi}(H_o) - I_{2i}(H_o) + \{ I_{3i}(H_o) - r^2 I_{1i}(H_o) \} / a - G_i(a-y_1) \right] / \{ 2\nu \, I_{oi}(H_o) \} \qquad (A3.8.1.56)$$

Substituting Eq. (A3.8.1.56) and Eq. (A3.8.1.35) into Eq. (A3.8.1.32) results in the probability distribution function of R and is given by

$$F_R(r) = \sum p_i \left[r^2 I_{oi}(H_o) - I_{2i}(H_o) + \{ I_{3i}(H_o) - r^2 I_{1i}(H_o) \} / a - G_1(a-y_1) \right] / V_i^* \quad ; H_o \leq r \leq R_o \qquad (A3.8.1.57)$$

where

$$R_o = \sqrt{a^2 + (a-H_o)^2 - 2a(a-H_o)\cos\nu} \qquad (A3.8.1.58)$$

Differentiating Eq. (A3.8.1.57) with respect to r, the probability density function of R is obtained as

$$f_R(r) = \sum p_i \left[2r \{ I_{oi}(H_o) - I_{oi}(a-y_1) + [I_{1i}(a-y_1) - I_{1i}(H_o)] / a \} + q_i(a-y_1) \right] / V_i^* \quad ; H_o \leq r \leq R_o \qquad (A3.8.1.59)$$

c) Probability Distribution function of Focal Depth, H, is lognormal in $(0, H_o]$

The probability distribution and density function of focal distance, R, for volume earthquake source for the lognormal focal depth H can be obtained from the previous section by following substitution

$p_1 = 1$ and $p_2 = 0$

$\theta_{1i} = \theta_1$ and $\theta_{2i} = \theta_2$

The probability distribution function, $f_R(.)$, of the focal distance, R, after above substitution is the following:

$$F_R(r) = [\, r^2 I_o(r) - I_2(r) + \{I_3(r) - r^2 I_1(r)\}/a \,]/V^* \quad ; \quad 0 \leq r \leq a \sin \nu \qquad (A3.8.1.60)$$

$$F_R(r) = [\, r^2 I_o(r) - I_2(r) + \{I_3(r) - r^2 I_1(r)\}/a + G(a-y_2) - G(a-y_1)\,]/V^* \quad ; a \sin \nu \leq r \leq 2a \sin(\nu/2) \qquad (A3.8.1.61)$$

$$F_R(r) = [\, r^2 I_o(r) - I_2(r) + \{I_3(r) - r^2 I_1(r)\}/a - G(a-y_1)\,]/V^* \quad ; \; 2a \sin(\nu/2) \leq r \leq H_o \qquad (A3.8.1.62)$$

$$F_R(r) = [\, r^2 I_o(H_o) - I_2(H_o) + \{I_3(H_o) - r^2 I_1(H_o)\}/a - G(a-y_1)\,]/V^* \quad ; \; H_o \leq r \leq R_o \qquad (A3.8.1.63)$$

where

$$I_m(x) = \exp\{(\theta_1 - 1/2\, m\theta_2)m\}\,\Phi[\,(\ell n\, H_o - \theta_1 - m\theta_2)/\sqrt{\theta_2}\,] \; ; \; m \geq 0 \qquad (A3.8.1.64)$$

$$V^* = 2(1-\cos \nu)\,[\, a^2 I_o(H_o) + I_2(H_o) - 2a\, I_1(H_o)\,] \qquad (A3.8.1.65)$$

$$G(x) = \{r^2 - 2a^2(1-\cos \nu)\}\, I_o(x) + \{4a(1-\cos \nu) - 1/a\, r^2\}\, I_1(x) + \{2 \cos \nu - 3\}\, I_2(x) + 1/a\, I_3(x) \qquad (A3.8.1.66)$$

$$y_1 = a \cos \nu - \sqrt{r^2 - a^2 \sin^2 \nu} \qquad (A3.8.1.67)$$

$$y_2 = a \cos \nu - \sqrt{r^2 - a^2 \sin^2 \nu} \qquad (A3.8.1.68)$$

$$R_o = \sqrt{a^2 + (a-H_o)^2 - 2a(a-H_o) \cos \nu} \qquad (A3.8.1.69)$$

and $\Phi(.)$ is the probability distribution function of $N(0,1)$.

The corresponding probability density function, $f_R(.)$, is given by

$$f_R(r) = 2r\,[\,I_o(r) - 1/a\ I_1(r)]\,/V^* \ ;\ 0 \leq r \leq a \sin \nu \qquad (A3.8.1.70)$$

$$f_R(r) = [\,2r\ \{I_o(r) - I_o(a-y_1) + I_o(a-y_2)$$

$$- [\,I_1(r) - I_1(a-y_1) + I_1(a-y_2)\,]/a\} \qquad (A3.8.1.71)$$

$$+\ q(a-y_1) + q(a-y_2)]\,/V^* \ ;\ a \sin \nu \leq r \leq 2a \sin(\nu/2) \qquad (A3.8.1.72)$$

$$f_R(r) = [\,2r\ \{I_o(r) - I_o(a-y_1) - [\,I_1(r) - I_1(a-y_1)]\,/a\}$$

$$+\ q(a-y_1)]\,/V^* \quad ;\ 2a \sin(\nu/2) \leq r \leq H_o \qquad (A3.8.1.73)$$

$$f_R(r) = [\,2r\ \{I_o(H_o) - I_o(a-y_1) + [\,I_1(a-y_1) - I_1(H_o)]\,/a\}$$

$$+\ q(a-y_1)]\,/V^* \quad ;\ H_o \leq r \leq R_o \qquad (A3.8.1.74)$$

where

$$g(x) = \exp[\,-(\ln x - \theta_1)^2/(2\theta_2)]\,/\,(\sqrt{2\pi\theta_2}\ x) \qquad (A3.8.1.75)$$

$$q(x) = s\,[\,2a^2(1-\cos\ \nu) - r^2 + x\,\{r^2/a - 4a(1-\cos\ \nu)\}$$

$$+\ x^2(3-2\cos\ \nu) - x^3/a\,]\ g(x) \qquad (A3.8.1.76)$$

and $$s = r/\sqrt{r^2 - a^2 \sin^2 \nu} \qquad (A3.8.1.77)$$

APPENDIX A3.8.2

PROBABILITY OF GENERALIZED PEAK SEISMIC INTENSITY, Y

a) Magnitude of earthquakes is cutoff at lower level m_o i.e. $m \varepsilon (m_o, \infty)$.

The probability of the event $[Y > y]$ is to be derived for the defined probability density function of magnitude, $f_M(.)$, Eq. (3.3) and for different hypotheses of focal depth distribution Eqs. (3.6-3.8). The attenuation law, Eq. (3.10), can be written as

$$Y = Z\,W \qquad (A3.8.2.1)$$

where $$Z = C_1 \exp\,(C_2 M) \qquad (A3.8.2.2)$$

and $$W = \exp[\,-C_3\,\ell n(R + C_4)\,] \qquad (A3.8.2.3)$$

according to section 3.7. The joint probability density function of Z and W is given by Eq. (3.4) as

$$f_{ZW}(z,w) = f_Z(z)\,f_W(w) \qquad (A3.8.2.4)$$

The probability density function, $f_Z(.)$, of Z is obtained by substitution of Eq. (3.3) into Eq. (3.15) and is given by

$$f_Z(z) = \exp[\,\beta m_o + \beta/C_2\ \ell n\ C_1 + \ \ell n\ \beta\ \ell n\ C_2 - (\beta + C_2)/C_2\ \ell n\ z\,]$$

$$;\ z\ \varepsilon\,(z_1, \infty) \qquad (A3.8.2.5$$

where $$z_1 = C_1 \exp\,[\,C_2 m_o\,] \qquad (A3.8.2.6$$

The probability density function, $f_W(.)$, of W is given by Eq. (3.14) as

$$f_W(w) = 1/\left[C_3 w^{(C_3+1)/C_3}\right] f_R(w^{-1/C_3} - C_4);\ w \in (w_1, w_2) \qquad (A3.8.2.9)$$

where
$$w_1 = (R_o + C_4)^{-C_3} \qquad (A3.8.2.10)$$

$$w_2 = C_4^{-C_3} \qquad (A3.8.2.11)$$

and R_o is the maximum focal distance and $f_R(.)$ is the probability density function of focal distance, R. The details of probability distribution function, $F_R(.)$, and the probability density function, $f_R(.)$, of focal distance, R, are given in Appendix A3.8.1.

To find the probability of the event $[Y > y]$, there exist three different regions in the domain of y, which are shown in Fig. (A3.8.2.1). From this figure and Eq. (3.8) the required probability of the event is obtained as

$$P[Y > y] = S_Y(y) = 1 \quad ;\ 0 \le y \le z_1 w_1 = y_1 \qquad (A3.8.2.12)$$

For $y \in [z_1 w_1, z_1 w_2]$ from Fig. (A3.8.2.1) and Eq. (3.19), the required probability is obtained as,

$$P[Y > y] = S_Y(y) = \int_{w_1}^{y/z_1} dw \int_{y/w}^{\infty} f_{ZW}(z,w)dz + \int_{y/z_1}^{w_2} dw \int_{z_1}^{\infty} f_{ZW}(z,w)dz$$

Substitution of Eq. (A3.8.2.4) and Eq. (A3.8.2.5) into this and integrating with respect to z results in

$$S_Y(y) = \int_{w_1}^{y/z_1} S_Z(y/w)\, f_W(w)dw + \int_{y/z_1}^{w_2} f_W(w)dw \qquad (A3.8.2.13)$$

where

$$S_Z(u) = \exp\ [\beta\{m_o + 1/C_2(\ell n\ C_1 - \ell n\ u)\}] \qquad (A3.8.2.14)$$

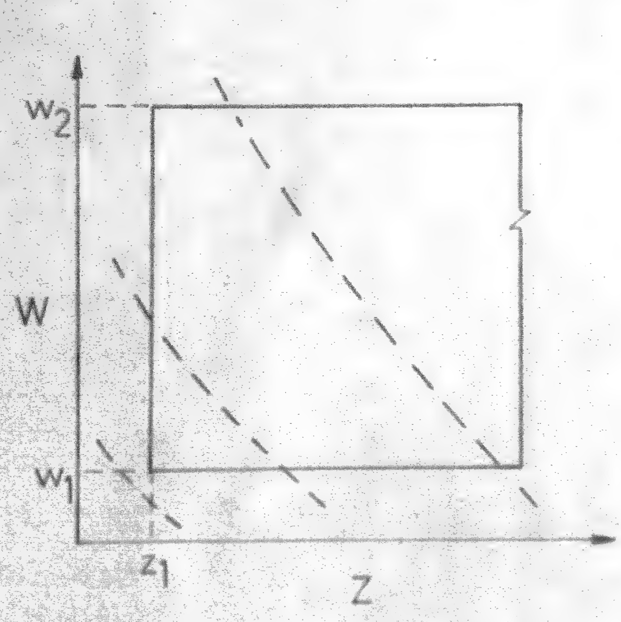

FIG. A3·8·2·1 DOMAIN OF DIFFERENT [Y>y]

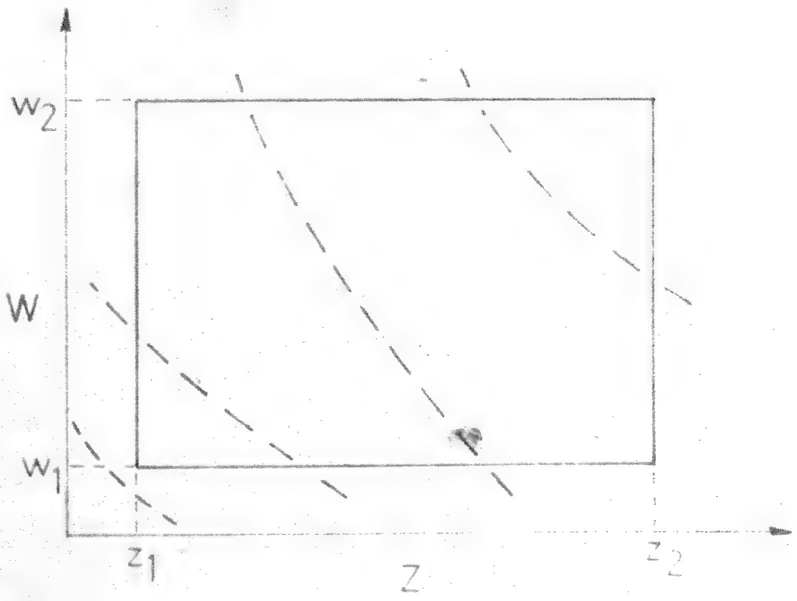
W
w_2
w_1
z_1
Z
z_2

FIG. A3·8·2·2 DOMAIN OF DIFFERENT [Y>y]

Substituting $r = w^{-1/C_3} - C_4$ into Eq. (A3.8.2.11) and integrating gives

$$S_Y(y) = \int_{x_1}^{R_o} S_Z[(r + C_4)^{C_3} y]\, f_R(r)dr + F_R(x_1)$$

$$; \; y_1 \leq y \leq z_1 w_2 = y_2 \qquad \text{(A3.8.2.15)}$$

where $\quad x_1 = \exp[(C_2 m_o + \ell n\, C_1 - \ell n\, y)/C_3] - C_4 \qquad$ (A3.8.2.16)

For $y \geq y_2$, from Fig. (A3.8.2.1) and Eq. (3.19), the required probability is

$$P[Y > y] = S_Y(y) = \int_{w_1}^{w_2} dw \int_{y/w}^{\infty} f_{ZW}(z,w)dz$$

Similar procedure and substitution as above results in

$$S_Y(y) = \int_{o}^{R_o} S_Z[(x + C_4)^{C_3} y]\; f_R(r)dr \; ; \; y \geq y_2 \qquad \text{(A3.8.2.17)}$$

For different hypotheses of focal depth, H, the required probability density and probability distribution function of focal distance, R , from Appendix A3.8.1 to be substituted and final form can be obtained.

(b) Magnitude of earthquakes is cutoff at both ends; i.e. $m \; \varepsilon \; (m_o, m_1]$

The probability density function, $f_Z(.)$, of Z is obtained by substitution of Eq. (3. 4) into Eq. (3.15) and is

$$f_Z(z) = K \exp[\beta\, m_o + \beta/C_2\, \ell n C_1 + \ell n\, \beta - \ell n\, C_2 - (\beta + C_2)/C_2 \ell n\, z]$$

$$; \; z \; \varepsilon \; (z_1, z_2] \qquad \text{(A3.8.2.18)}$$

where

$$z_2 = C_1 \; \exp\,(C_2 m_1) \qquad \text{(A3.8.2.19)}$$

The probability of the event $[Y \geq y]$ is obtained from Fig. (A3.8.2.2) and Eq. (3.19) as

$$P\,[Y > y] = S_Y(y) = 1 \qquad y \leq z_1 w_1 = y_1 \qquad (3.8.2.20)$$

From Fig. (A3.8.2.2) and Eq. (3.19), the probability of the event $[\,Y \geq y]$ when $y_1 \leq y \leq \min\,(y_2 = z_1 w_2, y_3 = z_2 w_1)$ is given by

$$P\,[Y > y] = S_Y(y) = \int_{w_1}^{y/z_1} dw \int_{y/w}^{z_2} f_{ZW}\,(z,w) + \int_{y/z_1}^{w_2} dw \int_{z_1}^{z_2} f_{ZW}(z,w)dz$$

Substituting Eq. (A3.8.2.4) and Eq. (A3.8.2.18) into this and integrating with respect to z results in

$$S_Y(y) = \int_{w_1}^{y/z_1} S_Z(y/w)\, f_W(w)dw + \int_{y/z_1}^{w_2} f_W(w)dw \qquad (A3.8.2.21)$$

where

$$S_Z(x) = K\,\{(C_1/x)^{\beta/C_2} - \exp\,(-\beta m_1)\}\exp\,(\beta m_o) \qquad (A3.8.2.22)$$

Substituting $r = w^{-1/C_3} - C_4$ into Eq. (A3.8.2.21) and integrating yields

$$S_Y(y) = \int_{x_1}^{R_o} S_Z\,[(r + C_4)^{C_3}\, y]\;\; f_R(r)dr + F_R(x_1) \qquad (A3.8.2.23)$$

where

$$x_1 = \exp\;[(\ell n\, C_1 - \ell n\, y + C_2\, m_o)/C_3] - C_4 \qquad (A3.8.2.24)$$

Using the definition of $S_Z(.)$ Eq. (A3.8.2.22) into Eq. (A3.8.2.23) results in

$$S_Y(y) = 1-K[\,1-F_R(x_1)] + \int_{x_1}^{R_o} S_Z^*\,[(r + C_4)^{C_3} y\,]\,f_R(r)dr$$

$$; \; y_1 \le y \le \min\,(y_2, y_3) \qquad (A3.8.2.25)$$

where

$$S_Z^*(x) = K \exp\,[\beta\,\{m_o-(\ell n\; x - \ell n\; C_1)/C_2\}\,] \qquad (A3.8.2.26)$$

and $F_R(.)$ is the probability distribution of focal distance, R.

Using Eq. (3.19) and from Fig. (A3.8.2.2), the probability of $[\,Y \ge y\,]$ when $y_3 \le y \le y_2$ is given by

$$S_Y(y) = \int_{y/z_2}^{y/z_1} dw \int_{y/w}^{z_2} f_{ZW}(z,w)dz + \int_{y/z_1}^{w_2} dw \int_{z_1}^{z_2} f_{ZW}(z,w)dz$$

Adopting similar procedure of Eq. (A3.8.2.25) for this yields

$$S_Y(y) = (1-K)\,F_R(x_2) + K\,F_R(x_1) + \int_{x_1}^{x_2} S_Z^*[\,(r+C_4)^{C_3}y]\,f_R(r)dr$$

$$; \; y_3 \le y \le y_2 \qquad (A3.8.2.27)$$

where

$$x_2 = \exp\,[(C_2 m_1 + \ell n\; C_1 - y)/C_3] - C_4 \qquad (A3.8.2.29)$$

For $y_2 \le y \le y_3$ from Fig. (A3.8.2.2) and Eq. (3.19), the probability of $[Y \ge y]$ is

$$S_Y(y) = \int_{w_1}^{w_2} dw \int_{y/w}^{z_2} f_{ZW}\,(z,w)dz$$

Using the steps as in Eq. (A3.8.2.25) reduces to

$$S_Y(y) = 1-K + \int_0^{R_o} S_Z^*\left[(r+C_4)^{C_3} y\right] f_R(r)dr \;;\; y_2 \leq y \leq y_3 \qquad (A3.8.2.29)$$

For $y \geq \max(y_2, y_3)$, the same probability from Fig. (A3.8.2.2) and Eq. (3.19) is

$$S_Y(y) = \int_{y/z_2}^{w_2} dw \int_{y/w}^{z_2} f_{ZW}(z,w)dz$$

By similar method of Eq. (A3.8.2.25) this results in

$$S_Y(y) = (1-K)\; F_R(x_2) + \int_0^{x_2} S_Z^*\left[(r+C_4)^{C_3} y\right] f_R(r)dr$$

$$; \; y \geq \max(y_2, y_3) \qquad (A3.8.2.30)$$

One of Eq. (A3.8.2.27) and Eq. (A3.8.2.29) will conform to the numerical values of relative parameters. Above results and the results of Appendix A3.8.1 will produce probability of generalized peak seismic intensity for the combination assumed distribution of focal depth, H, and magnitude, M.

APPENDIX A5.1

SECTION OF A SPHERE (EARTH) BY A PLANE (FAULT)

The equation of a fault passing through the points (a,θ_1,ϕ_1) and (a,θ_2,ϕ_2) on the surface of the sphere and passing through the origin of sphere is given by

$$\ell \cos\theta + m \sin\theta + n \tan\phi = 0$$

where

$$\ell = (\sin\theta_1 \tan\phi_2 - \sin\theta_2 \tan\phi_1)/\Delta \qquad (A5.1.1)$$

$$m = (\cos\theta_2 \tan\phi_1 - \cos\theta_1 \tan\phi_2)/\Delta \qquad (A5.1.2)$$

$$n = 1/\Delta \ \sin(\theta_2-\theta_1) \qquad (A5.1.3)$$

and

$$\Delta = \sqrt{\sin^2(\theta_2-\theta_1) + \tan^2\phi_1 + \tan^2\phi_2 - 2\tan\phi_1 \tan\phi_2 \cos(\theta_2-\theta_1)} \qquad (A5.1.4)$$

Taking OZ' in Fig. (A5.1), the new axis of Z, the normal to the fault plane which passes through 0 and makes an acute angle with OZ, the equation to OZ', referred to OX, OY, OZ, are

$$1/\ell \ \cos\phi \cos\theta = 1/m \cos\phi \sin\theta = 1/n \ \sin\phi \qquad (A5.1.5)$$

Taking OY', the new axis of Y, the line in the plane ZOZ' which is at right angle to OZ' and makes an acute angle with OZ, and choosing OX', the new X-axis, at right angle to OZ' and OY', so that the system OX', OY', OZ' can be brought to coincide with OX, OY, OZ. The given plane is X'OY', and since OX' is at right angles to OZ'

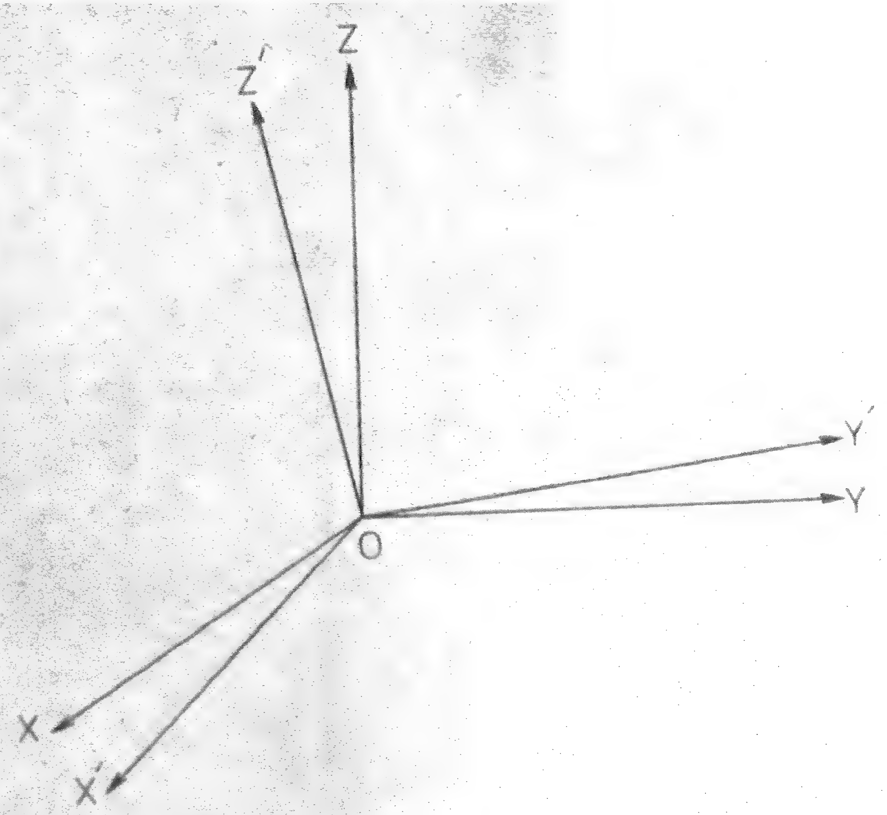

FIG-A5·1 ROTATION OF AXIS FOR FAULT PLANE X'OY' and OY', it is at right angles to OZ which lies in the plane Y'OZ'. Hence OX' lies in the plane XOY, and therefore is the line of intersection of given plane and the plane XOY. The equation of the plane Y'OZ' is

$$1/\ell \quad \cos\theta \; = 1/m \quad \sin\theta \tag{A5.1.6}$$

Since OY' makes an acute angle with OZ, the values of ℓ', m', n' – the direction-cosines of OY' are obtained as

$$\ell' \; = - \ell n/ \sqrt{\ell^2 + m^2} \tag{A5.1.7}$$

$$m' \; = - mn/ \sqrt{\ell^2 + m^2} \tag{A5.1.8}$$

$$n' \; = \sqrt{\ell^2 + m^2} \tag{A5.1.9}$$

The direction-cosines of OX' – at right angles to OY' and OZ' are

$$\ell'' = -m/ \sqrt{\ell^2 + m^2} \tag{A5.1.10}$$

$$m'' = \ell / \sqrt{\ell^2 + m^2} \tag{A5.1.11}$$

$$n'' = 0 \tag{A5.1.12}$$

Hence the transformation is given

$$\underset{\sim}{X}' = \underset{\sim}{T} \; \underset{\sim}{X} \tag{A.5.1.13}$$

where

$$\underset{\sim}{X}^t = <\cos\phi \; \cos\theta \quad \cos\phi \; \sin\theta \quad \sin\phi> \tag{A5.1.14}$$

$$\underset{\sim}{X}'^{t} = \langle \cos\phi' \quad \cos\theta' \quad \cos\phi' \sin\theta' \quad \sin\phi' \rangle \qquad (A5.1.15)$$

and

$$\underset{\sim}{T} = \begin{bmatrix} -m/\sqrt{\ell^2+m^2} & \ell/\sqrt{\ell^2+m^2} & 0 \\ -\ell n/\sqrt{\ell^2+m^2} & -mn/\sqrt{\ell^2+m^2} & \sqrt{\ell^2+m^2} \\ \ell & m & n \end{bmatrix} \qquad (A5.1.16)$$

This transformation is used to rotate a fault such that its position after rotation is equator.

APPENDIX A5.2

PROBABILITY DISTRIBUTION FUNCTION AND PROBABILITY DENSITY FUNCTION OF FOCAL DISTANCE, R, FOR AREA SOURCE

a) Focal depth, H, has probability density function, $f_H(.)$, and probability distribution function, $F_H(.)$ in $(0,H_o]$

The part of the fault which influences the seismic intensity at a site can be represented as shown in Fig. (A5.2.1) without loss of generality. The site 0 is at a distance z_1 out of plane. The transformation required to represent a fault plane as in Fig. (A5.2.1) is given in Appendix A5.1. The focal distance, R, from site to a point at source is given by

$$R = \sqrt{S^2 + z_1^2} \qquad (A5.2.1)$$

The probability distribution of focal distance, R, may be obtained by finding probability distribution of S and transforming it according to Eq. (A5.2.1). The location of earthquakes in the fault plane is assumed to be uniform in the direction of θ. The focal depth posseses a density $f_H(.)$ implying that the distance, D, from the centre of earth has a density

$$f_D(d) = f_H(a-d) \quad ; \quad d \varepsilon [a - H_o, a) \qquad (A5.2.2)$$

The probability distribution of S, assuming statistical independence of θ and H may be given as

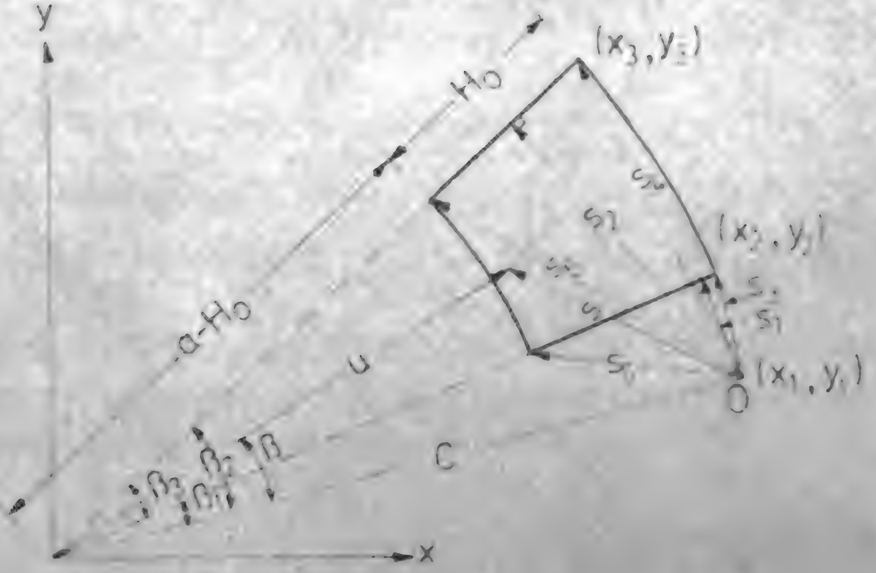
y
x
H_0
a-H_0
(x_3, y_3)
(x_2, y_2)
(x_1, y_1)
O
s_2
s_1
s_3
s
s_0
u
C
β
β_1
β_2
β_3

a = Radius of earth

H_0 = Maximum focal depth

FIG A521 AREA SOURCE DUE TO FAULT WITH PROJECTION OF SITE O AT FAULT PLANE

$$F_S(s) = \mathbf{P}\,[S \leq s] = 1/(K\beta_3) \iint u\, f_D(u)\, d\theta\, du \tag{A5.2.3}$$

with

$$K = E\,[D] = a - E\,[H] \tag{A5.2.4}$$

$$\beta_3 = \arctan\,(y_3/x_3) - \arctan\,(y_2/x_2) \tag{A5.2.5}$$

and $E\,[\,.\,]$ represents expected value of the variable. The probability distribution of focal distance, R, is obtained using Eq. (A5.2.1) and Eq. (5.2.3)

$$F_R(r) = F_S\,(\sqrt{r^2 - z_1^2}) \tag{A5.2.6}$$

From Fig. (A5.2.1), the required probability distribution, F_R, is

$$F_R(r) = 0 \qquad ; \quad z_1 \leq r \leq r_1 = \sqrt{C^2 \sin^2 \beta_1 + z_1^2} \tag{A5.2.7}$$

where

$$C = \sqrt{x_1^2 + y_1^2} \tag{A5.2.8}$$

$$\beta_1 = \arctan\,(y_2/x_2) - \arctan\,(y_1/x_1) \tag{A5.2.9}$$

Corresponding probability density is

$$f_R(r) = 0 \quad ; \quad z_1 \leq r \leq r_1 \tag{A5.2.10}$$

For the region $s_1 \leq s \leq \min\,(s_2, s_3)$, the probability distribution of S from Fig. (A5.2.1) and Eq. (A5.2.3) is

$$F_S(s) = 1/(K\beta_3) \int_{u_1}^{u_2} u\, f_D(u) \int_{\beta_1}^{\beta^*} d\theta\, du$$

where

$$\beta^* = \arccos\ [(C^2 + u^2 - s^2)/2Cu]$$

$$u_1 = C \cos\ \beta_1 - \sqrt{s^2 - C^2 \sin^2\ \beta_1}$$

$$u_2 = C \cos\ \beta_1 + \sqrt{s^2 - C^2 \sin^2 \beta_1}$$

$$s_2 = C \sin\ \beta_2$$

$$s_3 = \sqrt{a^2 + C^2 - 2aC \cos\ \beta_1}$$

$$\beta_2 = \arctan\ (y_3/x_3) - \arctan\ (y_1/x_1) \qquad (A5.2.11)$$

Integration with respect to θ and use of Eq. (A5.2.2) leads to

$$F_S(s) = 1/(K\beta_3) \int_{u_1}^{u_2} u(\beta^* - \beta_1)\, f_H(a - u)\, du$$

Using the transformation Eq. (A5.2.6) in this yields

$$F_R(r) = 1/(K\beta_3) \int_{t_1}^{t_2} (\beta - \beta_1)\, u\, f_H(a - u) du\ ;\ r_1 \leq r \leq \min\ (r_2, r_3) \qquad (A5.2.12)$$

where

$$t_1 = C \cos \beta_1 - \sqrt{r^2 - z_1^2 - C^2 \sin^2 \beta_1} \qquad (A5.2.13)$$

$$t_2 = C \cos \beta_1 + \sqrt{r^2 - z_1^2 - C^2 \sin^2 \beta_1} \qquad (A5.2.14)$$

$$\beta = \arccos\ [(C^2 + z_1^2 + u^2 - r^2)/2Cu] \qquad (A5.2.15)$$

$$r_2 = \sqrt{C^2 \sin^2\ \beta_2 + z_1^2} \qquad (A5.2.16)$$

$$r_3 = \sqrt{a^2 + C^2 - 2aC \cos \beta_1 + z_1^2} \qquad (A5.2.17)$$

Differentiation of Eq. (A5.2.12) leads to probability density of R as

$$f_R(r) = \int_{t_1}^{t_2} g(u)\ f_H(a-u)du \quad ; \quad r_1 \le r \le \min\ (r_2, r_3) \qquad (A5.2.18)$$

where

$$g(u) = 2ru/\left[K\beta_3 \sqrt{\{r^2 - z_1^2 - (u+C)^2\}\ \{(u-C)^2 + z_1^2 - r^2\}}\,\right] \qquad (A5.2.19)$$

Similar procedure yields probability distribution and probability density of focal distance, R, for various regions as under:

if $r_2 \le r \le r_3$

$$F_R(r) = 1/(K\beta_3)\ \left[\int_{t_1}^{v_1} (\beta - \beta_1)u\ f_H(a-u)du + \int_{v_2}^{t_2} (\beta - \beta_1)u\ f_H(a-u)du\right] + 1/K \int_{v_1}^{v_2} uf_H(a-u)du \qquad (A5.2.20)$$

where

$$v_1 = C\cos\beta_2 - \sqrt{r^2 - z_1^2 - C^2\sin^2\beta_2} \qquad (A5.2.21)$$

$$v_2 = C\cos\beta_2 + \sqrt{r^2 - z_1^2 - C^2\sin^2\beta_2} \qquad (A5.2.22)$$

Corresponding probability density is given by

$$f_R(r) = \int_{t_1}^{v_1} g(u)\ f_H(a-u)du + \int_{v_2}^{t_2} g(u)\ f_H(a-u)du \quad ; \quad r_2 \le r \le r_3 \qquad (A5.2.23)$$

If $r_3 \le r \le r_2$, the probability distribution of R is given by

$$F_R(r) = 1/(K\beta_3) \int_{t_1}^{a} (\beta - \beta_1)\ u\ f_H(a-u)du \qquad (A5.2.24)$$

Differentiation of this yields probability density of R as

$$f_R(r) = \int_{t_1}^{a} g(u)\ f_H(a-u)du \quad ; \quad r_3 \leq r \leq r_2 \qquad (A5.2.25)$$

For max $(r_2,r_3) \leq r \leq r_4 = \sqrt{a^2+C^2+z_1^2 - 2aC\cos\beta_2}$, the probability distribution of R is given by

$$F_R(r) = 1/(K\beta_3)\ [\ \int_{t_1}^{v_1} (\beta-\beta_1)\ u\ f_H(a-u)du + \int_{v_2}^{a} (\beta-\beta_1)u\ f_H(a-u)du\ ]$$

$$+\ 1/K \int_{v_1}^{v_2} u\ f_H(a-u)du \qquad (A5.2.26)$$

Corresponding probability density is

$$f_R(r) = \int_{t_1}^{v_1} g(u)\ f_H(a-u)du + \int_{v_2}^{a} g(u)\ f_H(a-u)du$$

$$;\ \max\ (r_2,r_3) \leq r \leq r_4 \qquad (A5.2.27)$$

The probability distribution of R for $r_4 \leq r \leq r_5 = \sqrt{(a-H_o)^2+C^2+z_1^2 - 2C(a-H_o)\cos\beta_1}$ is

$$F_R(r) = 1/(K\beta_3) \int_{t_1}^{v_1} (\beta-\beta_1)\ uf_H(a-u)du + 1/K \int_{v_1}^{a} uf_H(a-u)du \qquad (A5.2.28)$$

Probability density is given by

$$f_R(r) = \int_{t_1}^{v_1} g(u)\ f_H(a-u)du \quad ;\ r_4 \leq r \leq r_5 \qquad (A5.2.29)$$

Probability distribution of R for $r_5 \leq r \leq r_6 = \sqrt{(a-H_o)^2+C^2+z_1^2-2(a-H_o)C\cos\beta_2}$ is given by

$$F_R(r) = 1/(K\beta_3) \int_{a-H_o}^{v_1} (\beta-\beta_1)u\, f_H(a-u)du + 1/K \int_{v_1}^{a} uf_H(a-u)du \quad (A5.2.30)$$

Corresponding probability density is given by

$$f_R(r) = \int_{a-H_o}^{v_1} g(u)\, f_H(a-u)du \quad ; \quad r_5 \leq r \leq r_6 \qquad (A5.2.31)$$

The probability distribution and density of R beyond r_6 is given by

$$\left.\begin{array}{l} F_R(r) = 1 \\ f_R(r) = 0 \end{array}\right. \quad ; \ r \geq r_6 \qquad (A5.2.32)$$

b) Focal depth, H, is lognormal and mixed lognormal in $(0,H_o]$.

The probability distribution and density functions of the focal distance, R, for any distribution of focal depth, H, has been given in the previous section. The formulae given in the previous section have to be integrated for the given probability density, $f_H(.)$. However, the focal depth is assumed to be either lognormally distributed or mixed lognormally distributed. For both these cases analytical integration is not possible. Hence numerical integration technique has been employed to obtain the required probability distribution and density functions.

c) Focal depth, H, is uniform in $(0,H_o]$.

For uniform probability distribution of focal depth, H, Eq. (A5.2.4) yields

$$K = a - H_o/2 \qquad (A5.2.33)$$

The probability distribution of R is obtained using uniform distribution of H and integration formulae for different regions given in section A5.2a. These are

$$F_R(r) = 0 \qquad ; \; z_1 \leq r \leq r_1 = \sqrt{C^2 \sin^2 \beta_1 + z_1^2} \tag{A5.2.34}$$

$$F_R(r) = 1/E \;\; \eta_1(r,\beta_1) \qquad r_1 \leq r \leq \min\,(r_2,r_3) \tag{A5.2.35}$$

$$F_R(r) = 1/E\,[\,\eta_1(r,\beta_1) - \eta_1(r,\beta_2) - \eta_2(r,\beta_2) \quad ; \; r_2 \leq r \leq r_3 \tag{A5.2.36}$$

$$F_R(r) = 1/E\,[\,\eta_3(r,\beta_1,a) + \eta_4(r,\beta_1) - \eta_5(r,a)\,] \, ; \; r_3 \leq r \leq r_2 \tag{A5.2.37}$$

$$\begin{aligned} F_R(r) = 1/E\,[\,&\eta_3(r,\beta_1,a) + \eta_4(r,\beta_1) - \eta_1(r,\beta_2) \\ &- \eta_5(r,a)\,] \, ; \; \max\,(r_2,r_3) \leq r \leq r_4 \end{aligned} \tag{A5.2.38}$$

$$F_R(r) = 1/E\,[\,\eta_4(r,\beta_1) - \eta_4(r,\beta_2)\,] + G \quad ; \; r_4 \leq r \leq r_5 \tag{A5.2.39}$$

$$\begin{aligned} F_R(r) = 1/E\,[\,&\eta_5(r,a-H_o) - \eta_4(r,\beta_2) - \eta_3(r,\beta_1,\, a-H_o)\,] + G \\ &; \; r_5 \leq r \leq r_6 \end{aligned} \tag{A5.2.40}$$

$$F_R(r) = 1 \qquad ; \; r \geq r_6 \tag{A5.2.41}$$

where

$$E = 2\beta_3 \; H_o(a - H_o/2) \tag{A5.2.42}$$

$$\begin{aligned} \eta_1\;(r,u) = (r^2-z_1^2)[\,&\arcsin\,\{(C \sin^2 u + \sqrt{r^2-z_1^2-C^2\sin^2 u}\,\cos u)/\sqrt{r^2-z_1^2}\,\} \\ &- \arcsin\,\{(C \sin^2 u - \sqrt{r^2-z_1^2-C^2\sin^2 u}\,\cos u)/\sqrt{r^2-z_1^2}\,\}\,] \end{aligned} \tag{A5.2.43}$$

$$\eta_2(r,u) = 4(\beta_2-\beta_1)\;\sqrt{r^2-z_1^2 - C^2\sin^2 u}\;C\cos u \tag{A5.2.44}$$

$$\eta_3(r,u,v) = v^2\,[\arccos\{(C^2+v^2+z_1^2-r^2)/(2Cv)\} - \beta_1]$$

$$-\sqrt{\{r^2-z_1^2-(v+C)^2\}\{(v-C)^2+z_1^2-r^2\}}\;/2 \qquad \text{(A5.2.45)}$$

$$\eta_4(r,u) = C[\,C\cos u - \sqrt{r^2-z_1^2-C^2\sin^2 u}\,]\sin u$$

$$+\,(r^2-z_1^2)\,[\arcsin\{(C\sin^2 u + \sqrt{r^2-z_1^2-C^2\sin^2 u}\,\cos u)/\sqrt{r^2-z_1^2}\}]$$

$$\text{(A5.2.46)}$$

$$\eta_5(r,u) = (r^2-z_1^2)\arcsin\{(C^2+r^2-z_1^2-u^2)/(2C\sqrt{r^2-z_1^2})\} \qquad \text{(A5.2.47)}$$

$$G = a^2/[(2a-H_o)\,H_o] \qquad \text{(A5.2.48)}$$

Differentiation of Eqs. (A5.2.34 - A5.2.41) lead to probability density of R for various regions. They are the following

$$f_R(r) = 0 \qquad ;\ r \le r_1 \ \text{ and } \ r \ge r_6 \qquad \text{(A5.2.49)}$$

$$f_R(r) = 1/T\ [\xi_1(r,\beta_1) - \xi_2(r,\beta_1)]\,;\ r_1 \le r \le \min(r_2,r_3) \qquad \text{(A5.2.50)}$$

$$f_R(r) = 1/T\ [\xi_1(r,\beta_1) - \xi_2(r,\beta_1) - \xi_1(r,\beta_2) + \xi_2(r,\beta_2)]$$

$$;\ r_2 \le r \le r_3 \qquad \text{(A5.2.51)}$$

$$f_R(r) = 1/T\ [\xi_1(r,\beta_1) - \xi_3(r,a)]\ ;\ r_3 \le r \le r_2 \qquad \text{(A5.2.52)}$$

$$f_R(r) = 1/T\ [\xi_1(r,\beta_1) - \xi_3(r,a) - \xi_1(r,\beta_2) + \xi_2(r,\beta_2)]$$

$$;\ \max(r_2,r_3) \le r \le r_4 \qquad \text{(A5.2.53)}$$

$$f_R(r) = 1/T\,[\,\xi_1(r,\beta_1) - \xi_1(r,\beta_2)\,]\ ;\ r_4 \le r \le r_5 \qquad \text{(A5.2.54)}$$

$$f_R(r) = 1/T\ [\xi_3(r,a-H_o) - \xi_1(r,\beta_2)]\,;\ r_5 \le r \le r_6 \qquad \text{(A5.2.55)}$$

where

$$T = \sqrt{r^2 - z_1^2} / [\,(a - H_o/2)\,\beta_3\,H_o\,] \qquad (A5.2.56)$$

$$\xi_1\,(r,u) = \arcsin[\,(C \sin^2 u + \sqrt{r^2 - z_1^2 - C^2 \sin^2 u}\,\cos u) / \sqrt{r^2 - z_1^2}\,] \qquad (A5.2.57)$$

$$\xi_2\,(r,u) = \arcsin[\,(C \sin^2 - \sqrt{r^2 - z_1^2 - C^2 \sin^2 u}\,\cos u) / \sqrt{r^2 - z_1^2}\,] \qquad (A5.2.58)$$

$$\xi_3\,(r,u) = \arcsin[\,(r^2 - z_1^2 - u^2) / (2C\sqrt{r^2 - z_1^2})] \qquad (A5.2.59)$$

APPENDIX A6.4.1

THE PROBABILITY DISTRIBUTION FUNCTION OF Z

a) The Magnitude, M, is cutoff at lower level i.e. $m \varepsilon (0, \infty)$

The probability distribution function, $F_Z(.)$, can be easily obtained from Fig. (A6.4.1) as

$$F_Z(z) = 0 \qquad ; \; z \leq \exp(x_1 + C_2 m_o) = z_1 \tag{A6.4.1.1}$$

The probability distribution function of z is given by

$$P[Z \leq z] = P[X + C_2 M \leq \ell n \, z]$$

Assuming statistical independence of $X = \ell n \, C_1$ and M and Fig. (A6.4.1.2) yields

$$F_Z(z) = \int_{x_1}^{\ell nz - C_2 m_o} \int_{m_o}^{(\ell nz - x)/C_2} f_X(x) \, f_M(y) dy \, dx$$

Integration of this results in

$$F_Z(z) = \int_{x_1}^{\ell nz - C_2 m_o} f_X(x) \, F_M \{(\ell nz - x)/C_2\} \, dx$$

Integration and simplification of this results in

$$F_Z(z) = q_1(z, x_1, m_o, \Delta_1) + q_2(z, e_1, \Delta_1)$$

$$; \; z_1 \leq z \leq z_2 = \exp(x_2 + C_2 m_o) \tag{A6.4.1.2}$$

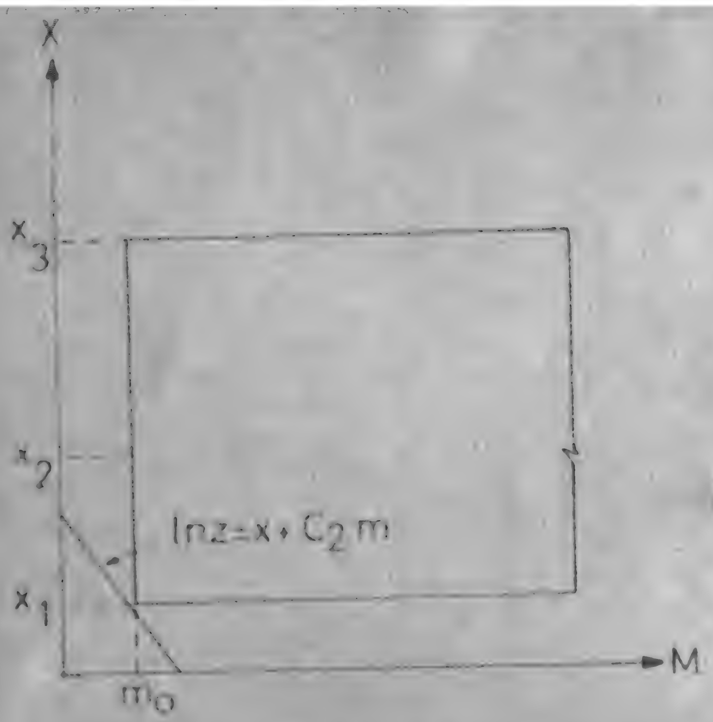
X
x_3
x_2
x_1
$\ln z = x + C_2 m$
m_0
M

FIG. A 6·4·1·1 $Z \leq z_1$

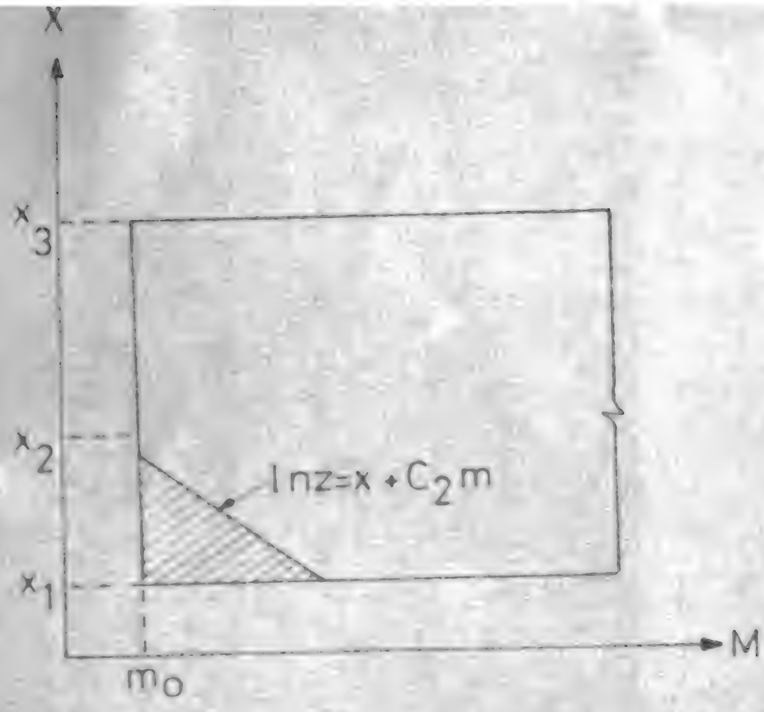
X
x_3
x_2
x_1
$\ln z = x + C_2 m$
m_0
M

FIG. A 6·4·1·2 $z_1 \leq Z \leq z_2$

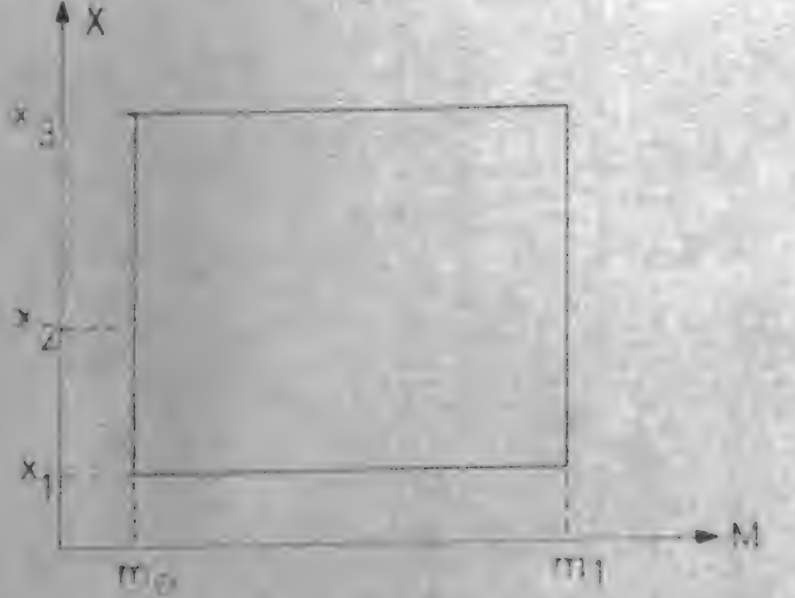
X
x_3
x_2
x_1
m_0
m_1
M

FIG. A 6·4·1·3 DOMAIN OF Z

where

$$q_1(u,v,w,y) = (\ln u-v-C_2w)\,(\ln u-v-C_2w - 2C_2/\beta)y \qquad (A6.4.1.3$$

$$q_2(u,v,y) = 2y\, C_2^2/\beta^2\, F_M(v) \qquad (A6.4.1.4$$

$$1/\Delta_1 = (x_3 - x_1)\,(x_2 - x_1) \qquad (A6.4.1.5)$$

$$e_1 = (\ln z - x_1)/C_2 \qquad (A6.4.1.6)$$

$$F_M(x) = 1-\exp\,[\beta(m_o-x)] \;\; ; \; x \geq m_o \qquad (A6.4.1.7)$$

Proceeding along similar lines the probability distribution function of Z is obtained in different regions as under

$$F_Z(z) = q_1(z,x_1,m_o,\Delta_1) + q_2(z,e_1,\Delta_1) - q_1(z,x_2,m_o,\Delta_1)$$

$$- q_2(z,e_2,\Delta_2)\; ; \; z_2 \leq z \leq \exp\,(C_2m_o + x_3) \qquad (A6.4.1.8)$$

$$F_Z(z) = 1+q_2(z,e_1,\Delta_1) - q_2(z,e_2,\Delta_2) + q_2(z,e_3,\Delta_3);\;\; z \geq z_3 \qquad (A6.4.1.9)$$

where

$$e_i = (\ln z - x_i)/C_2 \; ; \; i = 1,2,3 \qquad (A6.4.1.10)$$

$$1/\Delta_2 = (x_3 - x_2)\,(x_2 - x_1) \qquad (A6.4.1.11)$$

$$1/\Delta_3 = (x_3 - x_1)\,(x_3 - x_2) \qquad (A6.4.1.12)$$

b) The Magnitude, M, is cutoff at both level i.e. $M \in (m_o\, , m_1]$

The domain of M and X are shown in Fig. (A6.4.1.3). From Fig. (A6.4.1.3) it is easily seen that probability distribution function, $F_Z(.)$, is

$$F_Z(z) = 0 \qquad ; \; z \leq z_1 = \exp\,(x_1 + C_2 m_o) \qquad (A6.4.1.13)$$

The probability distribution as well as density function of Z in the region $z_1 \leq z \leq \min\,(z_2, z_4)$ is obtained from Fig. (A6.4.1.4) and the mutual statistical independence of C_1 and M as

$$P[\,Z \leq z\,] \;=\; P[\,X + C_2 M \leq \ln z\,]$$

or $$F_Z(z) = \int_{x_1}^{\ln z - C_2 m_o} \int_{m_o}^{(\ln z - x)/C_2} f_{X,M}(x,y)\,dy\,dx$$

$$= K \int_{x_1}^{\ln z - C_2 m_o} f_X(x)\; F_M\,\{(\ln z - x)/C_2\}\,dx \qquad (A6.4.1.14)$$

where $$1/K = 1 - \exp\,[\,\beta\,(m_o - m_1)\,] \qquad (A6.4.1.15)$$

Substitution of $f_X(.)$ from Eq. (6.22) into Eq. (A6.4.1.14) and subsequent integration and simplification results in

$$F_Z(z) = K\,[\,q_1(z_1 x_1, m_o, \Delta_1) + q_2(z, e_1, \Delta_1)]$$

$$; \; z_1 \leq z \leq \min\,(z_2, z_4) \qquad (A6.4.1.16)$$

where

$$z_2 = \exp\,(x_2 + C_2 m_o) \qquad (A6.4.1.17)$$

$$z_4 = \exp\,(x_1 + C_2 m_1) \qquad (A6.4.1.18)$$

The probability distribution of Z for various regions is obtained by employing similar procedure as in Eq. (A6.4.1.16), giving

$$F_Z(z) = u\Delta_1 + Kq_1(z,x_1,m_o,\Delta_1) - K_1q_1(z,x_1,m_1,\Delta_1)$$

$$; \; z_4 \leq z \leq z_2 \qquad \text{(A6.4.1.19)}$$

$$F_Z(z) = K\left[1-q_1(z,x_3,m_o,\Delta_3) + q_2(z,e_1,\Delta_1) - q_2(z,e_2,\Delta_2)\right]$$

$$; \; z_2 \leq z \leq \min(z_3,z_4) \qquad \text{(A6.4.1.20)}$$

$$F_Z(z) = u\Delta_1 - K_1q_1(z,x_1,m_1,\Delta_1) + K\left[1-q_1(z,x_3,m_o,\Delta_3)\right.$$

$$\left. - q_2(z,e_2,\Delta_2)\right] ; \; z_2,z_4 \leq z \leq z_3,z_5 \qquad \text{(A6.4.1.21)}$$

$$F_Z(z) = 1-u\Delta_3 - Kq_1(z,x_3,m_o,\Delta_3) + K_1q_1(z,x_3,m_1,\Delta_3)$$

$$; \; \max(z_2,z_5) \leq z \leq \min(z_3,z_6) \qquad \text{(A6.4.1.22)}$$

$$F_Z(z) = 1+K_1 + K\left[q_2(z,e_1,\Delta_1) + q_2(z,e_3,\Delta_3) - q_2(z,e_2,\Delta_2)\right]$$

$$; \; z_3 \leq z \leq z_4 \qquad \text{(A6.4.1.23)}$$

$$F_Z(z) = 1+u\Delta_1 - K_1q_1(z,x_1,m_1,\Delta_1) + K_1$$

$$- q_2(z,e_2,\Delta_2) + q_2(z,e_3,\Delta_3) ; \; \max(z_3,z_4) \leq z \leq z_5 \qquad \text{(A6.4.1.24)}$$

$$F_Z(z) = 1 - u\Delta_1 + K_1q_1(z,x_3,m_1,\Delta_1) + Kq_2(z,e_3,\Delta_3)$$

$$; \; z_5 \leq z \leq z_6 \qquad \text{(A6.4.1.25)}$$

$$F_Z(z) = 1 \qquad ; \; z \geq z_6 \qquad \text{(A6.4.1.26)}$$

where

$$K_1 = K - 1 \qquad \text{(A6.4.1.27)}$$

$$z_3 = \exp\left(x_3 + C_2 m_o\right) \qquad \text{(A6.4.1.28)}$$

$$z_5 = \exp\left(x_2 + C_2 m_1\right) \qquad \text{(A6.4.1.29)}$$

$$z_6 = \exp\left(x_3 + C_2 m_1\right) \qquad \text{(A6.4.1.30)}$$

APPENDIX A6.4.2

THE PROBABILITY DENSITY AND DISTRIBUTION FUNCTION OF W

The domain of $W = (R + C_4)^{C_3}$ is shown in Fig. (A6.4.2.1). The probability distribution function of W is given by

$$P[W \leq w] = P[C_3 \,\ell n\,(R + C_4) \leq \ell n\, w] \qquad (A6.4.2.1)$$

and is evaluated using statistical independence of R and C_3. From Fig. (A6.4.2.1) it is obvious that the probability distribution function, $F_W(.)$, and probability density function, $f_W(.)$ are given by

$$F_W(w) = 0 \qquad ; w \leq C_4^{a_1} = w_1 \qquad (A6.4.2.2)$$

$$f_W(w) = 0 \qquad (A6.4.2.3)$$

For $w_1 \leq w \leq \min(w_2, w_4)$, the probability distribution from Eq. (A6.4.2.1) and Fig. (A6.4.2.2) is given by

$$F_W(w) = \int_0^{w^{1/a_1} - C_4} \int_{a_1}^{\frac{\ell n\, w}{\ell n(r + C_4)}} f_{C_3}(y)\, f_R(r)\, dy\, dr$$

Integration with respect to y and use of Eq. (6.23) lead to

$$F_W(w) = \int_0^{r_1} g(w, r, a_1, \lambda_1)\, f_R(r) dr \quad ; w_1 \leq w \leq \min\ (w_2, w_4) \qquad (A6.4.2.4)$$

where

$$g(x, y, z, \alpha) = \{\ell n\, x/\ell n(y + C_4) - z\}^2\ \alpha \qquad (A6.4.2.5)$$

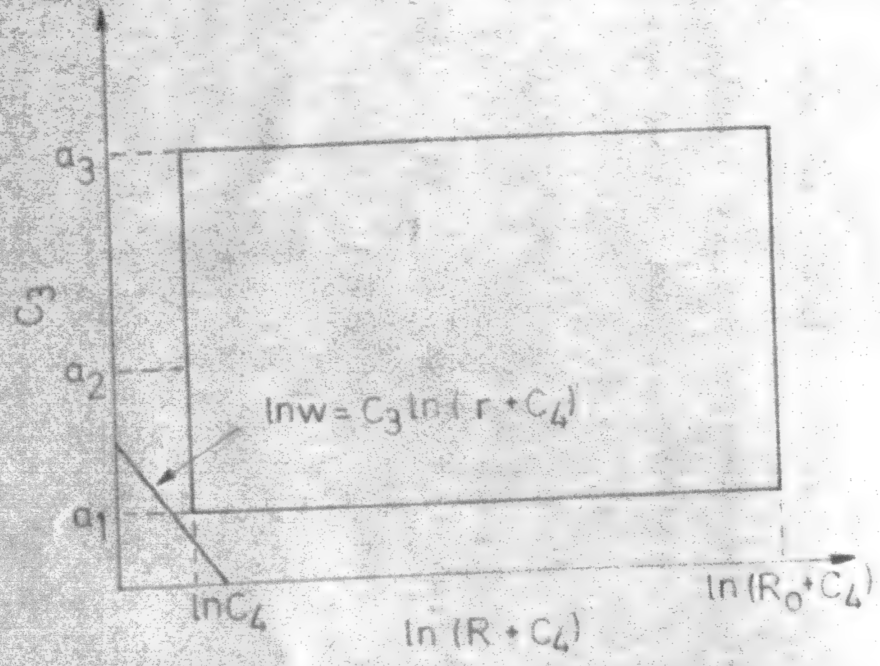

C_3
a_3
a_2
a_1
$\ln w = C_3 \ln(r + C_4)$
$\ln C_4$
$\ln(R + C_4)$
$\ln(R_0 + C_4)$

FIG. A6·4·21 EVENT $[W \leq w_1]$

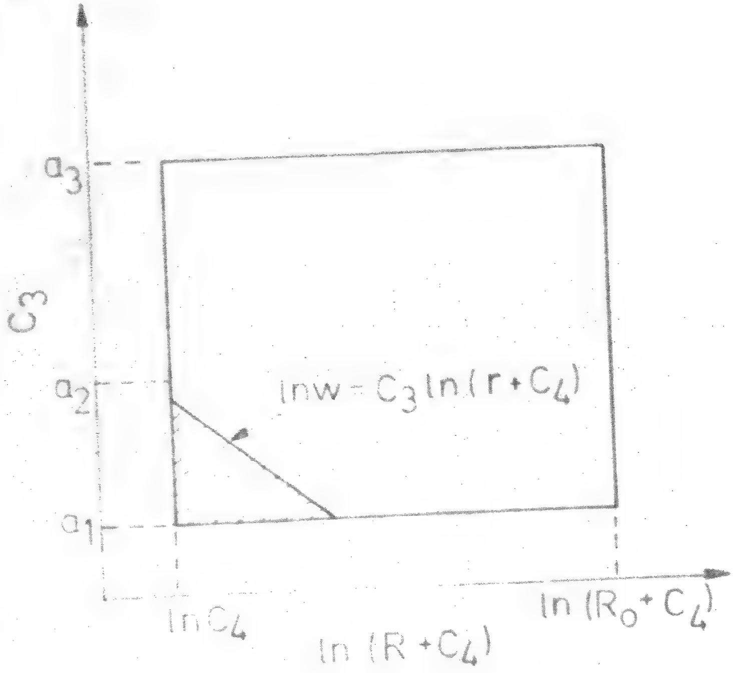

C_3
a_3
a_2
a_1
$\ln w = C_3 \ln(r + C_4)$
$\ln C_4$
$\ln(R + C_4)$
$\ln(R_0 + C_4)$

FIG. A6·4·2·2 EVENT $[w_1 \leq W \leq \min(w_2, w_4)]$

$$1/\lambda_1 = (a_3 - a_1)\,(a_2 - a_1) \qquad (A6.4.2.6)$$

$$w_2 = C_4^{a_2} \qquad (A6.4.2.7)$$

$$r_1 = w^{1/a_1} - C_4 \qquad (A6.4.2.9)$$

and $f_R(.)$ is the probability density of focal distance, R. Differentiation of Eq. (A6.4.2.4) with respect to r yields the probability density function of W as

$$f_W(w) = \int_0^{r_1} h(w,r,a_1,\lambda_1)\, f_R(r)dr \qquad (A6.4.2.10)$$

where

$$h(x,y,z,\alpha) = 2\alpha\, [\ell n\, x/\ell n(y+C_4)-z] \,/\, [\, x\, \ell n(y + C_4)\,] \qquad (A6.4.2.11)$$

The probability distribution function of W for other regions are obtained adopting similar procedure as in Eq. (A6.4.2.4). These are

$$F_W(w) = F_R(r_2) + \int_{r_2}^{r_1} g(w,r,a_1,\lambda_1)\, f_R(r)dr \int_0^{r_2} g(w,r,a_3,\lambda_3) f_R(r)dr$$

$$; \; w_2 \le w \le \min(w_3,w_4) \qquad (A6.4.2.12)$$

$$F_W(w) = \int_0^{R_o} g(w,r,a_1,\lambda_1)\, f_R(r)dr \quad ; \; w_4 \le w \le \min(w_2,w_5) \qquad (A6.4.2.13)$$

$$F_W(w) = F_R(r_2) + \int_{r_2}^{R_o} g(w,r,a_1,\lambda_1)\, f_R(r)dr - \int_0^{r_2} g(w,r,a_3,\lambda_3)\, f_R(r)dr$$

$$; \; \max(w_2,w_4) \le w \le \min\,(w_3,w_5) \qquad (A6.4.2.14)$$

$$F_W(w) = 1 - \int_0^{R_o} g(w,r,a_3,\lambda_3)\, f_R(r)dr \; ; \; \max(w_2,w_5) \le w \le \min(w_3,w_6)$$

$$(A6.4.2.15)$$

$$F_W(w) = F_R(r_2) - \int_{r_3}^{r_2} g(w,r,a_3,\lambda_3)\, f_R(r)dr + \int_{r_2}^{r_1} g(w,r,a_1,\lambda_1)\, f_R(r)dr; \quad w_3 \leq w \leq w_4 \qquad \text{(A6.4.2.16)}$$

$$F_W(w) = F_R(r_2) - \int_{r_3}^{r_2} g(w,r,a_3,\lambda_3)\, f_R(r)dr + \int_{r_2}^{R_o} g(w,r,a_1,\lambda_1)\, f_R(r)dr; \quad \max(w_3,w_4) \leq w \leq w_5 \qquad \text{(A6.4.2.17)}$$

$$F_W(w) = 1 - \int_{r_3}^{R_o} g(w,r,a_3,\lambda_3)\, f_R(r)dr \; ; \quad \max(w_3,w_5) \leq w \leq w_6 \qquad \text{(A6.4.2.18)}$$

$$F_W(w) = 1 \qquad ; \quad w \geq w_6 \qquad \text{(A6.4.2.19)}$$

where

$$r_2 = w^{1/a_2} - C_4 \qquad \text{(A6.4.2.20)}$$

$$r_3 = w^{1/a_3} - C_4 \qquad \text{(A6.4.2.21)}$$

$$w_3 = C_4^{a_3} \qquad \text{(A6.4.2.22)}$$

$$w_5 = (R_o + C_4)^{a_2} \qquad \text{(A6.4.2.23)}$$

$$w_6 = (R_o + C_4)^{a_3} \qquad \text{(A6.4.2.24)}$$

$$1/\lambda_3 = (a_3 - a_1)(a_3 - a_2) \qquad \text{(A6.4.2.25)}$$

and $F_R(.)$ is the probability distribution function of focal distance, R, and R_o is the maximum focal distance.

Differentiation of the Eq. (A6.4.2.12) to Eq. (6.4.2.19) leads to the probability density function of W and they are given in the followings.

$$f_W(w) = \int_{r_2}^{r_1} h(w,r,a_1,\lambda_1)\, f_R(r)dr - \int_{o}^{r_2} h(w,r,a_3,\lambda_3)\, f_R(r)dr$$

$$; \; w_2 \leq w \leq \min\,(w_3,w_4) \qquad (A6.4.2.26)$$

$$f_W(w) = \int_{o}^{R_o} h(w,r,a_1,\lambda_1)\, f_R(r)dr; \; w_4 \leq w \leq \min(w_2,w_5) \qquad (A6.4.2.27)$$

$$f_W(w) = \int_{r_2}^{R_o} h(w,r,a_1,\lambda_1)\, f_R(r)dr; \; \max(w_2,w_4) \leq w \leq \min(w_3,w_5) \qquad (A6.4.2.28)$$

$$f_W(w) = -\int_{o}^{R_o} h(w,r,a_3,\lambda_3)\, f_R(r)dr; \; \max(w_2,w_5) \leq w \leq \min(w_3,w_6) \qquad (A6.4.2.29)$$

$$f_W(w) = \int_{r_2}^{r_1} h(w,r,a_1,\lambda_1)\, f_R(r)dr - \int_{r_3}^{r_2} h(w,r,a_3,\lambda_3)\, f_R(r)dr$$

$$; \; w_3 \leq w \leq w_4 \qquad (A6.4.2.30)$$

$$f_W(w) = \int_{r_2}^{R_o} h(w,r,a_1,\lambda_1)\, f_R(r)dr - \int_{r_3}^{r_2} h(w,r,a_3,\lambda_3) f_R(r)dr$$

$$; \; \max\,(w_3,w_4) \leq w \leq w_5 \qquad (A6.4.2.31)$$

$$f_W(w) = \int_{r_3}^{R_o} h(w,r,a_3,\lambda_3)\, f_R(r)dr \; ; \; \max\,(w_3,w_5) \leq w \leq w_6 \qquad (A6.4.2.32)$$

$$f_W(w) = 0 \qquad \text{otherwise} \qquad (A6.4.2.33)$$

Only some of the formulae given above will be valid for the numerical values of the parameters involved.

APPENDIX A6.4.3

PROBABILITY OF PEAK GENERALIZED SEISMIC INTENSITY, Y

The probability of $[Y > y]$ of peak generalized intensity is obtained using the distribution laws for W and Z derived in Appendix A6.4.1 and A6.4.2. Since M, R, C_1 and C_2 are mutually independent so will be Z and W. This probability for magnitude cutoff at lower ends and magnitude cutoff at both ends are given in the following.

a) Magnitude cutoff at lower end i.e. $m \varepsilon (m_o, \infty)$

The domain of Y is shown in Fig. (A6.4.3.1)

The required probability

$$P[Y > y] = 1 \quad ; y \leq z_1/w_6 = y_1 \qquad (A6.4.3.1)$$

where $z_1 = \exp(x_1 + C_2 m_o)$ (A6.4.3.2)

and $w_6 = (R_o + C_4)^{a_3}$ (A6.4.3.3)

This probability is obtained for $y_1 \leq y \leq y_2$ from Fig. (A6.4.3.2) and is given by

$$P[Y > y] = S_Y(y) = 1 - \int_{z_1/y}^{w_6} dw \int_{z_1}^{wy} f_{Z,W}(z,w)dz$$

Use of statistical independence of Z and W and subsequent integration with respect to z results in

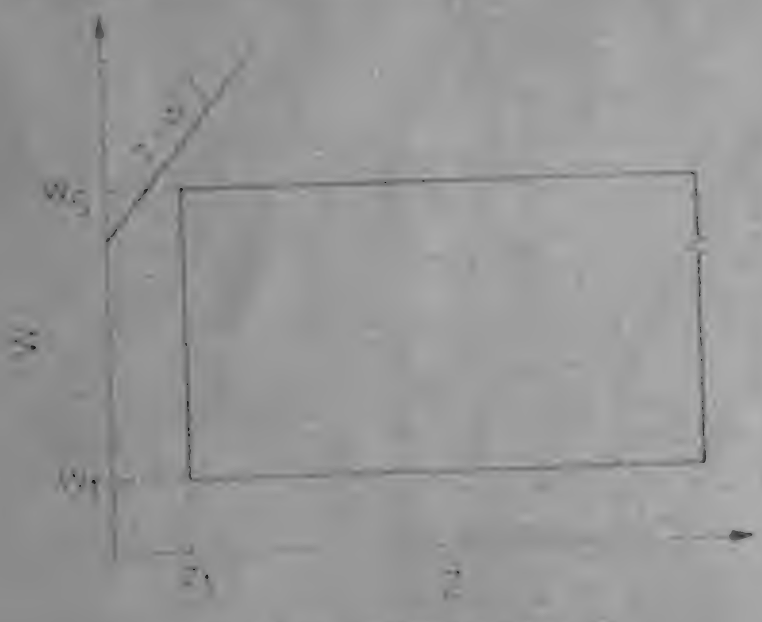

FIG. A6·4·3·1 EVENT [$Y \leq y_1$]

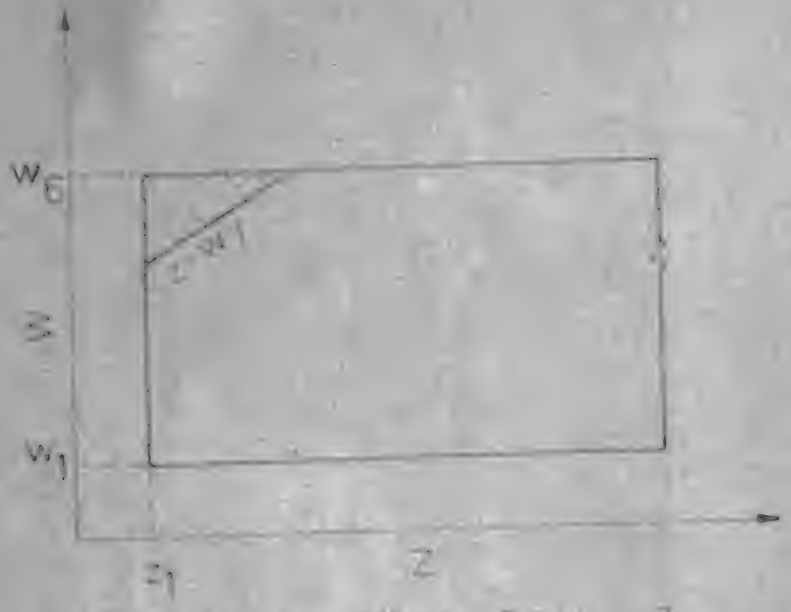

FIG. A6·4·3·2 EVENT [$y_1 < Y \leq y_2$]

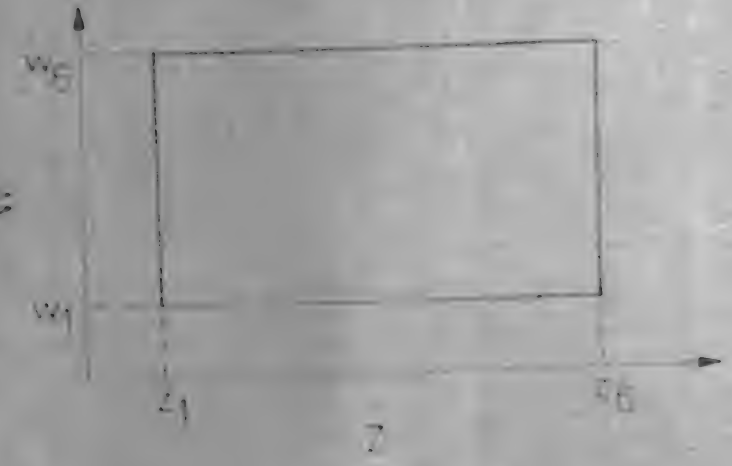
w_6
w
w_1
z_1
z_6
z

FIG. A6·4·[illegible] DOMAIN OF Z AND W

$$S_Y(y) = 1 - \int_{z_1/y}^{w_6} f_W(w)\, F_Z(wy)\, dw; \quad y_1 \leq y \leq y_2 \tag{A6.4.3.4}$$

where

$$y_1 = \exp\,(x_1 + C_2 m_o)/(R_o + C_4)^{a_3} \tag{A6.4.3.5}$$

$$y_2 = \exp\,(x_1 + C_2 m_o)/\,C_4^{\;a_1} \tag{A6.4.3.6}$$

The probability distribution of Z given in Appendix A6.4.1 for suitable region has to be used in Eq. (A6.4.3.4). However further simplification is not possible analytically. Numerical integration has to be used to integrate the integral in Eq. (A6.4.3.4). Similar procedure lead to

$$S_Y(y) = 1 - \int_{w_1}^{w_6} F_Z(wy)\, f_W(w)dw\ ; \quad y \geq y_2 \tag{A6.4.3.7}$$

b) Magnitude cuttoff at both ends i.e. $m \in (m_o, m_1)$

The domain of Z and W are shown in Fig. (A6.4.3.3). Following similar procedure as in previous section the required probability is obtained as

$$S_Y(y) = P[Y > y] = 1 \quad ; \; y \leq y_1 = z_1/w_6 \tag{A6.4.3.8}$$

$$S_Y(y) = 1 - \int_{z_1/y}^{w_6} F_Z(wy)\, f_W(w)dw\ ; \quad y_1 \leq y \leq \min(y_2, y_3) \tag{A6.4.3.9}$$

$$S_Y(y) = 1 - \int_{w_1}^{w_6} F_Z(wy)\, f_W(w)dw; \quad y_2 \leq y \leq y_3 \tag{A6.4.3.10}$$

$$S_Y(y) = F_W(z_1/y) \int_{z_1/y}^{z_6/y} F_Z(wy)\, f_W(w)dw; \; y_3 \leq y \leq y_2 \qquad (A6.4.3.11)$$

$$S_Y(y) = F_W(z_6/y) - \int_{w_1}^{z_6/y} F_Z(wy)\, f_W(w)dw; \; \max\,(y_2,y_3) \leq y_4 \qquad (A6.4.3.12)$$

$S_Y(y) = 0$ otherwise

where

$$y_1 = z_1/w_6 = \exp\,[\,x_1 + C_2 m_o\,]\,(R_o + C_4)^{-a_3} \qquad (A6.4.3.13)$$

$$y_2 = z_1/w_1 = \exp\,[\,x_1 + C_2 m_o\,]\; C_4^{-a_1} \qquad (A6.4.3.14)$$

$$y_3 = z_6/w_6 = \exp\,[\,x_3 + C_2 m_o\,]\,(R_o + C_4)^{-a_3} \qquad (A6.4.3.15)$$

$$y_4 = z_6/w_1 = \exp\,[\,x_3 + C_2 m_o\,]\; C_4^{-a_1} \qquad (A6.4.3.16)$$

Appendix A7.1

Table A7.1

List of Earthquakes before 1917

Date	Time hr - min - Sec	Latitude degree	Longitude degree	Focal depth Kms.	Magnitude	Remarks
08930000	-	-	-	-	> 7.0	Diabul (unknown)
15050706	-	N 34.45	E 69.16	-	> 8.0	
16680502	-	-	-	-	> 7.0	delta of Indus
16680511	-	-	-	-	> 7.0	delta of Indus
16690604	-	-	-	-	> 6.0	**Madran**
17200715	-	N 28.39	E 77.13	-	6.5	4-5 shocks/day for 40 days, occasional 4 to 5 months.
17620402	-	N 22.24	E 90.42	-	> 7.5	-
17640604	-	-	-	-	> 6.0	Bank of Ganges, Several shocks
18030901	-	N 27.31	E 77.42	-	6.5	
18080000	-	-	-	-	6.5	Kumaon
18160526	-	N 30.00	E 80.00	-	6.5	2-shocks
18190616	-	-	-	-	8.0	Rann of Kutch
18210813	-	N 23.13	E 70.08	-	> 5.0	
18220129	-	N 13.14	E 79.06	-	5.0	Several shocks (S.S.)
18220403	-	-	-	Deep	6.5	Manipur-Burma Border, S.S.

Table contd. A7.1

18230209	-	-	-	-	> 6.0	Indian Ocean
18261029	-	N 27.50	E 86.50	-	6.0	8 minor after-shocks (A.S.)
18270900	-	-	-	-	-	In hills-Ravi emerges in plain
18280606	-	N 34.04	E 74.49	-	> 6.0	
18280708	-	-	-	Deep	> 5.0	Manipur-Burma Border
18280822	-	N 14.04	E 72.85	-	> 5.0	
18301231	-	N 22.24	E 90.42	-	> 5.0	
18310000	-	N 30.00	E 70.00	-	6.0	
18320221	-	N 36.50	E 70.50	Deep	7.0	S.S.
18330826	-	N 27.50	E 86.50	-	7.5-8.0	
18331002	-	-	-	-	>6.0	A.S.of 18330826
18331018	-	-	-	-	>6.0	A.S.of 18330826
18390323	-	N 22.00	E 96.08	-	7.5-8.0	
18420116	-	N 27.31	E 77.42	-	-	
18420219	-	N 34.25	E 70.26	-	7.5	100 A.S. in a month
18420305	-	N 30.29	E 78.06	-	5.5	
18421111	-	-	-	Deep	>6.0	Manipur-Burma Border
18430401	-	N 15.12	E 75.57	-	5.5-6.0	
18430411	-	N 30.00	E 80.00	-	> 5.0	
18450419	-	N 23.48	E 68.47	-	6.0	To 18450425, 66 A.S.

Table contd. A7.1

18450806	-	N 24.43	E 91.55	-	6.5	
18461018	-	N 24.62	E 72.70	-	6.0	
18520124	-	N 33.94	E 73.39	-	6.0	
18520500	-	N 27.55	E 81.10	-	6.5	
18560407	-	-	-	-	5.0	Near Kotghur (Simla hills)
18580824	-	N 19.00	E 90.50	-	7.5	
18631118	-	N 22.00	E 75.00	-	5.0	
18640429	-	N 24.00	E 70.00	-	6.0	
18651219	-	-	-	Deep	6.0	Manipur-Burma Border
18660523	-	N 27.5	E 86.5	-	7.0	
18680630	-	-	-	-	> 5.0	Manipur-Burma Border
18680800	-	-	-	-	-	Peshavar, I Milne
18690110	-	-	-	-	> 7.5	Near Cachar (Assam)
18690400	-	-	-	-	-	Peshwar, I Milne
18690707	-	N 27.5	E 86.5	-	6.5	
18691220	-	-	-	-	-	Rawalpindi, I Milne
18700422	-	-	-	-	-	Dacca, I Milne
18701028	-	-	-	-	-	Sind, I Milne
18721215	-	-	-	-	-	Sind, III Miln
18750426	-	-	-	-	-	Darjiling, I Milne
18751212	-	-	-	-	-	Lahore, II Milne

Table contd. A7.1

18780302	–	–	–	–	–	Punjab, I Milne
18811231	–	–	–	–	> 8.0	Bay of Bengal
18830400	–	–	–	–	–	Peswar, II Milne
18850530	–	N 34.6	E 74.35	–	7.0	
18850714	–	N 23.5	E 90.25	–	> 7.0	N-W of Dacca
18881020	–	–	–	–	–	Srinagar, I Milne
18881223	–	–	–	–	–	Burma, I Milne
18891017	–	–	–	–	–	Or 18, Serajganj, Dharma-I Milne
18921222	–	N 30.56	E 66.25	–	–	
18931105	–	–	–	–	–	Peshavar, Nausar -I Milne
18970612	11-06-00	N 26.0	E 91.0	–	8.7	A.S. for years, Darjiling, III Milne
18990925	–	–	–	–	–	
19000208	–	N 10.7	E 76.7	70	6.0	
19020418	–	N 36.5	E 70.5	Deep	7.0	
19020616	–	N 31.0	E 79.0	–	6.0	Felt at Dhera-dun at 07 hr 20 min.
19020822	–	N 37.0	E 77.0	–	7.0	
19020920	–	N 36.5	E 70.5	Deep	7.0	
19030114	–	N 24.0	E 70.0	–	6.0	
19050404	–	N 32.5	E 76.25	–	8.0	
19050928	01-26-09	N 29.0	E 74.00	–	7.0	
19060228	–	N 32.0	E 77.00	–	7.0	

Table contd. A7.1

19060520	-	N 36.5	E 70.5	Deep	7.0	
19060613	-	N 31.0	E 79.0	-	5.5-6.0	
19060815	-	N 24.62	E 72.7	-	5.0	
19060831	14-57-30	N 28.00	E 94.0	-	6.5	
19061024	14-42-51	N 40.00	E 68.0	Shallow	7.0	
19070413	-	N 36.5	E 70.5	260	7.0	
19071021	04-23-36	N 38.0	E 69.0	Shallow	8.0	
19071225	22-36-00	N 36.5	E 70.5	240	6.75	
19080112	-	N 32.0	E 68.0	-	6.0	
19080209	18-13-00	N 36.6	E 90.0	Shallow	7.0	
19080305	-	N 32.0	E 68.0	-	5.0	13 A.S.
19080312	19-26-24	N 36.5	E 70.5	220	6.75	
19081023	20-14-06	N 36.5	E 70.5	220	7.0	
19081211	-	N 31.0	E 79.0	-	7.5	
19081212	12-54-54	N 26.0	E 79.0	-	7.5	
19090217	-	N 27.0	E 87.0	-	5.0	
19090409	-	N 24.62	E 72.7	-	5.0	7 moderate shocks
19090707	21-37-50	N 36.50	E 70.5	230	7.75	
19090707	21-39-05	N 36.5	E 70.5	Shallow	8.0	
19090907	-	N 36.5	E 70.5	-	6.0	
19091020	23-41-12	N 30.0	E 68.0	-	7.2	
19100712	07-36-12	N 38.0	E 66.0	Shallow	8.7	
19110101	10-18-00	N 38.0	E 66.0	50	7.2	
19110704	-	N 36.0	E 70.5	Deep	7.6	

Table contd. A7.1

19111207	-	N 30.0	E 88.0	-	5.0
19120425	02-24-06	N 21.0	E 97.0	-	8.0
19120425	10-27-48	N 36.5	E 70.5	220	6.75
19120523	02-24-26	N 21.0	E 97.0	-	8.0
19120523	23-08-18	N 36.5	E 70.5	220	6.25
19120823	21-14-30	N 36.5	E 70.5	200	7.5
19121128	20-55-06	N 36.5	E 70.5	230	6.5
19140206	11-42-18	N 29.5	E 65.0	100	7.0
19140328	10-44-48	N 25.0	E 90.0	100	6.7
19141011	16-17-06	N 12.0	E 94.0	80	7.2
19151114	-	N 63.3	E 92.7	-	5.0
19151205	-	N 63.3	E 92.7	-	5.0
19160107	-	N 13.0	E 77.83	-	5.0
19160828	-	N 30.0	E 81.00	-	7.5